

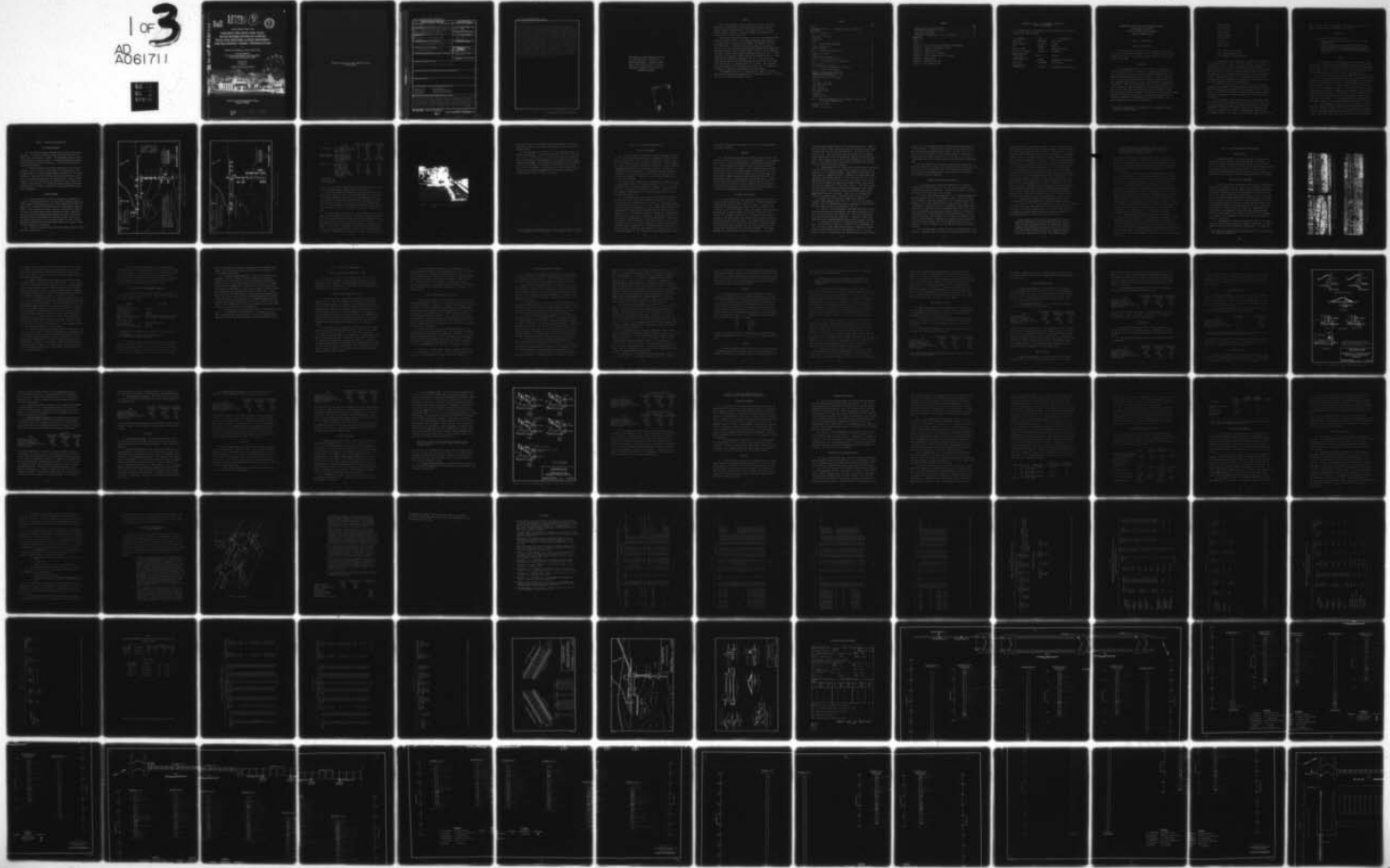
AD-A061 711 ARMY ENGINEER WATERWAYS EXPERIMENT STATION VICKSBURG MISS F/G 13/2
CONCRETE AND ROCK CORE TESTS, MAJOR REHABILITATION OF STARVED R--ETC(U)
SEP 78 R L STOWE, B A PAVLOV, G S WONG

UNCLASSIFIED

WES-MP-C-78-12

NL

| OF 3
AD
A061711



DDU FILE COPY A061711



LEVEL

2
B.S.



MISCELLANEOUS PAPER C-78-I2

CONCRETE AND ROCK CORE TESTS
MAJOR REHABILITATION OF STARVED
ROCK LOCK AND DAM, ILLINOIS WATERWAY
CHICAGO DISTRICT, PHASE I, REHABILITATION

by

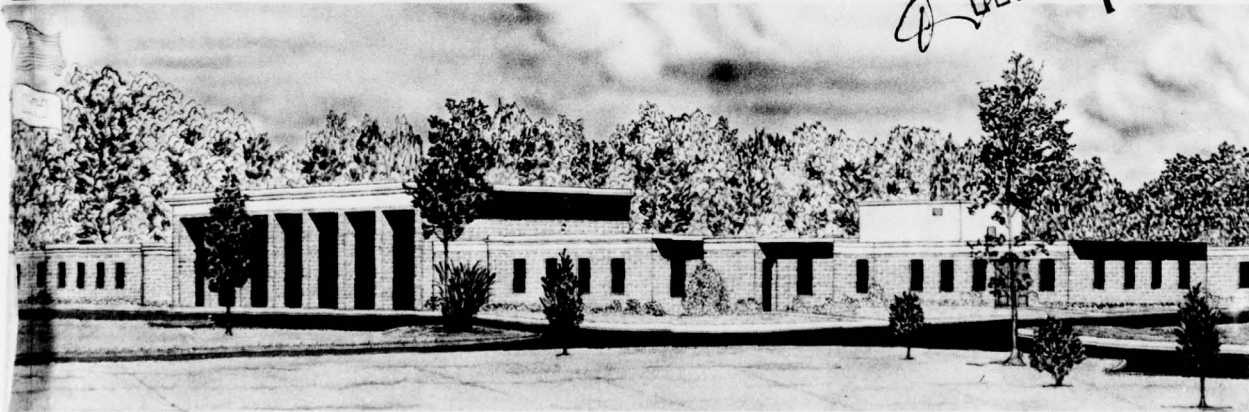
Richard L. Stowe, Barbara A. Pavlov, Ging S. Wong

Concrete Laboratory
U. S. Army Engineer Waterways Experiment Station
P. O. Box 631, Vicksburg, Miss. 39180

September 1978

Final Report

Approved For Public Release; Distribution Unlimited



Prepared for U. S. Army Engineer District, Chicago
Chicago, Ill. 60604

48 11:28 033

Destroy this report when no longer needed. Do not return
it to the originator.

Unclassified

(19) WES-MP-C-78-12

SECURITY CLASSIFICATION OF THIS PAGE (When Data Entered)

REPORT DOCUMENTATION PAGE		READ INSTRUCTIONS BEFORE COMPLETING FORM
1. REPORT NUMBER Miscellaneous Paper C-78-12	2. GOVT ACCESSION NO.	3. RECIPIENT'S CATALOG NUMBER
4. TITLE (and Subtitle) CONCRETE AND ROCK CORE TESTS, MAJOR REHABILITATION OF STARVED ROCK LOCK AND DAM, ILLINOIS WATERWAY, CHICAGO DISTRICT, PHASE I, REHABILITATION.		5. TYPE OF REPORT & PERIOD COVERED Final report
6. AUTHOR(s) Richard L. Stowe, Barbara A. Favlov Ging S. Wong		7. PERFORMING ORG. REPORT NUMBER
8. CONTRACT OR GRANT NUMBER(s)		(12) 184P
9. PERFORMING ORGANIZATION NAME AND ADDRESS U. S. Army Engineer Waterways Experiment Station P. O. Box 631, Vicksburg, Miss. 39180		10. PROGRAM ELEMENT, PROJECT, TASK AREA & WORK UNIT NUMBERS
11. CONTROLLING OFFICE NAME AND ADDRESS U. S. Army Engineer District, Chicago 219 South Dearborn Street Chicago, Ill. 60604		12. REPORT DATE Sept 1978
13. NUMBER OF PAGES 152		14. SECURITY CLASS. (of this report) Unclassified
15a. DECLASSIFICATION/DOWNGRADING SCHEDULE		
16. DISTRIBUTION STATEMENT (of this Report) Approved for public release; distribution unlimited.		
17. DISTRIBUTION STATEMENT (of the abstract entered in Block 20, if different from Report)		
18. SUPPLEMENTARY NOTES		
19. KEY WORDS (Continue on reverse side if necessary and identify by block number) Concrete cores Rock foundations Concrete tests Rock tests (Laboratory) Core drilling Starved Rock Lock and Dam Rock cores		
20. ABSTRACT (Continue on reverse side if necessary and identify by block number) Drilling for laboratory testing of concrete and foundation rock was carried out for the U. S. Army Engineer District, Chicago, as part of a major rehabilitation program at the Starved Rock Lock and Dam. The structures are on the Illinois Waterway. Laboratory testing of the concrete core was done to ascertain the extent of concrete deterioration and to determine selected physical properties of the concrete. Foundation rock core was tested for purposes of (Continued) cont >		

DD FORM 1 JAN 73 1473

EDITION OF 1 NOV 65 IS OBSOLETE

Unclassified

SECURITY CLASSIFICATION OF THIS PAGE (When Data Entered)

030 700

Gu

~~Unclassified~~

~~SECURITY CLASSIFICATION OF THIS PAGE(When Data Entered)~~

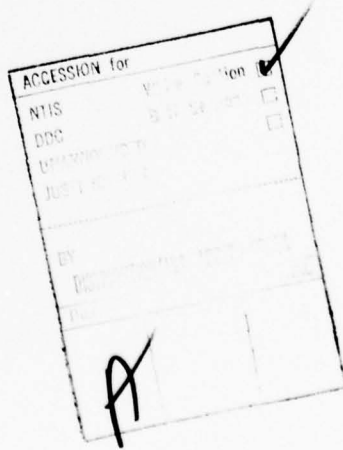
20. ABSTRACT (Continued).

obtaining characterization properties and engineering design parameters. The rock test results, if found to be significantly lower than previously reported, are to be used for checking a structural stability analysis. Laboratory testing included the determination of compressive strength, unit weight, compressional wave velocity, elastic modulus, triaxial strength, and direct shear strength. Direct shear tests were conducted on intact and discontinuous rock specimens. The concrete core indicates moderate to severe deterioration on most all exposed concrete surfaces. The predominant cause of the deterioration has been cycles of freezing and thawing. The average depth of frost-damaged concrete in the lock chamber walls is 0.20 ft; in the upper gate bays, it is 0.23 ft; and lower gates bays, none. The top 0.75 ft of concrete in the lower approach wall is frost damaged while the wall's vertical surface is not damaged. Frost action and alkali-silica reaction have caused the concrete deterioration in the dam structures. The average depth of damaged concrete in the head gate piers, the ice chute pier, and in 8 out of 11 tainter gate piers is 2.0 ft, 1.7 ft, and 1.4 ft, respectively. Three of the tainter gate piers have localized concrete damage to depths of about 0.3 ft. Maximum damage extends to 3.1 ft in the nose section of two piers. An assessment of the foundation condition was made and guidance is presented as to proper choice of design values for the foundation rock.

~~Unclassified~~

~~SECURITY CLASSIFICATION OF THIS PAGE(When Data Entered)~~

THE CONTENTS OF THIS REPORT ARE NOT TO BE
USED FOR ADVERTISING, PUBLICATION, OR
PROMOTIONAL PURPOSES. CITATION OF TRADE
NAMES DOES NOT CONSTITUTE AN OFFICIAL EN-
DORSEMENT OR APPROVAL OF THE USE OF SUCH
COMMERCIAL PRODUCTS.



PREFACE

This testing program, "Concrete and Rock Core tests, Major Rehabilitation of Starved Rock Lock and Dam, Illinois Waterway, Chicago District, Phase I, Rehabilitation," was conducted for the U. S. Army Engineer District, Chicago. The work was authorized by DA Form 2544 No. NCC-IA-77-31, dated 5 April 1977.

Drilling was conducted by personnel of the Soils and Pavements (S&PL) Laboratory (S&PL) of the U. S. Army Engineer Waterways Experiment Station (WES) during the period June 1977-August 1977 under the direction of Mr. Mark Vispi. Laboratory tests were performed at the Concrete Laboratory (CL) and the S&PL during the period September 1977-November 1977 under the direction of Messrs. Bryant Mather, Chief of Concrete Laboratory and John M. Scanlon, Chief, Engineering Mechanics Division. Mr. G. P. Hale supervised the laboratory testing conducted in the S&PL; and Mr. G. S. Wong conducted the petrographic examination. Mr. R. L. Stowe was Project Leader and was assisted in performing laboratory work at the CL by Messrs. F. S. Stewart and J. B. Eskridge and Ms. B. A. Pavlov. This report was prepared by Messrs. Stowe and Wong and Ms. Pavlov. Mr. J. B. Warriner of the S&PL wrote Appendix E concerning possible slide wedges.

The Commander and Director of WES during the conduct of the investigation and the preparation and publication of this report was COL J. L. Cannon, CE. Mr. F. R. Brown was Technical Director.

CONTENTS

	<u>Page</u>
PREFACE	1
CONVERSION FACTORS, U. S. CUSTOMARY TO METRIC (SI) UNITS OF MEASUREMENT	4
PART I: INTRODUCTION	5
Location of Study Area.	5
Background.	5
Objectives.	7
Scope	7
PART II: DRILLING AND EXPLORATION.	8
Previous Explorations	8
Current Drilling.	8
PART III: GEOLOGICAL CHARACTERISTICS	14
Bedrock Stratigraphy.	14
Backfill.	15
Geologic Cross Sections	15
Bedrock Structural Characteristics.	17
PART IV: TEST SPECIMENS AND TEST PROCEDURES.	20
Cores Received.	20
Selection of Test Specimens	20
Test Procedures and Petrographic Examination.	23
PART V: TEST RESULTS AND ANALYSIS.	25
Results of Petrographic Examination	25
Characterization Properties of Rock	25
Modulus and Poisson's Ratio of Rock	26
Peak and Ultimate Shear Strength.	27
Backfill.	29
General	29
Lock Chamber Land Wall.	31
Lock Chamber River Wall	32
Upper Gate Bays	32
Lower Gate Bay.	33
Upper Approach Wall	34
Lower Approach Wall	34
Head Gates.	37
Ice Chute Pier.	38
Tainter Gate Piers.	39
PART VI: GEOLOGICAL CHARACTERISTICS AND SUMMARY OF CONCRETE CON- DITION AND RECOMMENDATIONS.	43
Bedrock Stratigraphy.	43
Backfill.	43
Geologic Cross Section.	44

CONTENTS

	<u>Page</u>
Bedrock Structural Characteristics	44
Recommended Design Values for Rock	47
Lock Concrete Condition	48
Dam Concrete Condition	49
Recommended Instrumentation of Left Dam Abutment	51
REFERENCES	55
TABLES 1-6	
PLATES 1-23	
APPENDIX A: DETAIL GEOLOGIC AND STRUCTURAL CROSS SECTIONS	
APPENDIX B: RESULTS OF PETROGRAPHIC REPORT	
APPENDIX C: SEISMIC COEFFICIENT	
APPENDIX D: HYPOTHETICAL SLIDE WEDGES	
APPENDIX E: CAPPING EXPOSED SURFACE OF CONCRETE	
APPENDIX F: ABBREVIATIONS	
EXHIBIT A: PHOTOGRAPHS OF CORES	
EXHIBIT B: FIELD DRILLING LOGS	

CONVERSION FACTORS, U. S. CUSTOMARY TO METRIC (SI)
UNITS OF MEASUREMENT

U. S. customary units of measurement used in this report can be converted to metric (SI) units as follows:

Multiply	By	To Obtain
cubic feet	0.02831685	cubic metres
degrees (angle)	0.0174533	radians
feet	0.3048	metres
feet per second	0.3048	metres per second
miles (U. S. statute)	1.609344	kilometres
pounds (force) per square inch	6894.757	pascals
pounds (mass) per cubic foot	16.01846	kilograms per cubic metre
square feet	0.09290394	square metres
tons (mass) per square foot	9,764,856	kilograms per square metre

CONCRETE AND ROCK CORE TESTS, MAJOR REHABILITATION OF
STARVED ROCK LOCK AND DAM
ILLINOIS WATERWAY, CHICAGO DISTRICT
PHASE I, REHABILITATION

PART I: INTRODUCTION

Location of Study Area

1. The Starved Rock Lock and Dam site is located some 8 miles west of Ottawa, Illinois in LaSalle County, Illinois. The site is near mile 231 on the Illinois River; the approximate driving distance is about 85 miles southwest of Chicago.

Background

2. At a meeting held at the offices of the U. S. Army Engineer District, Chicago (NCC) on 11 February 1977, representatives of the Concrete Laboratory (CL) and the Soils and Pavements Laboratory (S&PL) of the Waterways Experiment Station (WES) were requested to submit a proposal for work to assist the Chicago District in connection with concrete and rock exploration and laboratory testing. The work would be accomplished in two phases. Phase I work concerned concrete and rock exploration, laboratory testing for a major rehabilitation of the Starved Rock Lock and Dam. Phase II work concerned drilling and laboratory testing to comply with certain Office, Chief of Engineers (OCE) and North Central Division (NCD) comments as outlined in Reference 1. The following tabulation gives the name and affiliations of the attendees at the February meeting. This report presents the results of the Phase I work.

* A table for converting U. S. customary units of measurement to metric (SI) units is given on page 4.

Fred Patterson	NCD
Terrence Smith	NCD
Ignas Juzenas	CDO
Jim Przwoznik	CDO
Richard Huelsman	CDO
George Sanborn	CDO
C. Ruiter	CDO
Richard Stowe	WES
Mark A. Vispi	WES

NCD - North Central Division
 CDO - Chicago District Office
 WES - Waterways Experiment Station

3. The major work effort during Phase I would be to resurface most of the exposed concrete surfaces of the lock and dam. WES was asked to ascertain the extent of concrete deterioration on these surfaces. The number and location of borings to be drilled were assigned by NCC personnel. Specific boring locations on the separate structures were assigned by the author after a field inspection and a review of a periodic inspection report.² A secondary effort was to obtain characterization properties and engineering design parameters of foundation rock at given locations. These data supplement previously reported data.³

4. Phase II work involved drilling and then testing of concrete and bedrock for purposes of obtaining certain characterization properties and engineering design properties as outlined on pages 53 and 54 in Reference 3. The District will check previous structural stability analyses if certain rock properties differ significantly from those reported in Reference 3.

5. In the summer of 1976, concrete cores were recovered from the lock chamber walls at Starved Rock Lock and were tested at the WES. The cores were examined for extent of deterioration and tested for strength and modulus of elasticity. Pertinent results of that examination and testing are included in this report for completeness. See Reference 4 for complete report. As a result of an interim field inspection in July 1977,

eight additional borings were selected. The results of tests on the core taken from these borings are included in this report.

Objectives

6. The objectives of this study were to:
 - a. Conduct drilling for laboratory testing of concrete and foundation rock.
 - b. Make an analysis of test conducted and a summary of the concrete condition over the project site. The rock test results, if found to be significantly different than previously reported, are to be used for checking a stability analysis.

Scope

7. The drilling was accomplished using a WES drilling crew, plant, and supplies. Floating plant, barge-mounted crane, and tow boat were supplied by NCC. A Bureau of Reclamation geologist on contract to WES logged and preserved the core for testing. Delivery of the core to WES was made in three shipments, one each in mid June, July, and August 1977.

8. The objectives of this study were accomplished by drilling concrete and rock core and sampling backfill material, conducting petrographic examinations, characterization property tests (unconfined compression, unit weight, and ultrasonic pulse velocity), and engineering design property tests (modulus of elasticity, Poisson's ratio, and direct shear). Direct shear tests were conducted on concrete to rock, intact rock, shale-filled partings oriented parallel to bedding, and on specimens oriented to obtain cross-bedded shear strengths. Precut surfaces were not tested in direct shear because sufficient testing on precut surfaces had been performed previously; see Reference 5. One clayey shale sample was subjected to a petrographic examination to determine nomenclature and mineral content.

9. At the completion of the Phase II work a final report, to include the compliance drilling together with previous drilling (NCC, see Reference 3 and WES drilling), will be used to develop the site geology in more detail than presented herein; the report will follow in the near future. This report is the final report for the concrete rehabilitation.

PART II: DRILLING AND EXPLORATION

Previous Exploration

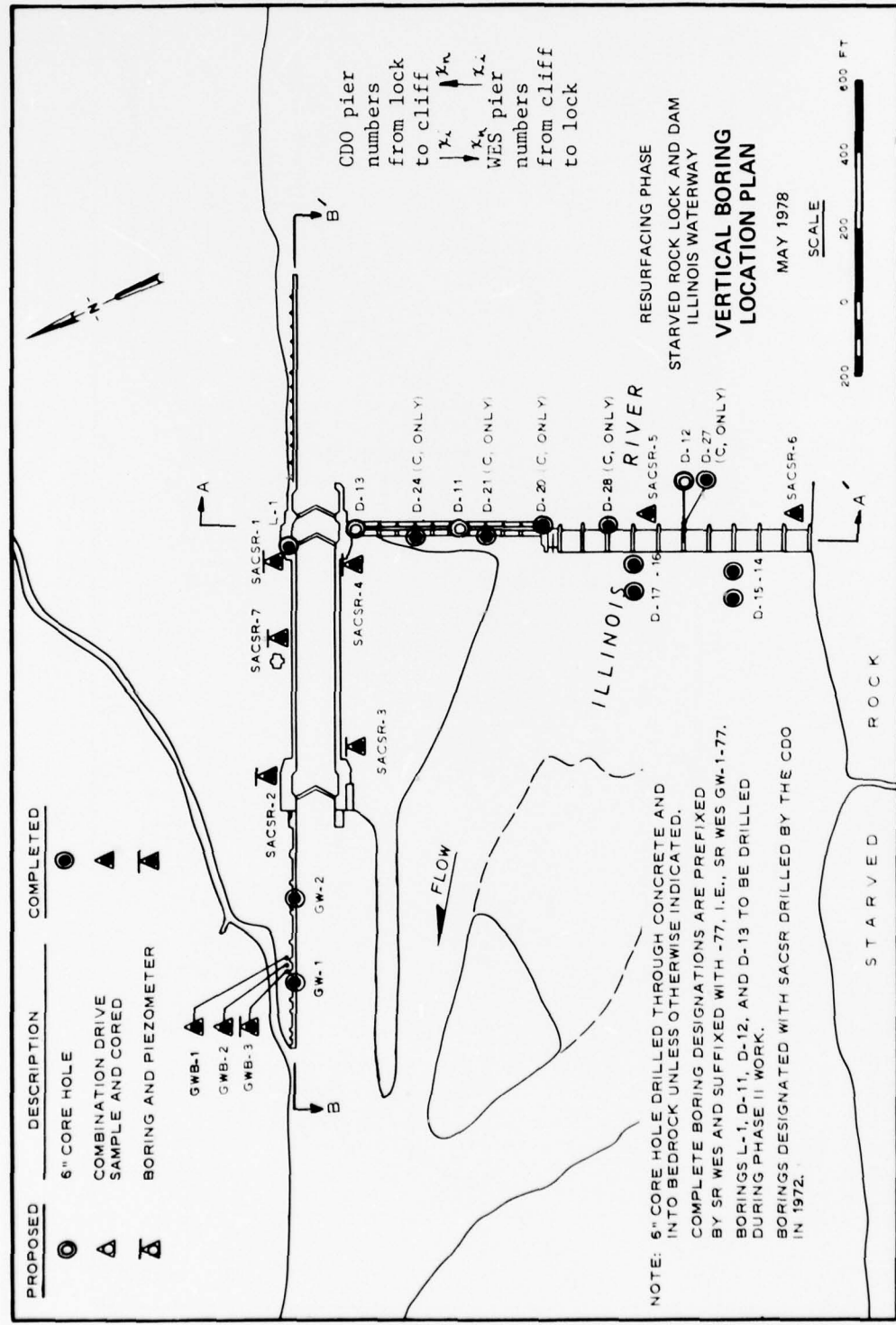
10. The concrete sampling conducted by WES in 1976 is pertinent to this study. In 1976, 20 horizontal borings were drilled into the lock chamber walls from inside the chamber. The approximate boring locations within monoliths are shown in Plate 1. The monolith numbering system is the same as used in Plate 13, Reference 2. The cores were examined for extent of deterioration.

11. Previous foundation explorations pertinent to this study were conducted in 1972 by the NCC (see Reference 3 for details) and in 1974 through the NCC by a private drilling company (see Reference 5 for boring locations). During the 1972 drilling program seven borings were located near the lock walls and upstream of the dam structures. During the 1974 program a total of 19 borings were put down north of and on three lines parallel to the lock axis. The geologic information obtained from these borings serves as a valuable reference for the work accomplished during this investigation.

Current Drilling

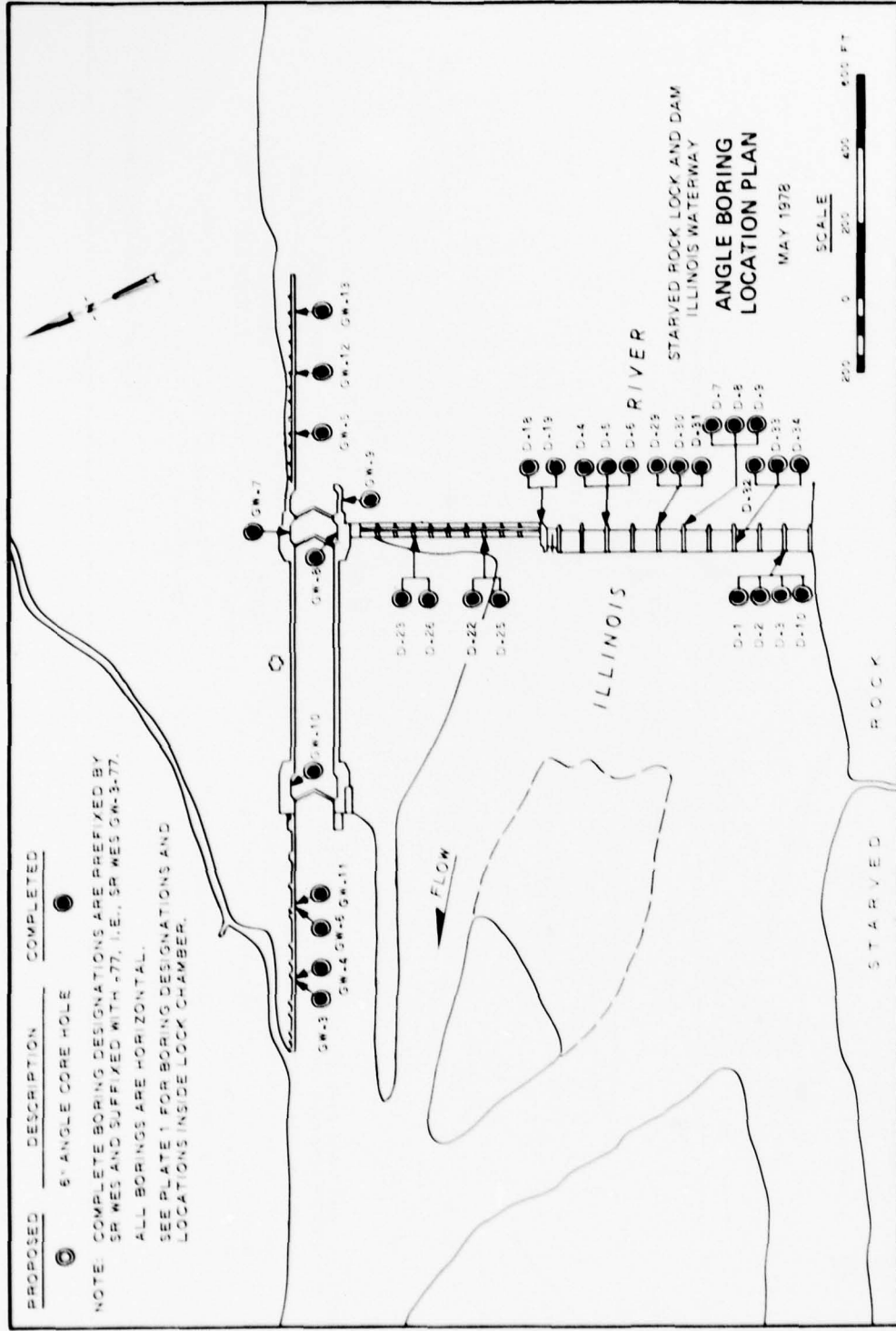
12. Drilling was begun on 4 June and completed on 13 August 1977. A total of 67 borings were drilled into concrete and foundation rock; this figure includes the 20 borings put into the lock chamber walls during the summer 1976. The general boring location plan is presented in Figures 1a and 1b. Plate 2 gives the location of section lines and Plate 3 depicts the sections on which specific boring locations are shown. During the drilling operation the WES personnel numbered the head gate and tainter gate piers from the Starved Rock cliff towards the lock. The District has numbered coming from the lock and going towards the cliff. The WES numbering system will be used in this report because this system is cited in the two exhibits to this report.

13. A summary of boring locations, direction number, material drilled, and depth is given below:



a. Vertical boring location plan

Figure 1. General boring location plans



b. Angle Boring Location Plan

Figure 1. General boring location plans

	<u>Location</u>	<u>Direction</u>	<u>No. of Holes/</u>	<u>Material</u>
			<u>Depth, ft</u>	<u>Drilled</u>
Lock Structure	Lock chamber land wall	H ¹	10/3	Con ³
	Lock chamber river wall	H	10/3	Con
	Miter gate bays	H	4/3	Con
Upper and Lower Approach Walls	Upper approach wall	H	3/3	Con
	Lower approach wall	H	4/3	Con
	Lower approach wall	V ²	2/55	Con & Rock
	Lower approach wall in backfill	V	1/28; 2/19	Con & Soil
Dam Structure	Head gate piers	H	4/3	Con
	Head gate piers	V	2/3	Con
	Ice chute pier	H	2/3	Con
	Ice chute pier	V	1/3	Con
	Tainter gate pier	H	16/3	Con
	Tainter gate pier	V	3/11	Con
	Downstream of tainter gate sill	V	4/20	Rock

1 Horizontal = H

2 Vertical = V

3 Con = Concrete

Totals of 24, 12, and 31 borings were put into the lock structure, upper and lower approach walls, and dam structure, respectively.

14. Drilling equipment consisted of an Acker Toredo Mark II skid-mounted rotary drill rig, and a Concord portable drill rig. Six-inch inside diameter diamond core bits and a 5-ft-long doubletube barrel was used to drill the concrete and the bedrock in the deep holes. A single core barrel was used with the Concord rig to drill the shallow holes. Access to the drill holes was by a marine floating plant and for holes on top of structures by crane. A typical drill rig setup is shown in Figure 2.

15. Total footage drilled was 261.7, 160.0, and 63.1 ft in concrete, bedrock, and overburden, respectively. All concrete and bedrock samples were preserved for laboratory testing. Procedure for handling the core and preserving it for testing was the same as given in Reference 5. Color photographs of all the core recovered are included in a notebook as Exhibit A to this report. The Exhibit is on file at the Chicago District Office. Core recovery was 100 percent in the concrete and 96 percent in the bedrock. The backfill material consists of sandy clay and gravel and

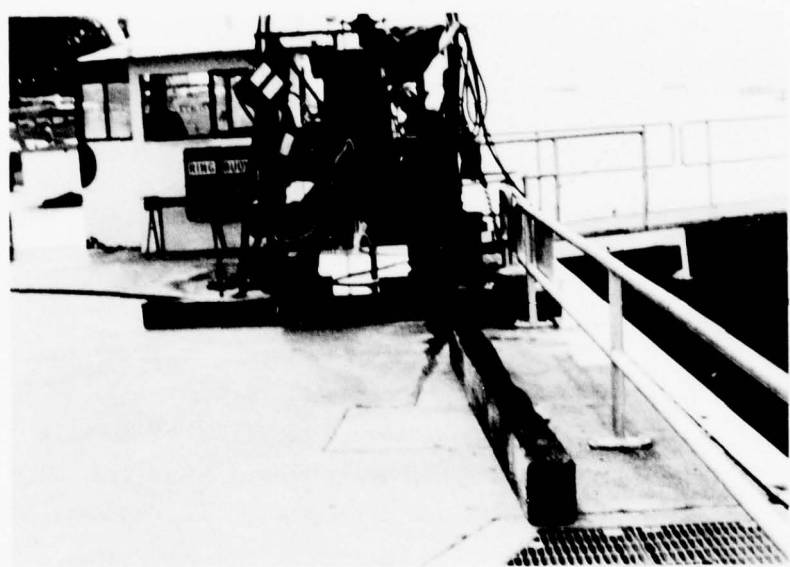


Figure 2. Typical drill rig setup, Starved Rock Lock and Dam

was easily recovered. All drilled holes were backfilled to their full depth with concrete produced using a commercially available packaged dry combined mixture.

16. One piezometer of the slotted 1-1/4-inch PVC pipe type was installed in boring GWB-1. It was set at elevation (el) * 430.5 (piez. tip). Plate 4 gives pertinent data; daily drill reports on file at the NCC district office contain a few measurements of water heights that were taken by WES field geologist. The presentation and summarization of piezometer data as to its pertinence to a stability analysis was not within the scope of this investigation. An assessment of current readings from all piezometers and possible recommendations for additional piezometer installations by WES could be made if so desired.

* All elevations (el) cited herein are in feet referred to mean sea level.

PART III: GEOLOGICAL CHARACTERISTICS

Bedrock Stratigraphy

17. The bedrock beneath and adjacent to the lock and dam is assigned to the St. Peter Sandstone Formation and the Shakopee Dolomite Formation, both of Ordovician age. The St. Peter is represented at Starved Rock by two of its members, the Tonti and the Kress sandstones. The Tonti member is a medium to fine grained, well-sorted, noncalcareous, friable sandstone. A total of only 10 ft was uncovered in the boreholes. The Tonti lies conformably on the Kress Member.⁶ The designation "Kress" was given to all deposits closely associated with the St. Peter but underlying the typical, pure sandstone.⁶ A total of 33 ft of the Kress Member was uncovered in the boreholes.

18. The Kress is a coarse rubble or conglomerate of angular chert in a sometimes layered matrix of sand, green shale, or clay. It is a residue from the solution of the underlying cherty dolomites. Some of the chert is oolitic. The Kress contains layers of shale up to 1 ft thick. The Kress Member is approximately 10 ft thick in borings drilled in back of the dam (D-14 through 17).

19. The Shakopee Dolomite is a thin to medium-bedded, fine-grained, argillaceous to pure, light brown to light grey dolomite. It contains lenses and layers of sandstone up to 4 ft thick. It contains blue green to grey green shale seams up to 0.3 ft thick. Shale-filled bedding planes are found throughout the dolomite. It also contains lenticular masses of laminated dark grey medium grained dolomite that are algal reefs which measure up to 1 ft in thickness. Within the dolomite are found bands and nodules of chert, some oolitic, some sandy. Several beds are brecciated or disrupted.⁷ Separating the St. Peter and the Shakopee in the Starved Rock area is a major unconformity. There was an interval of erosion and non-deposition at this time which created the irregular erosional surface separating these two bodies of rock. Residual material (chert rubble) from the erosion of the underlying carbonates is included in the St. Peter as the Kress Member.^{7,8} This irregular surface may explain some of the

differences in elevation of the contact of the St. Peter and the Shakopee found in the boreholes.

Backfill

20. Three boreholes were made into backfill material (GWB-1, GWB-2, GWB-3); see Figure 1a for boring locations. Approximately 55 ft of material was recovered. Only one borehole (GWB-1) reached bedrock and penetrated 1 ft. Bedrock overburden was probably spoil from the lock and dam excavations and consists of a mixture of clay, sand, and gravel. The backfill material varies in proportions ranging from 80 percent loose sand on top (clayey sand) to 80 percent compact clay near bottom (sandy clay) with pockets of gravel interspersed with the sand and clay layers. Up to 20 percent gravel is found within the sand and clay layers. Bedrock recovered was a green gray shale layer topping a sandstone reached at el 431. This puts the rock in the Kress Sandstone or at the contact of the Shakopee Dolomite and Kress Sandstone as inferred from comparison of this hole with surrounding lower approach wall boreholes.

Geologic Cross Sections

21. Log of boring sheets were drawn and include the seven vertical borings drilled during the Phase I work and the L-1 boring scheduled to be drilled during Phase II work; see Plates 5, 6, and 7. Boring L-1 was scheduled to be drilled during the Phase II work. Due to heavy river traffic the drill crew was unable to drill horizontally into the approach walls and gate recesses; therefore they drilled L-1 during this time period. The information from boring L-1 is presented in this report for continuity. The log of borings were drawn to give a general overview of the bedrock material that was drilled. The foundation material is quite complex and in order to correlate strata and select representative material for testing, detail geologic cross sections and structural cross sections were compiled; they are presented in Appendix A. Two general geologic cross sections are presented in Plates 8 and 9. One section

was drawn along the land lock wall and the lower approach wall. Another section was drawn from the upper gate recess on the land lock wall, across the dam to the cliff into which the dam abutts. See Figure 1a for section locations. These two sections show the continuity of the bedrock beneath and adjacent to the lock and dam and indicate possible weak zones. Tight contacts between concrete and rock were observed on core from GW-1 and L-1. Core from GW-2 had a loose contact and boreholes D-14 through D-17 were drilled directly into bedrock.

22. Approximately 80 ft of bedrock was recovered from the four borings in the back of the tainter gate dam section of which 46 ft was St. Peter Sandstone and 34 ft Shakopee Dolomite. The sandstone contains many shale seams spaced at irregular intervals. Thickness of the shale ranges from coatings on some bedding surfaces to a 2-ft thick layer in D-17. The 2-ft layer broke into pieces about 0.4 ft long as it came out of core barrel. The rock was unsuitable for compressive strength testing. Chert nodules and bands are abundant and, in some areas, oolitic. The chert is black, grey, and white with some of the white chert displaying a soft, porous, chalk-like nature. The dolomite contains shale-filled bedding planes spaced from 0.05 ft to a foot apart. There is a 4-ft sandstone layer found in the dolomite which is continuous across the lock and dam.

23. Eighty feet of bedrock was recovered from boreholes on the lock and guidewalls (GW-1, GW-2, L-1). All of this is Shakopee Dolomite. The 4-ft sandstone bed previously mentioned is present here at the same elevation in all three boreholes (414 ft).

24. There are a few discontinuous clay seams and pockets in the St. Peter and near the top of the Shakopee. The largest occurrence of clay is a 1-ft section of grey clay found in D-14. The clay was analyzed by X-ray diffraction and consists essentially of kaolinite, illite, and a mixed layer clay containing montmorillonite, which will swell in water.

25. Boring D-14 is located 4 ft downstream from tainter gate pier No. 4. The clay was not found in D-15, which is 15 ft downstream from D-14. Nor was it found in the Phase II boring D-12 which goes through Pier No. 6 located about 140 ft to the northeast of D-14. It is not known if the clay is present under the tainter gate section just upstream

from D-14. It is recommended that one boring be drilled through the sill ofainter gate No. 4 (counting from the bluff side of the dam) during the scour detection program scheduled in FY78. The top of the clay is at el 412.25, the design el of concrete-rock contact is 425.48, and the actual contact of concrete and rock in D-12 is el 416.5. The presence of clay and the concrete-rock contact needs to be verified just upstream from D-14.

26. The bedrock in the two cross sections has been divided into three lithologic units on Plates 8 and 9 on the basis of size and continuity of a unit over the lock and dam area. The divisions marked are the St. Peter Sandstone, the Shakopee Dolomite and the nominal 4-ft sandstone lens contained within the Shakopee.

Bedrock Structural Characteristics

27. The general bedrock structural characteristics relevant to foundations are presented in Plates 5, 6, and 7 and the detailed characteristics are presented in Appendix B. The plates are similar to the cross sections described in Geologic Cross Sections.

28. Dips in local bedding range from <1 to 12 degrees when measured between boreholes at the St. Peter/Shakopee contact. However, bedding dips uniformly <1 degree when measured on the 4-ft sandstone bed in the Shakopee or some other continuous feature other than this contact. This is explained by the fact that the St. Peter/Shakopee contact marks a major unconformity, as mentioned in the Stratigraphy, where the St. Peter rests on a very irregular erosional surface caused by solution of underlying cherty dolomites. Bedding along the lock and approach walls is very consistent and regular. Beds as small as 0.2-ft-thick were traceable across the lock in the boreholes. Among the more prominent features which were found in all three boreholes are the 4-ft sandstone layer (el 413), an algal reef (el 405), stylolites (el 404), and a 0.2-ft-thick chert bed at (el 403).

29. The nearest major regional structure is the Sandwich Fault Zone. Reference 3 contains a map of the fault zone erroneously placing it 5 miles

from Starved Rock Lock and Dam and Reference 5 locates it in the same area. The fault zone is actually located 5.8 miles northeast of Dresden Island Lock and Dam which puts it 26 miles northeast of Starved Rock at its closest approach.⁶ Small faults were found in two of the boreholes. The largest occurred in the 4-ft sandstone layer in the Shakopee in borehole D-16 and had an apparent displacement of 0.9-1.2 ft. The other two had displacements of only 0.05 ft. See Appendix C for a brief discussion on using the standard zone value for seismic coefficient for the Illinois Waterway System.

30. Thirteen structural breaks in the cores were interpreted as joints, including four pairs of conjugate joints. One pair of conjugate joints was nearly vertical (80 degrees), the other pairs had average dips of 25 degrees. Two of the remaining unpaired joints had dips of 80 degrees. The joint dip frequency was similar to that reported in Reference 5, i.e., a greater number of low angle (15 to 25 degrees) groups exist and a high angle group of joints dipping 80 to 85 degrees exists in the core taken during this study. Although the joint orientation was not measured during this investigation, the similar joint dip frequencies suggest that the joint described in this report belong to the same joint sets reported previously for the Starved Rock Duplicate Lock site.⁵ The joint orientation over the duplicate lock site can be projected to the dam sections.

31. Dolomite and sandstone breccias were found in GW-2. Other cores contained "disrupted bedding" which designates dolomite which is beginning to break up or deform and probably marks the onset of the brecciation. At the base of the brecciated dolomite in GW-2 is an area which is just beginning to break up into angular pieces. This implies that the breccia was formed in place and probably broke up in response to pressure from surrounding material.¹⁰ Reference 10 clarifies this point.

"Many sediments display intricately folded beds or laminae, sometimes accompanied by breccia, strongly suggesting that deformation occurred during or shortly after deposition. Some deformation structures apparently occur in deposits laid down on inclined slopes independent of the action of turbidity currents. Inasmuch as some fine-grained sediments contain up to 80 percent water when freshly deposited, such loosely aggregated material may readily yield to forces and slide down a relatively gentle slope or shear under gentle stresses. The original bedding

becomes intricately folded during the sliding, the stiffer materials in the beds may break into angular fragments, developing intraformational conglomerates. Sliding may readily occur at the edges of reefs."

The "soft sediment deformation" noted in other areas of the cores is a different type of response to these pressures. Here pressures put on a weaker bed cause the material to flow and become folded instead of break up. The flow occurred along shale seams interbedded with the dolomite. Stylolites with small vertical projections were found in five of the seven boreholes.

32. Fractured bedrock was found in a substantial portion of the cores. Sixteen percent of the rock recovered under the lock and approach wall was fractured while 24 percent of the rock in the four cores taken from in back of the dam was fractured. Within these four boreholes, the top 15 ft of rock contained the highest concentration of fractures.

33. The fractured bedrock constitutes possible weak zones in the bedrock especially under the lower approach wall in borings CW-1 and CW-2. The rock from these borings is not only fractured, but it consists of clayey shale, friable sandstone with shale seams, and dolomite with clay pockets. Another possible weak zone in the bedrock is located just downstream of tainter gate Pier 4 in boring D-14. This weak zone is composed of clay (1-ft thick) and was encountered about 9 ft below top of rock; see Plate A1 of Appendix A. Were the clay to be a lens, and the concrete-rock contact as low as observed in boring D-12 (140-ft away), then the clay would occur under Pier 4 within 4 to 12 ft of the concrete-rock contact. This possibility will be explored during the scour detection drilling.

34. The extremely low strength of the intact shale parallel to its bedding prescribes that any shale bed be considered as a potential sliding plane parallel to its bedding. The numerous joints in the bedrock described in Reference 5 are oriented such that they could participate in a shear failure involving a rock wedge in front of the lower approach wall or the dam sections. The recommended shear strength parameters for natural joints in the sandstone and shale, presented in Reference 5 and given in paragraph 105 of this report, should be considered in a structural stability analysis.

PART IV: TEST SPECIMENS AND TEST PROCEDURES

Cores Received

35. Approximately 396 ft of concrete and rock core along with 11 sacks and 9 tubes of backfill material were received from a total of 47 borings. Pertinent information concerning the core received at WES is presented in Table 1. Upon receipt of the core at WES, the boxes containing rock samples were kept in the laboratory until the selection of test specimens was completed; this process took about one week. Selected test specimens were then stored in a moist curing room until time for testing.

Selection of Test Specimens

36. The concrete core varied greatly in its physical condition over the project (see Figures 3 and 4). Some core was so badly deteriorated (broken to gravel-size pieces) that intact samples could not be obtained for testing. Therefore concrete test specimens were selected from the intact near surface portion and the bottom portion of the core. The near surface core sometimes contained cracks but remained intact. This procedure was used for the short core and for core with lengths up to 5.1 ft. For the deeper borings, GW-1 and GW-2 test specimens were selected from the near surface, middle, and bottom portions of the core. Characterization properties, effective (wet) unit weight (m), compressional wave velocity (V_p), and compressive strength (UC), and engineering design properties Young's Modulus (E), and Poisson's ratio (ν)^{*} were determined or calculated. Test assignment locations can be gotten from appropriate tables of test results.

37. Recommendations were made in References 3 and 5 to test shale during any future testing program for compressive strength and E ; adequate samples were not recovered during these investigations. The shale that

* For convenience, symbols and usual abbreviations are listed and defined in the Notation (Appendix F).

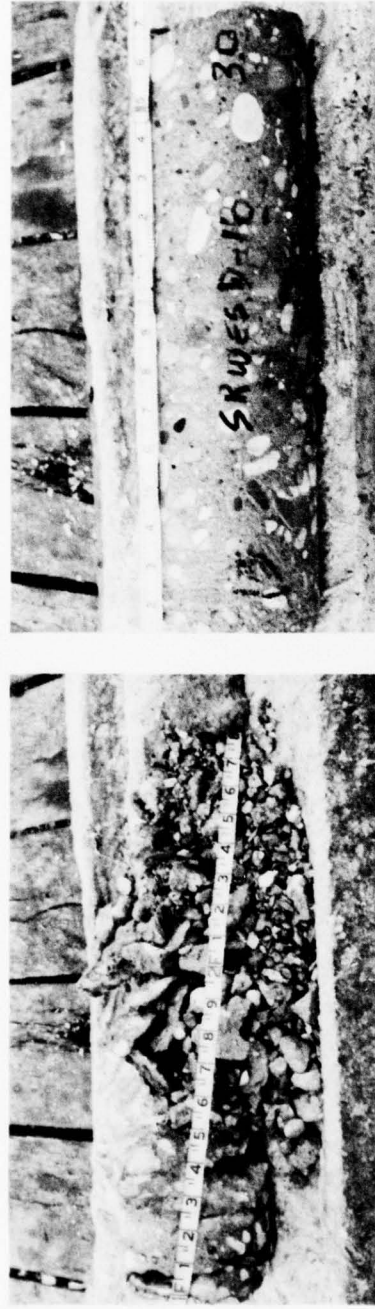


Figure 3. Concrete core from ice chute pier (horizontal boring SR WES D-18-77) showing broken condition of core



Figure 4. Concrete core from tainter gate pier No. 2 (horizontal boring SR WES D-10-77) showing subparallel cracking due to frost action

was previously recovered was either broken by drilling action or too thin for testing. From the geologic sections presented herein, it is evident that adequate shale was not encountered in the bedrock for other than direct shear testing. Three intact shale samples were obtained with one being taken from boring L-1.

38. Whenever possible bedrock specimens were selected for characterization property tests from the full length of core. A few tests were performed on the available assumed weaker rock close to the concrete-bedrock contact, namely friable sandstone, sedimentary breccia, and interbedded dolomite and sandstone. The more competent bedrock (dolomite, competent sandstone) was quite similar to the material tested during the investigation reported in Reference 5; therefore this rock was not tested.

39. For the engineering design tests (moduli, Poisson's ratio, and direct shear) an attempt was made to select test specimens to be representative of the rock in close proximity to the concrete-bedrock contact. This applied to the lower approach wall and tainter gate Piers No. 4 and No. 8. Due to the fractured and friable condition of the first 4 ft of bedrock, assumed to underlay the lower approach wall, test specimens could not be prepared for shear testing. Specimens for direct shear testing had to be taken about 7 to 15 ft below the base of the wall; some difficulty was encountered preparing test specimens from this zone. Lower bound shear strengths that could be used to represent the bedrock within the first 4 ft below the wall will be mentioned in Part V. Test assignment locations can be gotten from the tables of rock test results.

40. There were four types of specimens tested in direct shear; concrete cast to rock, intact, shale-filled partings, and cross-bedded. Most of the specimens selected were friable sandstone and brecciated dolomite; the specimens represent the bedrock adjacent to the base of the lower approach wall. Representative specimens of the thinly bedded shale were tested in direct shear as a filler material in the friable sandstone or brecciated rock and designated as filled partings. Clay seams generally occurred in highly fractured zones and specimens containing them could not be tested in direct shear.

41. Due to the extent and number of joints in the foundation, attempts were made to obtain test specimens that contained these features. In selecting dolomite cores containing joints, it was observed that the surfaces were undulated such that the differential between high and low portions was too great for the direct shear apparatus. Consequently, no natural dolomite joints were tested. Naturally jointed sandstone specimens could not be obtained for direct shear testing.

Test Procedures and Petrographic Examination

42. The characterization properties tests and the engineering design properties tests were conducted in accordance with the appropriate test methods tabulated below:

Property	Test Method
<u>Characterization</u>	
Effective Unit Weight (As Received), γ_m	RTM 109*
Dry Unit Weight, γ_d	RTM 109
Water Content, w	RTM 106
Compressional Wave Velocity, V_p	RTM 110 (ASTM D 2845)** (CRD-C 151)***
Compressive Strength, UC	RTM 111 (ASTM D 2938) (CRD-C 150)***
<u>Engineering Design</u>	
Elastic Modulus, E	RTM 201 (ASTM D 3148)
Direct Shear Strength	RTM 203
Multistage Triaxial Strength	RTM 204

* Proposed Rock Test Method, Corps of Engineers, in review prior to publication.

** See appropriate ASTM 1977 Book of ASTM Standards.

*** WES, Handbook for Concrete and Cement.

43. The concrete-on-rock specimens for direct shear testing were fabricated using a general mass concrete mixture having an approximate compressive strength of 2000 psi at 28 days age. The concrete was wet sieved over a 1-in. sieve-size screen, and the portion passing was cast on top of rock cores contained in the bottom section of 6-in.-diameter

molds. Rock surfaces onto which the concrete was cast were gently undulating. Rock cores used for these tests were taken from within 10 ft of the concrete-rock contact.

44. A detailed visual examination of all the core was made in the laboratory. Pieces of concrete core were selected for petrographic examination from all structures of the lock and dam that were drilled. Some pieces of cores were sawed along the long axis of the core to allow better and easier examination of the concrete; a few were ground smooth and examined for entrained air. Some of the new surface concrete recovered were highly fractured and examination was made of the pieces. A photograph was made of the sawed surfaces of each condition represented by the cores. The concrete cross-sections were examined megascopically and with a stereomicroscope. Selected particles were examined using a polarizing microscope and identified using X-ray diffraction. Portions of the cement paste in a deteriorated area of concrete were compared to the cement paste from an area of concrete that was considered good.

45. A sample of grey clay was ground to pass a 45 micrometre (No. 325) sieve and then examined by X-ray diffraction. A sedimented slide was made in the usual manner and also X-rayed. The X-ray examinations were made with an X-ray diffractometer using nickel-filtered copper radiation.

PART V: TEST RESULTS AND ANALYSIS

Results of Petrographic Examination of Rock

46. A piece of greyish clay recovered from D-14 and el 411.3 to 412.2 was analyzed to determine its mineralogical composition. It was composed of quartz, dolomite, clay-mica, kaolinite, and mix-layer montmorillonite and is a swelling clay. The other rocks were visually identified; they are described in Part III.

Characterization Properties of Rock

47. The results of the characterization properties tests are presented in Table 2. Only four specimens were tested for γ_m , V_p , and UC for the following reasons. The dolomite recovered during this investigation was quite similar to the dolomite reported on in Reference 5; it was well documented in Reference 5 and therefore was not tested again. The friable sandstone did not occur in long enough pieces for compressive testing; smaller pieces were tested in direct shear. Two sandstone specimens, one slightly to moderately friable and one competent, were obtained and tested. One piece each of sedimentary breccia (Ss, Sh, and Dol well cemented) and interbedded dolomite sandstone and reef carbonate were tested.

48. The average γ_m of the sandstone is $148.6 \text{ lb}/\text{ft}^3$; this compares quite well with the previously reported value of $149.9 \text{ lb}/\text{ft}^3$ for competent sandstone given in Reference 5. The average water content of 6.2 percent compares well with a water content of 7.4 reported previously.⁵ The V_p averages 9440 fps and is reasonable for this type of sandstone. The compressive strengths of the two specimens differ by a factor of 2.4. The specimen having the lower UC (3200 psi) contained inclusions of shale and chert and was slightly to moderately friable. The competent specimen had a UC equal to 7560 psi. The previously tested competent sandstone had an average UC equal to 4810 psi.⁵

49. The characterization properties of the sedimentary breccia specimen and the interbedded specimen approach, and for one case surpasses, similar properties of the intact dolomite previously tested.⁵ The compressive strengths of the sedimentary breccia and the interbedded dolomite and sandstone are 4870 psi and 7560 psi, respectively. Both rocks are quite competent in the in situ condition. Bearing capacity values presented in Reference 5 are lower than those presented in this report and are recommended for use in any design considerations or structural stability analyses.

Modulus and Poisson's Ratio of Rock

50. Results of the modulus of elasticity and Poisson's ratio tests are presented in Table 2. The stress-strain relation for four rocks tested is presented in Plates 10 through 13. A tangent E was computed for each of the curves. The E was calculated as an incremental value between 2000 and 3000 psi, which corresponds to the linear portion of the stress-strain curve for all four specimens except the friable sandstone from GW-1; it was obtained between 1000 and 2000 psi. The stress-strain curves have a concave upwards initial portion which represents closure of cracks formed from stress relieving the core and closure of microfractures. The incremental E should represent the in situ rock. Poisson's ratio was calculated at a stress value of 2000 psi.

51. There are too few data to present average values of E and v for the three rocks (friable sandstone with chert inclusions, sedimentary breccia and interbedded dolomite and sandstone). The lowest E was obtained from the sedimentary breccia (2.12×10^6 psi), which is slightly higher than the previously recommended design value for dolomite.⁵ Sedimentary breccia was not previously tested, therefore, an $E = 2.12 \times 10^6$ psi and $v = 0.24$ is recommended when this rock type is considered for design.

52. The E and v for the slight to moderate friable sandstone and competent sandstone is 2.22×10^6 psi, 0.35 and 4.35×10^6 psi, 0.18, respectively. The interbedded E and v are 3.22×10^6 psi and 0.10.

Peak and Ultimate Shear Strength

53. The stress values from the direct shear tests are presented in Table 3 along with water contents and dry densities. The rock shear test envelopes are given in Table 4. The direct shear envelopes are plotted on Plates 14 and 15 for the sandstone and shale, respectively.

54. Two types of direct shear tests were conducted to ascertain peak strength of intact specimens and sliding friction characteristics of discontinuous specimens. Peak strengths were measured for the sandstone containing a concrete-rock interface, intact competent and friable sandstone, intact shales, and cross-bedded dolomites. Sliding friction properties were measured for specimens of sandstone and dolomite along shale-filled partings.

55. All specimens were tested in the single-plane shear device designated the MRD shear device. The tests performed on intact, concrete-on-rock, and cross-bedded specimens produced on moderate amount of scatter. The tests of the precut specimens had a very small amount of scatter. All envelopes were calculated using a linear regression analysis.

56. Three concrete-on-competent sandstone tests were conducted along the interface of the two materials; the rock contained the natural rock bedding planes. The very friable sandstone crumbled and could not be prepared for testing. The peak shear strength parameters of cohesion (c) and angle of internal friction (ϕ) is 0.2 tsf and 73.9 degrees; the ultimate values of c_u and ϕ_u are 1.0 tsf and 59.8 degrees. These peak and ultimate values are approximately equal to similar values of the intact competent sandstone. The shear surface in the concrete-sandstone test specimens occurred totally in the sandstone portion of the specimens.

57. Two series of competent sandstone specimens were tested for intact strength and the series with the lower shear strength had a $c = 0.9$ tsf and a $\phi = 64.6$ degrees; the $c_u = 1.3$ and $\phi_u = 51.7$ degrees. The increase in cohesion between values for peak and ultimate is attributed to interlocking of asperities along the already failed surface.

58. One series of friable (moderately soft by NCC definitions as presented in Reference 3) sandstone specimens yielded shear strength

values of $c = 6.5$ tsf and $\phi = 29.1$ degrees, ultimate values of $c_u = 5.9$ tsf and $\phi_u = 27.1$ degrees were obtained. The angle of internal friction for the friable sandstone is about one-half that of the competent sandstone. A $c_u = 5.9$ tsf and a $\phi_u = 27.1$ degrees is recommended for the friable sandstone and a $c = 0.9$ tsf and $\phi_u = 51.7$ degrees is recommended for competent sandstone when either rock is considered in stability analysis. Shear strength parameters for the bedrock within the first 4 ft under the lower approach wall were not obtained as discussed earlier. Shear strengths, thought to approach lower bound values for this zone, are the strengths presented for friable sandstone and shale-filled partings in shaley sandstone. Except for the material not being fractured, the friable sandstone used in obtaining shear strengths was similar to the friable sandstone found in the 4-ft zone beneath the lower approach wall.

59. The shear strength parameters for intact shale are $c = 3.7$ tsf and $\phi = 11.9$ degrees and the ultimate values are $c_u = 3.1$ tsf and $\phi_u = 11.9$ degrees. These values were obtained from specimens tested parallel to bedding. Previously reported ϕ values for intact shale in Reference 5 compare quite well with the current values. Previous ϕ is 14.5 degrees. The values for intact shale do not compare well with similar values presented in References 2 and 3. These references reported ϕ 's of 49.5 degrees and c 's of 2.3 tsf. It is recommended that the lower shear strength values be used to reanalyze portions of the structural stability analysis that incorporated shale for bedrock.

60. Five sliding friction tests were conducted. Two tests along shale-filled partings in competent sandstone yielded low values of $c = 1.1$ tsf and $\phi = 26.2$ degrees. Two tests along shale-filled partings in dolomite yielded low values of $c = 1.7$ tsf and $\phi = 20.6$ degrees. One test along a shale parting in shaley sandstone (boring L-1, el 410.0 ft) had a $c = 2.9$ tsf and a $\phi = 13.7$ degrees; the $\phi = 13.7$ degrees is nearly the same as the ϕ for intact shale (11.9 degrees). The shear strength parameters for intact shale are recommended to be used when rock containing shale-filled partings is considered in stability analysis.

61. One series of cross-bedded shear tests on dolomite yielded a $c = 22.2$ tsf and a $\phi = 73.1$ degrees; ultimate values are $c_u = 20.0$ tsf

and $\phi_u = 73.1$ degrees. Dolomitic rock occurs beneath the lower approach wall, however, sliding along shale seams is likely to occur before cross bedded shear through the dolomite or any other rock present in the foundation. No rock-on-rock (precut) direct shear tests were conducted during this program. These shear strength parameters can be found tabulated in paragraph 105; they are taken from Reference 5.

Backfill

62. One piezometer was set in boring SR-WES GWB 1-77 which is located in the backfill adjacent to the lower approach wall. Pertinent information concerning the piezometer installation is presented in Plate 4.

63. The peak stress values obtained from the R triaxial and the direct shear tests of overburden are presented in Table 5. The stress circles, stress-strain plots and selected characterization properties for the triaxial tests are presented on Plates 16-19. The shear stress-normal stress plots and other pertinent information from the direct shear tests are presented on Plates 20-23. Recommended soil design parameters were based on this data and are as follows:

γ_{wet}	115.4 pcf
γ_{dry}	96.5 pcf
γ_{sub}	60.3 pcf
$c' =$	0.0
$\phi' =$	28°

A value for coefficient of lateral earth pressure for similar backfill material is presented in Reference 3; it is $k_r = 0.55$ and appears reasonable.

General

64. Because a majority of work effort was to ascertain the extent of deteriorated concrete at the lock and dam, it appears appropriate to present a definition of deteriorated concrete. The authors concur with

the definition of deterioration as stated in the report by ACI Committee 201 (see ACI Journal, November 1968):

"Deterioration is any adverse change of normal mechanical, physical, and chemical properties either on the surface or in the whole body of concrete generally through separation of its components."

65. The following general comments pertain to the condition of the concrete over the entire lock and dam. Individual structures within the lock and dam will be discussed separately. The results of the concrete characterization and engineering design tests are presented in Table 6. These data will be referred to when appropriate. Results of the detailed petrographic report is presented in Appendix B. General description of the concrete from 41 borings are presented in Plates B1-B10 of Appendix B; and a description of the concrete cores examined in detail is presented in Plates B11-B22 of Appendix B. The field drilling logs for all borings except those on the inside faces of the lock walls are presented in Exhibit B to this report. Exhibit B is on file at the Chicago District Office.

66. All of the concrete examined, except for the near surface concrete in a few borings, did not contain any entrained air. The non-air entrained concrete was considered old concrete and the air entrained concrete was considered new. The new concrete normally consisted of coarse aggregates less than one in. in diameter and was cemented with a light grey paste. The old concrete consisted of gravel aggregate with a maximum size about three in. in diameter and was cemented with a brown paste. The aggregate consists of dolomite, chert, siltstone, limestone, shale and other varieties of rock. The concrete sampled appeared to be well consolidated. Minor amounts of honeycombing were detected; however, the void areas should not affect the structural adequacy of the structures.

67. Examination of the core shows that while some of the concrete is in good condition from the old finished surface to the greatest depth drilled, many of the cores show cracks subparallel to the face surface of the concrete and to depths ranging from 2 in. to 3 ft. These subparallel

cracks are the results of freezing and thawing. All structures at the lock and dam contain frost-damaged concrete. Within some of the frost-damaged zones cracks at right angles to the free surface (formed surfaces) of the core were observed. Similar cracking occurred outside frost-damaged zones. Longitudinal cracks normal to the free surface are associated with alkali-silica reaction in hydraulic structures and some bridges. Core SR WES D-22 is a good example of both types of cracking; see photograph B2 in Appendix B. The photograph shows a particle of white chert next to the large longitudinal crack that goes to a depth of 3.0 ft; the chert is apparently the most reactive aggregate in the structure. Similar cracks were found in about one-fourth of cores examined.

Lock Chamber Land Wall

68. Depth of Deterioration. The average depth of concrete deterioration throughout the eroded portion of the wall is 0.2 ft; maximum depth of frost-damaged concrete is 0.3 ft (see Plate 1 for individual depths of frost-damaged concrete at each boring location).

69. The total depth of deterioration as measured from the original face of the lock wall is the sum of the eroded depth and of the present frost-damaged concrete. The deepest damaged concrete is near the top of the wall.

70. Average Physical Properties. The average physical properties of the land wall concrete are tabulated below:

Test	Near Surface Concrete	Bottom of Core Specimens	Percentage * Difference
Effective Unit Wt, pcf	148.2	145.1	+2.1
Comp Wave Velocity, fps	14,272	15,070	-5.3
Compressive Strength, psi	5,310	5,260	+1.0
Modulus of Elasticity, $\times 10^6$ psi	2.41	2.15	+12.0
Poisson's Ratio	0.16	0.18	-11.1

* The percentage difference was calculated using the bottom of core specimen value as the base number.

The concrete is sound just beyond the outer few inches of concrete. The percentage differences indicate minor changes between the near and bottom of core concrete.

Lock Chamber River Wall

71. Depth of Deterioration. The average depth of deteriorated concrete throughout this side of the wall is 0.2 ft; the maximum depth is 0.2 ft (see Plate 1 for depth of deteriorated concrete for each boring). The deepest frost-damaged concrete is near the top of the wall. All of the core except the one taken from monolith 40 exhibited frost damage near the vertical lock wall surface.

72. Average Physical Properties. The average physical properties of the river wall concrete are listed below:

<u>Test</u>	<u>Near Surface Concrete</u>	<u>Bottom of Core Specimens</u>	<u>Percentage Difference</u>
Effective Unit Wt, pcf	146.5	144.2	+1.6
Comp Wave Velocity, fps	13,600	14,953	-9.1
Compressive Strength, psi	5,750	5,260	+9.3
Modulus of Elasticity, $\times 10^6$ psi	2.15	2.83	-24.0
Poisson's Ratio	0.16	0.20	-20.0

Generally, the near surface concrete in the top portion of the lock walls has lower physical properties than the near surface concrete near the low pool elevation. In general the bottom of core specimens exhibit slightly higher physical properties than the near surface concrete. Although the percentage difference indicates that the modulus and Poisson's ratio of the near surface concrete is about 80 percent of the bottom concrete, both are reasonable values. The difference should be taken into account if a stress analysis was being made of the lock chamber walls.

Upper Gate Bays

73. Depth of Deterioration. The average depth of deterioration in the gate bays is 0.23 ft with the maximum depth of 0.5 ft in boring

GW 8 (H). This boring is located in the riverward side of the bay. At about 0.9 ft a fracture surface was noted along with alkali-silica gel. The fracture is normal to the free surface. This extent of damaged concrete in a location subjected to high stress as a gate bay is considered dangerous. Immediate repair of the gate bays is necessary for the preservation of the lock.

74. Average Physical Properties. The average physical properties of the upper gate bays concrete are tabulated below:

<u>Test</u>	<u>Near Surface Concrete</u>	<u>Bottom of Core Specimens</u>	<u>Percentage Difference</u>
Effective Unit Wt, pcf	146.1	147.3	-0.8
Comp Wave Velocity, fps	12,236	14,126	-13.4
Compressive Strength, psi	6,070	5,380	+12.8
Modulus of Elasticity, $\times 10^6$ psi	--	4.00	--
Poisson's Ratio	--	0.16	--

The near surface concrete shows about a 13 percent reduction in the Vp compared to the concrete at a depth of about 1.5 ft. Frost damage has affected the velocity of the near surface concrete.

Lower Gate Bay

75. There was no deterioration due to frost action detected in the one boring (GW-10) in the lower gate bay. A minor amount of scaling was observed on the core end which represented the present wall face of the bay.

76. The near surface and bottom end of the core had similar physical properties:

<u>Test</u>	<u>Near Surface Concrete</u>	<u>Bottom of Core Specimens</u>	<u>Percentage Difference</u>
Effective Unit Wt, pcf	153.0	151.7	+0.9
Comp Wave Velocity, fps	15,625	15,625	0.0
Compressive Strength, psi	6,610	6,560	+0.8
Modulus of Elasticity, $\times 10^6$ psi	4.65	5.93	21.6
Poisson's Ratio	0.19	0.26	26.9

The full length of the core is considered to be sound concrete. The near surface concrete exhibits a similar deformation response to a compressive loading as did the lock chamber land wall concrete; i.e., the modulus and Poisson's ratio of the near surface concrete is about 75 percent of the deeper concrete.

Upper Approach Wall

77. Depth of Deterioration. There was no evidence of frost-damaged concrete in the three cores taken from the upper approach wall. Two cores contained new concrete as an overlay and one core contained all old concrete. Scrapping by barge traffic has resulted in minor amounts of concrete loss at the edges of the armor plates.

78. Average Physical Properties. The average physical properties of the upper approach wall concrete are presented below:

Test	Near Surface Concrete	Bottom of Core Specimens
Effective Unit Wt., pcf	--*	149.5
Comp Wave Velocity, fps	--	15,799.0
Compressive Strength, psi	--	7,970
Modulus of Elasticity, $\times 10^6$ psi	--	5.00
Poisson's Ratio	--	0.19

* The near surface concrete was not tested due to the high concentration of steel bars and pieces of armor plate within that core.

The high velocity and compressive strength represents concrete apparently not affected by freezing and thawing. It is sound concrete. No repair to the concrete is necessary in the upper approach wall.

Lower Approach Wall

79. Depth of Deterioration. There were two vertical borings drilled into the lower approach wall and four horizontal borings. No new concrete was encountered in these borings. The results of frost damage was evident

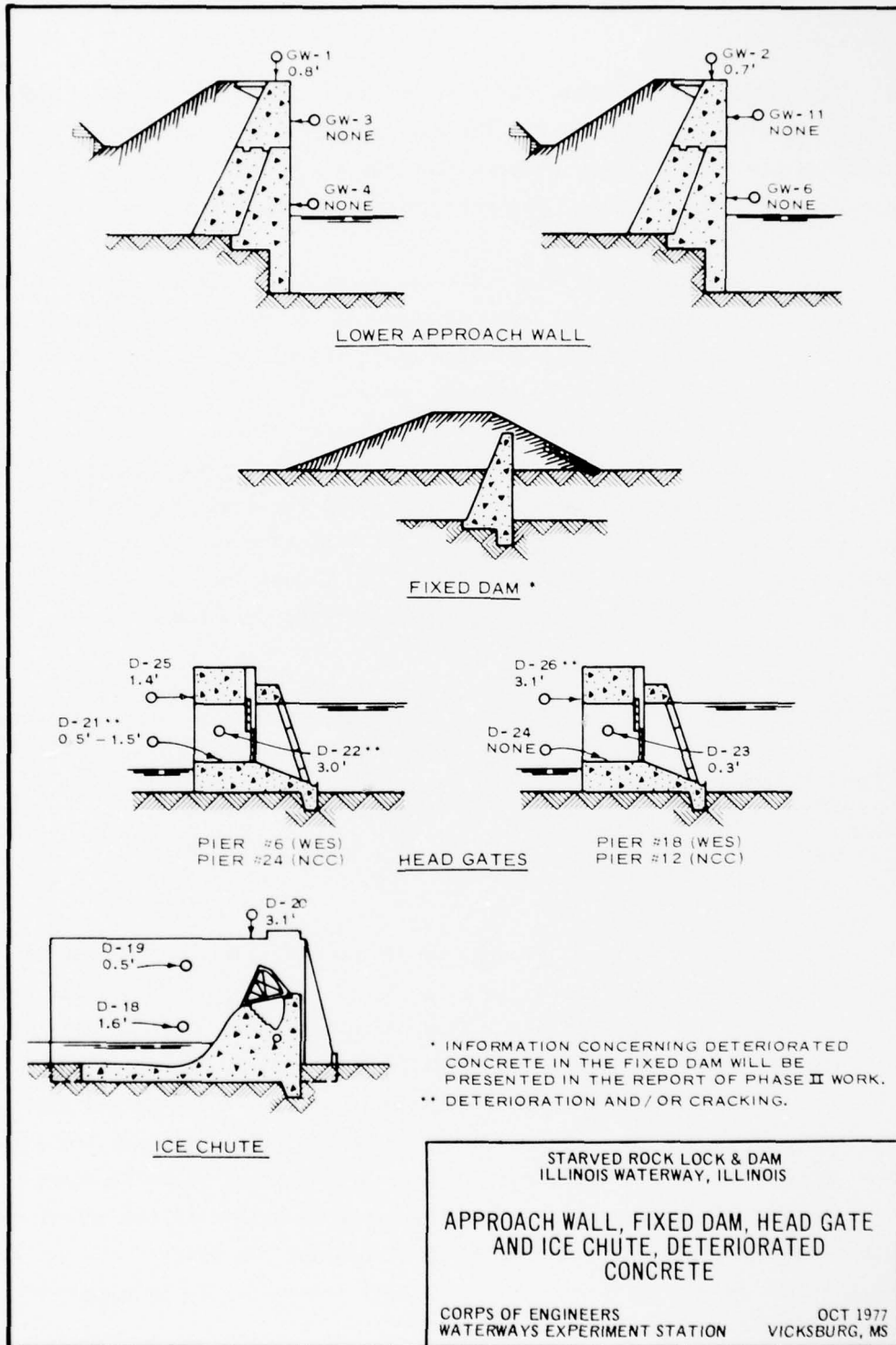


Figure 5. Deteriorated concrete in lower approach wall

in the two vertical borings, however, no frost damage was detected in the horizontally drilled core. The average depth of frost-damaged concrete in the core from the vertical borings was 0.75 ft. The maximum depth was 0.8 ft. Figure 5 presents details of the damaged concrete in the lower approach wall.

80. Longitudinal cracks, starting at the free surface and extending to maximum depths of 1.5 ft, were observed in three of the four cores from the horizontal borings. Alkali-silica gel was present on the crack surface of core GW-3; the longitudinal cracks are thought to be caused in part by alkali-silica reaction.

81. Average Physical Properties. The average physical properties of the concrete from the two vertical holes in the lower approach wall are presented below. Test specimens were obtained from the near surface, middle, and bottom of the approach wall; the values from core at the middle and bottom of hole were averaged because they were nearly equal.

Test	Middle and		
	Near Surface Concrete	Bottom of Core Specimens	Percentage Difference
Effective Unit Wt, pcf	153.6	149.9	+2.5
Comp Wave Velocity, fps	11,000	15,257	-27.9
Compressive Strength, psi	5,470	6,920	-21.0
Modulus of Elasticity, $\times 10^6$ psi	1.57	5.29	-70.0
Poisson's Ratio	0.17	0.20	-15.0

The velocity and modulus of elasticity of the near surface concrete is considerably less than the concrete in the other portions of the boring; 28 and 70 percent, respectively. These lower values are expected in view of the amount of deteriorated concrete in the upper 0.7 ft of boring GW-2. The test specimens that represented the near surface concrete did contain frost-damaged concrete. The strength of the same core does not indicate the damaged concrete. The reason is that often times cracks in cores that are perpendicular to the axis of applied load have little effect on compressive strength. From a material standpoint the concrete in the top of the wall is not performing as originally intended. It is suggested

that consideration be given to replacing the top 9 in. of concrete in the lower approach wall during the upcoming major rehabilitation program.

82. Average Physical Properties. The average physical properties of the concrete from the four horizontal holes in the lower approach wall are presented below:

Test	Near Surface Concrete	Bottom of Core Specimens	Percentage Difference
Effective Unit Wt., pcf	151.1	151.9	-0.5
Comp Wave Velocity, fps	16,094	16,103	-0.1
Compressive Strength, psi	7,420	8,190	-9.4
Modulus of Elasticity, $\times 10^6$ psi	5.21	6.19	-15.8
Poisson's Ratio	0.24	0.24	0.0

Very small difference exists between the near and bottom of core concrete (distance of about 3 ft). No repair to the vertical face of the wall is necessary.

Head Gates

83. Depth of Deterioration. The depth of deteriorated concrete and cracking associated with alkali-silica reaction observed in the core from the head gate piers are presented in Figure 5; also see Plate B4 in Appendix B.

84. Frost action and alkali-silica reaction have combined to cause extensive damage to the concrete in Piers 6 and 18 (Piers 24 and 12, respectively, using the CDO numbering system). Most of the damaged concrete is located in the downstream top portion of Piers 6 and 18. The maximum depth of frost damage (1.2 ft) was found in Boring D-26 (Pier 18), however, cracks were observed to continue to the end of the core (depth 3.1 ft). Core D-22 has longitudinal cracks to its full depth of 3.1 ft. The average depth of damaged concrete (including frost-damaged and cracked concrete) in the piers is 2.0 ft. The core from the sill section of the headgate bays showed no evidences of frost damage. Longitudinal cracking is present in one of the two cores from the sills; D-21 from a depth interval of 0.5 to 1.5 ft.

85. Average Physical Properties. The average concrete physical properties of the headgate piers and sills are presented below:

Test	Near Surface Concrete	Bottom of Core Specimens	Percentage Difference
Effective Unit Wt, pcf	154.4	153.8	+0.4
Comp Wave Velocity, fps	12,875	15,083	-14.6
Compressive Strength, psi	5,280	5,050	+4.6
Modulus of Elasticity, $\times 10^6$ psi	3.02	3.93	-23.0
Poisson's Ratio	0.11	0.20	-45.0

An extremely low value of velocity was recorded for the near surface core (first 1 ft of core) in Boring D-23, it was 8318 fps or about one-half the value of the sounder concrete. The modulus for this particular specimen is also low compared to sound concrete; 0.71×10^6 psi as compared to 4.00×10^6 psi. It is recommended that for the headgate piers 9 to 12 in. of concrete be removed from the downstream face and replaced with new concrete. Local areas may require deeper removal. The sides of those piers that are heavily spalled and cracked should have the exterior concrete removed and replaced with at least 6 in. of concrete.

Ice Chute Pier

86. Depth of Deterioration. The most severe freezing and thawing has taken place in the ice chute pier; this is the pier that the boiler house rests upon. The average depth of frost-damaged concrete is 1.7 ft with a maximum depth of 3.1 ft in the core from Boring D-20; see Figure 5. Boring D-20 is a vertical boring about 6 ft from the upstream edge of the ice chute pier. The upstream section of the ice chute pier near the water line is heavily eroded and the exterior right side of the ice chute pier is heavily spalled and cracked.

87. Average Physical Properties. The average physical properties of the ice chute pier are presented below:

Test	Near Surface Concrete	Bottom of Core Specimens	Percentage Difference
Effective Unit Wt., pcf	149.5	146.7	+1.9
Comp Wave Velocity, fps	7,766	15,300	-49.2
Compressive Strength, psi	3,030	6,500	-53.4
Modulus of Elasticity, $\times 10^6$ psi	1.43	4.33	-66.9
Poisson's Ratio	0.10	0.17	-41.2

The average velocity and compressive strength for the near surface concrete (first 1 ft of core) is the lowest recorded over the project. The lowest velocity and strength was recorded for core D-20 which is from the vertical boring. The velocity and strength is 2840 fps and 2400 psi, respectively. The percentage difference indicates that the near surface concrete is of poor quality compared to the deeper concrete.

88. Nine to twelve in. of concrete from the top of the pier should be removed and replaced. Both sides of the pier are heavily spalled and cracked. At least 9 in. of concrete from both sides of the pier should be removed and replaced with new concrete.

Tainter Gate Piers

89. Depth of Deterioration. Based in part on visual observations and on boring information, Piers 1, 2, 3, 6, 7, 9, 10, and 11 (1, 2, 3, 5, 6, 9, 10, and 11 CDO numbering system) have been severely damaged by frost action. Piers 4, 5, and 8 are considered to be moderately damaged. Refer to Figure 6 for depths of frost damage and boring locations. The average depth of frost damage for the severely damaged piers is 1.4 ft; maximum depth of frost damage combined with cracking extends to 3.1 ft near the nose of Piers 6 and 9. The cracking is in part due to alkali-silica reaction. The greatest amount of frost-damaged concrete in the tainter gate piers occurs in the upstream one-half portion to about 1 ft below upper pool elevation. Severe erosion has occurred at the upstream water line around the nose of the piers. The least amount of damaged concrete is located near the downstream edge of the piers.

90. No damaged concrete due to frost action was detected in the three borings drilled into Pier 4. However, there were signs of erosion on the sides of the piers.

91. It is recommended that, for the severely frost-damaged piers, 9 to 12 in. of concrete be removed and replaced with new concrete. The top horizontal surfaces of the moderately damaged piers should be repaired to a depth of 9 to 12 in. The new concrete should be tied to the old using grouted anchor bolts. To further insure a good bond, an epoxy adhesive between the old and new concrete is recommended in areas where it is practical to use. The average depth of deteriorated concrete over the severely damaged piers is 1.4 ft. Presently for each 1 sq ft of exposed surface there is 1.4 cu ft of concrete readily susceptible to freezing and thawing. A 9-in.-thick cap of new concrete would reduce the volume of deteriorated concrete by 54 percent. If the porous concrete under the 9-in. cap contained water, it would probably freeze and could crack from beneath. The least amount of porous concrete left, the greater the possibility that a cap would not crack from beneath. Injection of an epoxy resin or chemical grout into the remaining porous concrete should fill voids and increase the concrete strength. Names and addresses of companies dealing with epoxy injection can be obtained from the following agency. The address appears in Reference 12.

"Division of General Research, Bureau of Reclamation, Engineering and Research Center, Denver Federal Center, Denver, Colorado 80225."

One or more of these companies may have had experience with injecting epoxies or chemical grout into porous concrete. It is assumed that the techniques used would be different than techniques used for injecting these materials into single or multiple cracks. The effectiveness of such a procedure should be studied.

92. Average Physical Properties. The average physical properties of the severely and moderately deteriorated concrete from the tainter gate piers are presented below:

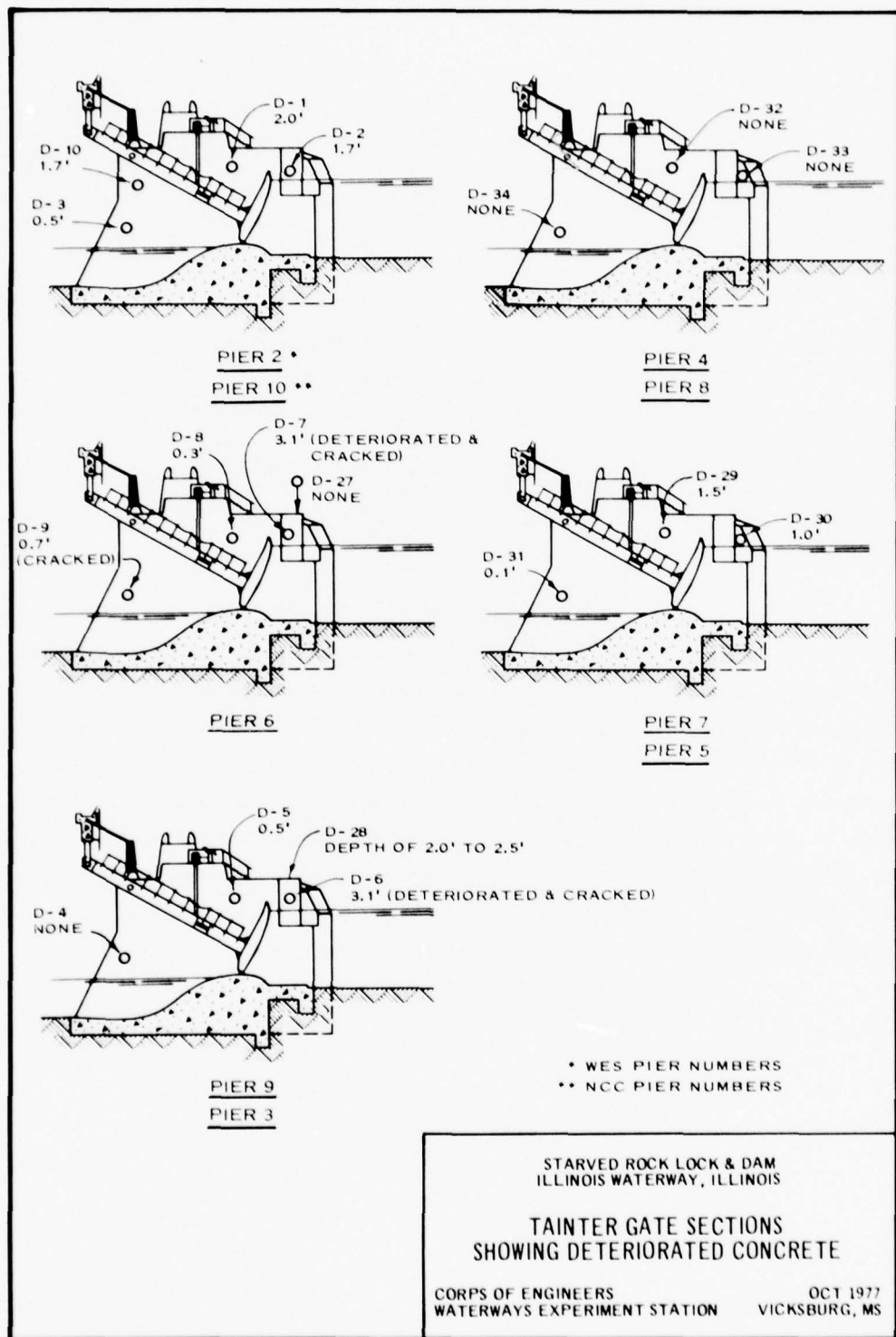


Figure 6. Location of deteriorated concrete, tainter gate sections

Severely Deteriorated Piers

Test	Near Surface Concrete	Bottom of Core Specimens	Percentage Difference
Effective Unit Wt, pcf	150.7	151.1	-0.3
Comp Wave Velocity, fps	13,949	15,484	-9.9
Compressive Strength, psi	5,770	5,510	+4.7
Modulus of Elasticity, $\times 10^6$ psi	4.04	4.32	-6.5
Poisson's Ratio	0.16	0.18	-11.1

Moderately Deteriorated Piers

Test	Near Surface Concrete	Bottom of Core Specimens	Percentage Difference
Effective Unit Wt, pcf	147.8	149.6	-1.2
Comp Wave Velocity, fps	15,813	16,585	-4.7
Compressive Strength, psi	5,440	5,340	+1.8
Modulus of Elasticity, $\times 10^6$ psi	3.70	5.00	-26.0
Poisson's Ratio	0.15	0.23	-34.7

93. The percentage difference indicates minor changes in the near and bottom of core specimens. Tests on the near surface concrete included only a few pieces of damaged concrete. Had a larger number of damaged specimens been tested, the difference in properties between the near and bottom of core concrete would be greater. The cores that were tested represent sound concrete. A major difference in the modulus and Poisson's ratio is seen for the moderately deteriorated piers, however, the values for these two parameters represent sound concrete. A number of near surface cores could not be prepared for testing because of their broken condition; some were saved for petrographic examination.

PART VI: GEOLOGICAL CHARACTERISTICS AND
SUMMARY OF CONCRETE CONDITION AND RECOMMENDATIONS

Bedrock Stratigraphy

94. Two stratum were encountered under the lock and dam site, the Ordovician St. Peter Sandstone and the Shakopee Dolomite. The Tonti and Kress sandstones of the St. Peter Formation were uncovered at Starved Rock. The Tonti member is a medium- to fine-grained, well-sorted, non-calcareous, friable sandstone. The Kress is a coarse rubble or conglomerate of angular chert in a sometimes layered matrix of sand, green shale, or clay. The Kress contains layers of shale up to 1-ft-thick. The Shakopee Dolomite is a thin- to medium-bedded, fine-grained, argillaceous to pure, light brown to light grey dolomite. It contains lenses and layers of sandstone up to 4-ft-thick, blue green to grey shale seams up to 0.3-ft-thick, and shale-filled bedding planes throughout. Lenticular masses of dolomite that are algal reefs up to 1 ft in thickness are found in the Shakopee.

95. A major unconformity separates the St. Peter and the Shakopee in the Starved Rock area. An interval of erosion and non-deposition created the irregular erosional surface that separates these two bodies of bedrock. This irregular surface may explain some of the differences in elevation of the contact between the St. Peter and the Shakopee.

Backfill

96. Bedrock overburden behind the lower approach wall is probably spoil from the lock and dam excavations and consists of a mixture of clay, sand, and gravel. Proportions of fill range from 80 percent loose sand (clayey sand) on top to an equal percent of compact clay (sandy clay) near the bottom. The overburden rests on the Kress sandstone or at the contact of the Shakopee Dolomite and Kress as inferred from borings in the adjacent lower approach wall.

Geologic Cross Section

97. Two cross sections were drawn; one along the dam and one along the lock chamber land wall and the lower approach wall. A tight contact (between the concrete and bedrock) was noted in two of the three borings drilled in the lock and approach walls. The borings in back of the dam were drilled directly into rock. These sections give an overview of the bedrock under the lock and just in back of the dam and show the variations in the two major rock units. The location of weak materials such as shale, clay, and friable sandstone can be readily detected which should be beneficial in assigning strength parameters for stability analysis. The unconformable contact between the St. Peter and Shakopee exists under the project. The 4-ft-thick sandstone layer in the dolomite is also continuous under the lock and dam.

98. There are a few discontinuous clay seams and clay lens in the St. Peter and near the top of the Shakopee. The thickest unit of clay (a 1-ft lens or seam) was encountered just 4 ft downstream of tainter gate pier No. 6. The lens is assumed to be within 4 to 12 ft of the concrete-bedrock contact. The clay was analyzed by X-ray diffraction and contains, among other minerals, the mineral montmorillonite which is a swelling type clay. The extent of the clay is unknown.

Bedrock Structural Characteristics

99. Dips in local bedding range from <1 to 12 degrees when measured between boreholes (three-point problem) at the St. Peter/Shakopee contact. The 4-ft sandstone bed in the Shakopee dips uniformly <1 degree over the project; this is consistent with regional dips cited in the literature.

100. The first 3 and 4-1/2 ft of bedrock beneath the lower approach walls in borings GW-1 and GW-2, respectively, is fractured. The fractured rock in these two borings consists of shale, clayey shale, friable sandstone with shale-filled partings, and cherty dolomite. This fractured zone constitutes a weakness in the bedrock and should be considered in a structural stability analysis. Similar amounts of fracturing in the same

type of rock exist under the downstream portion of the landside lock wall (see Plate 2, Reference 3). The bedrock under the upper portion of the landside lock wall and under the riverside lock wall consists of dolomite with shale-filled partings and thin sandstone layers. About 5 ft beneath the base elevation of the lock is the nominal 5-ft-thick sandstone layer that is continuous over the lock and dam site. The lowest value of internal friction ($\phi = 13.7$ deg) obtained on a shale-filled parting was measured on a test specimen recovered from this sandstone layer.

101. Four ft downstream from tainter gate pier No. 4 is a 1-ft-thick lens or seam of clay containing fragments of dolomite. The top of the lens is located at el 412.3 which is 13.7 ft below the design base elevation of the tainter gate piers. It is 4.2 ft below the base of tainter gate pier No. 6 which is approximately 140 ft to the north; the contact of the base of pier 6 and bedrock was determined from boring D-12 drilled during the Phase II work. The lens was not found in any other boring put down during this investigation or the previous investigation.³ It is recommended that the extent of this material be determined by drilling during the scour detection program scheduled for FY 78. If it is present under a portion of the dam, then sliding stability analysis for this area of the dam should be checked using appropriate material properties of the clay; the clay would be sampled and tested.

102. The Sandwich Fault Zone is the nearest major regional structure to Starved Rock Lock and Dam; the fault zone is 26 miles to the northeast. Small local faults were observed on the core from two borings, the largest having an apparent displacement of 1.2 ft. These small faults will not affect the stability of the lock or dam.

103. The joints that were observed in the core during this investigation are considered to be within the same joint sets reported in Reference 5. No joint orientations were measured during this study, however, the previous joint orientations measured at the proposed duplicate lock site (adjacent to present lock, see Reference 5) could be extrapolated to the dam site. Individual joints and conjugate joints could possibly participate in failure of sections of the approach and lock walls and

the dam in one of the following ways. Individual joints could provide an inclined surface on which a horizontal shear failure could daylight. And if the orientation of joint sets form possible rock wedges, then sliding along the joint surfaces could occur. One potential sliding mass is a wedge bound on the top by concrete, exposed face due to scouring, and two intersecting cross-bed joints. The formation of potential wedges is illustrated in Figure 5 of Reference 5. In order to determine possible wedge sizes, joint frequency or joint spacing within joint sets must be determined. If the scour areas at the lock and dam are ever dewatered, detailed geologic structure mapping should be performed. Information from such a mapping effort could give realistic rock wedge sizes for use in a structural stability analysis. If the five joint attitudes listed on p 36 of Reference 5 are examined alone with the attitude of the bedding and hypothesized to have a significant probability of existing beneath the dam or lock wall, then they may be combined in various ways to produce representatives of possible slide wedges. These hypothetical slide wedges may then be analyzed as to their mode of sliding and their respective factors of safety. The six discontinuities can be combined into nine wedges that are visually apparent to have a possibility of moving into a scour or excavation parallel to the river. Of these nine possible wedges analysis indicates three have factors of safety against sliding by their dead weight of less than 1.0. The angle of sliding friction used was 13.7° , the lowest determined by testing. The calculations method is detailed in Reference 11. The following information pertains to the six discontinuities that can be combined into wedges.

<u>Plane</u>	<u>Strike</u>	<u>Dip</u>	<u>Sliding Mode</u>	<u>Volume for 10-ft Vertical Face</u>	ϕ Required for Stability
1	0°	16° E	Slide on plane 1	532 yd^3	16°
2	144°	17° SW alone			
4	52°	20° NW	Slide on plane 4	307 yd^3	20°
1	0°	16° E	alone		
4	52°	20° NW	Slide on plane 4	1850 yd^3	20°
Bedding	45°	10° SE	alone		

Paper exercises are presented in Appendix D and are intended as examples to show the possibility of critical discontinuity combinations and the nature of their evaluation. Realistic factors of safety or compliance can only be achieved using real geologic and laboratory data.

104. The extremely low strength of the intact shale parallel to its bedding dictates that, for conservative design, any shale bed be treated as a potential sliding plane parallel to its bedding. Sufficiently lower values of shear strength were obtained for intact shale than previously reported.³ It is recommended that the lower shear strength values be used to re-analyze those portions of the structural stability analysis that incorporated shale for bedrock.

Recommended Design Values for Rock

105. Design should consider rock type and the various bedrock structural characteristics described herein. Guidance is presented in the following tabulation as to proper choice of design parameters. The tabulation is taken from Reference 5 and updated with values obtained during this investigation where appropriate.

	Dolomite	Friable Sandstone	Competent Sandstone	Shale
Characterization Properties				
Effective Unit Weight, lb/ft ³	157.0	127.7	138.3	110.4
Wet Unit Weight, lb/ft	162.0	140.2	147.7	129.9
Bearing Capacity, tsf	350	39	320	--
Tensile Strength, psi	110	75	175	
Shear Strength				
Intact	c=90 tsf ϕ=56°	c=5.9 tsf ϕ=27.1°	c=0.9 tsf* ϕ=51.7°	c=3.7 tsf* ϕ=11.9°
Natural Joint	--	--	c=1.45 tsf ϕ=30.5°	c=0 ϕ=38°
Shale-Filled Parting	c=1.7 tsf* ϕ=20.6°	c=2.9 tsf* ϕ=13.7°	c=1.8 tsf* ϕ=26.2°	--
Precut, Rock-on-Rock	c=0.0 ϕ=31°	c=0.0 ϕ=33.5°	c=0.0 ϕ=31°	c=0.5 tsf ϕ=19°
Concrete on Rock	c=1.6 tsf ϕ=63°	--	c=0.2 tsf ϕ=73.9°	--

	Dolomite	Friable Sandstone	Competent Sandstone	Shale
Cross-Bed	c=22.2 tsf ϕ=73.1	--	--	--
Modulus of Elasticity x 10 ⁶ psi	1.82	--	2.00	--
Poisson's Ratio	0.13	--	0.12*	--
Shear Modulus x 10 ⁶ psi	0.65	--	--	--

* Newer lower value obtained during this investigation. See p 39, Reference 5, for values that have been updated.

Lock Concrete Condition

106. New concrete in repaired sections is in good condition. It is air entrained and has resisted the harsh winter environment on the river. The new concrete is structurally sound by itself but in certain locations could be knocked loose by barge impact because of the frost damaged concrete beneath. The old concrete in the lock structures is non-air entrained concrete that was well consolidated during placement. It is structurally sound in areas which have not been effected by frost action.

107. The exposed and near surface old concrete in the chamber walls and upper and lower gate bays is lightly to moderately deteriorated. Freezing and thawing is the major cause of the damaged concrete; alkali-silica reation is a minor cause. All of the exposed vertical surfaces have been effected by frost action to varying degrees. The results of frost damage is evidenced by erosion and scabbing of the concrete. The average depth of frost damaged concrete is as follows: lock chamber walls, 0.2 ft; upper gate bays, 0.23 ft; and lower gate bays, none in core, however, exposed aggregate on the wall indicates damaged has occurred.

108. There was no evidence of frost damage in the core from the upper approach wall. No repair to the concrete is required in this wall.

109. No frost damaged concrete was recovered from the horizontally drilled borings in the vertical face of the lower approach wall. The vertical face need not be repaired. The average depth of frost damaged concrete from the vertical borings in the wall (top of wall) is 0.75 ft. The concrete on top of the wall is not performing as originally intended. It is suggested that consideration be given to replacing the top 9 in. of concrete with new concrete during the upcoming major rehabilitation program.

110. It is suggested that 6 in. of concrete on the exposed vertical surfaces of the lock walls and gate bays be removed and replaced with new concrete. The thickness of concrete required to bring the existing wall out to its original position is not addressed in this report. Local areas may require deeper removal.

Dam Concrete Condition

111. New concrete, as an overlay over damaged concrete, was encountered in one of the borings in the dam masonry. It is sound by itself but subject to being broken off if impacted hard. The old concrete in the dam structures is non-air entrained concrete and structurally sound in areas which have not been affected by frost action and alkali-silica reaction.

112. Alkali-silica reaction is present in the concrete and is generally found behind the frost damaged concrete. The greatest amount of damage due to this reaction has occurred in the dam masonry. The effects of the alkali-silica reaction is confined to the outer 4 ft of concrete. Since the serious alkali-silica reaction seems to be expressed most often in association with cracks normal to free surfaces, it seems reasonable to assume that the alkali-silica reaction was encouraged when the exterior concrete began to crack up because of freezing and thawing, progressively letting water penetrate into the concrete. If the outer fragile concrete is repaired as recommended with air-entrained concrete, the structures should be stable in terms of the anticipated behavior of the concrete. The exception being if water in the old porous concrete behind the new concrete freezes, cracking of the new concrete could occur from beneath.

113. The exposed and near surface old concrete in the head gate piers, the ice chute pier, and the tainter gate piers is moderately to severely deteriorated. Erosion and scabbing of the concrete is in evidence on most of the dam masonry. Erosion is more prominent near mean upper and lower pool elevations, while scabbing occurs on most of the concrete surfaces.

114. The average depth of concrete deterioration in the head gate piers is 2.0 ft; sills of the gate bays are damaged only at the downstream edge which are rounded. The ice chute pier is deteriorated to an average depth of 1.7 ft. Tainter gate Piers 4, 5, and 8 are moderately deteriorated in localized areas to depths of about 4 in. The remaining tainter gate piers are severely deteriorated to an average depth of 1.4 ft. The greatest amount of damaged concrete is found in the upstream half of the piers; a maximum depth of 3.1 ft was observed near the nose in Piers 6 and 9.

115. It is recommended that 9 to 12 in. of concrete be removed and replaced with new concrete on the following dam sections and areas of sections; localized areas may require deeper removal:

- a. Downstream face of the head gate piers and edge of the sills.
- b. Ice chute pier.
- c. Tainter gate Piers 1, 2, 3, 6, 7, 9, 10, and 11.
- d. Horizontal surfaces of tainter gate Piers 4, 5, and 8.

116. Six-in. concrete removal and replacement with new concrete is recommended in the following areas:

- a. Sides of the head gate piers.
- b. Local areas on vertical surfaces of tainter gate Piers 4, 5, and 8. These areas are evident by leaching and scabbing.

117. The new concrete should be tied to the old concrete using anchor bolts. To improve the bond between old and new concrete, an epoxy adhesive is recommended in areas where it is feasible to be used; see Appendix E for brief discussion of capping the tainter gate piers with new concrete.

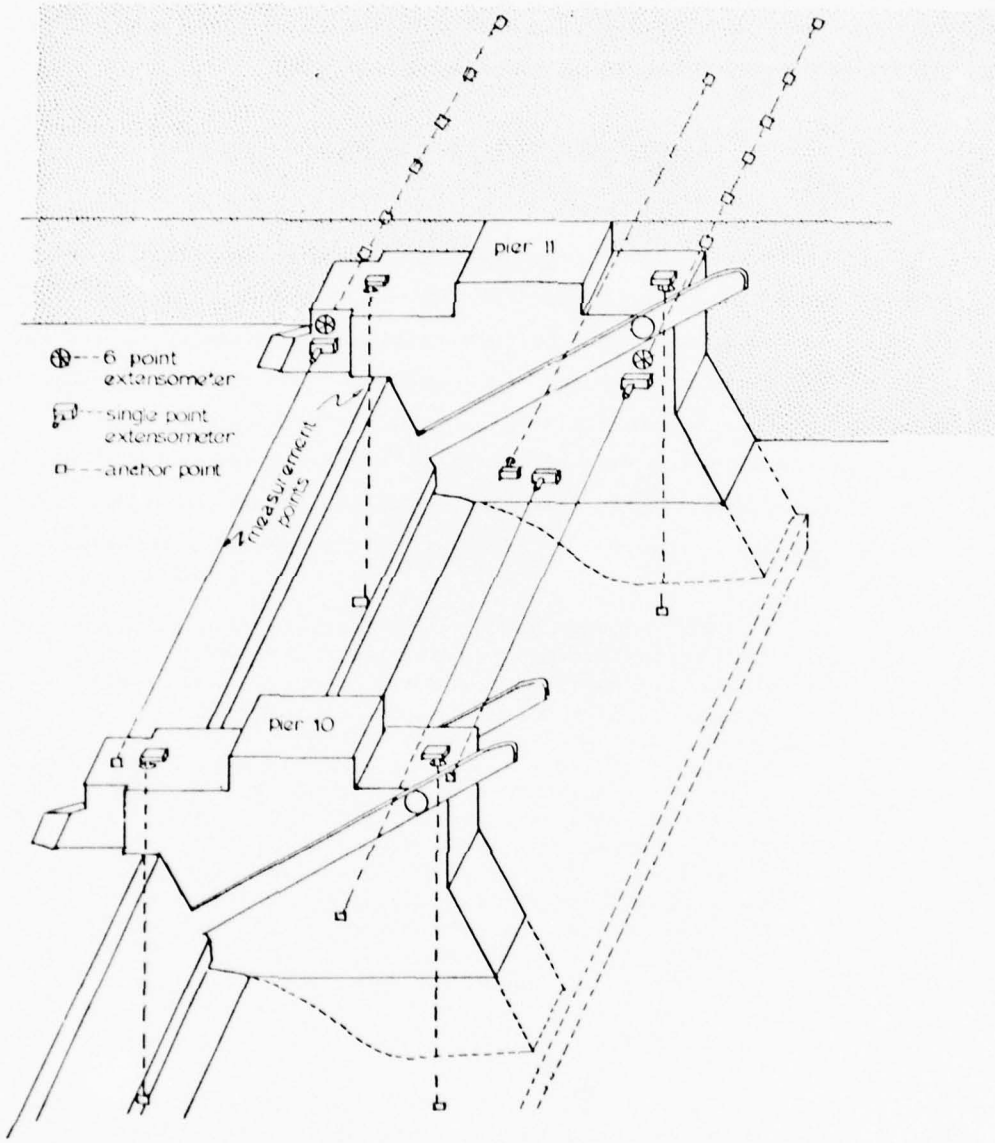
118. The concrete deterioration at Starved Rock Lock and Dam is in an advanced stage and the rate of deterioration will accelerate if the

concrete is left exposed to the freezing-and-thawing environment. This investigation concurs with the findings of the Chicago District; i.e., the concrete must undergo a major rehabilitation if the lock and dam is to continue in service for an extended length of time.

Recommended Instrumentation of
Left Dam Abutment

119. District and Lock personnel have encountered problems in operating tainter gate No. 10 near the left dam abutment. As part of the District's continuing ongoing investigation at Starved Rock Lock and Dam, WES is instrumenting the left dam abutment. The purpose for instrumenting is to ascertain the origin of movement which systematically (possibly seasonally) stresses or binds the left-most tainter gate causing opening to be extremely difficult. The proposed plan is presented below; the proposal has been sent to the District under separate cover in April 1978.

- a. In order to determine the appropriate remedial actions for the above-mentioned problem, the movements of piers 10 and 11 should be described as a function of time. To detect the pier movements, 10 extensometers are recommended. Two multiple-point borehole extensometers (MPBX) should be placed through the abutment pier and extended into the abutment to a depth beyond any possible movement. One MPBX should be located upstream of the tainter gate as far as practical and the other downstream of the gate (Figure 7). The third extensometer to be placed in the abutment should be a single-point extensometer placed through the lower center of the abutment pier. Three single-point extensometers should be used for spanning the tainter gate which has opening difficulties. The remaining four extensometers should be single-point, placed vertically through the piers and anchored to competent foundation rock.
- b. Precise location of the MPBX should be determined from visual inspection of the abutment adjacent to the pier. The depth of the deepest anchor should be determined from visual inspection of the top of the abutment for surface expressions of stress relief joints, conjugate joint sets, etc., and from the core obtained from the MPBX borings. Intermediate anchor points for the MPBX will be located from the borehole cores in an effort to



avoid multiple anchorage within the same rock block, anchorage within joints, etc. Location of the single-point extensometers between piers 10 and 11 should be adjacent to the abutment extensometers. The remaining extensometers are to be located toward each end of the two piers and the depth of anchor point should be determined from core logs of the respective borings.

- c. Data acquisition for the above system is a reasonably simple procedure, and with only limited training lock and dam personnel could read the instruments easily. Since the MPBX is, to a limited extent, temperature sensitive, temperature should be recorded anytime the system is read. Additionally, to complement the extensometer readings and possibly provide some insight to the pier movements, it is recommended that both upstream and downstream river stages be recorded at the time extensometer readings are acquired.
- d. The frequency at which readings are acquired should be set by the District Office; however, it is recommended that the reading schedule be flexible with provisions for increasing the frequency if the amount or rate of measured movement indicates the necessity. Field plots, maintained by lock and dam personnel, would insure the earliest possible detection of any adverse movement.
- e. Formal data reduction can be accomplished at the WES on an on-going basis with minimal effort. An evaluation of the data acquired from the recommended instrumentation system should indicate the mechanisms involved in the movement of the pier(s) and consequently remedial recommendations can be made to alleviate the tainter gate operation problems.
- f. Cost for installing the instrumentation system, including drilling and drill support costs, is \$66,700. The cost breakdown is given below:

	2 MPBX's	8 Single-Point Extensometers	Engineering and Support
Extensometer head	\$2300	\$5200	
Anchors, hardware, etc.	1250	1300	
Cables, connectors, etc.	500	2000	
Readout unit			\$ 1,175
Site investigation			1,900
Design and assembly			3,000
Installation			7,200
Drilling and drill support			40,870

Approximately two months "lead" time will be required by the WES for acquiring and fabricating the special "Invar" tape extensometers for use in spanning the tainter gate.

REFERENCES

1. Letter, NCD 1st Incl, dated 28 June 1972, subject: Field Conference on Concrete Exploration and Testing, Existing Locks and Dams, Illinois Waterway; Letter, NCDED-T (21 November 1973) 1st Incl, subject: Periodic Inspection and Continuing Evaluation of Completed Civil Works Structures - Periodic Inspection Report No. 2, Starved Rock Lock and Dam, Illinois Waterway, Illinois.
2. "Periodic Inspection, Report No. 2, Starved Rock Lock and Dam, Illinois Waterway," Illinois, Department of the Army, Corps of Engineers, Chicago District, October 1973.
3. "Appendix A, Soils and Geology For Structural Stability Analysis, Starved Rock Lock and Dam, Illinois Waterway," Department of the Army, Corps of Engineers, Chicago District, November 1972, Revised June 1973.
4. WESCC Letter Report to Chicago District, CE, dated 8 September 1976, Report of Concrete Core Tests, Lock Walls at Starved Rock Lock and Dam, Illinois Waterway, Chicago District.
5. Stowe, R. L., and Warriner, J. B., "Rock Core Tests, Proposed Duplicate Lock - Phase II, Starved Rock Lock and Dam, Illinois River, Illinois," MP C-75-9, US Army Engineer Waterways Experiment Station, CE, Vicksburg, MS, June 1975.
6. Templeton, J. S., and Willman, H. B., "Champlainian Series (Middle Ordovician) in Illinois," Bull 89, Ill. State Geol Survey, 1963.
7. Willman, H. B. et al, "Handbook of Illinois Stratigraphy," Bull 95, Ill. State Geol Survey, 1975.
8. Buschbach, T. C., "Cambrian and Ordovician Strata of Northeastern Illinois," Dept of Investigations #218, Ill. State Geol Survey, 1964.
9. Willman, H. B., "Summary of the Geology of the Chicago Area," Circular 460, Ill. State Geol Survey, 1971.
10. Krumbein, W. C. and Sloss, L. L., Stratigraphy and Sedimentation, 2nd ed, Freeman, San Francisco, 1963, p 132.
11. Hendron, A. J., Carding, E. J., and Aiyer, A. K., Analytical and Graphical Methods for the Analysis of Slopes in Rock Masses, Nuclear Cratering Group, Technical Report No. 36, 1971.
12. Concrete Manual, A Water Resources Technical Publication, 8th Edition, US Department of the Interior, 1975.

Table 1
WES Core from Starved Rock Lock and Dam, Illinois Waterway, Chicago District (Resurfacing Phase)

WES Reference	Drill Hole #	Date Rec'd	Core Diam. (In.)	Bag/Box No.	Depth (Ft.)	Elevation (ft.)		Top of Hole	Remarks
						Top Intervals	Depth Intervals		
CHI-13 CL-1	SR WES GWB-1-77	7-19-77	--	1 of 10	0 - 3.0	458.5 - 455.5	458.5	Clay	Vertical
		7-19-77	--	2 of 10	3.0-6.5	455.5 - 452.0	458.5	Clay	
		7-19-77	--	3 of 10	6.5-8.5	452.0 - 450.0	458.5	Clay	
		7-19-77	--	4 of 10	8.5-11.5	450.0 - 447.4	458.5	Clay	
		7-19-77	--	5 of 10	11.1-13.0	447.4 - 445.5	458.5	Clay	
		7-19-77	--	6 of 10	13.0-14.7	445.5 - 443.8	458.5	Clay	
		7-19-77	--	7 of 10	14.7-19.2	443.8 - 439.3	458.5	Clay	
		7-19-77	--	8 of 10	19.2-23.0	439.3 - 435.5	458.5	Clay	
		7-19-77	--	9 of 10	24.4-25.2	434.1 - 433.3	458.5	Clay	
		7-19-77	--	10 of 10	25.2-26.0	433.3 - 432.5	458.5	Clay	
CHI-13 CL-2	SR WES GWB-2-77	7-19-77	6	1 of 2	7.9-14.0	450.6 - 444.5	458.5	Clay (Tube 1, 2, and 3 in Box 1)	
CHI-13 CL-3	SR WES GWB-3-77	8-15-77	6	2 of 2	14.6-16.0	443.9 - 442.5	458.5	Clay (Tube 4 in Box 2)	
		8-15-77	6	1 of 3	5.5-10.5	453.0 - 448.0	458.5	Clay (0.5 ft sack sample, gravelly sand)	
		8-15-77	6	2 of 3	12.5-16.5	446.0 - 442.0	458.5	Clay	
		8-15-77	6	3 of 3	10.5-12.5	448.0 - 446.0	458.5	Clay	
		8-15-77	6	3 of 3	16.5-19.0	442.0 - 439.5	458.5	Clay	
CHI-13 CON-5	SR WES GW-3-77	7-19-77	6	1 of 1	0 - 3.1	452.9 - 451.9	452.9	Concrete	Horizontal
CHI-13 CON-6	SR WES GW-1-77	6-14-77	6	1 of 17	0 - 3.3	459.0 - 455.6	459.0	Concrete	Vertical
		6-14-77	6	2 of 17	3.30-7.8	455.6 - 451.2	459.0	Concrete	
		6-14-77	6	3 of 17	7.8-12.6	451.2 - 446.4	459.0	Concrete	
		6-14-77	6	4 of 17	12.6-17.4	446.4 - 444.6	459.0	Concrete	
		6-14-77	6	5 of 17	14.4-19.4	444.6 - 439.6	459.0	Concrete	
		6-14-77	6	6 of 17	19.4-23.3	439.6 - 434.5	459.0	Concrete	
		6-14-77	6	7 of 17	24.5-29.1	434.5 - 429.9	459.0	Concrete	
CHI-13 DG-5				8 of 17	29.1-32.3	429.9 - 426.7	459.0	Concrete	
				9 of 17	32.3-36.8	426.7 - 422.2	459.0	Dolomite	Sandstone
				10 of 17	36.8-41.4	422.2 - 417.6	459.0	Dolomite	Sandstone
				11 of 17	41.4-44.7	417.6 - 414.3	459.0	Dolomite	Sandstone
				12 of 17	44.7-48.6	414.3 - 410.4	459.0	Dolomite	Sandstone

(Continued)

(Sheet 1 of 4)

Table 1 (Continued)

WES Reference	Drill Hole #	Date Rec'd	Core Diam (In.)	Bag/Box No.	Elevation (Ft.)			Top of Hole Remarks
					Depth (ft.)	Depth Intervals	Top of Hole	
CHI-13 DC-5	SR WES GS-1-77	6-14-77	6	13 of 14	48.6-54.3	410.4 - 404.7	429.0	Dolomite, Sandstone
	SR WES GS-4-77	6-14-77	6	14 of 14	54.3-57.0	404.7 - 402.0	429.0	Dolomite, Sandstone
CHI-13 GS-7	SR WES GS-4-77	7-19-77	6	1 of 1	0 - 3.3	445.3 - 445.3	445.3	Concrete Horizontal
CHI-13 GS-8	SR WES GS-11-77	7-19-77	6	1 of 1	0 - 3.0	454.2 - 454.2	454.2	Concrete Horizontal
CHI-13 GS-9	SR WES GS-2-77	7-19-77	6	1 of 1	0 - 3.1	459.0 - 455.9	455.9	Concrete Vertical
	SR WES GS-2-77	7-19-77	6	2 of 17	3.1-7.5	455.9 - 451.5	451.5	Concrete
	SR WES GS-2-77	7-19-77	6	3 of 17	7.5-9.9	451.5 - 449.1	449.1	Concrete
	SR WES GS-2-77	7-19-77	6	7 of 17	9.-13.2	449.1 - 445.8	445.8	Concrete
	SR WES GS-2-77	7-19-77	6	3 of 17	13.2-14.3	445.8 - 444.7	444.7	Concrete
	SR WES GS-2-77	7-19-77	6	5 of 17	14.3-16.8	444.7 - 440.2	440.2	Concrete
	SR WES GS-2-77	7-19-77	6	6 of 17	18.8-23.0	440.2 - 435.5	435.5	Concrete
CHI-13 DC-6	SR WES GS-2-77	7-19-77	6	7 of 17	23.5-27.5	435.5 - 431.5	431.5	Concrete, Dolomite, Sandstone
	SR WES GS-2-77	7-19-77	6	8 of 17	27.5-31.8	431.5 - 427.2	427.2	Dolomite, Sandstone
	SR WES GS-2-77	7-19-77	6	9 of 17	31.8-36.1	427.2 - 422.9	422.9	Dolomite, Sandstone
	SR WES GS-2-77	7-19-77	6	10 of 17	36.1-40.1	422.9 - 418.9	418.9	Dolomite, Sandstone
	SR WES GS-2-77	7-19-77	6	11 of 17	40.1-43.9	418.9 - 415.1	415.1	Dolomite, Sandstone
	SR WES GS-2-77	7-19-77	6	12 of 17	43.9-47.5	415.1 - 411.5	411.5	Dolomite, Sandstone
	SR WES GS-2-77	7-19-77	6	13 of 17	47.-50.8	411.5 - 408.2	408.2	Dolomite, Sandstone
CHI-13 GS-10	SR WES GS-6-77	8-15-77	6	14 of 17	50.8-54.8	408.2 - 404.2	404.2	Dolomite, Sandstone
CHI-13 GS-11	SR WES GS-10-77	8-15-77	6	1 of 1	0 - 3.5	444.3 - 444.3	444.3	Concrete Horizontal
CHI-13 GS-12	SR WES GS-7-77	7-19-77	6	1 of 1	0 - 3.0	455.7 - 455.7	455.7	Concrete Horizontal
CHI-13 GS-13	SR WES GS-8-77	7-19-77	6	1 of 1	0 - 3.2	461.3 - 461.3	461.3	Concrete Horizontal
CHI-13 GS-14	SR WES GS-9-77	7-19-77	6	1 of 1	0 - 3.0	460.7 - 460.7	460.7	Concrete Horizontal
CHI-13 GS-15	SR WES GS-5-77	7-19-77	6	1 of 1	0 - 3.2	460.5 - 460.5	460.5	Concrete Horizontal
CHI-13 GS-16	SR WES GS-12-77	8-15-77	6	1 of 1	0 - 3.0	460.8 - 460.8	460.8	Concrete Horizontal
CHI-13 GS-17	SR WES GS-13-77	7-19-77	6	1 of 1	0 - 3.1	461.0 - 461.0	461.0	Concrete Horizontal
CHI-13 GS-18	SR WES D-23-77	7-19-77	6	1 of 1	0 - 2.9	448.9 - 448.9	448.9	Concrete Horizontal
CHI-13 GS-19	SR WES D-24-77	7-19-77	6	1 of 1	0 - 3.0	442.8 - 439.8	442.8	Concrete Vertical
CHI-13 GS-20	SR WES D-26-77	7-19-77	6	1 of 1	0 - 3.0	457.7 - 457.7	457.7	Concrete Horizontal
CHI-13 GS-21	SR WES D-22-77	7-19-77	6	1 of 1	0 - 3.1	448.8 - 448.8	448.8	Concrete Horizontal
CHI-13 GS-22	SR WES D-21-77	7-19-77	6	1 of 1	0 - 3.1	442.8 - 439.7	439.7	Concrete Vertical

(Continued)

(Sheet 2 of 4)

Table 1 (Continued)

WES Reference	Drill Hole #	Date Rec'd	Core Diam. (In.)	Bag/Box No.	Elevation (Ft.)			Remarks
					Top of Hole	Depth Intervals	Top of Hole	
CHI-13 CON-23	SR WES D-25-77	7-19-77	6	1 of 1	0 -3.3	456.7 - 457.7	456.7	Concrete
CHI-13 CON-24	SR WES D-19-77	7-19-77	6	1 of 1	0 -3.5	454.2 - 454.2	454.2	Concrete
CHI-13 CON-25	SR WES D-28-77	8-15-77	6	1 of 1	0 -3.6	448.3 - 448.3	448.3	Concrete
CHI-13 CON-26	SR WES D-20-77	7-19-77	6	1 of 1	0 -3.6	469.0 - 465.4	469.4	Concrete
CHI-13 CON-27	SR WES D-17-77	7-19-77	6	1 of 1	0 -3.3	445.5 - 445.5	445.5	Concrete
CHI-13 CON-28	SR WES D-2-77	7-19-77	6	1 of 1	0 -3.4	461.0 - 461.0	461.0	Concrete
CHI-13 CON-29	SR WES D-6-77	7-19-77	6	1 of 1	0 -3.1	461.4 - 461.4	461.4	Concrete
CHI-13 CON-30	SR WES D-28-77	8-15-77	6	1 of 3	0 -3.5	468.0 - 468.0	468.0	Concrete
CHI-13 DC-7	14 SR WES D-17-77	8-15-77	6	2 of 3	3.5 -8.0	464.5 - 460.0	468.0	Concrete
CHI-13	8-15-77	8-15-77	6	3 of 3	8.0 -13.0	460.0 - 455.0	468.0	Concrete
CHI-13	8-15-77	8-15-77	6	1 of 5	0 -4.2	428.2 - 424.0	428.2	Dolomite, Sandstone Vertical
CHI-13	8-15-77	8-15-77	6	2 of 5	4.2 -6.2	424.0 - 420.0	420.0	Dolomite, Sandstone
CHI-13	8-15-77	8-15-77	6	3 of 5	8.2 -13.4	420.0 - 414.8	428.2	Dolomite, Sandstone
CHI-13	8-15-77	8-15-77	6	4 of 5	13.4 -16.4	414.8 - 411.8	428.2	Dolomite, Sandstone
CHI-13	8-15-77	8-15-77	6	5 of 5	16.4 -19.8	411.8 - 409.4	428.2	Dolomite, Sandstone
CHI-13	8-15-77	8-15-77	6	1 of 6	0 -4.2	428.6 - 424.4	428.6	Dolomite, Sandstone
CHI-13	8-15-77	8-15-77	6	2 of 6	4.2 -6.7	424.4 - 421.9	421.9	Dolomite, Sandstone
CHI-13	8-15-77	8-15-77	6	3 of 6	6.7 -10.5	421.9 - 419.1	428.6	Dolomite, Sandstone
CHI-13	8-15-77	8-15-77	6	4 of 6	10.5 -14.6	418.1 - 414.0	428.6	Dolomite, Sandstone
CHI-13	8-15-77	8-15-77	6	5 of 6	14.6 -17.9	414.0 - 410.7	428.6	Dolomite, Sandstone
CHI-13	8-15-77	8-15-77	6	6 of 6	17.9 -19.9	410.7 - 408.7	428.6	Dolomite, Sandstone
CHI-13 CON-31	SR WES D-31-77	8-15-77	6	1 of 1	0 -3.1	442.2 - 444.2	444.2	Concrete
CHI-13 CON-32	SR WES D-19-77	8-15-77	6	1 of 1	0 -3.3	461.6 - 461.6	461.6	Concrete
CHI-13 CON-33	SR WES D-20-77	8-15-77	6	1 of 1	0 -3.0	462.3 - 462.3	462.3	Concrete
CHI-13 CON-34	SR WES D-9-77	7-19-77	6	1 of 1	0 -3.2	455.3 - 455.3	455.3	Concrete
CHI-13 CON-35	SR WES D-8-77	7-19-77	6	1 of 1	0 -3.5	461.3 - 461.3	461.3	Concrete
CHI-13 CON-36	SR WES D-1-77	7-19-77	6	1 of 1	0 -2.9	460.8 - 460.8	460.8	Concrete
CHI-13 CON-37	SR WES D-27-77	8-15-77	6	1 of 3	0 -3.5	468.0 - 464.5	468.0	Concrete
CHI-13 CON-37	SR WES D-27-77	8-15-77	6	2 of 3	3.5 -6.9	464.5 - 461.1	468.0	Concrete
CHI-13 CON-37	SR WES D-27-77	8-15-77	6	3 of 3	6.9 -10.2	461.1 - 457.8	468.0	Concrete
CHI-13 CON-37	8-15-77	8-15-77	6	1 of 6	10.2 -11.1	457.8 - 456.9	468.0	Concrete

(Continued)

(Sheet 2 of 4)

Table 1. (Concluded)

WES Reference	Drill Hole #	Date Rec'd	Core Diam. (In.)	Bag/Box No.	Depth (Ft.)	Elevation (Ft.)		
						Top of Hole	Depth Intervals	Top of Vertical
CHI-13 DC-9	SR WES D-15-77	8-15-77	6	1 of 6	0 -3.9	428.0	424.1	428.0
		8-15-77	6	2 of 6	3.9-8.4	424.1	419.6	428.0
		8-15-77	6	3 of 6	8.4-11.2	419.6	415.8	428.0
		8-15-77	6	4 of 6	11.2-14.7	416.8	413.7	428.0
		8-15-77	6		14.7-18.6	413.7	409.4	428.0
		8-15-77	6	5 of 6	18.6-20.7	409.4	407.3	428.0
		8-15-77	6	1 of 5	0 -2.2	418.2	415.0	418.2
		8-15-77	6	2 of 5	3.2-4.0	415.0	408.2	418.2
		8-15-77	6	3 of 5	8.0-12.7	408.2	405.5	418.2
		8-15-77	6	4 of 5	12.7-16.5	405.5	401.7	418.2
		8-15-77	6	5 of 5	16.5-20.1	401.7	398.1	418.2
		8-15-77	6	1 of 1	0 -3.0	444.7	444.7	444.7
		8-15-77	6	1 of 1	0 -2.9	460.9	460.9	460.9
		8-15-77	6	1 of 1	0 -2.4	462.9	462.9	462.9
		8-15-77	6	1 of 2	0 -1.5	452.5	452.5	452.5
		7-19-77	6	2 of 2	1.5-5.1	452.5	452.5	452.5
		7-19-77	6	1 of 1	0 -3.3	446.3	446.3	446.3
		7-19-77	6	1 of 1	0 -3.3	465.7	465.7	465.7
		7-19-77	6	1 of 1	0 -2.9	461.0	461.0	461.0
CHI-13 CON-38	SR WES D-34-77							
CHI-13 CON-39	SR WES D-32-77							
CHI-13 CON-40	SR WES D-33-77							
CHI-13 CON-41	SR WES D-10-77							
CHI-13 CON-42	SR WES D-3-77							
CHI-13 CON-43	SR WES D-1-77							
CHI-13 CON-44	SR WES D-2-77							

(Sheet 4 of 4)

Table 2
Bedrock Test Results, Starved Rock Lock and Dam

Drill Hole No. SR WES-77	Elev Ft	Effective γ_m , lb/ft ³	Unit Wt γ_d , lb/ft ³	Characterization Tests				Remarks
				Dry Content w, %	Water Velocity V_p , fps	Comp. UC, psi	Comp.	
GW-1	413.5	148.0	139.4	6.2	9,114	3200	Slight to mod. fri SS w/Sh and Ch inclusions	
GW-2	420.0	162.3	157.0	3.4	11,875	4870	Sed breccia, SS, Sh and Dol, well cemented	
GW-2	407.7	154.2	150.4	2.5	12,053	8300	Inter bed Dol, Ss and Reef Carb	
D-16	426.3	148.6	139.9	6.2	9,758	7560	Competent Ss	

Engineering Design Tests

Drill Hole No. or WES-77	Elev ft	Elastic Modulus $E \times 10^6$, psi	Poisson's Ratio
GW-1	413.5	2,22	0.35
GW-2	420.0	2.17	0.24
GW-2	407.7	3.22	0.10
D-16	426.3	4.35	0.18

Table 3
Laboratory Test Results - Starved Rock Lock and Dam
Single Plane Direct Shear Tests

Lithology	Borings No	Elevation MSL	Type Test	Normal Stress tsf		Peak Shear Stress tsf	Ultimate Shear Stress tsf	Water Content %	Dry Density pcf
				2	4				
Sandstone, C (H)*	L-1	413.3	conc on rock	2	8.4	3.2	1.9	128.4	
	D-14	417.1		4	12.0	9.6	5.5	134.9	
	D-17	428.2		8	28.5	14.1	1.7	152.2	
Sandstone, C (Mod H)	GW-2	414.0	intact	2	10.7	4.4	2.3	126.8	
		413.4		4	19.3	12.9	3.5	126.1	
		412.5		8	33.4	16.9	0.7	127.8	
Sandstone, C (Mod H)	GW-1	410.5	intact	2	4.2	4.1	5.8	117.6	
	L-1	412.4		4	6.3	6.1	4.5	141.1	
	D-15	423.7		8	16.4	11.6	7.3	144.2	
Sandstone, Fri (Mod Sf)	GW-1	414.8	intact	2	6.9	5.8	2.2	134.2	
		412.7		4	9.8	9.5	2.3	137.3	
		411.0		8	10.6	9.4	6.4	125.8	
Shale	L-1	409.4	intact	2	4.2	3.6	12.3	131.3	
	D-16	424.8		4	4.0	3.7	10.9	139.8	
	D-17	421.8		8	5.1	4.8	9.0	133.8	
Shale Ptg* in Sandstone, C (H)	GW-2	422.1	Filled Ptg	2	2.3	-	3.5	165.6	
				4	3.8	-			
				8	6.2	-			
Shale Ptg in Sandstone, C (Mod H)	D-14	416.6	Filled Ptg	2	3.5	-	6.7	140.7	
				4	2.7	-			
				8	6.1	-			
Shale Ptg in Shly Sandstone	L-1	410.0	Filled Ptg	2	4.3	-	10.2	124.8	
				4	2.5	-			
				8	5.3	-			

(Continued)

Table 3 (Concluded)

<u>Lithology</u>	Borings No	Elevation MSL	Type Test	Normal Shear Stress tsf		Ultimate Shear Stress tsf	Water Content pcf	Dry Density pcf
				tsf	tsf			
Shale Ptg in Dolomite	GK-2	416.3	Filled Ptg	2	2.7	-	6.7	153.6
Shale Ptg in Dolomite	L-1	416.8	Filled Ptg	4	2.7	-	-	-
Dolomite	GK-2	424.9	Cross Bed	8	4.8	-	-	-
		423.4		2	21.4	-	4.3	135.8
		423.1		4	28.4	-	-	-
				8	27.1	-	-	-
				2	23.9	23.3	-	-
				4	42.4	39.1	-	-
				8	46.1	45.6	-	-

* C = Competent; Fri = Friable; Mod = Moderately; H = Hard; SF = Soft; Ptg = Parting. Hard, moderate and soft, given in parentheses, are presented for correlating to previous District work as presented in Reference 3.

Table 4
Laboratory Test Results - Starved Rock Lock and Dam
Rock Shear Test Envelopes

Lithology	Boring No	Elevation MSL	Type Test	Peak		Ultimate	
				Cohesion tsf	Angle of Friction deg	Cohesion tsf	Angle of Friction deg
Sandstone, C (H)	L-1	413.3	Concrete on Rock	0.2	73.9	1.0	59.8
	D-14	417.1					
	D-17	428.2					
Sandstone, C (Mod H)	GW-2	414.0	Intact	3.7	75.1	2.4	62.6
		413.4					
		412.5					
Sandstone, C (Mod H)	GW-1	410.5	Intact	0.9	64.6	1.3	51.7
	L-1	412.4					
	D-15	423.7					
Sandstone, Fri (Mod Sf)	GW-1	414.8	Intact	6.5	29.1	5.9	27.1
		412.7					
		411.0					
Shale	L-1	409.4	Intact	3.7	11.9	3.1	11.9
	D-16	424.8					
	D-17	421.8					
Shale Ptg in Sandstone, C(H)	GW-2	422.1	Filled Ptg	1.1	32.7	-	-
Shale Ptg in Sandstone, C(Mod H)	D-14	416.6	Filled Ptg	1.8	26.2	-	-
Shale Ptg in Shly Sandstone	L-1	410.0	Filled Ptg	2.9	13.7	-	-
Shale Ptg in Dolomite	GW-2	416.3	Filled Ptg	1.7	20.6	-	-

(Continued)

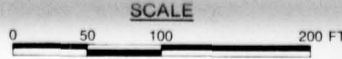


Table 4 (Concluded)

<u>Lithology</u>	<u>Boring No</u>	<u>Elevation MSL</u>	<u>Type Test</u>	<u>Peak</u>		<u>Ultimate</u>	
				<u>Cohesion tsf</u>	<u>Angle of Friction deg</u>	<u>Cohesion tsf</u>	<u>Angle of Friction deg</u>
Shale Ptg in Dolomite	L-1	416.8	Filled Ptg	22.1	37.5	-	-
Dolomite	GW-2	424.9	Cross Bed	22.2	73.1	20.0	73.1
		423.4					
		423.1					

Table 5
Engineering Design Test Results, Backfill, Starved Rock Lock
Triaxial, R Test

Drill Hole No SR WES-	Elevation ft	Triaxial			
		Total Stress ϕ'	c, tsf	Effective Stress ϕ'	c, tsf
GWB 2-77	450.6-449.3	10°	1.9	28°	0.8
GWB 2-77	443.9-442.5	15°	0.4	34°	0

Direct Shear

Drill Hole No SR WES-	Elevation ft	ϕ'	c, tsf
GWB 2-77	450.6-449.3	33°	0.0
GWB 2-77	448.3-447.4	28°	0.3
GWB 2-77	447.4-446.3	33°	0.0
GWB 2-77	443.9-442.5	33°	0.0

Table 6
Concrete Test Results, Starved Rock Lock and Dam

Drill Hole No. SR-WES- 77	Elev Ft	Depth of Core, Ft	χ_m , lb/ft	Characterization Tests					Engineering Design Tests		
				Effective Unit Wt	Dry χ_d , lb/ft	Unit Wt χ_d , lb/ft	Water Content W, %	Comp Velocity Vp, fps	Wave Strength UC, psi	Elastic Modulus E x 10 ⁶	Poisson's Ratio
GW1	445.2	151.1	142.4	6.1	16,129			8300	5.71	0.21	
GW1	431.1	151.1	143.0	5.7	14,705			5070	4.26	0.18	
GW2	458.5	153.6	147.1	4.4	11,000			5470	1.57	0.17	
GW2	445.3	149.8	138.6	8.1	15,156			6730			
GW2	434.0	145.6	134.8	8.0	13,888			5790	4.21	0.19	
GW3	452.9	154.8	147.4	5.0	16,290			8980	6.67	0.23	
GW4	445.3	150.5	142.4	5.7	15,625			6110	4.71	0.24	
GW6	444.3	0.5	149.8	141.9	5.6			16,530	7290		
GW6	444.3	2.9	149.2	139.0	7.3			16,293	6620		
GW7	461.3	0.8	146.1	134.9	8.3			12,236	6070	2.22	0.10
GW7	461.3	1.7	146.1	133.9	9.1			14,375	6360		
GW8	460.7	1.1	146.1	134.5	8.6			13,513	4700		
GW9	460.5	1.6	149.8	140.5	6.6			14,492	5080	4.00	0.16
GW10	455.7	0.6	153.0	142.2	7.6			15,625	6610	4.65	0.19
GW10	455.7	2.4	151.7	141.8	7.0			15,625	6560	5.93	0.26
GW11	454.2	0.5	154.2	147.4	4.6			16,129	8850	5.71	0.25
GW11	454.2	2.1	151.7	145.9	4.0			15,625	8960	5.71	0.24
GW12	460.8	2.5	149.8	140.5	6.6			16,597	7340		
GW13	461.0	1.3	149.2	142.5	4.7			15,000	8600	5.00	
D1	465.7	2.8	151.1	141.2	7.0			14,428	5200		
D2	461.0	2.2	153.0	143.7	6.5			15,161	7130	3.81	
D2	446.3	0.7	146.7	135.5	8.3			11,363	5270	3.81	
D3	446.3	2.8	149.2	140.0	6.6			14,705	3480	3.87	0.18
D4	445.5	0.7	156.1	146.2	6.8			14,705	6510	4.71	0.21
D4	445.5	2.4	152.3	144.5	5.4			15,625	6140	5.71	0.22
D5	461.0	1.0	149.2	138.7	7.6			13,157	4260	2.76	
D5	461.0	2.3	146.7	138.5	5.9			14,428	4190	3.81	0.14
D8	461.3	0.7	153.6	144.0	6.7			15,151	7440	4.00	0.10

(Continued)

(Sheet 1 of 3)

Table 6 (Continued)

Drill Hole No. SR-WES-#77	Elev Ft	Characterization Tests						Engineering Design Tests			
		Depth of Core, Ft	Effective Unit Wt Ft	Dry Unit Wt Ft	Unit Wt γ_m , lb/ft	Water Content W, %	Comp Vp, fps	Wave Vp, fps	Comp Strength UC, psi	Elastic Modulus $E \times 10^6$	Poisson's Ratio
D8	461.3	2.4	153.0	142.6	7.3	15,625	7130	5,41	0.14		
D9	445.3	1.6	154.8	144.3	7.3	15,873	6170				
D9	445.3	2.6	155.5	147.3	5.6	15,468	6590	5.71	0.21		
D10	452.5	2.2	149.2	140.0	6.6	13,698	4390	3.20	0.14		
D18	447.5	1.9	144.8	132.5	9.3	15,450	4530	3.66	0.12		
D19	454.2	0.9	149.8	139.2	7.6	12,692	3660	1.43	0.10		
D19	454.2	3.0	148.6	141.4	5.1	15,151	8470	5.00	0.21		
D20	468.4		149.2	137.1	8.8	2,840	2400				
D21	442.3		153.6	144.4	6.4	14,925	5170				
D23	448.9	0.5	154.8	145.6	5.6	8,318	4630	0.71	0.04		
D23	448.9	1.5	154.8	147.0	5.3	15,263	6400	4.30	0.24		
D24	442.3		154.8	145.5	6.4	15,384	6040	5.33	0.17		
D24	440.3		154.8	145.4	6.5	16,290	4470	5.33	0.21		
D25	456.7	1.4	151.7	142.2	6.7	13,698	4280	2.16	0.15		
D27	467.5		149.2	138.1	8.0	13,570	5210				
D27	458.4		146.7	135.3	8.4	16,130	5750	4.41	0.21		
D28	467.5		149.8	141.7	5.7	16,710	6890	4.94	0.21		
D28	456.2		148.6	134.6	10.4	15,625	5790				
D29	461.6	1.9	151.1	141.5	6.8	16,530	6530				
D30	462.3	1.0	151.7	140.5	8.0	15,730	5360	3.37	0.13		
D30	462.3	2.4	153.0	142.6	7.4	16,920	4730	3.87	0.16		
D31	444.2	0.5	150.5	139.1	8.2	15,715	4790				
D31	444.2	2.5	151.1	140.0	8.1	16,460	4040				
D32	460.9	0.5	145.5	133.7	8.8	14,985	4390	3.08	0.14		
D32	460.9	2.3	148.0	136.3	8.6	16,195	5230				
D33	462.9	0.5	149.2	139.2	7.2	16,530	6490	4.32	0.16		
D33	462.9	2.8	148.6	138.9	7.0	16,500	5820	5.00	0.23		
D34	444.7	0.5	148.6	138.1	7.6	15,925	5430				
D34	444.7	2.4	152.3	139.0	9.6	17,060	4960				

(Sheet 2 of 3)
(Continued)

Table 6 (Concluded)

Drill Hole No. SR-WES- 77	Elev Ft	Core, Ft	Characterization Tests						Engineering Design Tests		
			Depth of Effective Unit Wt γ_m , lb/ft	Dry	Water	Comp	Wave	Comp	Elastic Modulus $E \times 10^6$	Poisson's Ratio	
				χ_d , lb/ft	Unit Wt W, %	Content Vp, fps	Strength UC, psi	Modulus $E \times 10^6$	Poisson's Ratio		
L1	462.8		148.6	138.0	7.7	14,925	6220	4.44	0.31		
L1	444.5		152.3	142.2	7.1	15,512	7110	5.16	0.15		
L1	427.2		147.3	136.5	7.9	14,828	4620	4.00	0.20		

(Sheet 3 of 3)

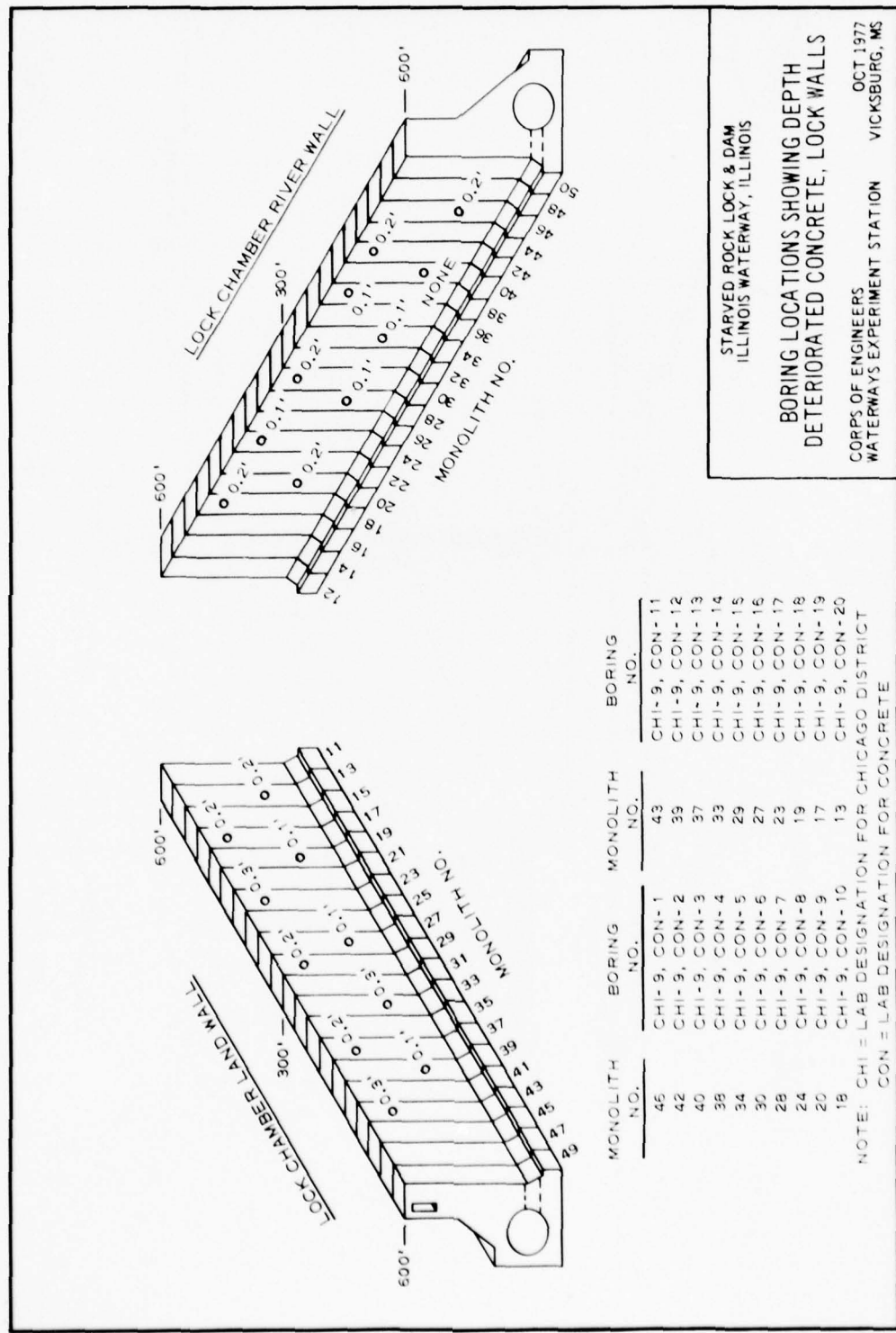
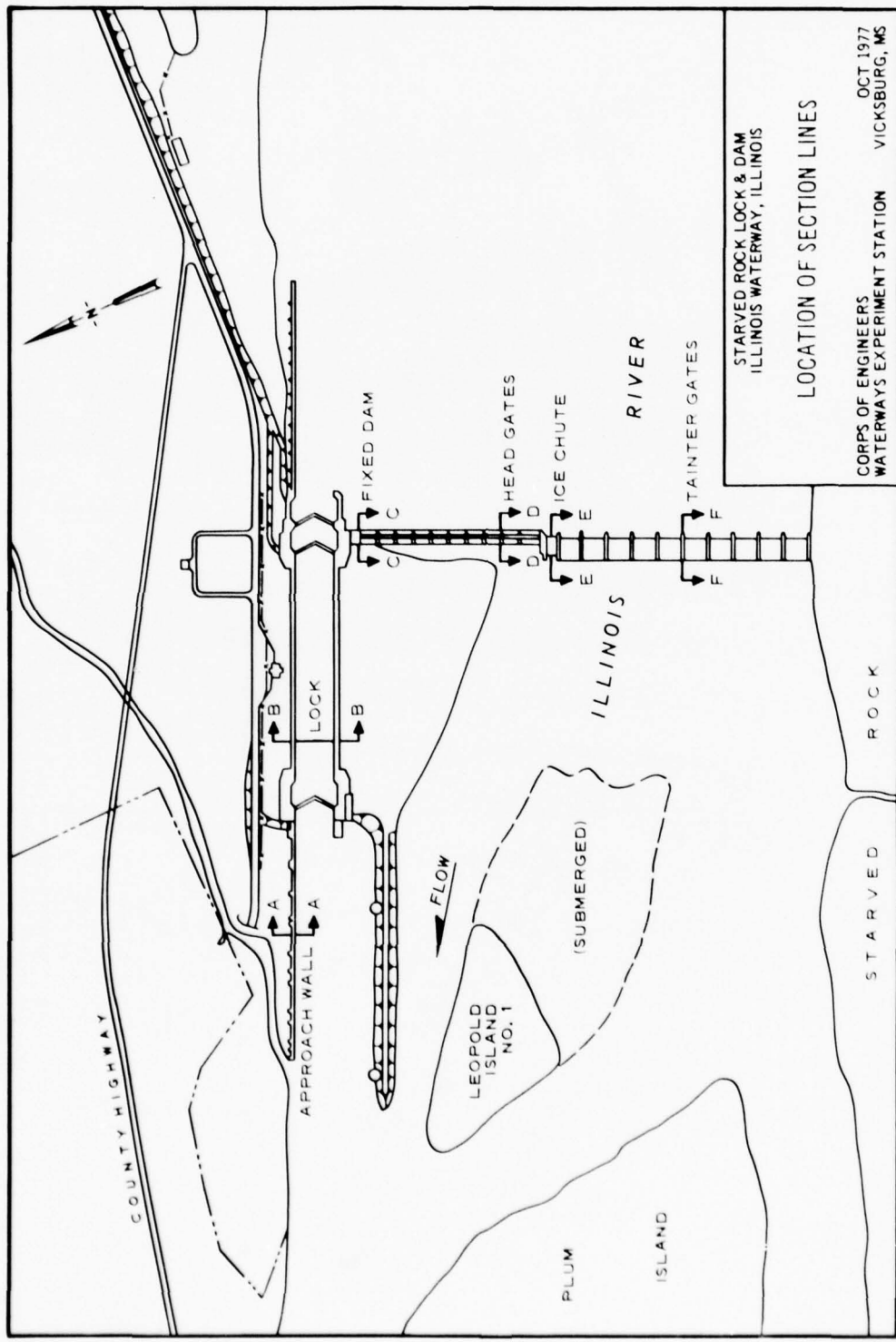
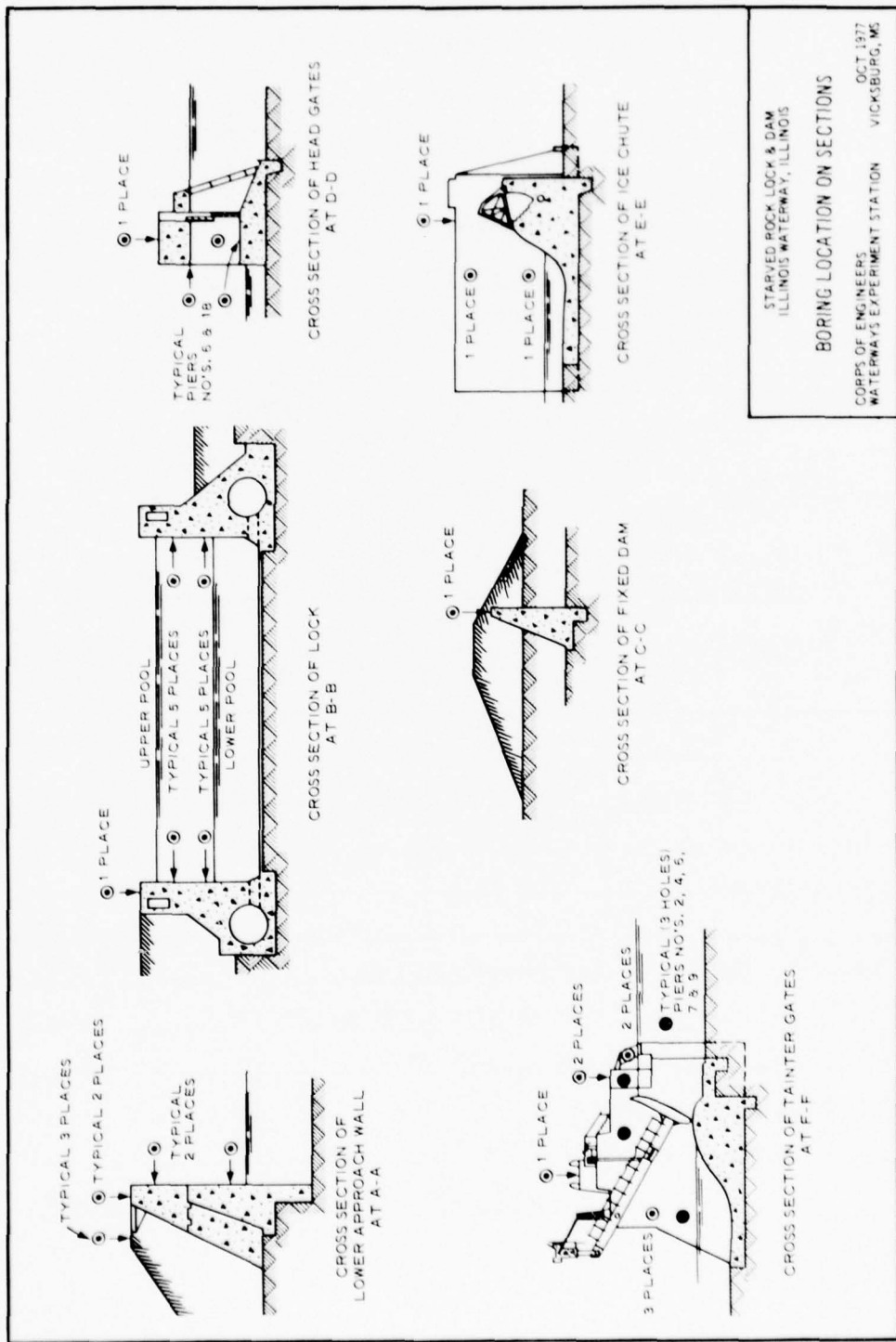


PLATE 1





PIEZOMETER INSTALLATION REPORT

Mark S. Taylor for Robert Neal
INVESTIGATOR

WES FORM 798
MAR. 53
REVISED OCT. 53

WES Re
CHI-13

CHI-13

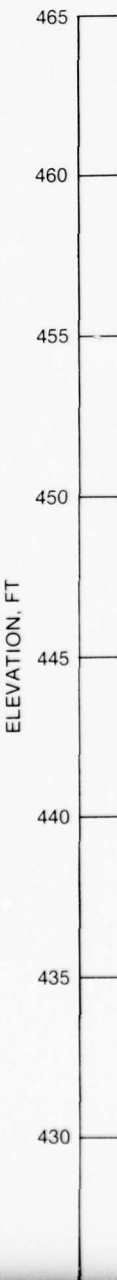
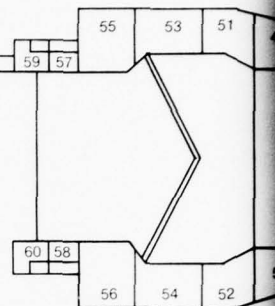
CHI-13
CHI-13
CHI-13
CHI-13

SR WES GWB-1-77



SR WES GW-1-77

SR WES GW-2-77



SR WES GW-1-77

4-9 JUNE 1977
ELEV. TOP OF HOLE = 459.0'

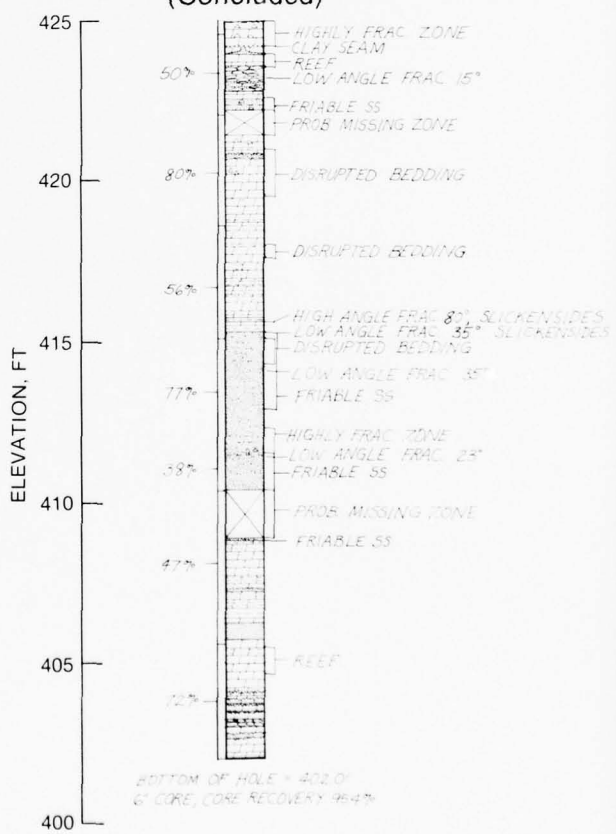


800

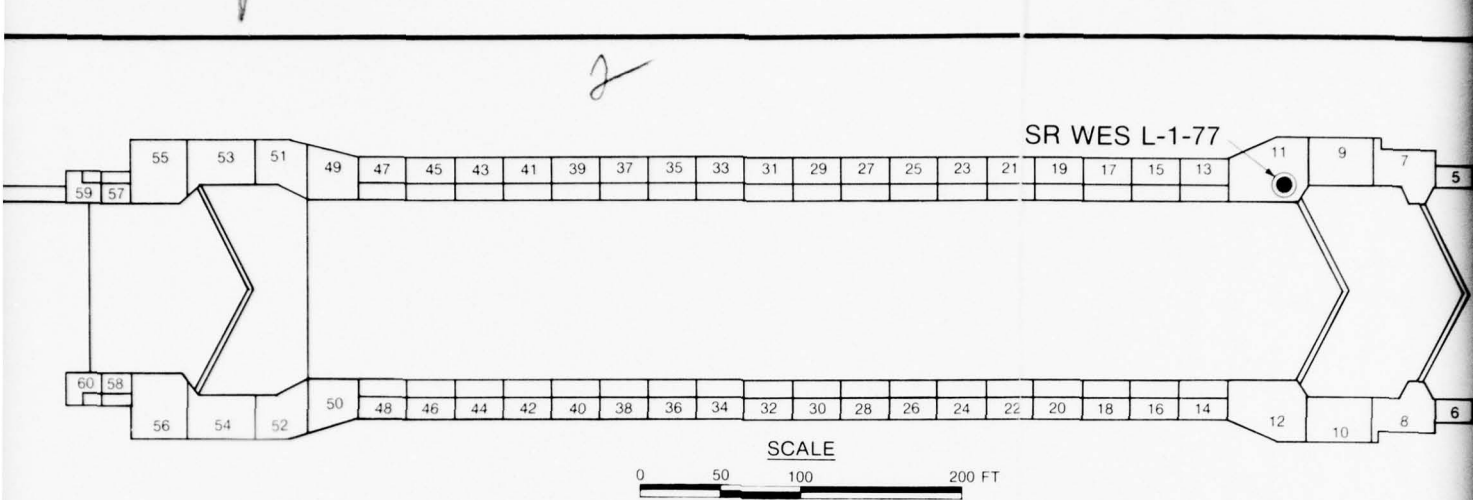
0%

0%

HIGHLY FRAC ZONE



Drill H
SR 1
G1
G2
G3
D



77

SR WES GW-2-77

9-14 JUNE 1977
ELEV. TOP OF HOLE = 457.0'

LY FRAC ZONE
SEAM

ANGLE FRAC 15°

BLE 55
MISSING ZONE

UPTED BEDDING

UPTED BEDDING

ANGLE FRAC 80° SLICKENSIDES
ANGLE FRAC 35° SLICKENSIDES
UPTED BEDDING

ANGLE FRAC 35°
BLE 55

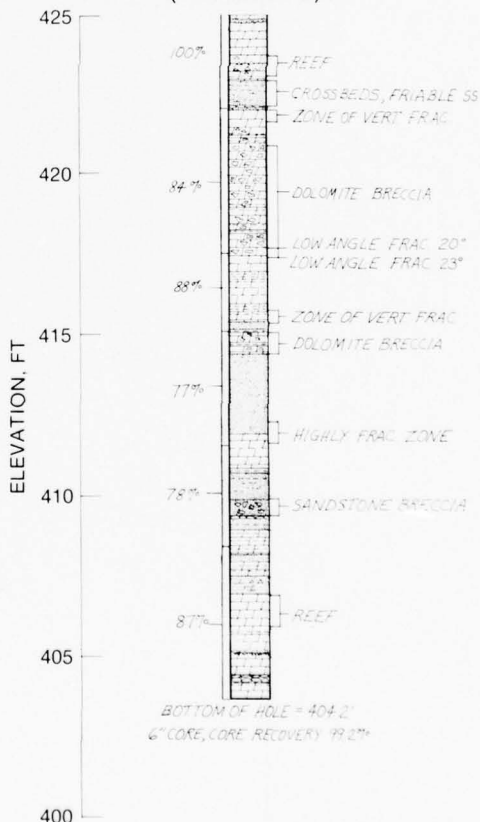
Y FRAC ZONE
ANGLE FRAC 23°
BLE 55

R MISSING ZONE
BLE 55

0'
95.4%

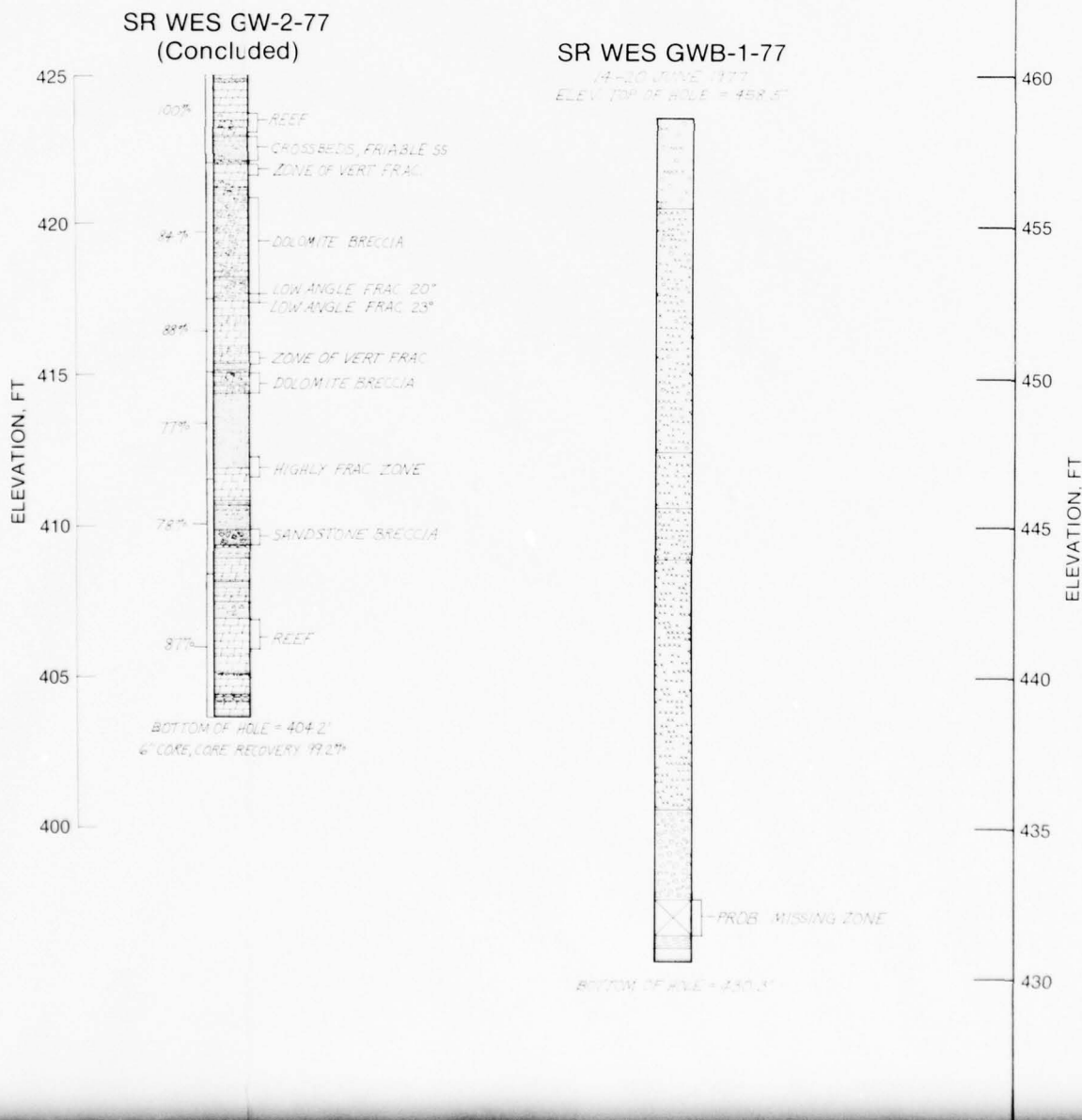
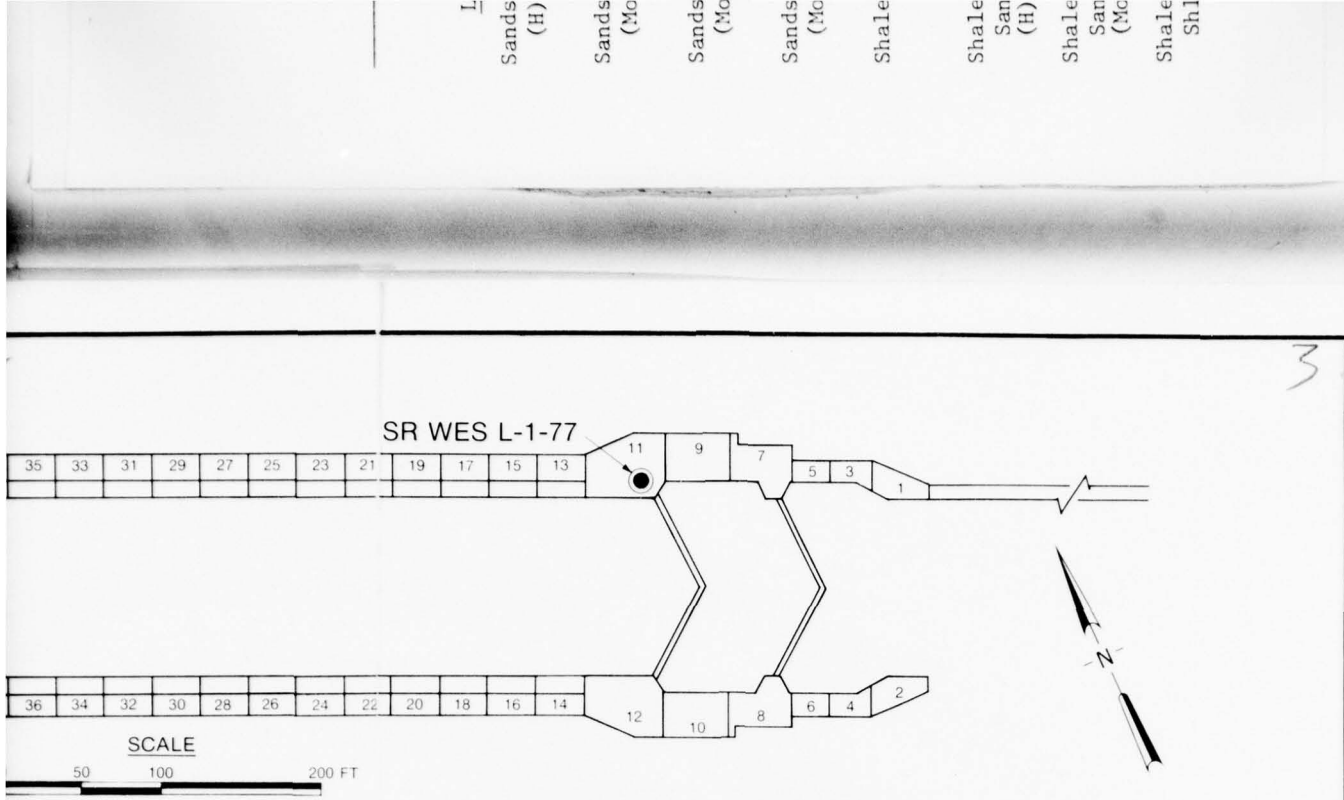


SR WES GW-2-77
(Concluded)



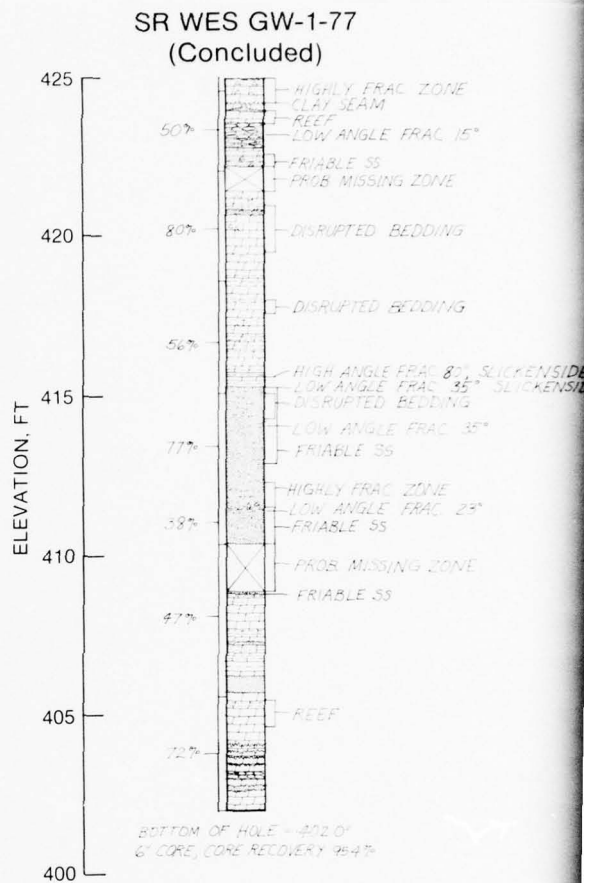
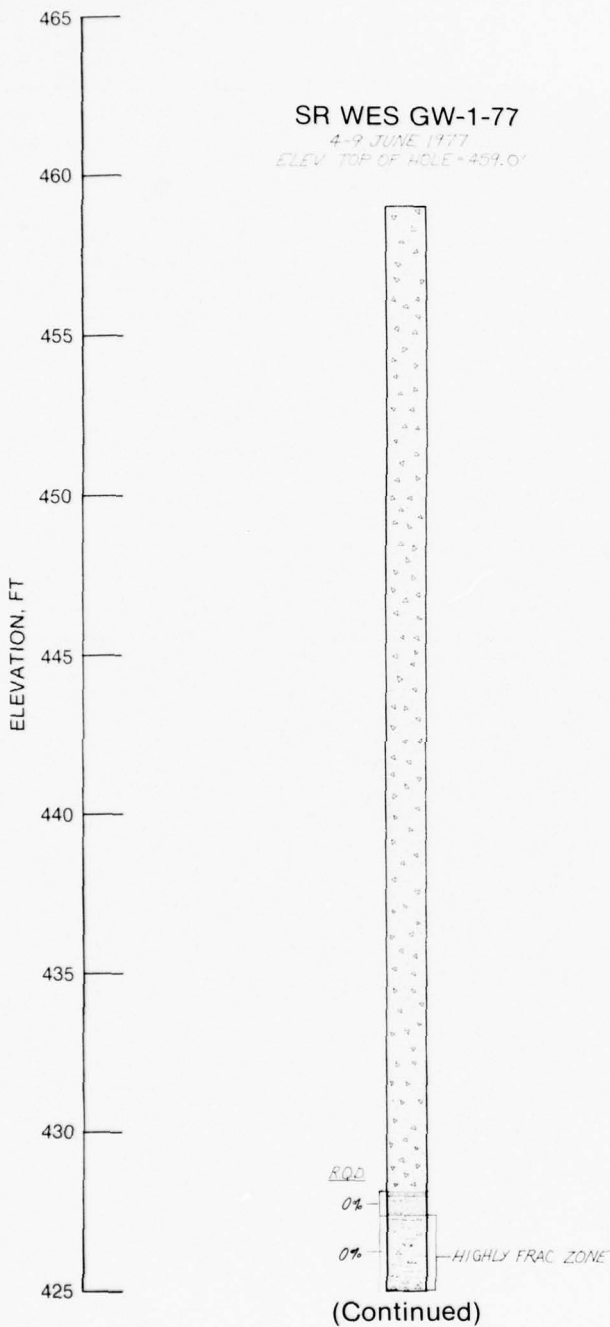
SR WES
9-20 JU
ELEV. TOP OF

BOTTOM OF



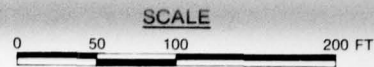
* C = Cr
Given

Lith
Shale Pt
Dolomi
Dolomite

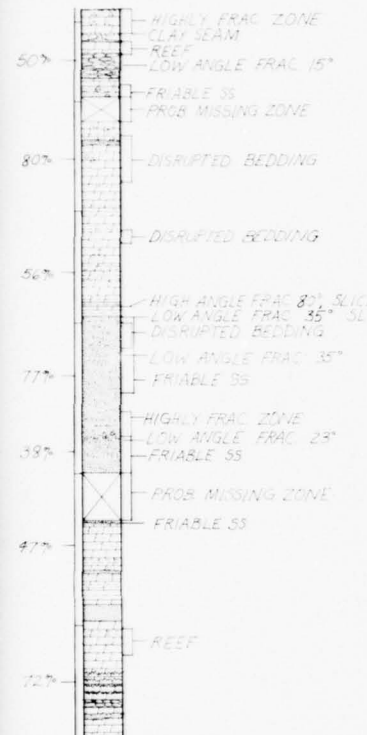


NOTE: FIELD LOGS INDICATE NO WATER LOSS.

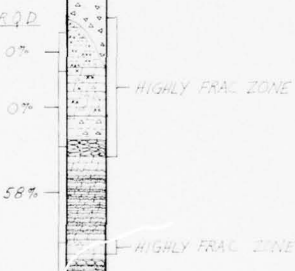
Sand (H) Sand (M) Sand (M) Sand (M) Shal Sa Shal Sa Shal Sh Shal Do



SR WES GW-1-77
(Concluded)

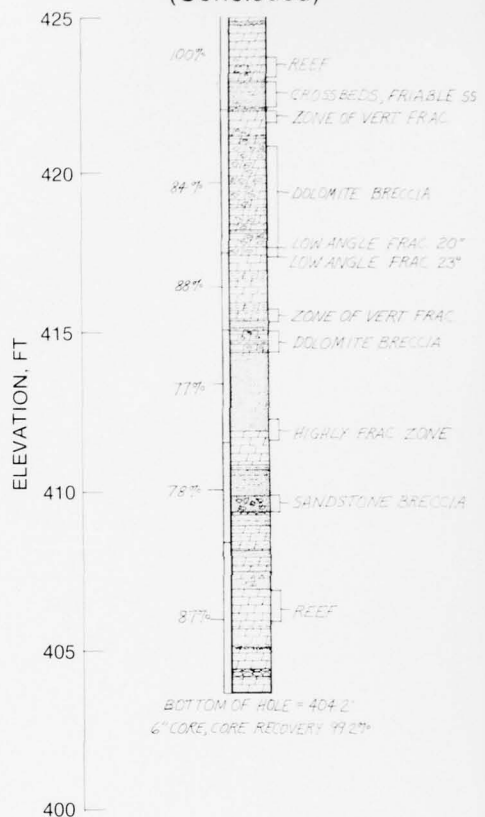


SR WES GW-2-77
9-14 JUNE 1977
ELEV. TOP OF HOLE = 457.0'



(Continued)

SR WES GW-2-77
(Concluded)



LEGEND

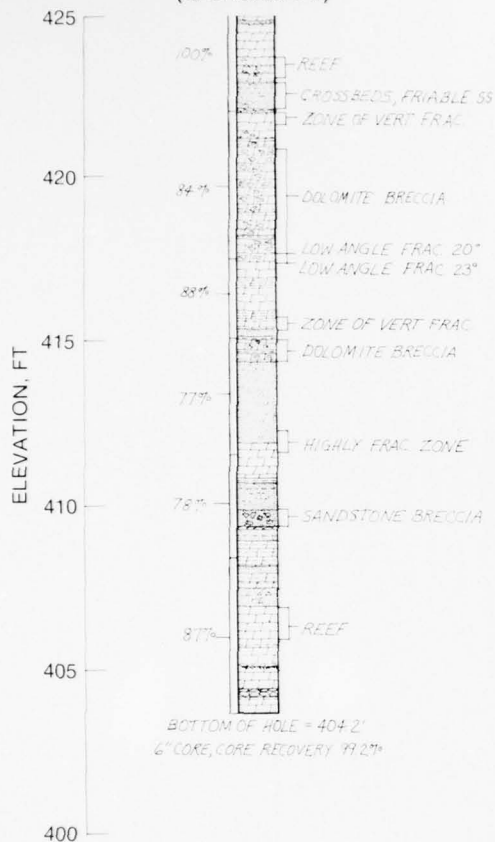
SEAM	CHERT NODULES
MITE	OOLITIC CHERT NODULES
RECCIA	BEDDED CHERT
TONE	OOLITIC BEDDED CHERT
SEAM	STYLOLITE
EL	CONCRETE
LOGS INDICATE NO WATER LOSS.	

<u>PROPOSED</u>	<u>SYMBOL</u>	<u>DESCRIPTION</u>	<u>COMPLETED</u>
	△	COMBINATION DRIVE SAMPLE AND CORED 6" CORE HOLE	●

SCALE

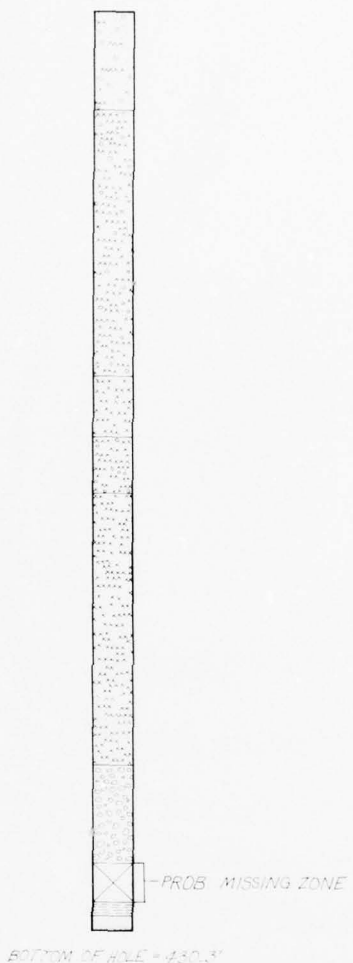
50 100 200 FT

SR WES GW-2-77
(Concluded)



SR WES GWB-1-77

7/20 JUNE 1977
ELEV. TOP OF HOLE = 458.5'



SYMBOL

<u>PROPOSED</u>	<u>DESCRIPTION</u>	<u>COMPLETED</u>
△	COMBINATION DRIVE	△
○	SAMPLE AND CORED	●
	6" CORE HOLE	

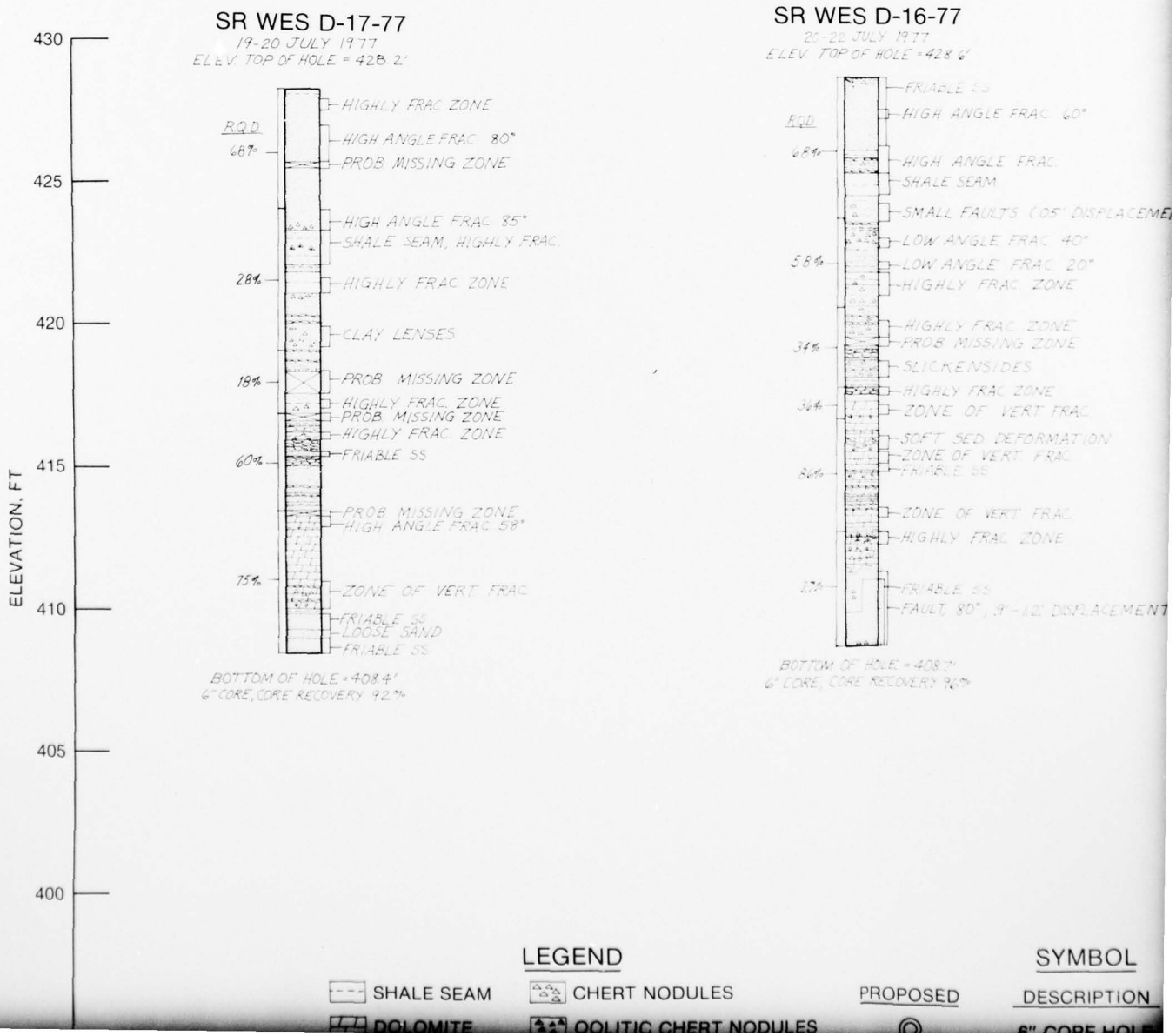
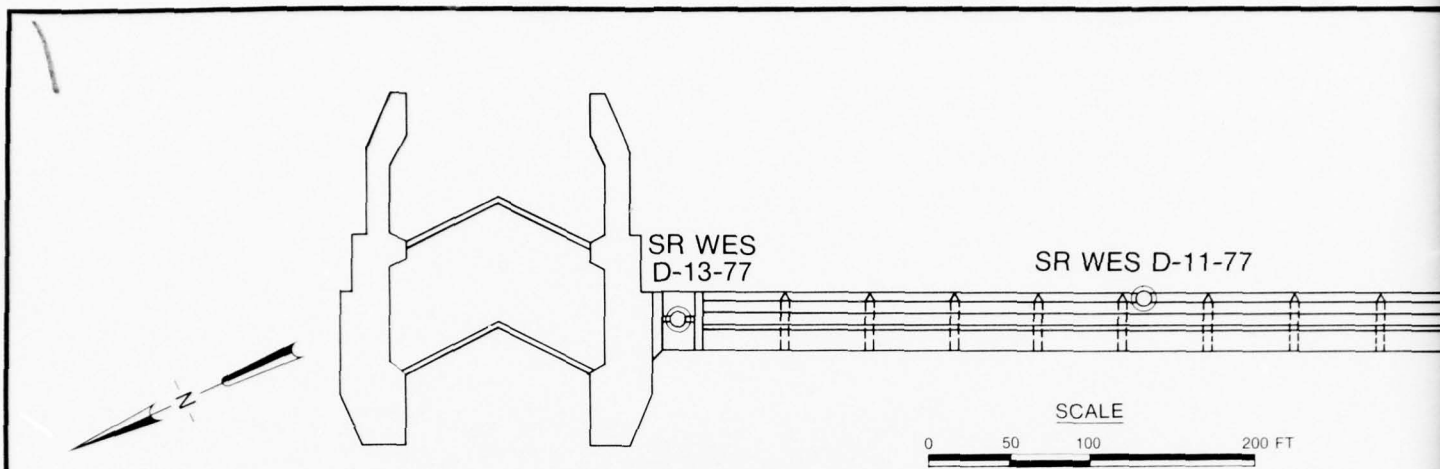
REHABILITATION PHASE
STARVED ROCK LOCK AND DAM
ILLINOIS WATERWAY

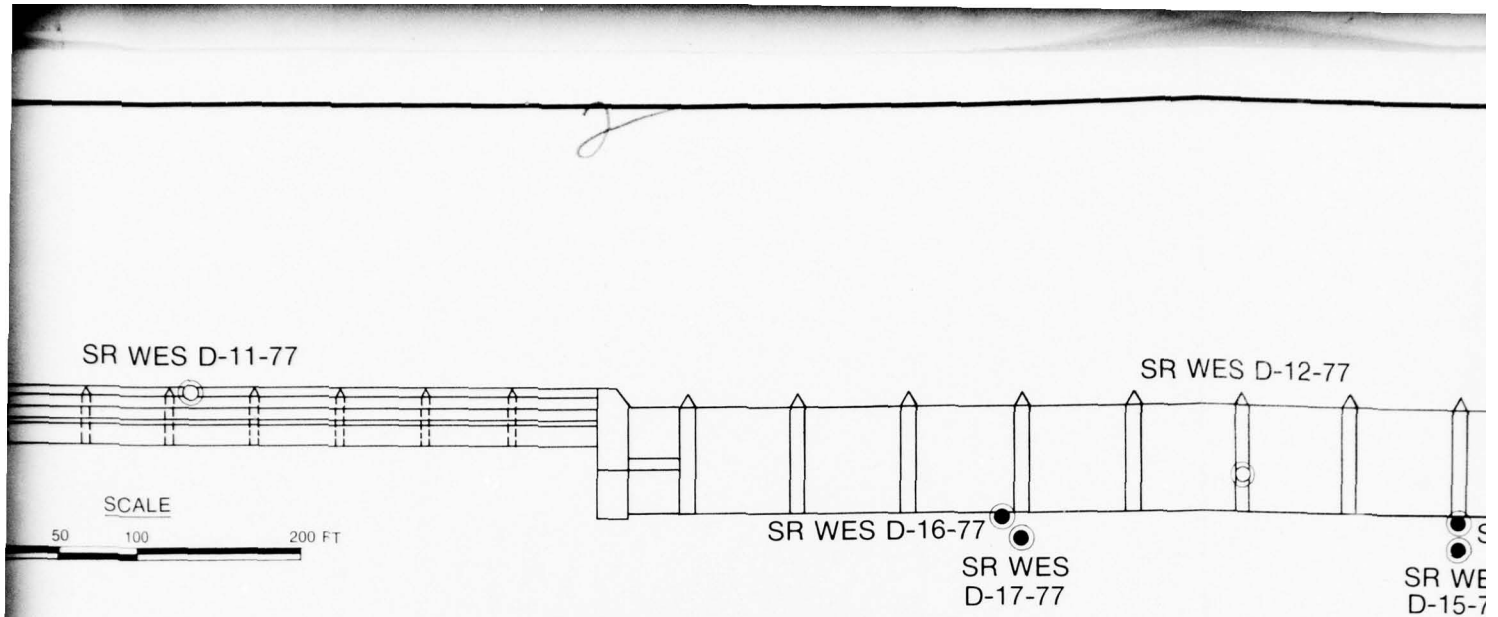
LOG OF BORINGS

(SHEET 1 of 3)

PLATE 5

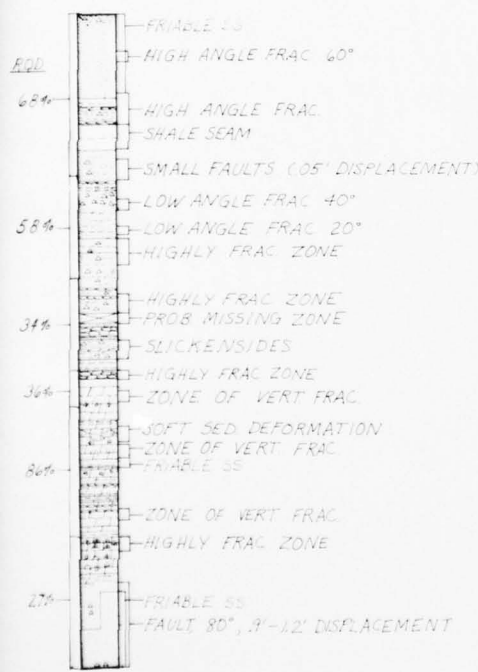
4





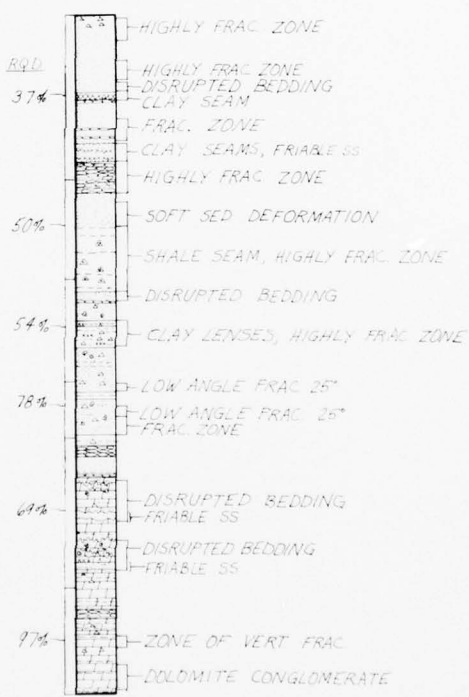
SR WES D-16-77

20-22 JULY 1977
ELEV. TOP OF HOLE = 428.6'



SR WES D-15-77

23-25 JULY 1977
ELEV. TOP OF HOLE = 428.0'



SR WES D-14

25-26 JULY 1977
ELEV TOP OF HOLE = 41



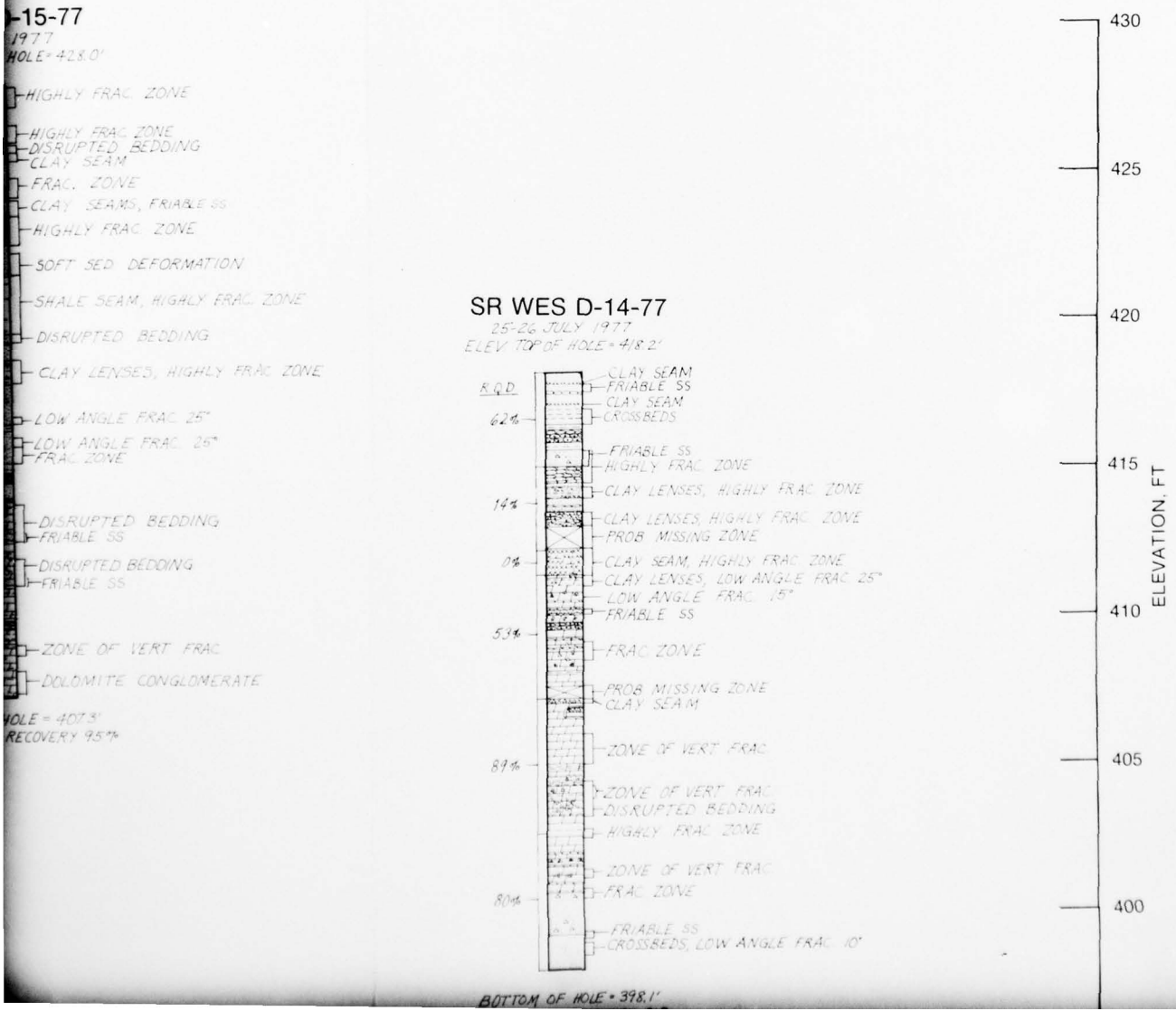
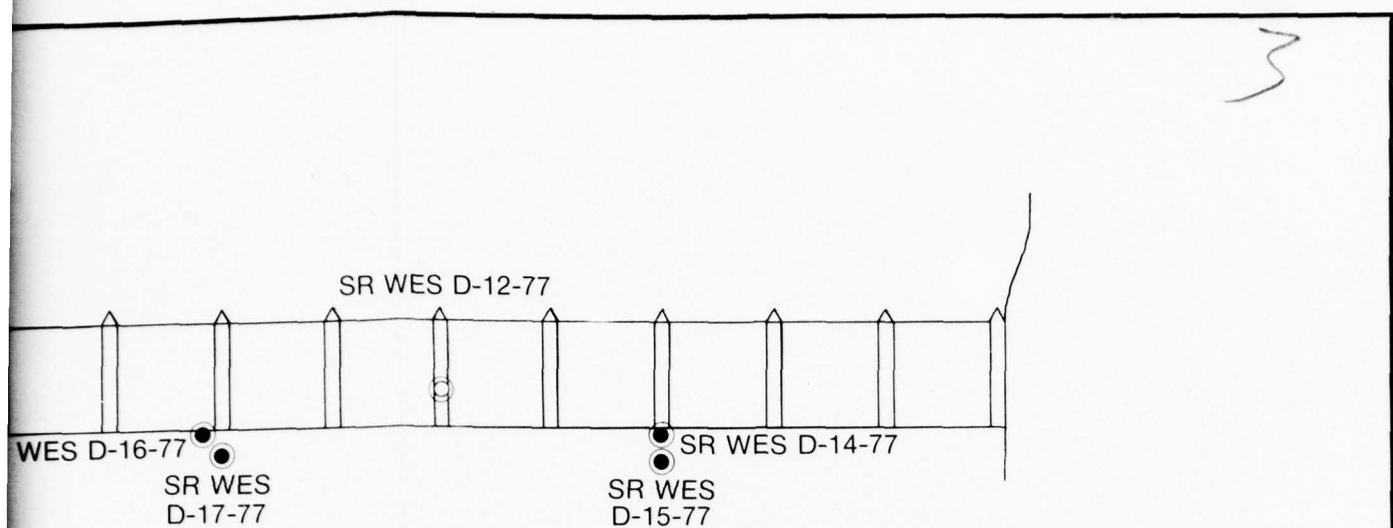
SYMBOL

PROPOSED

DESCRIPTION

COMPLETED

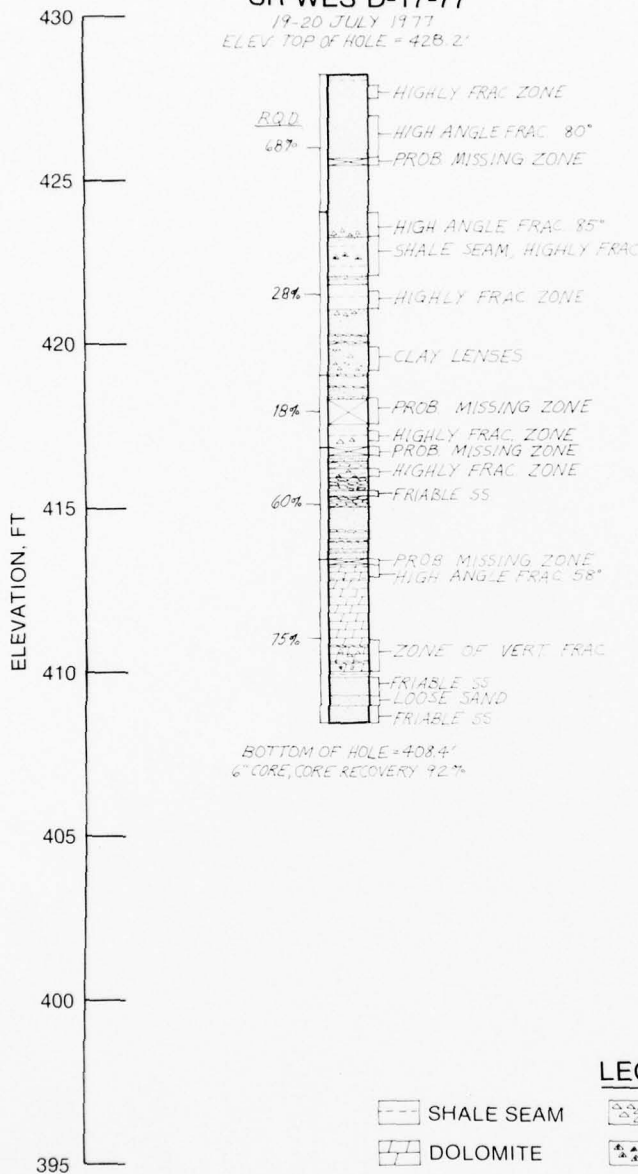
BOTTOM OF HOLE = 37
6" CORE, CORE RECOVERY



0 50 100 200 FT

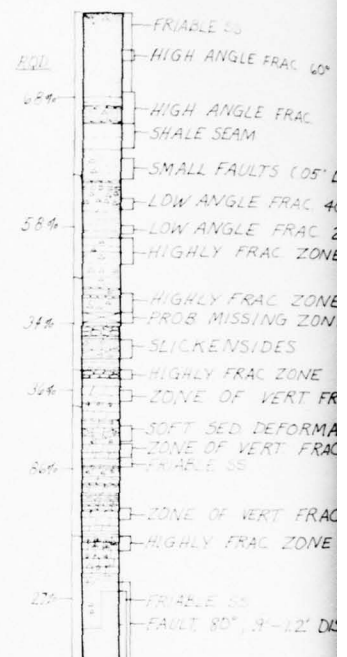
SR WES D-17-77

19-20 JULY 1977
ELEV. TOP OF HOLE = 428.2'



SR WES D-16-77

20-22 JULY 1977
ELEV. TOP OF HOLE = 428.6'



LEGEND

SHALE SEAM	CHERT NODULES
DOLOMITE	OOLITIC CHERT NODULES
DOL. BRECCIA	BEDDED CHERT
SANDSTONE	OOLITIC BEDDED CHERT
CLAY SEAM	STYLOLITE
GRAVEL	CONCRETE

PROPOSED



SY

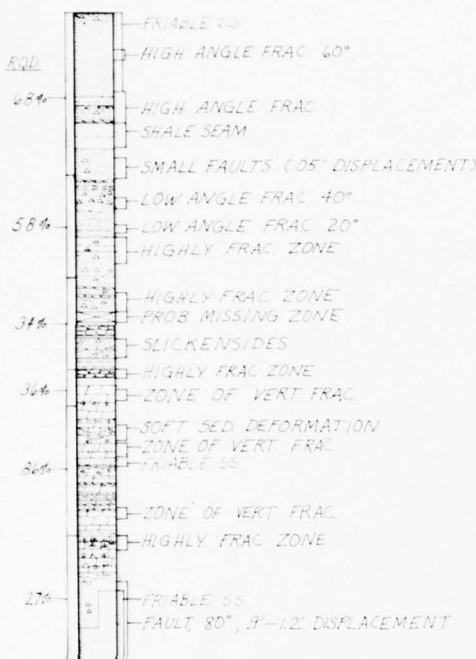
DES

6" C

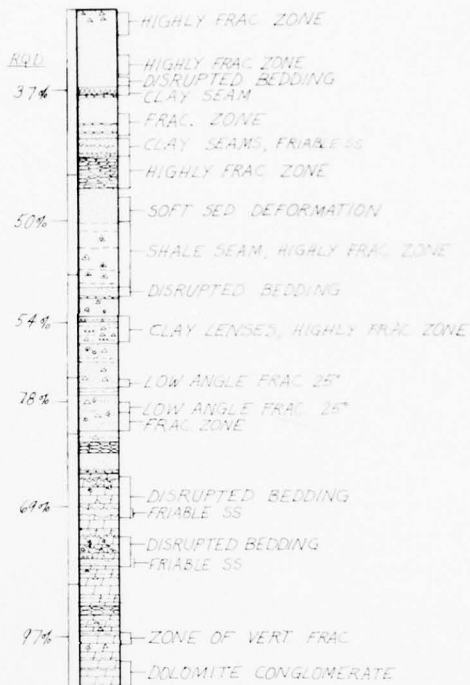
100 200 FT

SR WES
D-17-77SR W
D-15

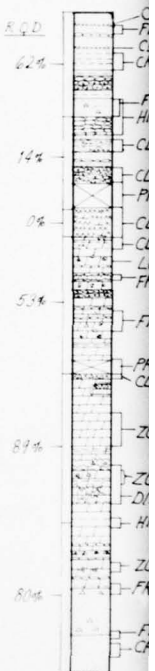
SR WES D-16-77

20-22 JULY 1977
ELEV. TOP OF HOLE = 428.6'BOTTOM OF HOLE = 408.7'
6" CORE, CORE RECOVERY 96%

SR WES D-15-77

23-25 JULY 1977
ELEV. TOP OF HOLE = 428.0'BOTTOM OF HOLE = 407.3'
6" CORE, CORE RECOVERY 95%

SR WES D-1

25-26 JULY 1977
ELEV. TOP OF HOLE =BOTTOM OF HOLE =
6" CORE, CORE RECOVERY

		<u>SYMBOL</u>	
LES	PROPOSED	DESCRIPTION	COMPLETED
ART NODULES	◎	6" CORE HOLE	●
ART			
DED CHERT			

5

SR WES
D-17-77

SR WES
D-15-77

5-77

77

E= 428.0'

HIGHLY FRAC ZONE

HIGHLY FRAC ZONE
DISRUPTED BEDDING
CLAY SEAM

FRAC. ZONE

CLAY SEAMS, FRIABLE SS

HIGHLY FRAC ZONE

SOFT SED. DEFORMATION

SHALE SEAM, HIGHLY FRAC ZONE

DISRUPTED BEDDING

CLAY LENSES, HIGHLY FRAC ZONE

LOW ANGLE FRAC 25°

LOW ANGLE FRAC 25°

FRAC. ZONE

DISRUPTED BEDDING
FRIABLE SS

DISRUPTED BEDDING
FRIABLE SS

ZONE OF VERT FRAC

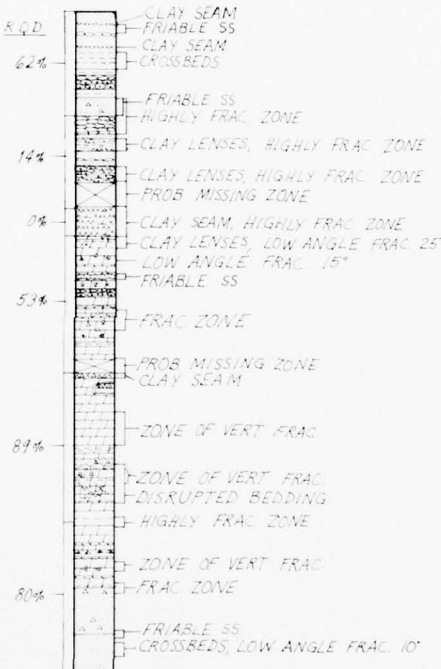
DOLOMITE CONGLOMERATE

- 407.3'

VERY 95%

SR WES D-14-77

25-26 JULY 1977
ELEV TOP OF HOLE = 418.2'



430
425
420
415
410
405
400
395

EL E V A T I O N , F T

REHABILITATION PHASE
STARVED ROCK LOCK AND DAM
ILLINOIS WATERWAY

LOG OF BORINGS

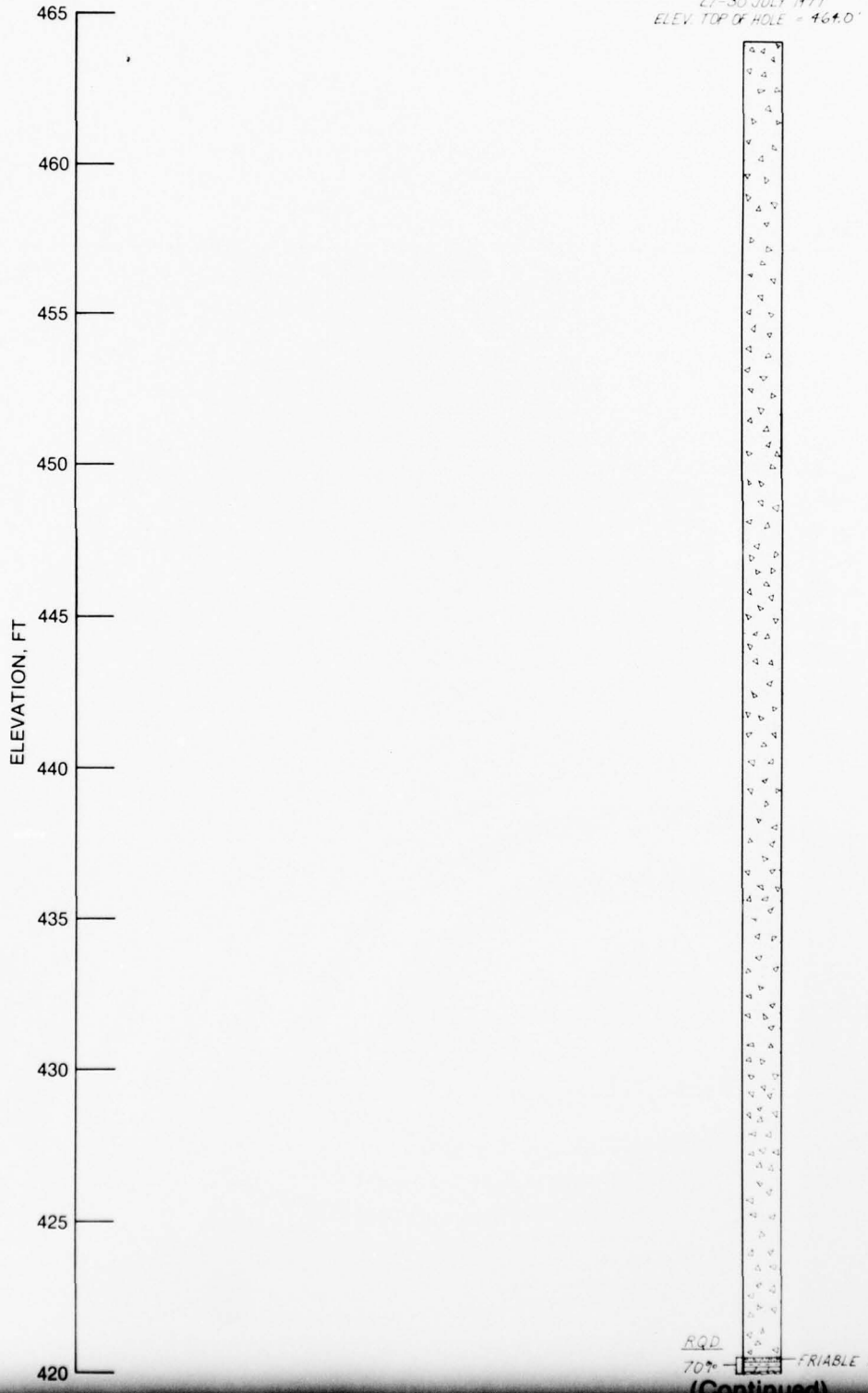
(SHEET 2 of 3)

4

PLATE 6

SR WES L-1-77

27-30 JULY 1977
ELEV. TOP OF HOLE = 464.0'



2

SR WES L-1-77

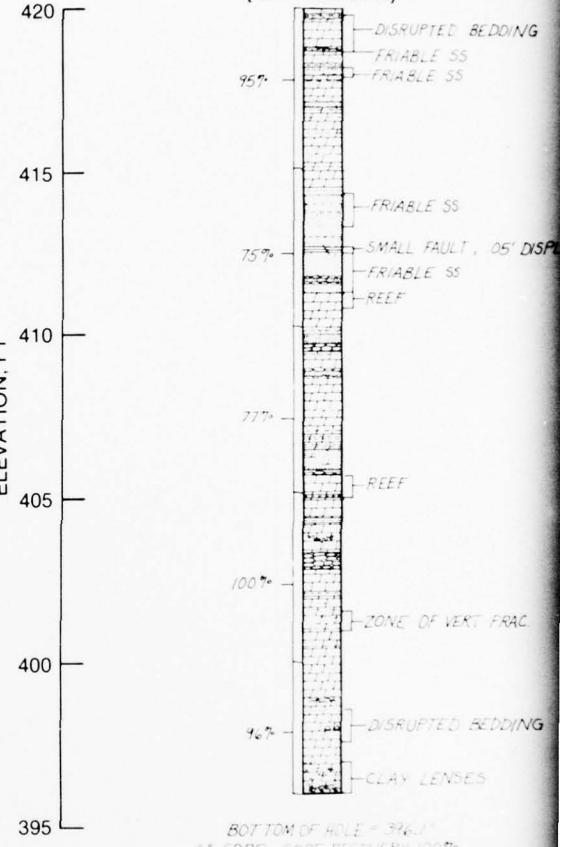
27-30 JULY 1977

ELEV. TOP OF HOLE = 464.0'



FRIABLE SS

SR WES L-1-77
(Concluded)



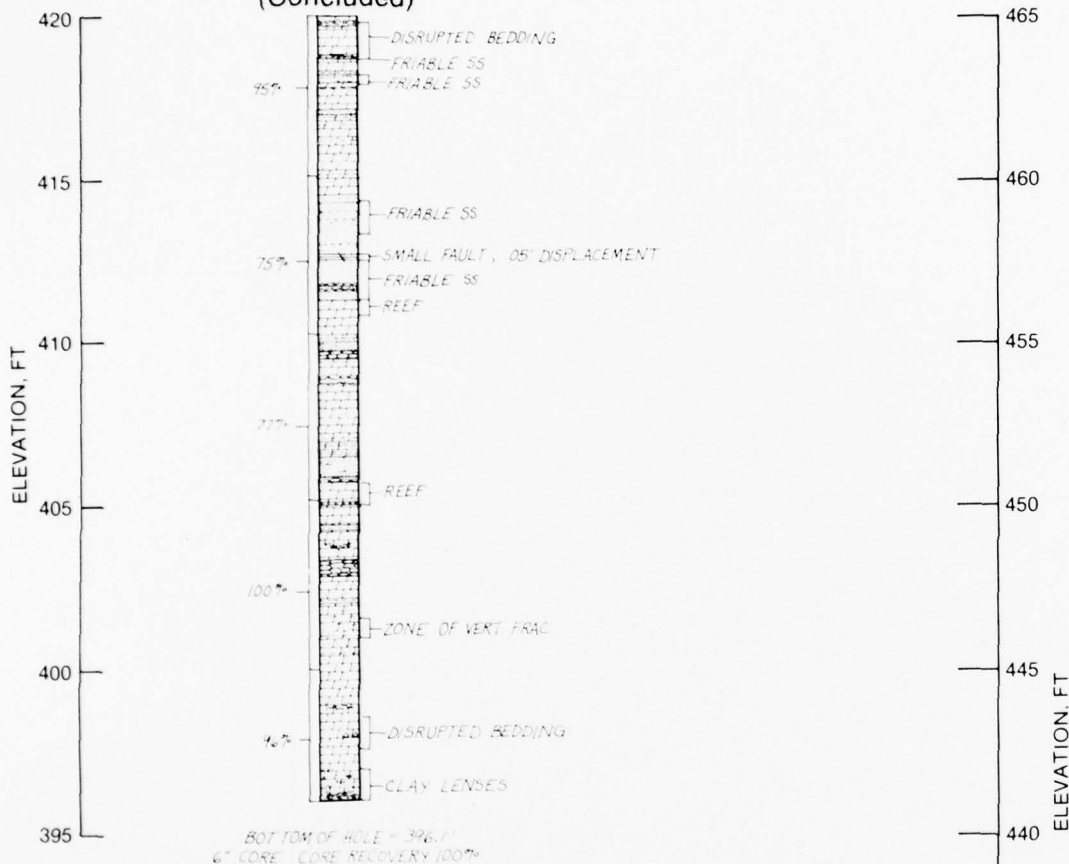
LEGEND

--- SHALE SEAM

--- CHERT NODULES

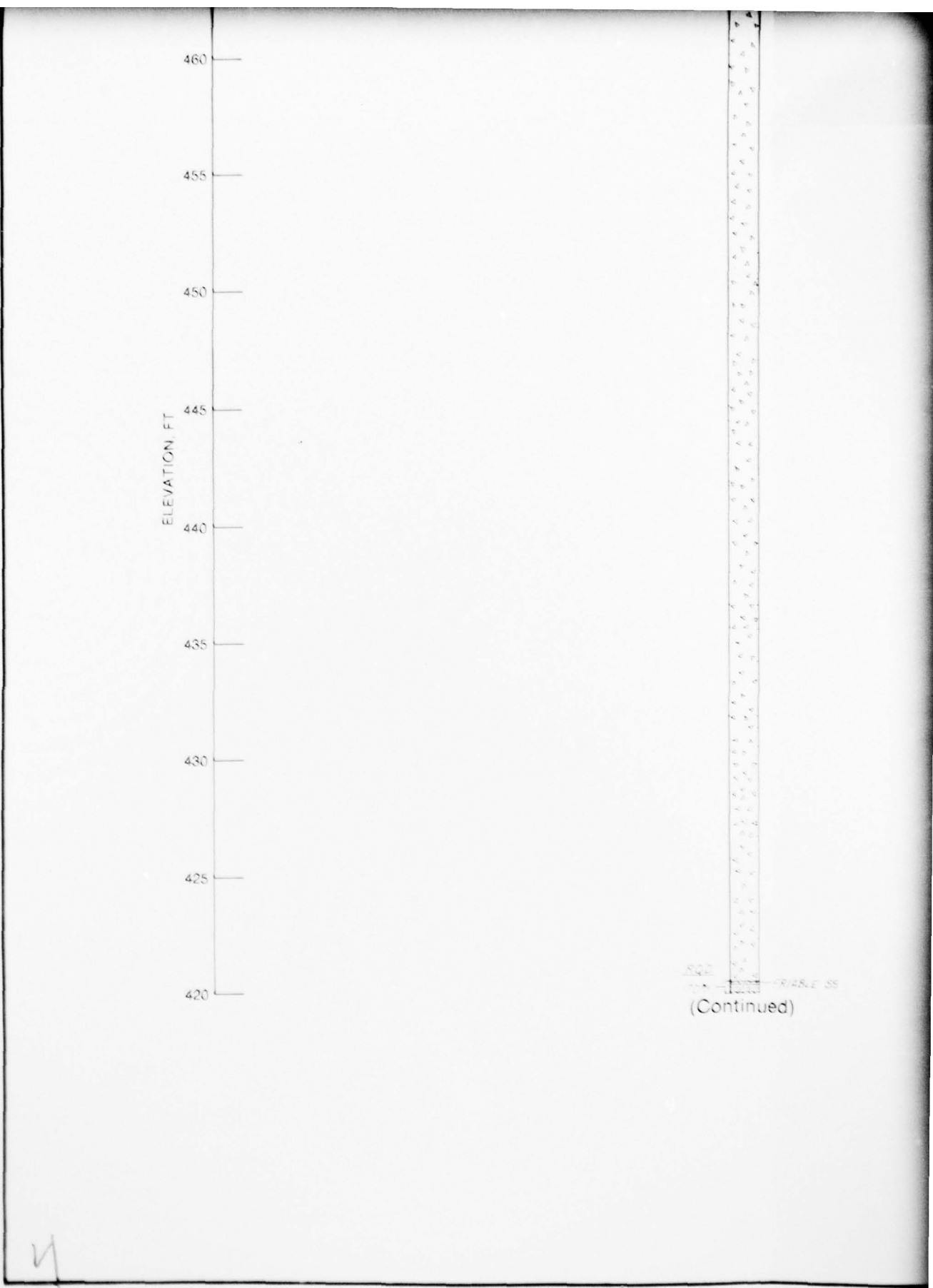
3

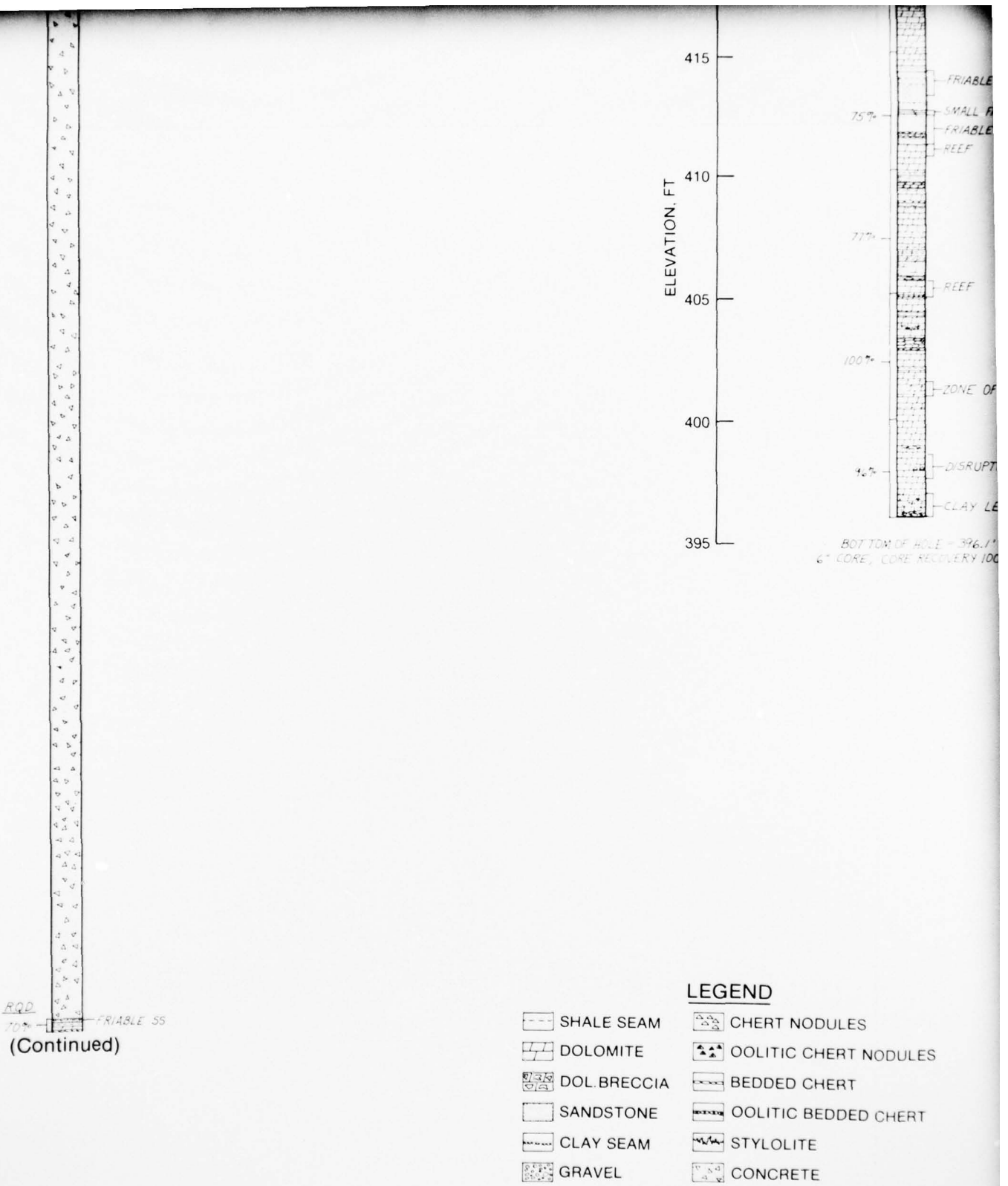
SR WES L-1-77
(Concluded)

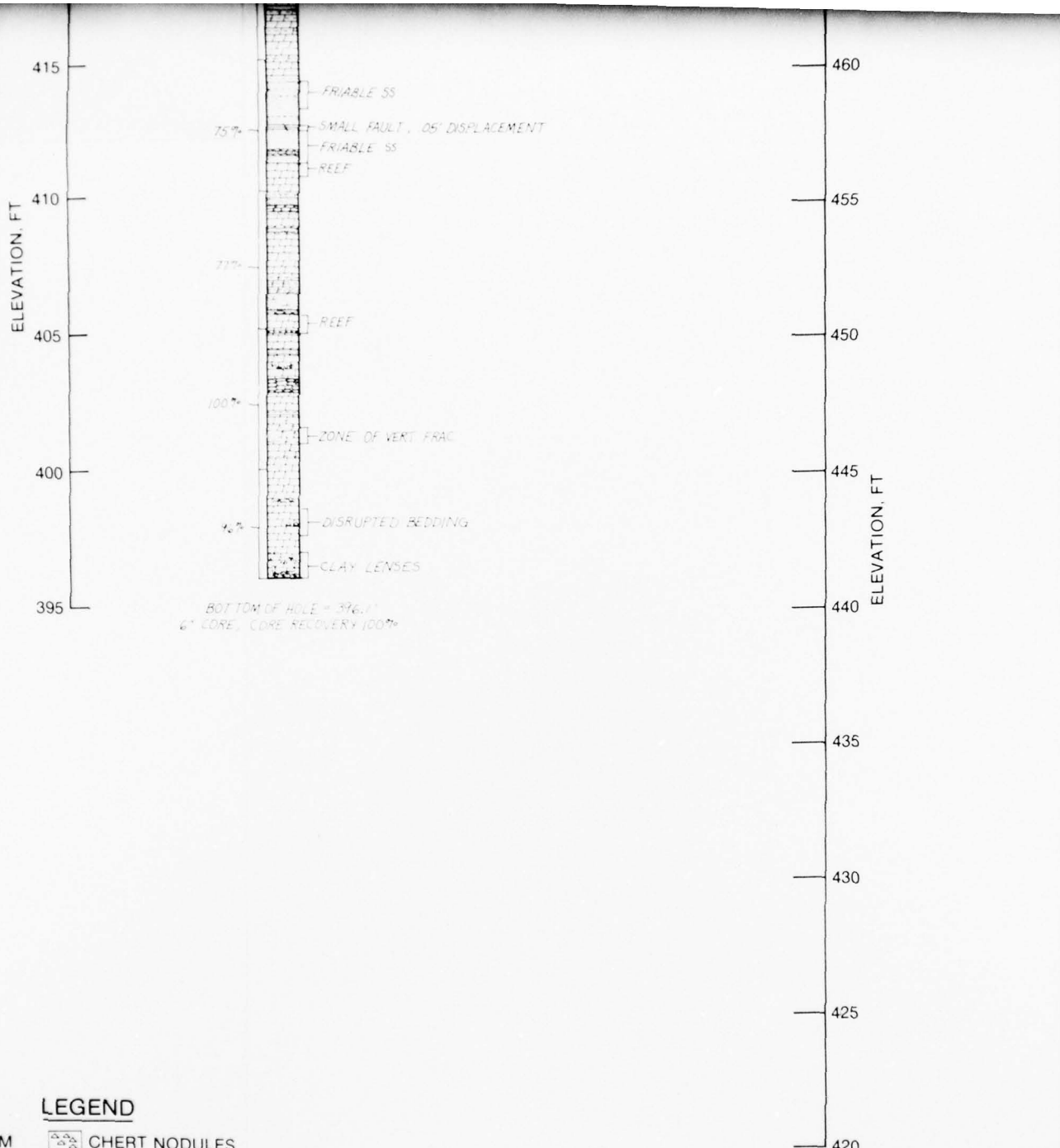


LEGEND

SEAM CHERT NODULES





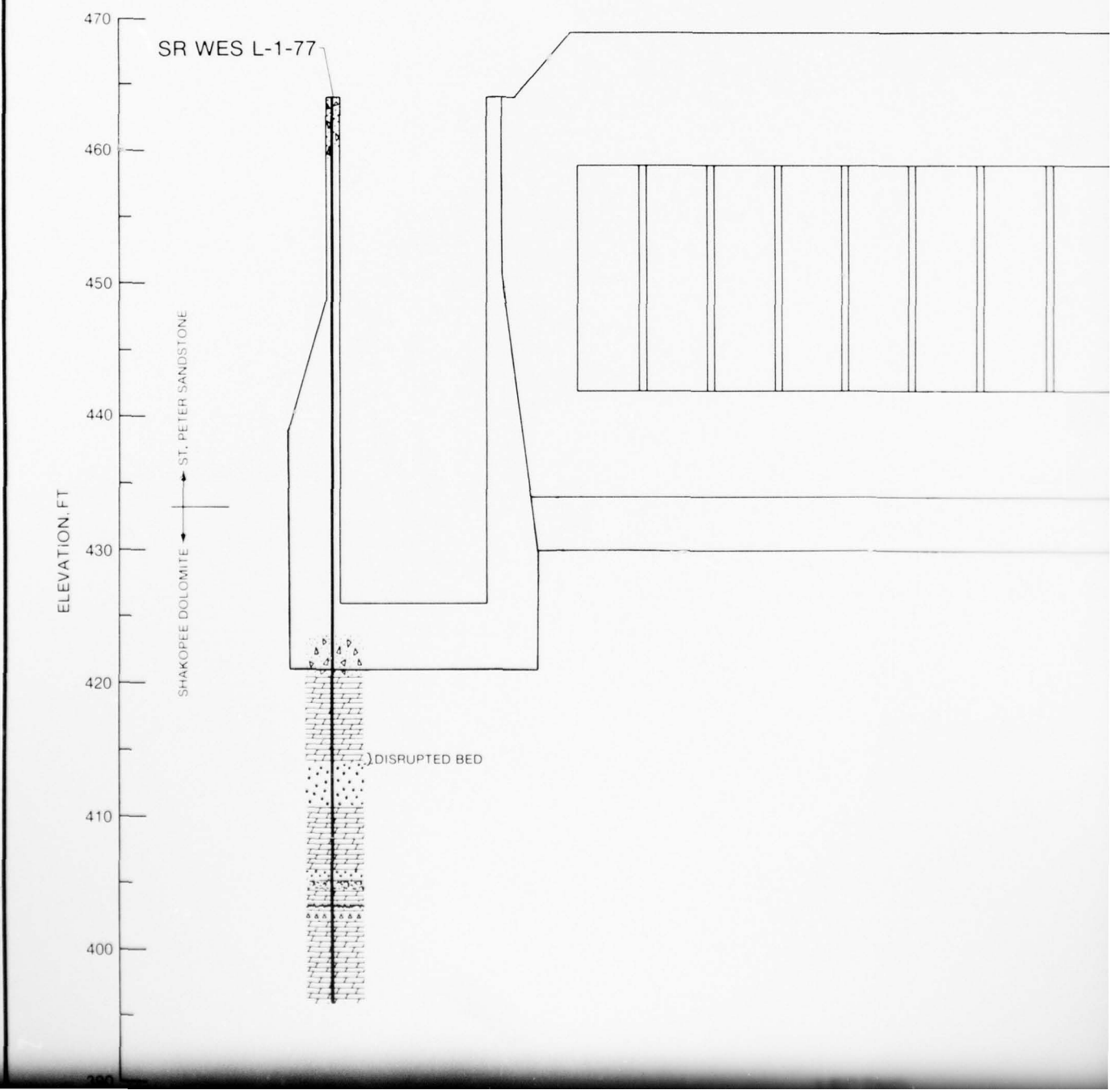
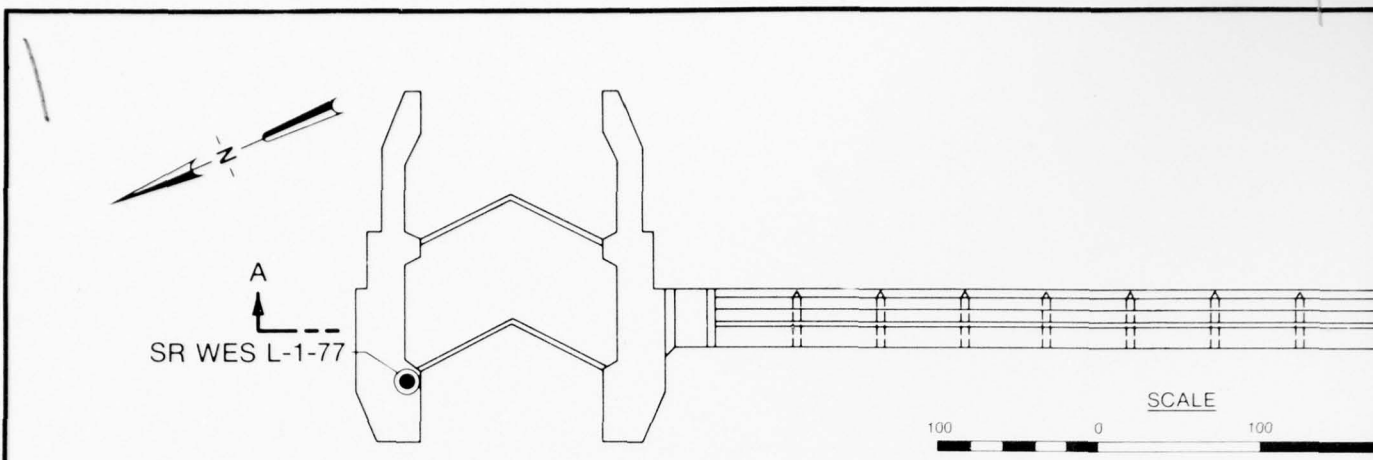


REHABILITATION PHASE
STARVED ROCK LOCK AND DAM
ILLINOIS WATERWAY

LOG OF BORINGS

(SHEET 3 of 3)

PLATE 7



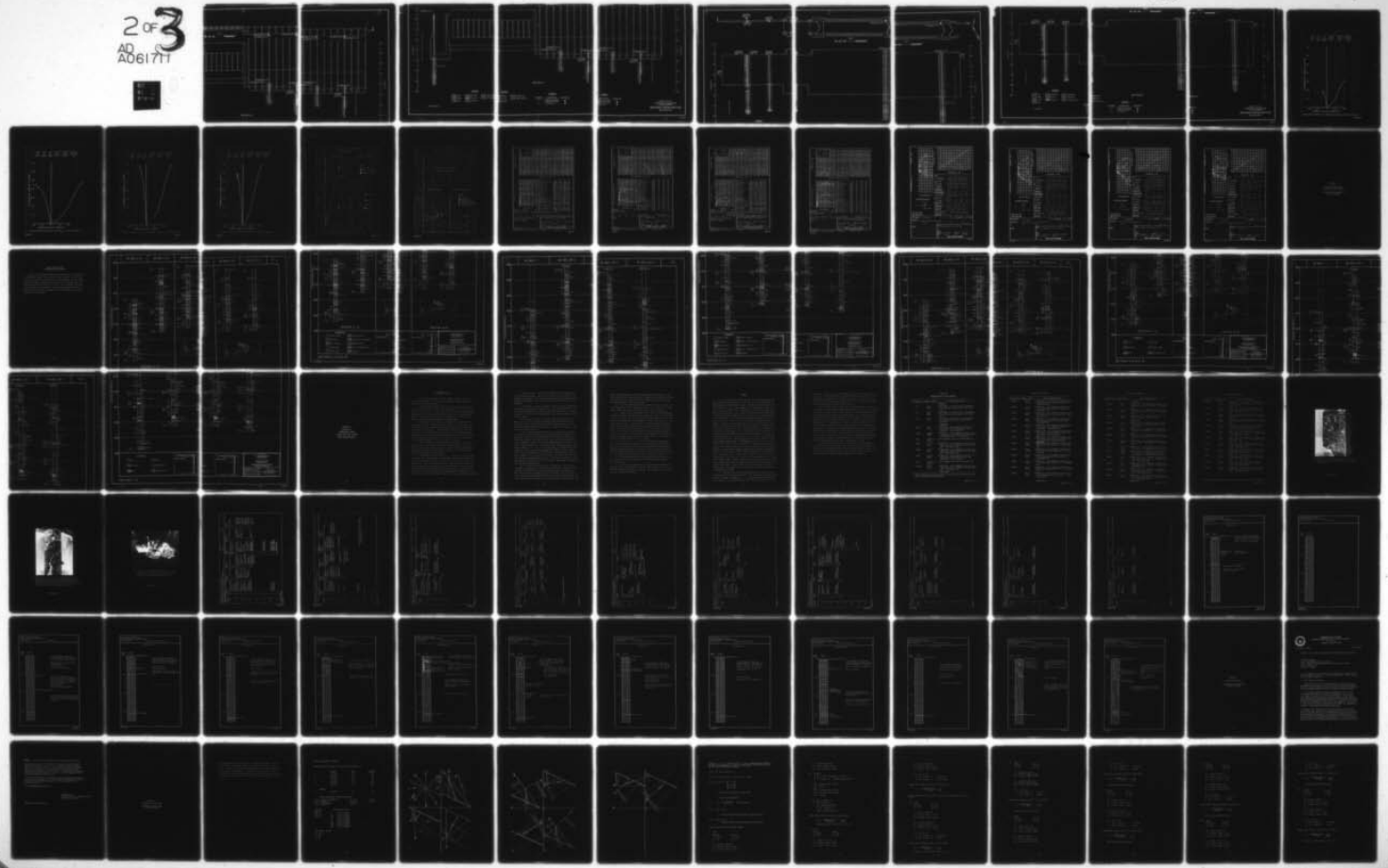
AD-A061 711 ARMY ENGINEER WATERWAYS EXPERIMENT STATION VICKSBURG MISS F/G 13/2
CONCRETE AND ROCK CORE TESTS, MAJOR REHABILITATION OF STARVED R--ETC(U)
SEP 78 R L STOWE, B A PAVLOV, G S WONG

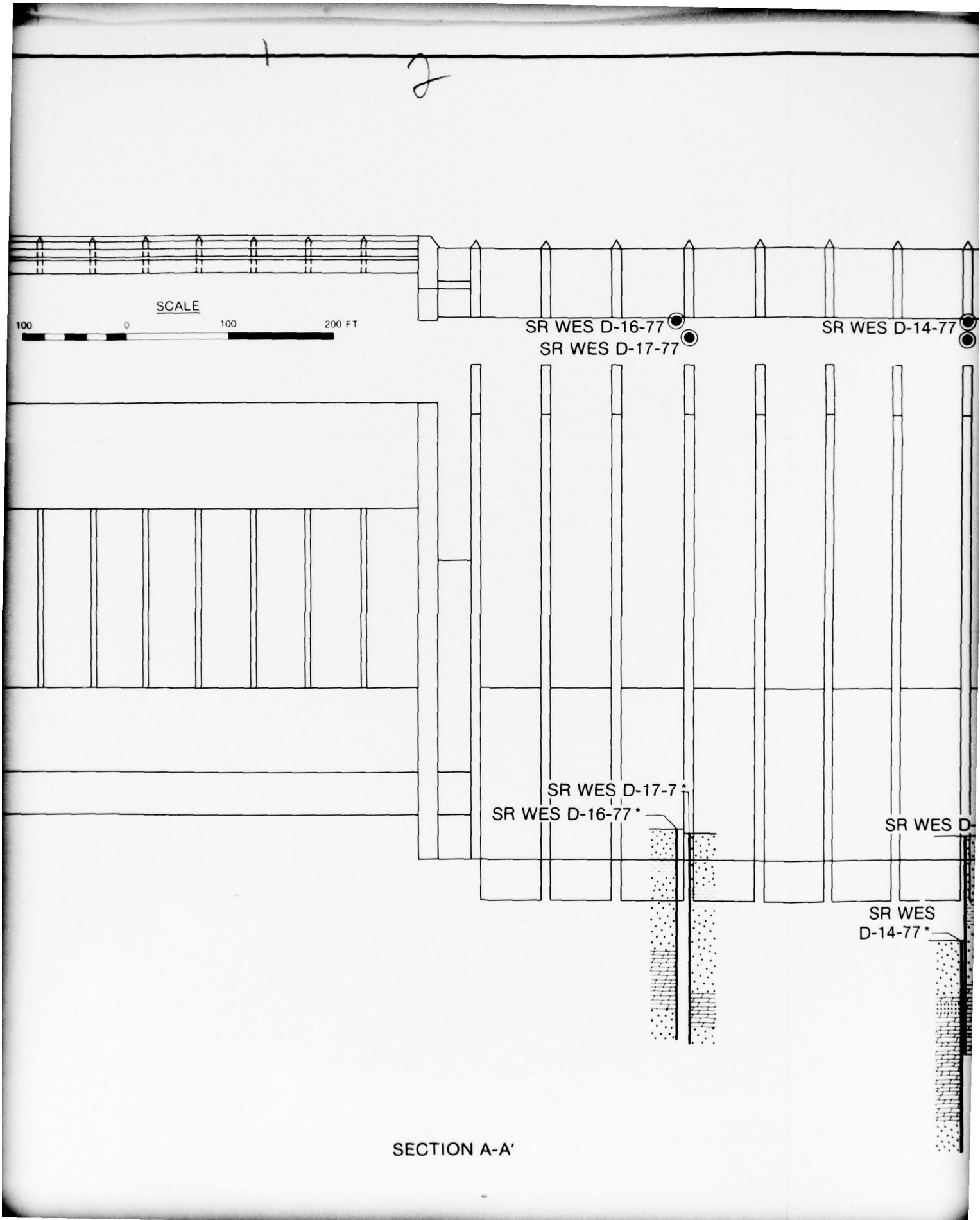
UNCLASSIFIED

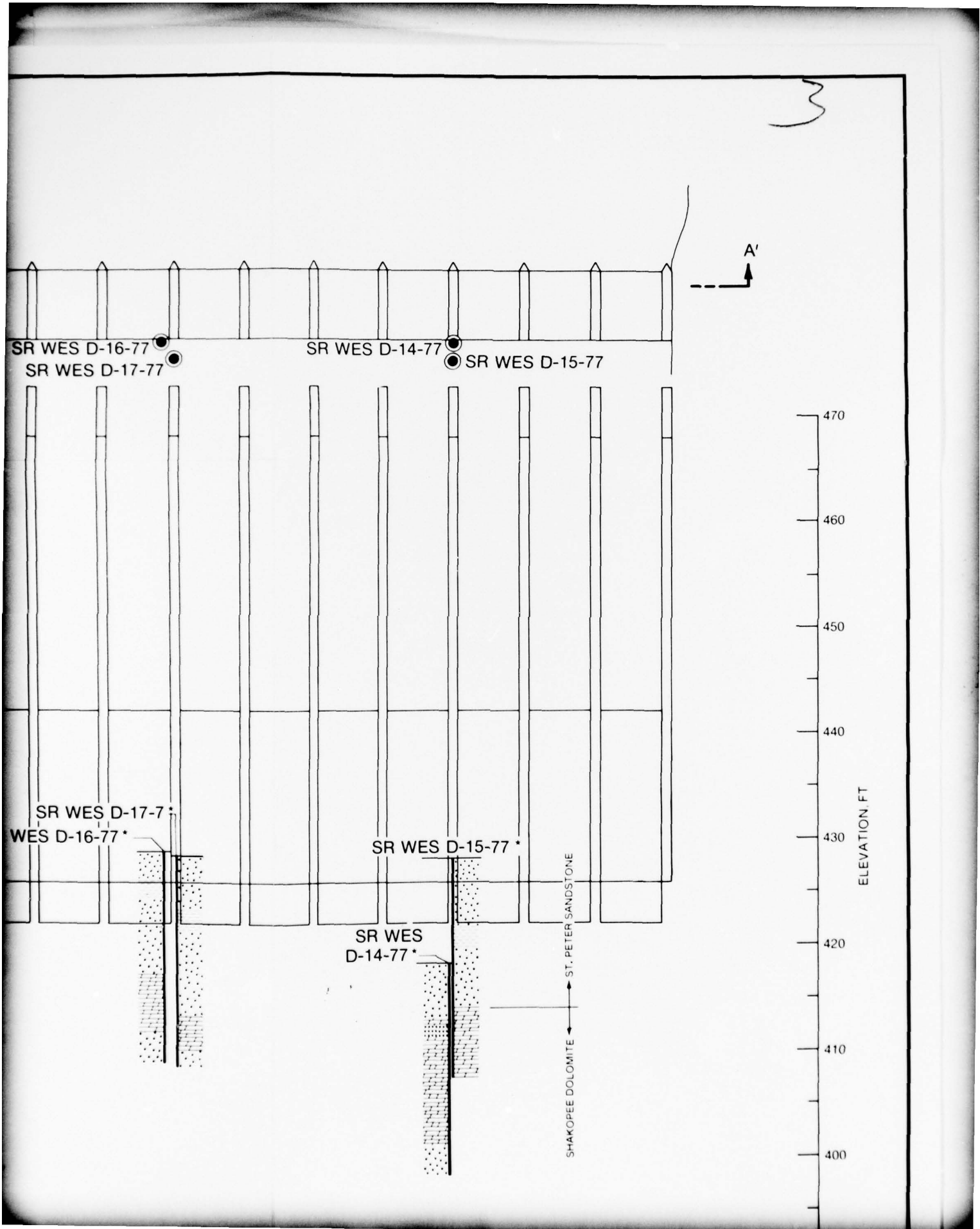
WES-MP-C-78-12

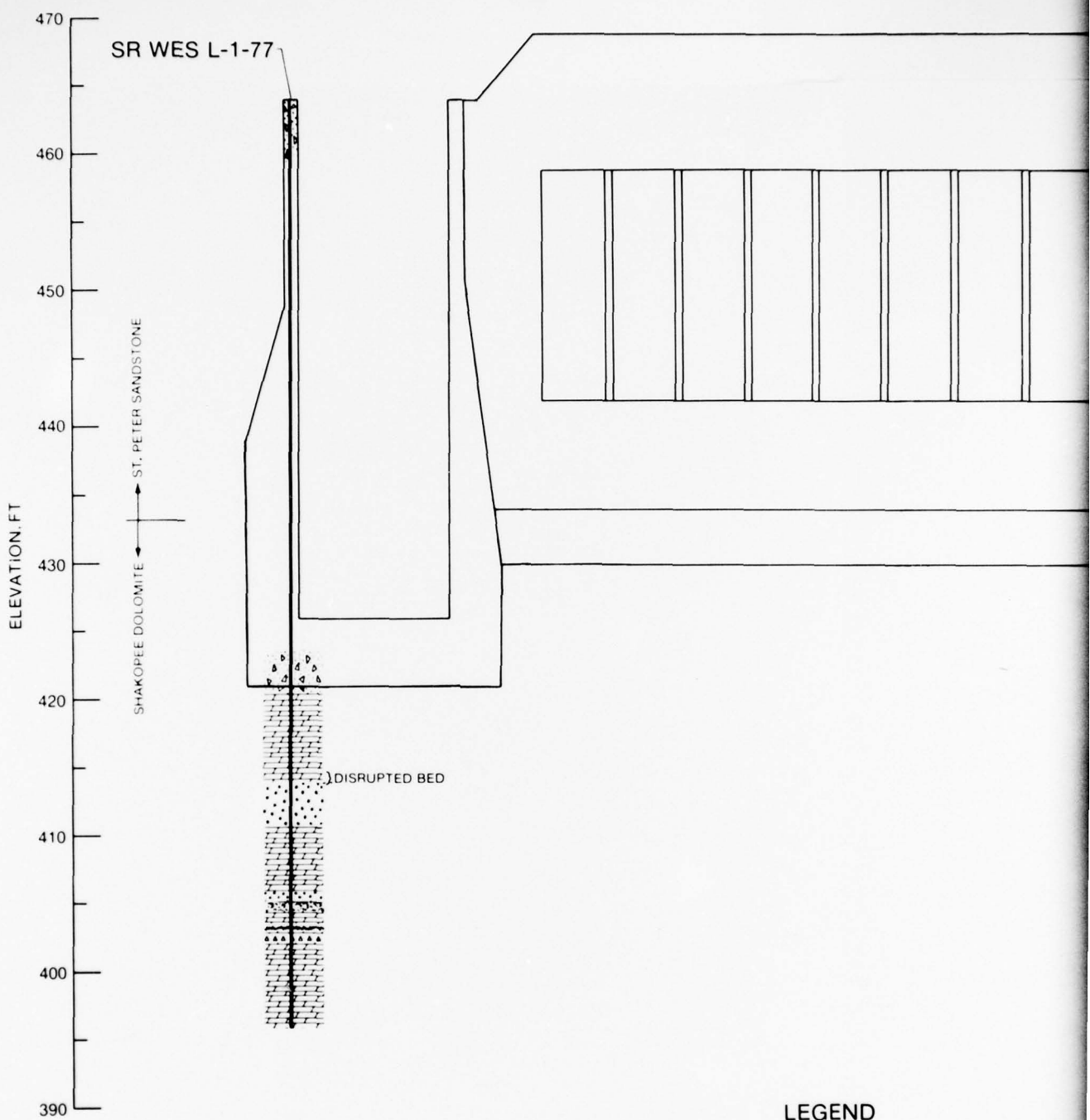
NL

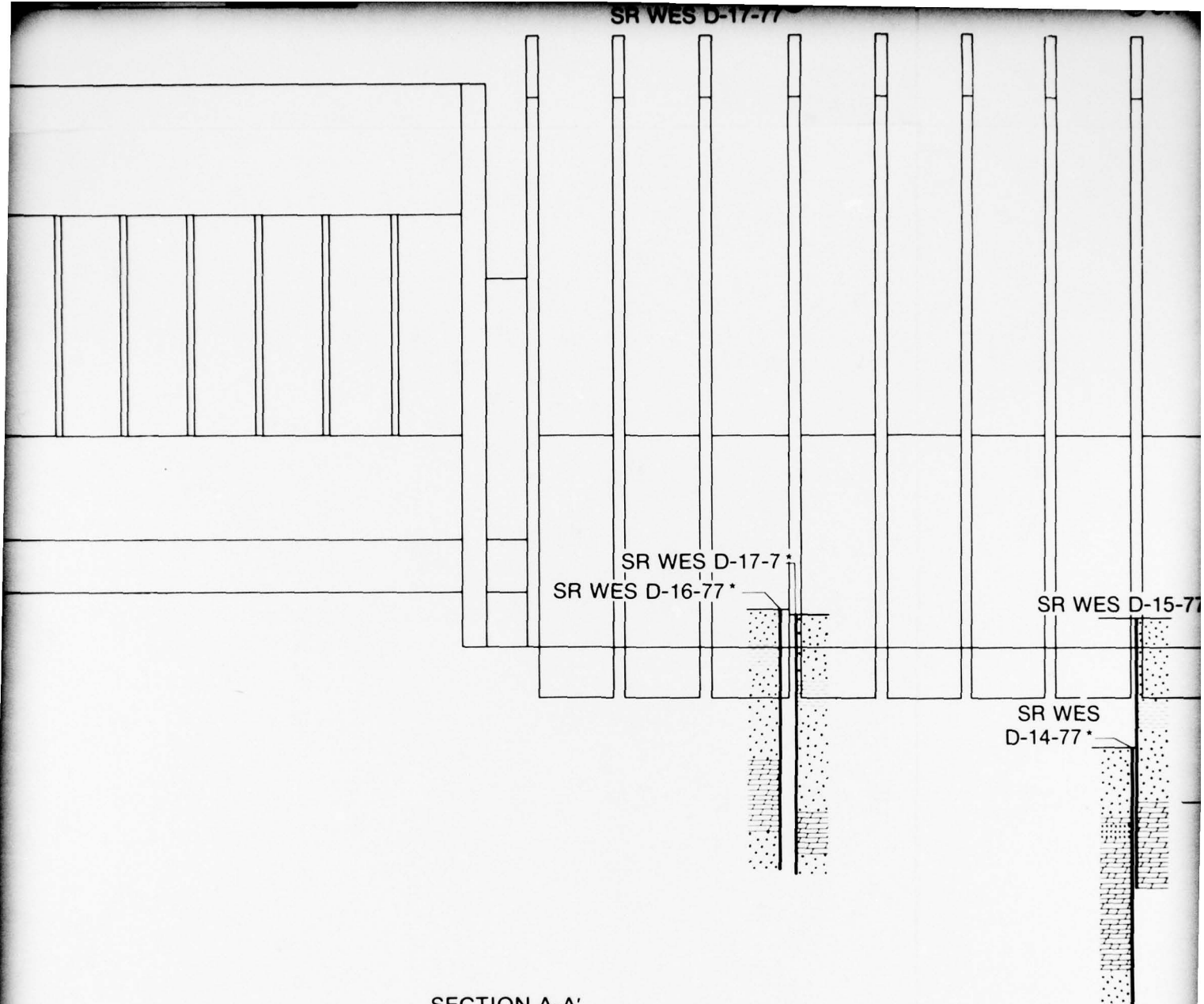
2 of 3
AD-A061 711











SECTION A-A'

LEGEND

DOLOMITE		SANDSTONE
STYLOLITE		CHERT NODULES
CONCRETE		

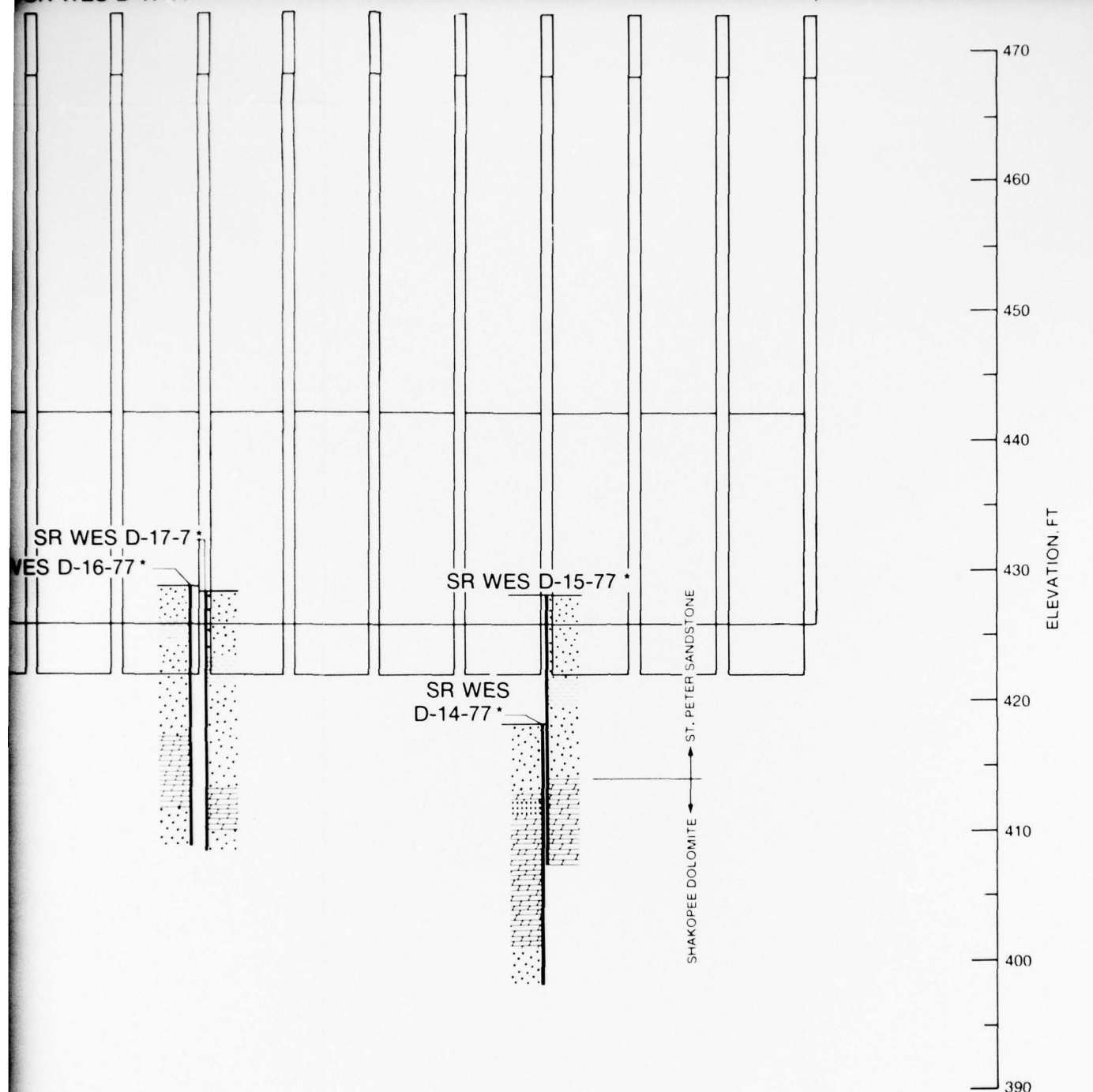
SYMBOL

PROPOSED	DESCRIPTION	COMPLETED
	COMBINATION DRIVE SAMPLE AND CORED	
	6" CORE HOLE	

5

SR WES D-17-77

SR WES D-15-77



SYMBOL

DESCRIPTION

COMPLETED

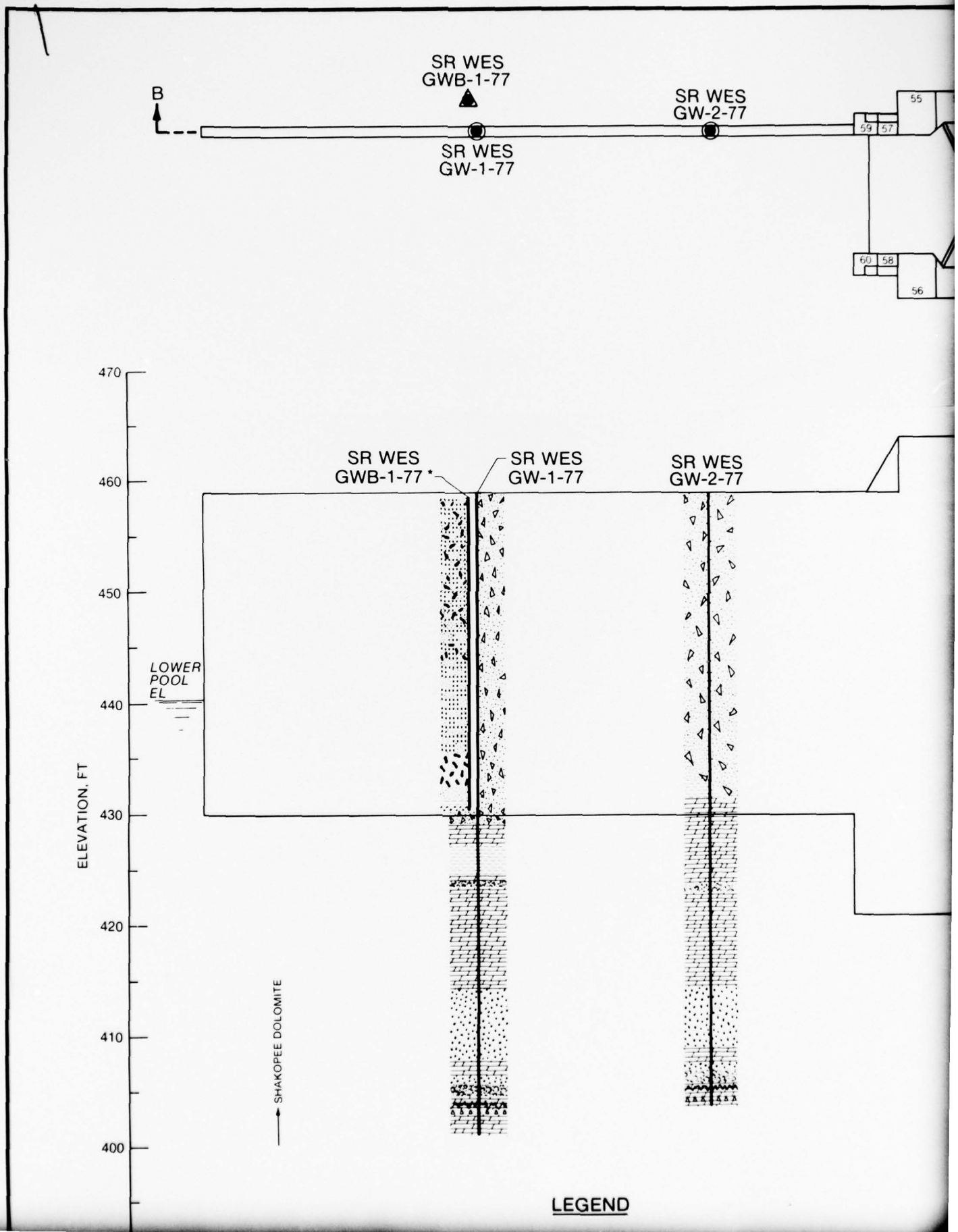


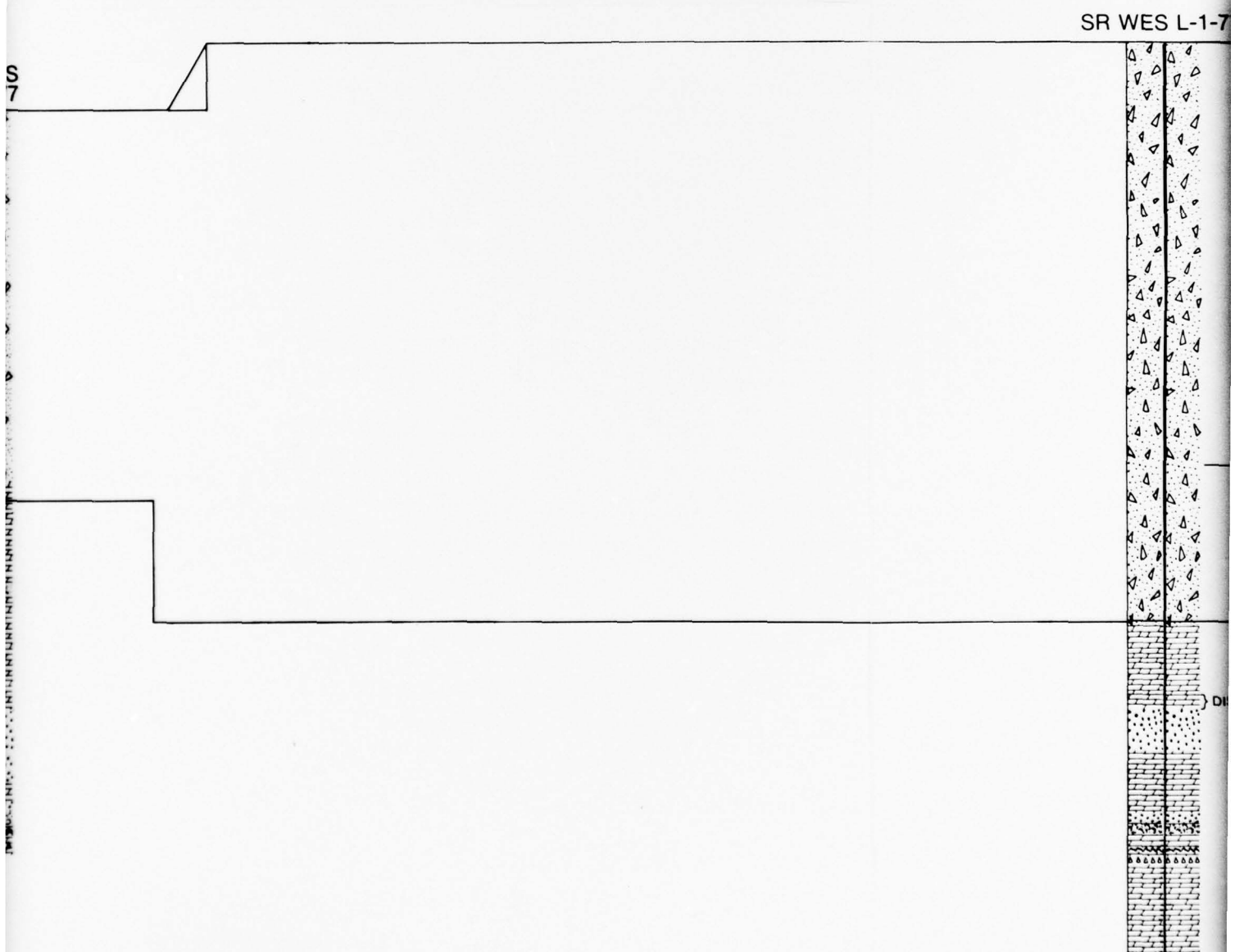
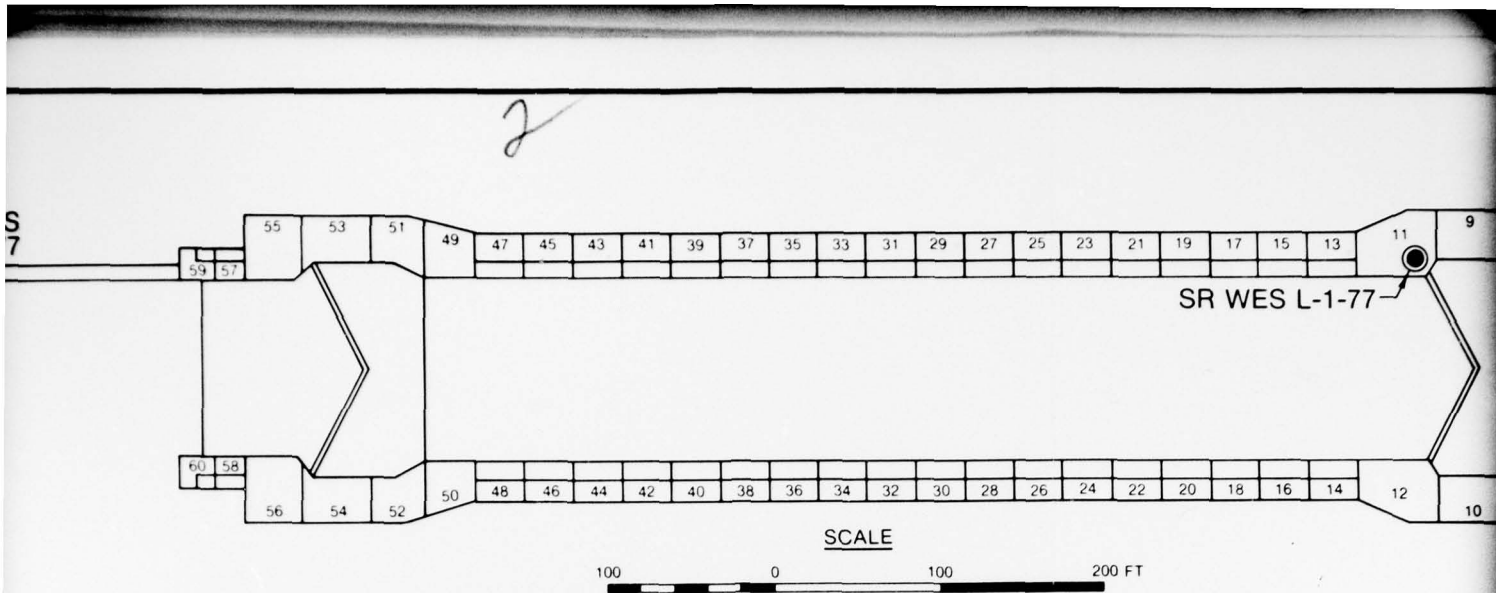
OMBINATION DRIVE
AMPLE AND CORED
CORE HOLE

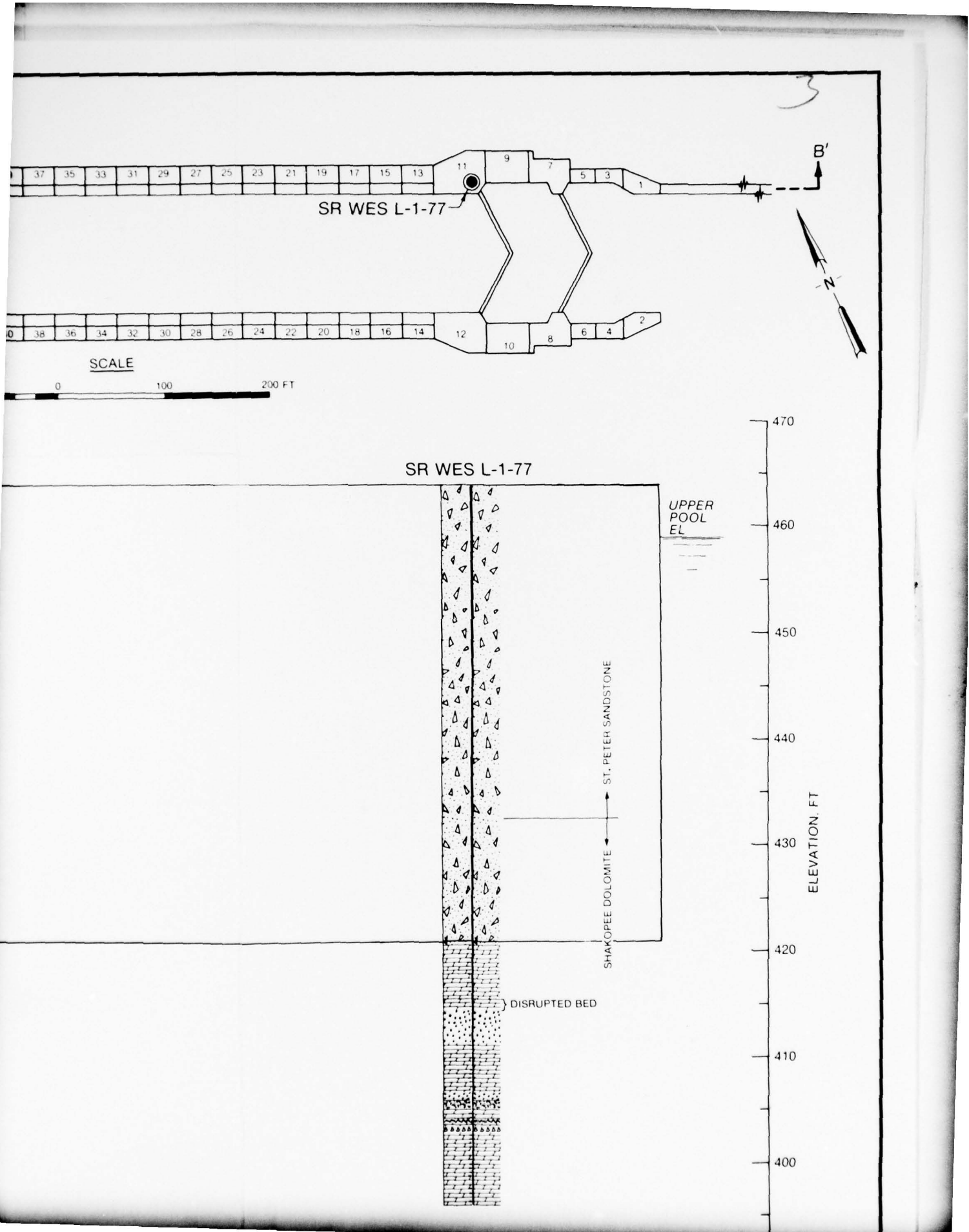


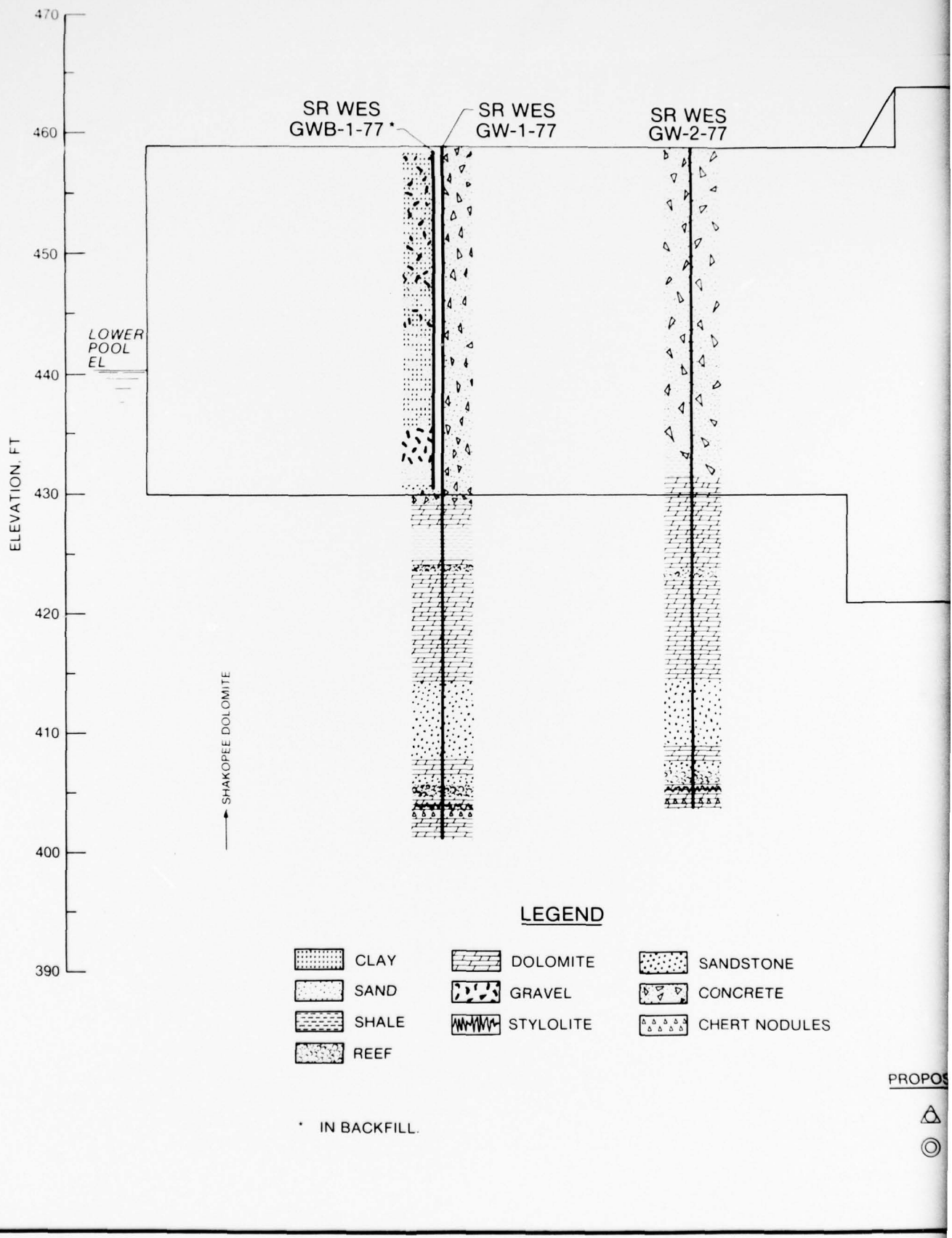
REHABILITATION PHASE
STARVED ROCK LOCK AND DAM
ILLINOIS WATERWAY

GEOLOGIC CROSS SECTION
SECTION A-A'









SCALE

100 0 100 200 FT

SR WES L-1-71



SECTION B-B'

NDSTONE

INCRETE

ERT NODULES

SYMBOL

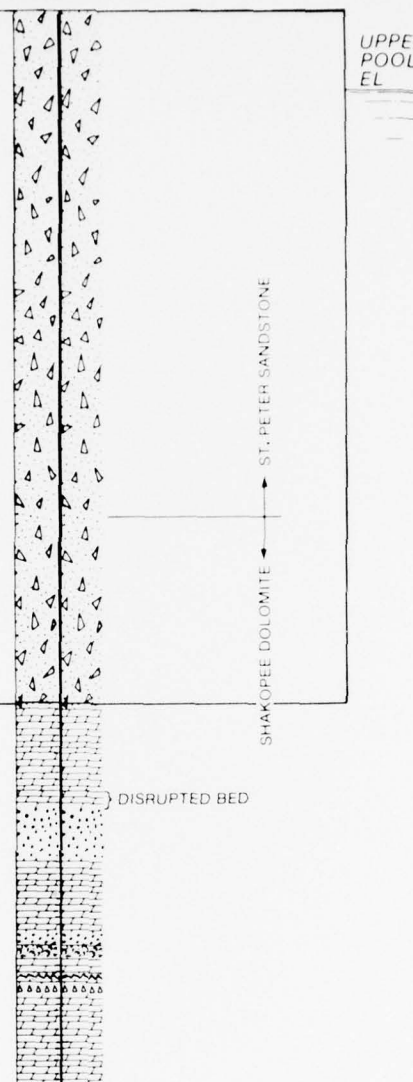
<u>PROPOSED</u>	<u>DESCRIPTION</u>	<u>COMPLETED</u>
△	COMBINATION DRIVE SAMPLE AND CORED	▲
○	6" CORE HOLE	●

5

SCALE

0 100 200 FT

SR WES L-1-77



ELEVATION, FT

SECTION B-B'

COMPLETED



REHABILITATION PHASE
STARVED ROCK LOCK AND DAM
ILLINOIS WATERWAY

GEOLOGIC CROSS SECTION
SECTION B-B'

b

PLATE 9

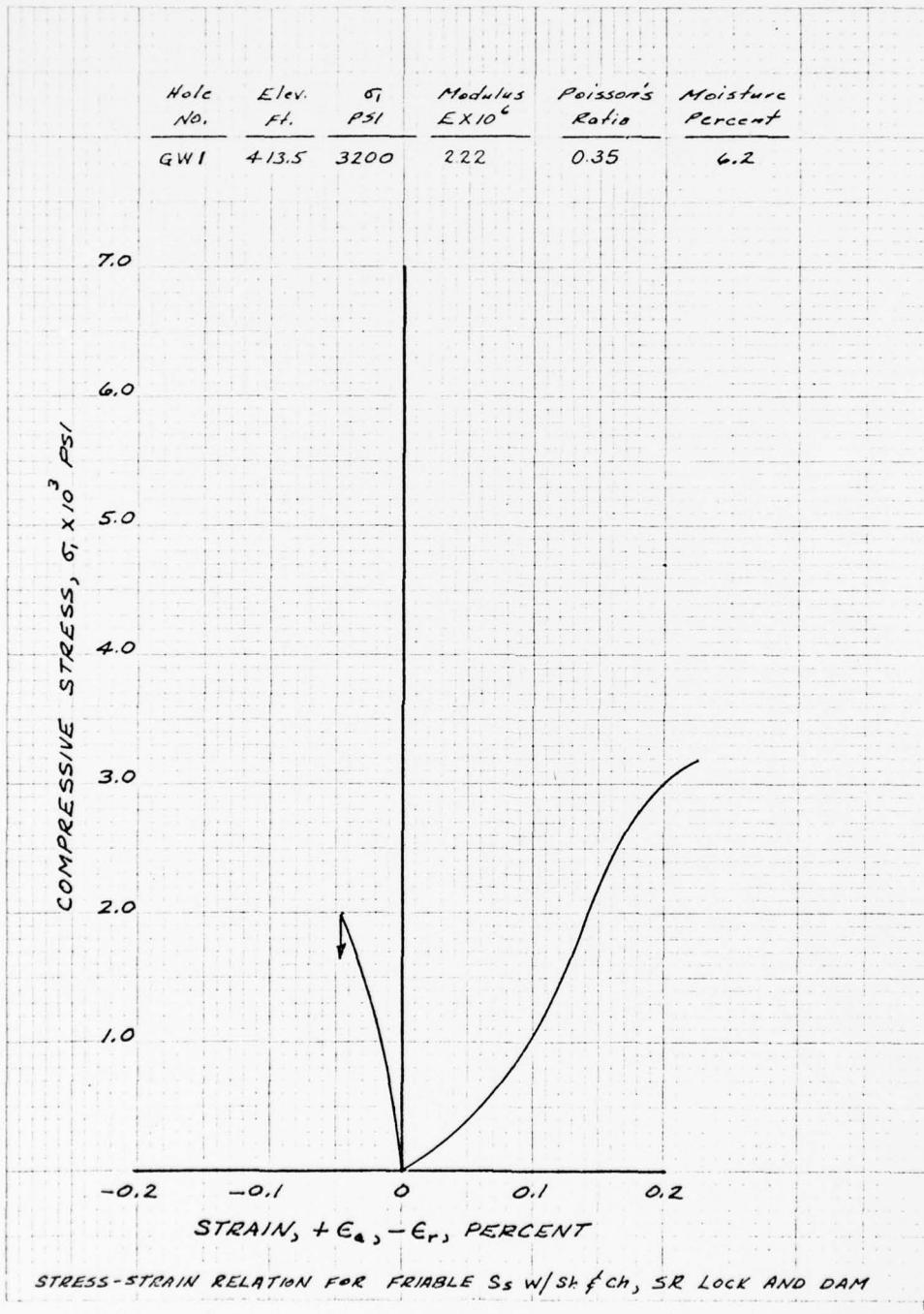


PLATE 10

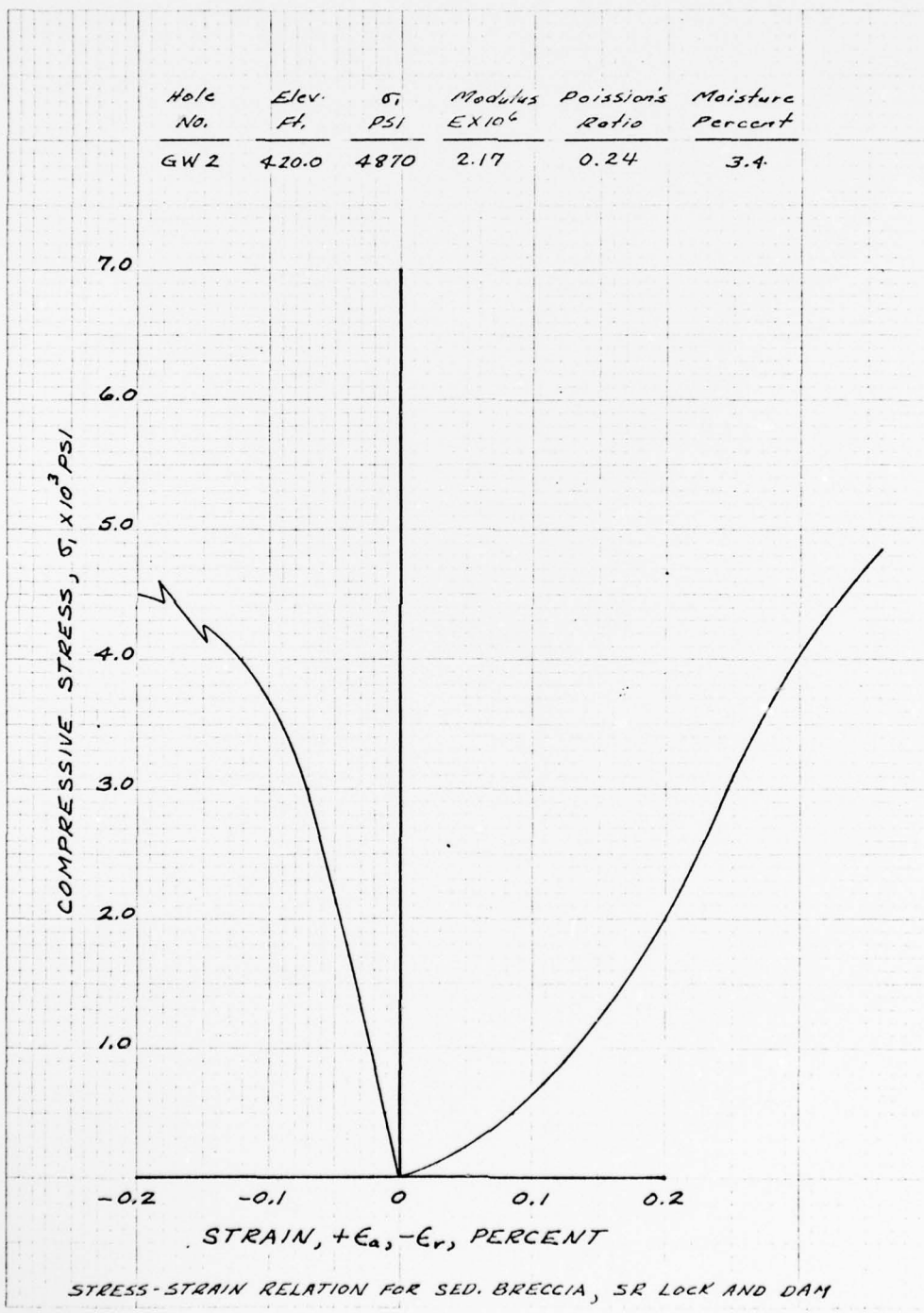


PLATE 11

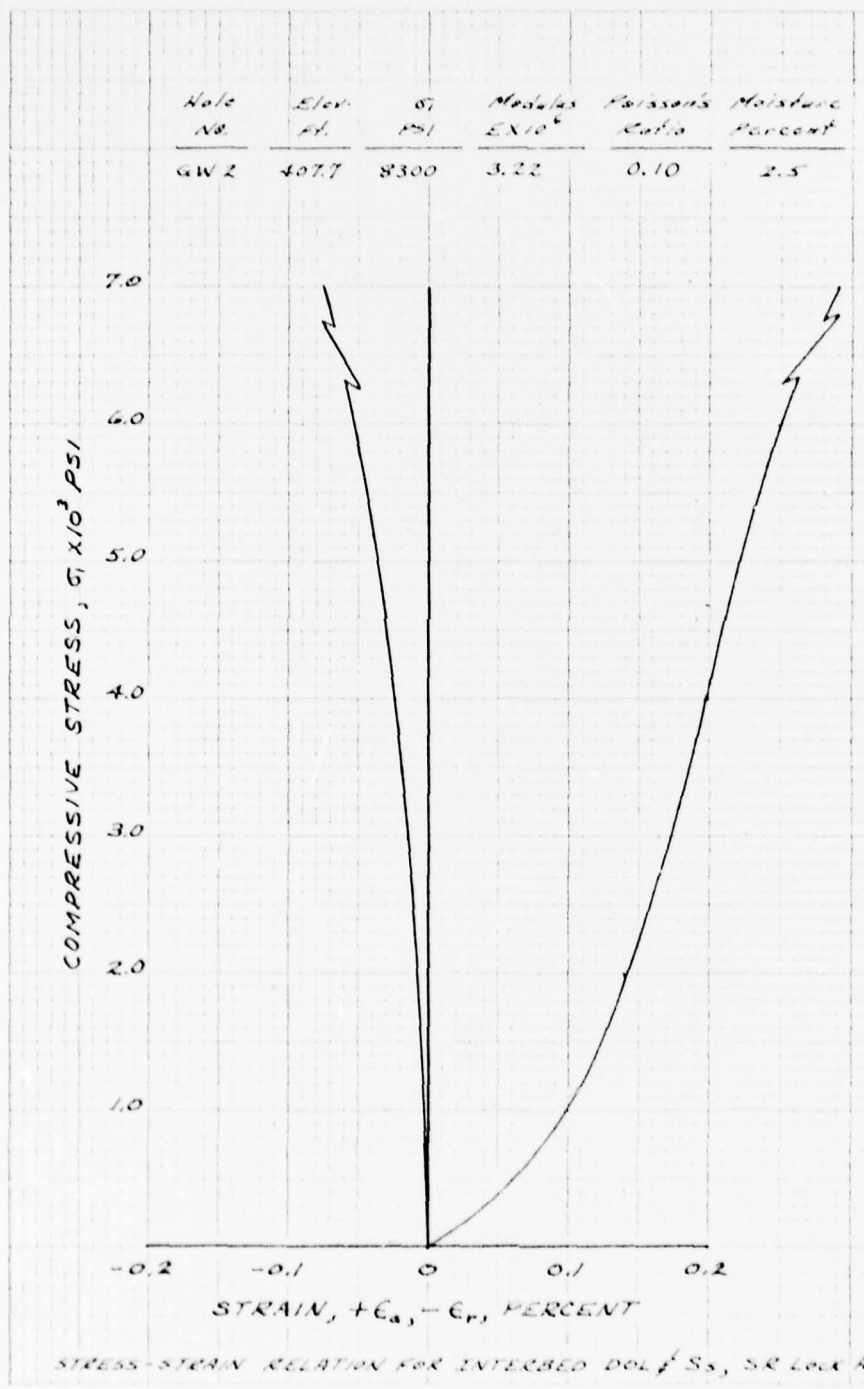


PLATE 12

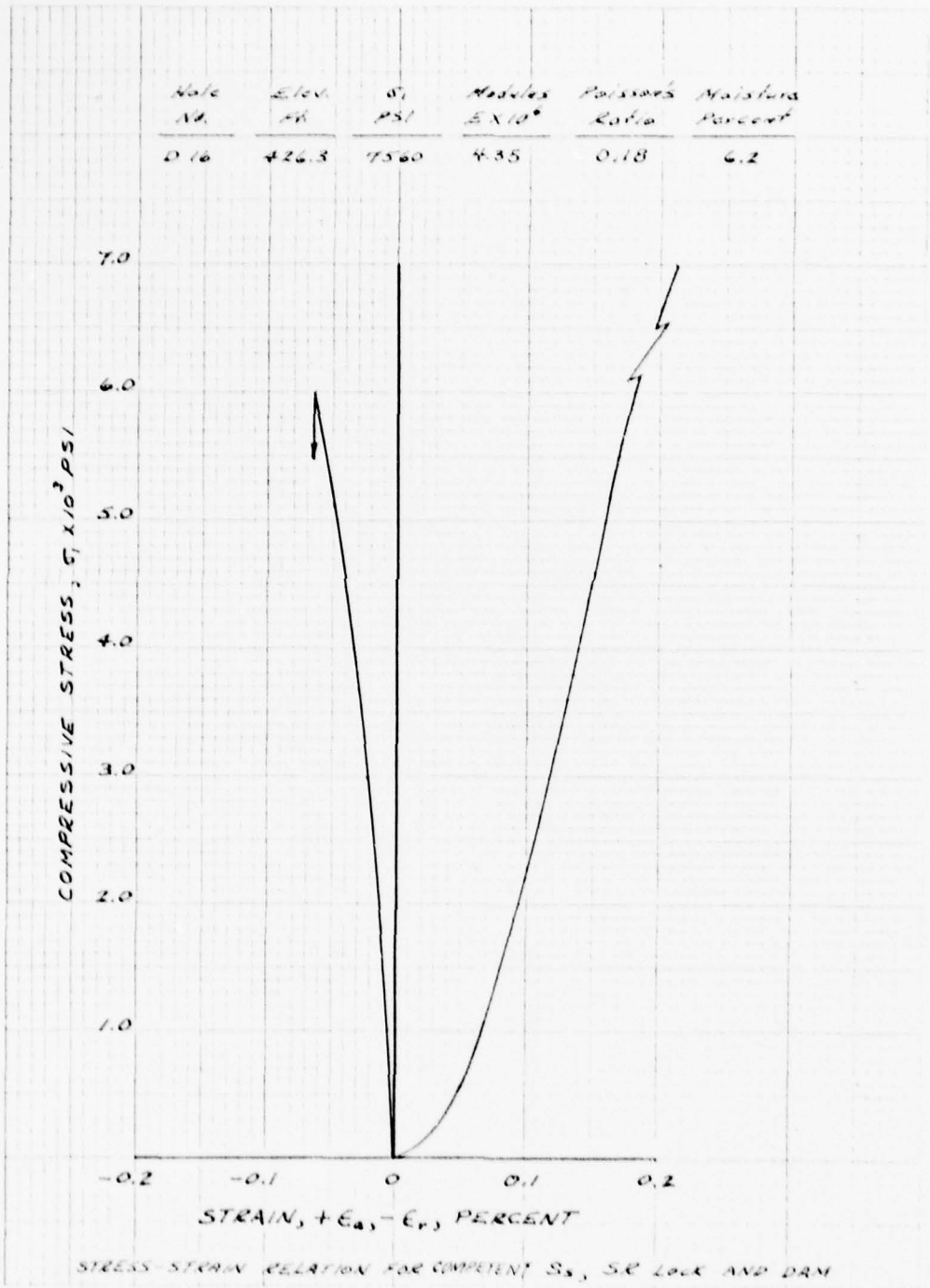


PLATE 13

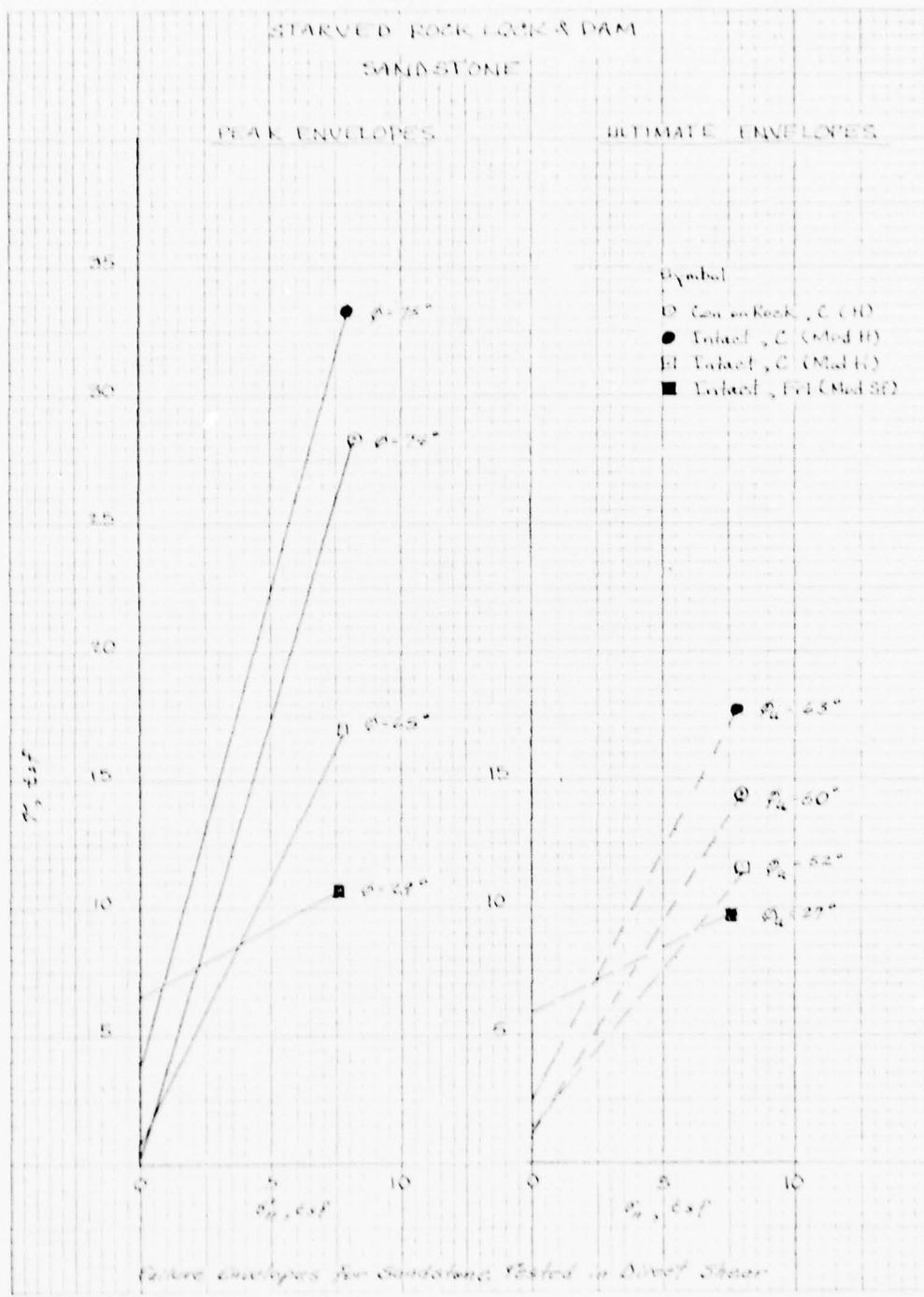


PLATE 14

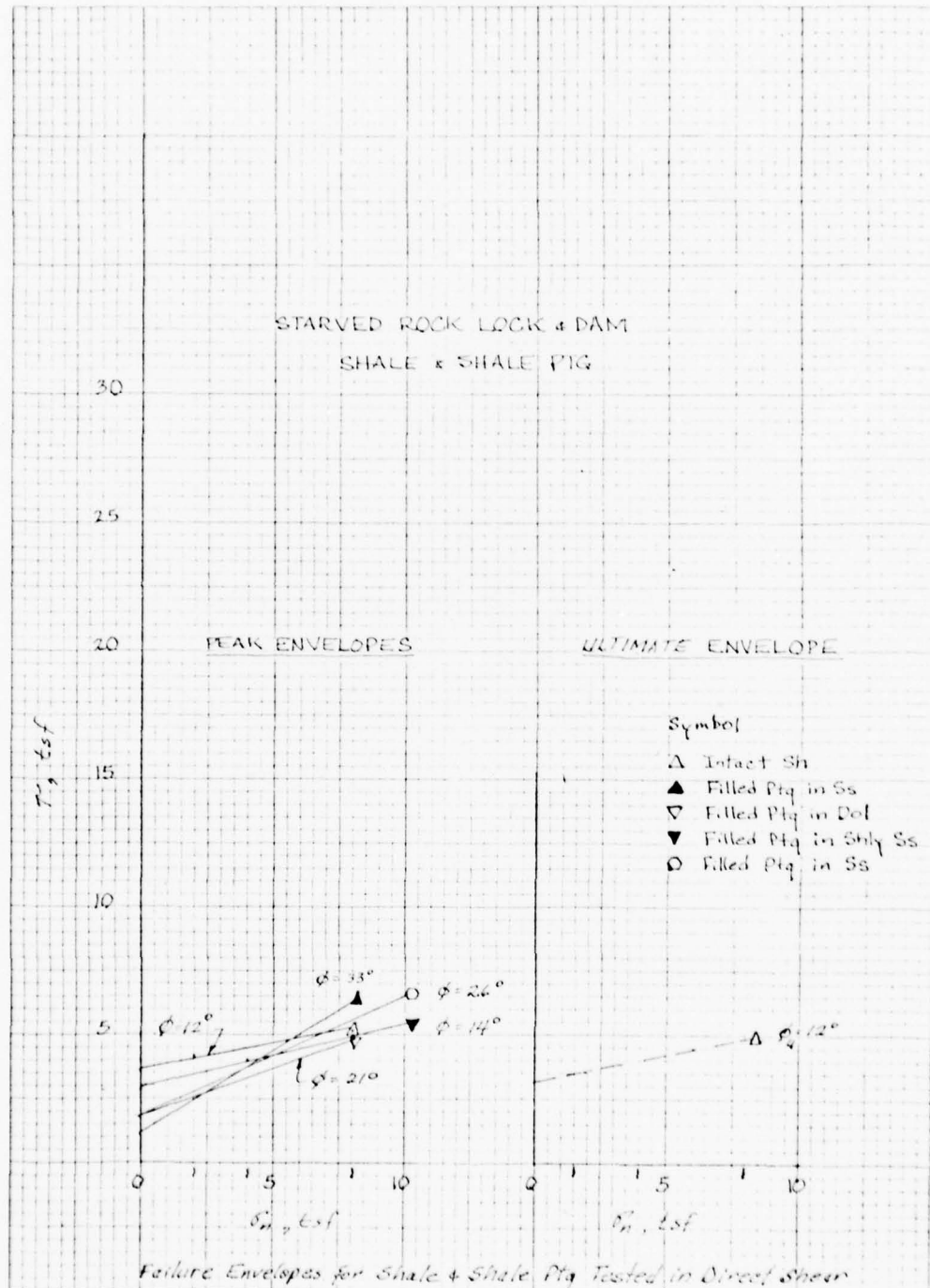
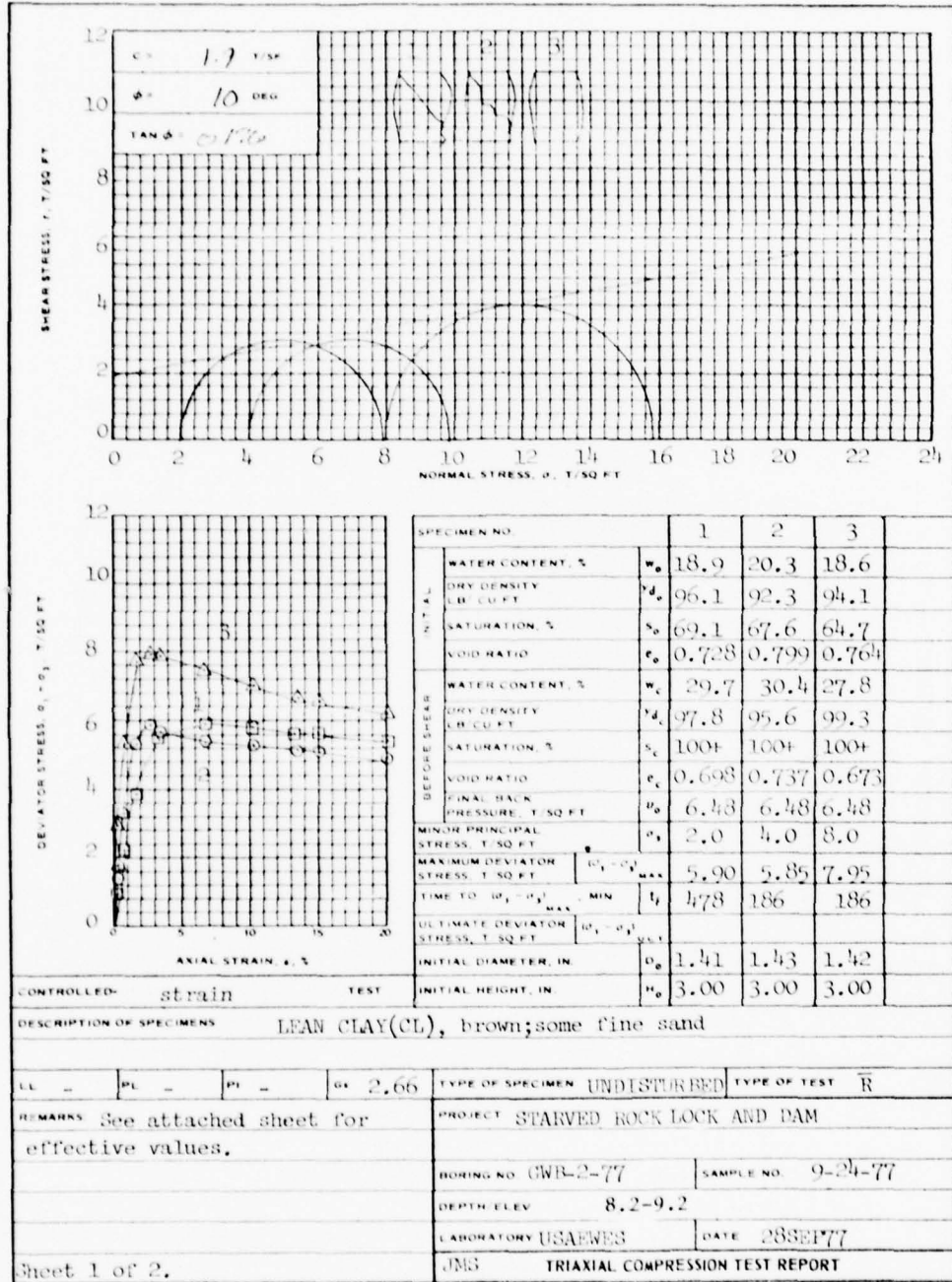
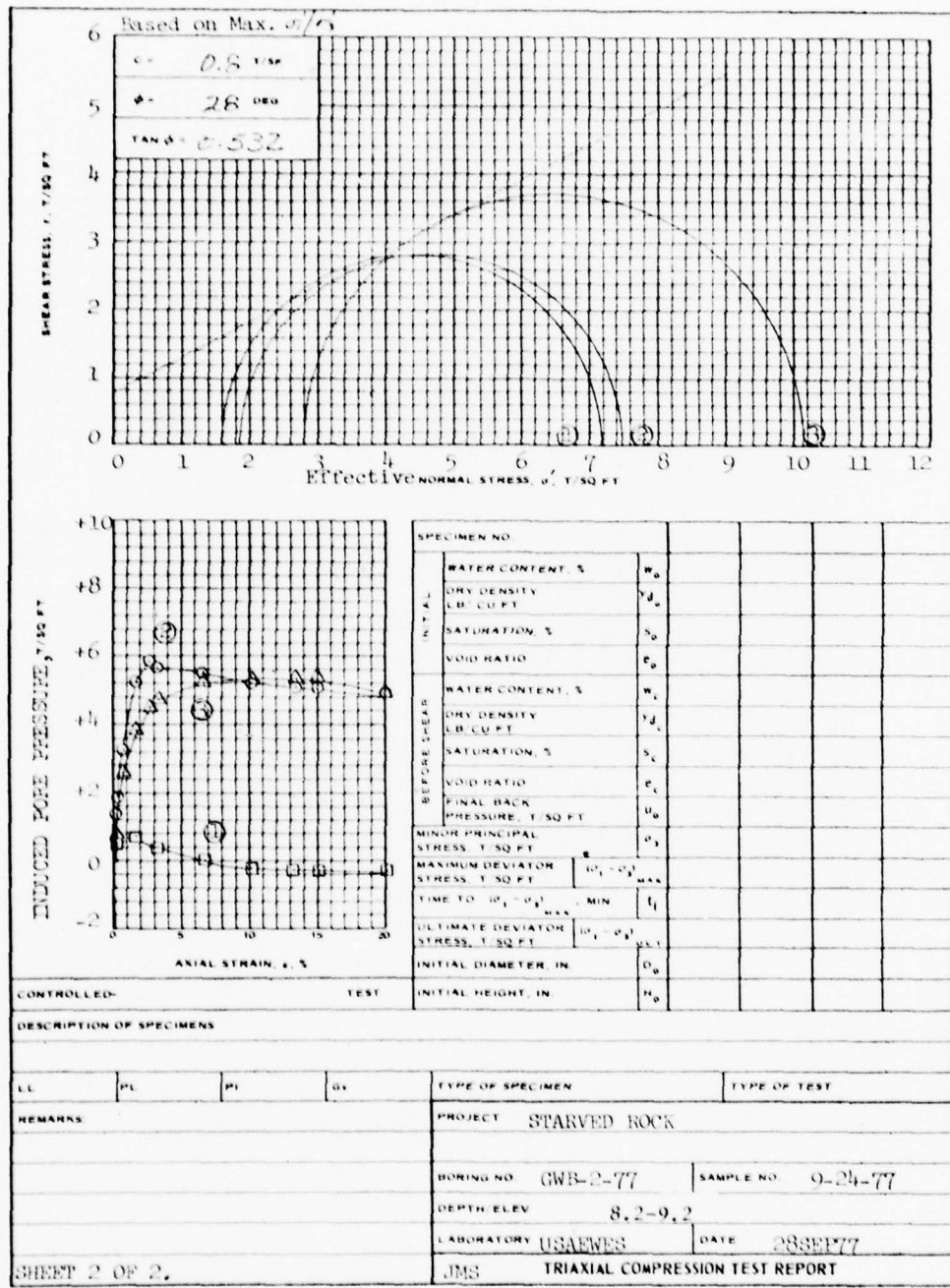
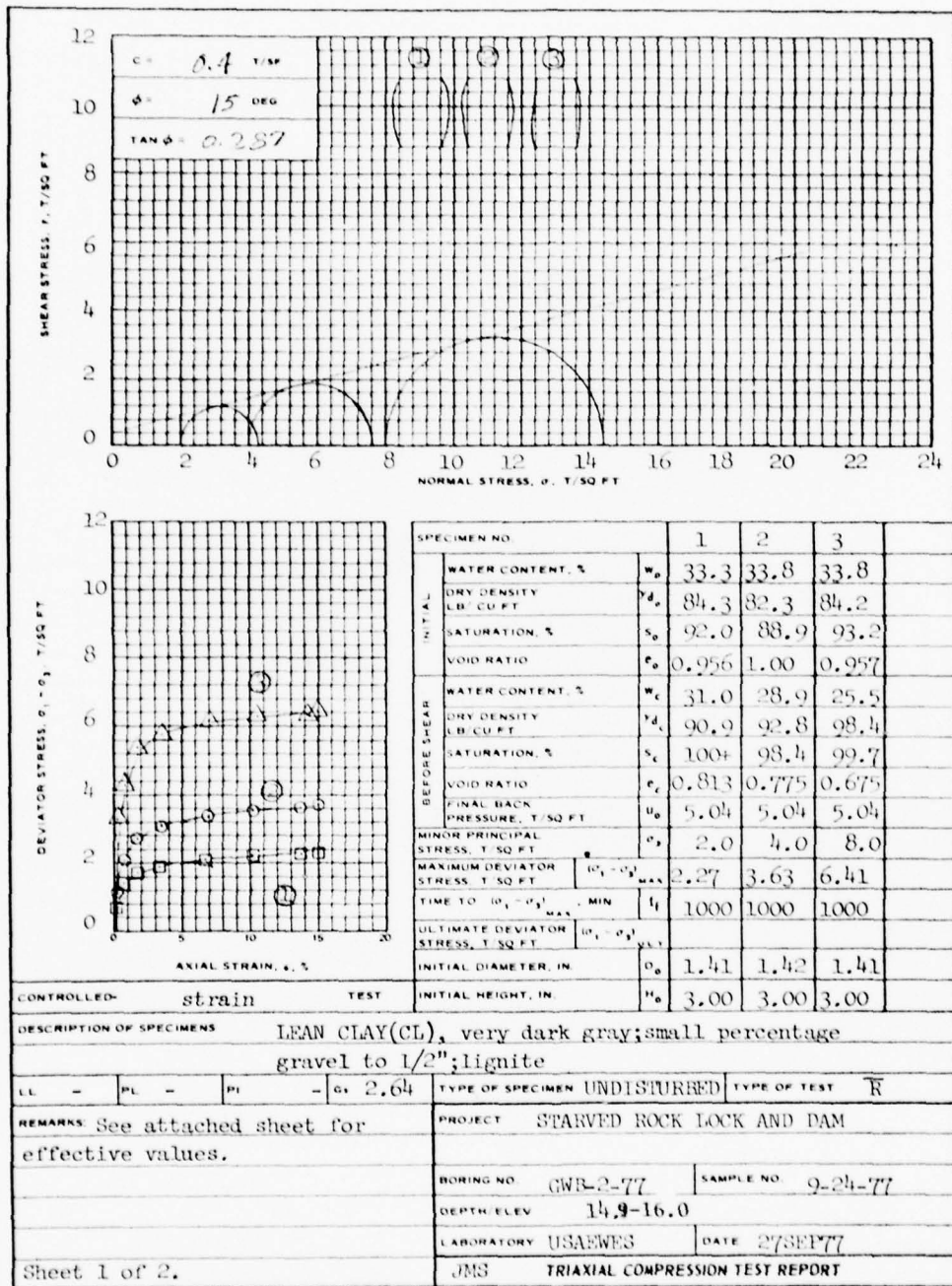
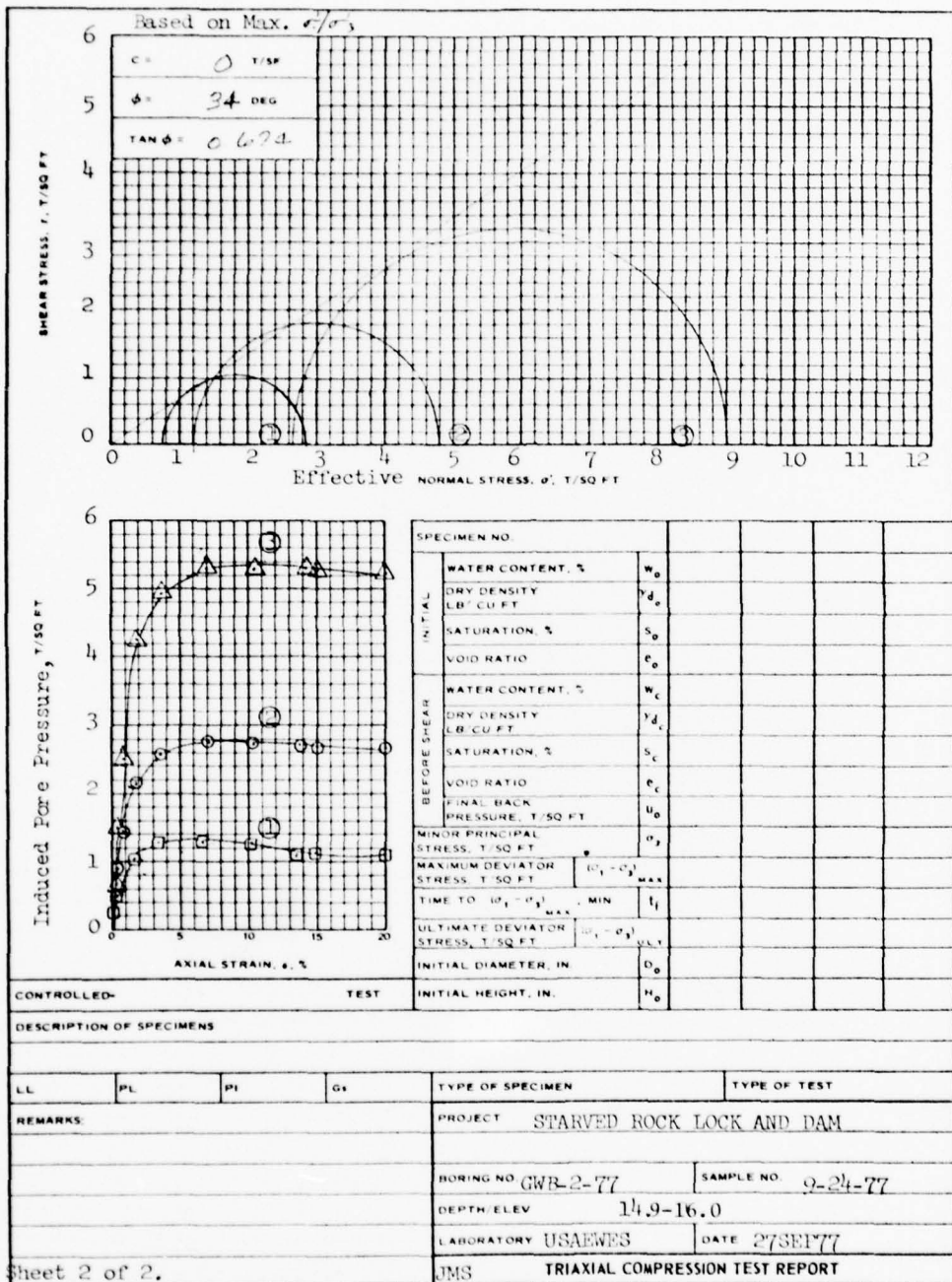


PLATE 15







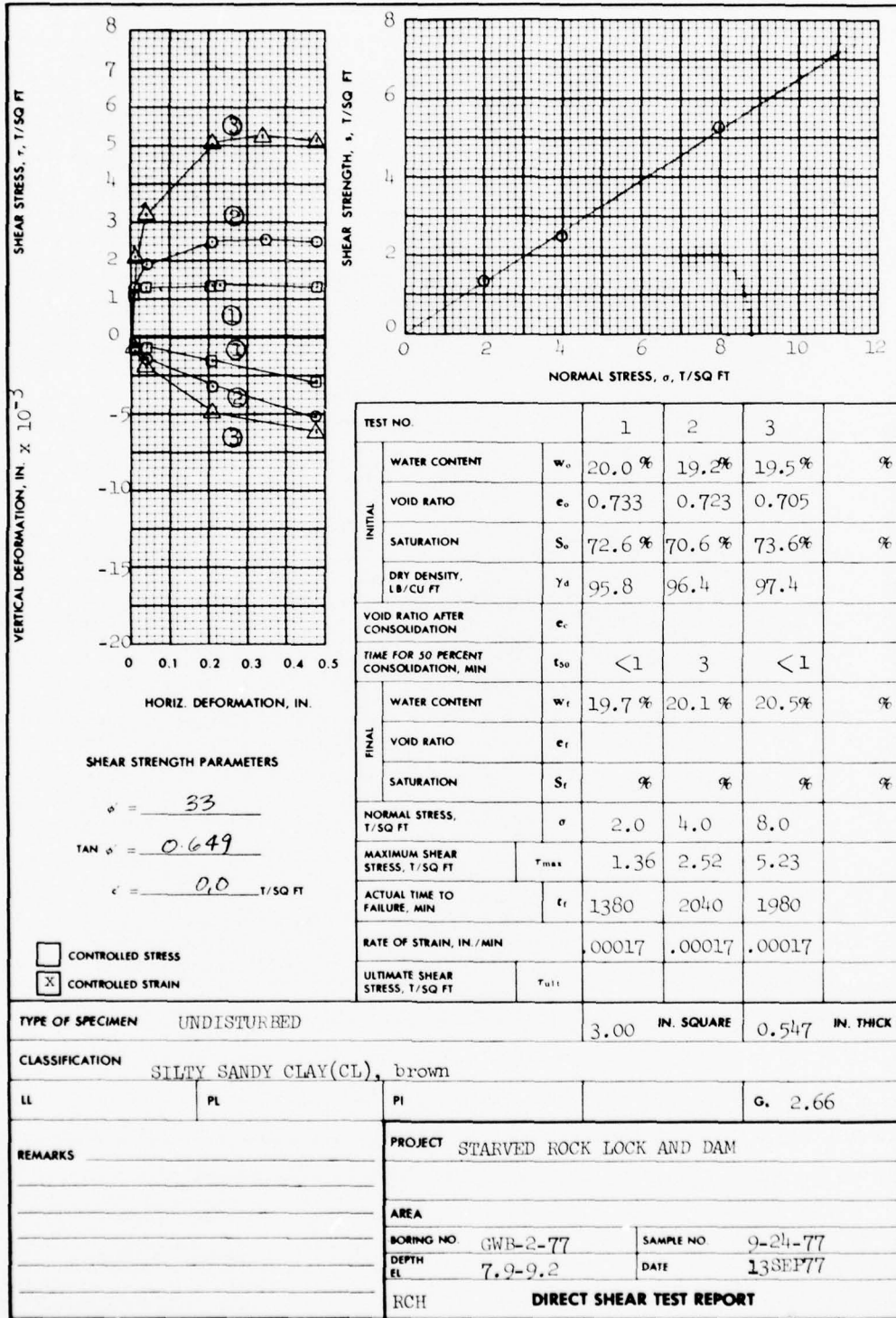


ENG FORM NO. 2089 PREVIOUS EDITION IS OBSOLETE
REV JUNE 1970

TRANSLUCENT

(EM 1110-2-1906)

PLATE 19



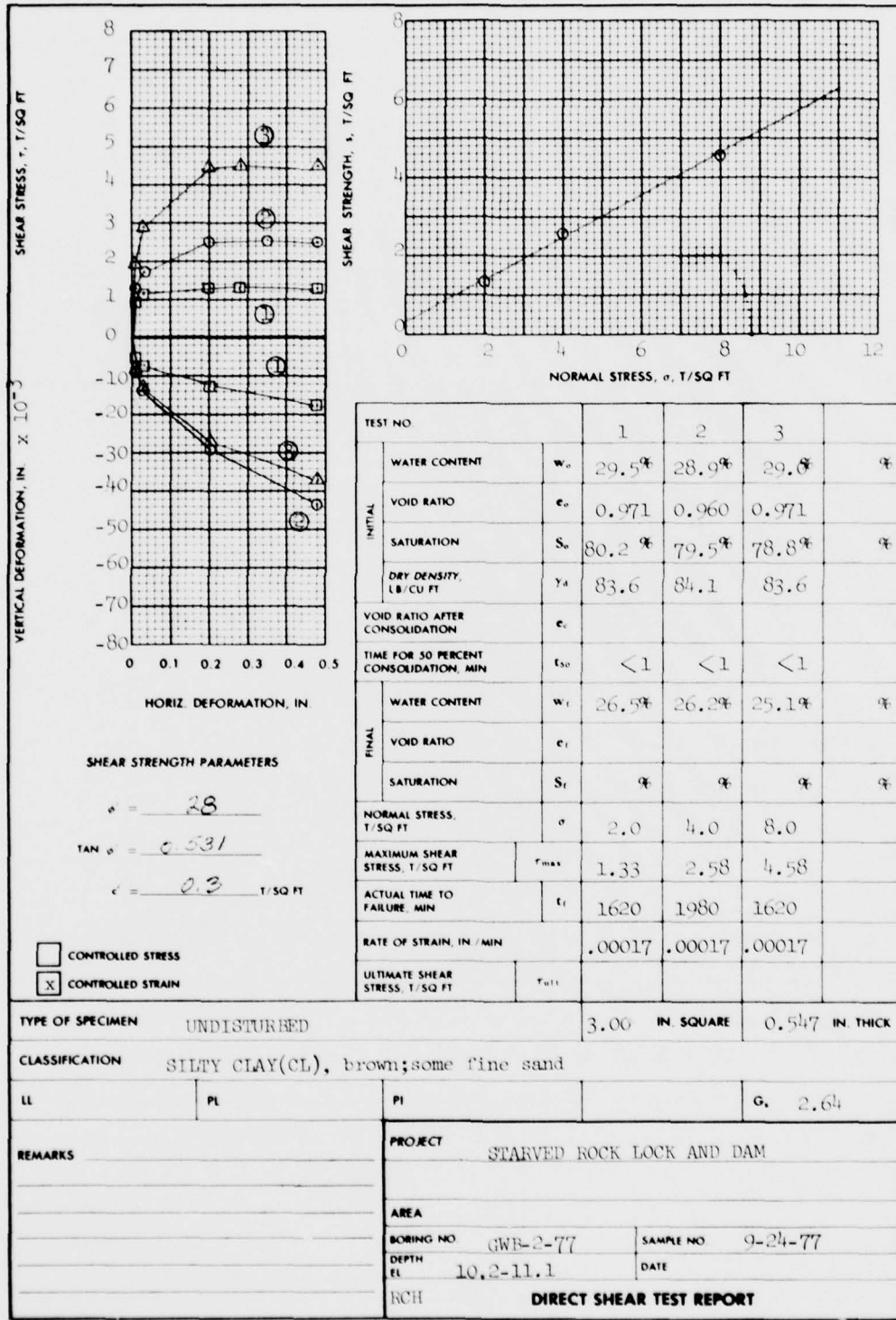
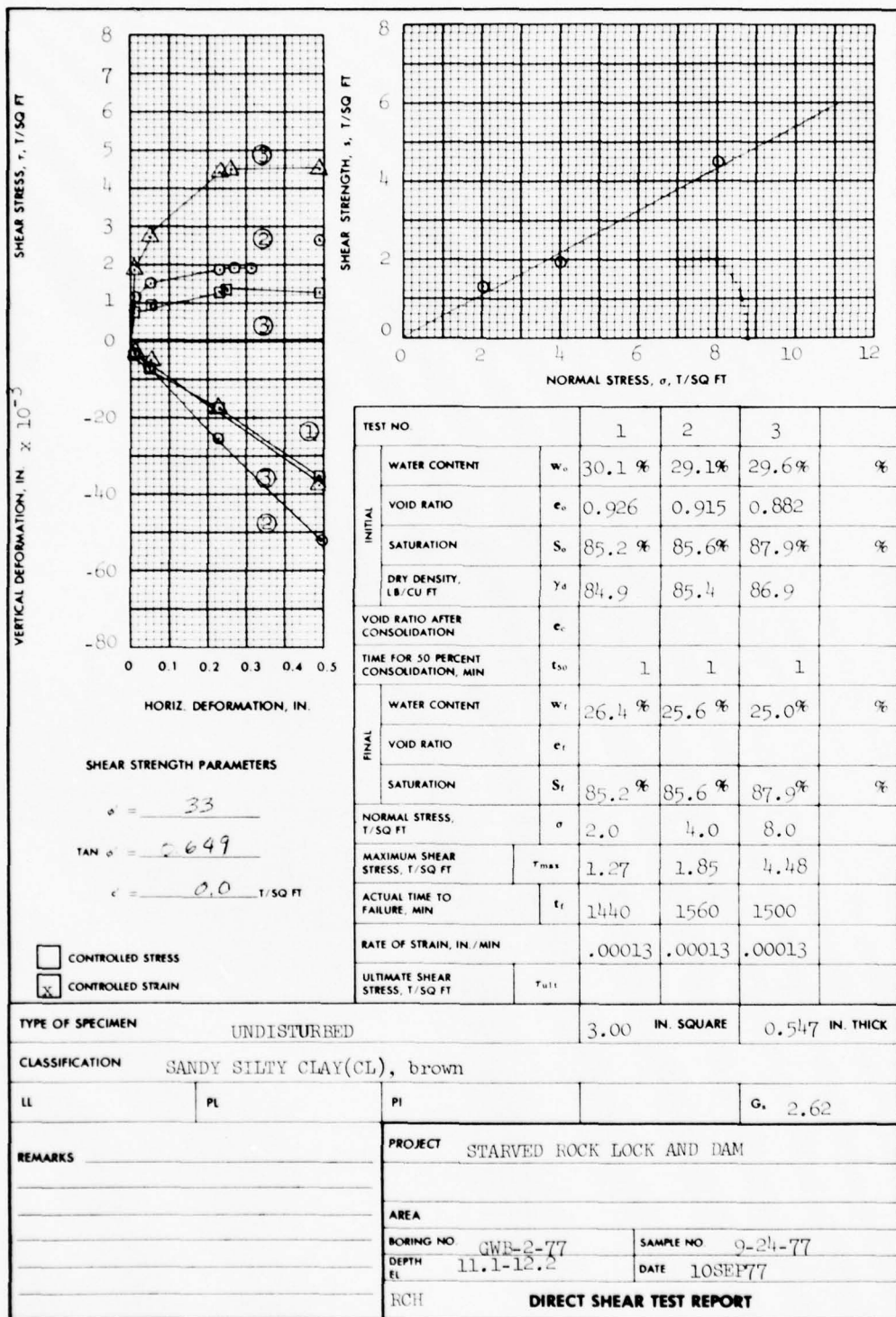
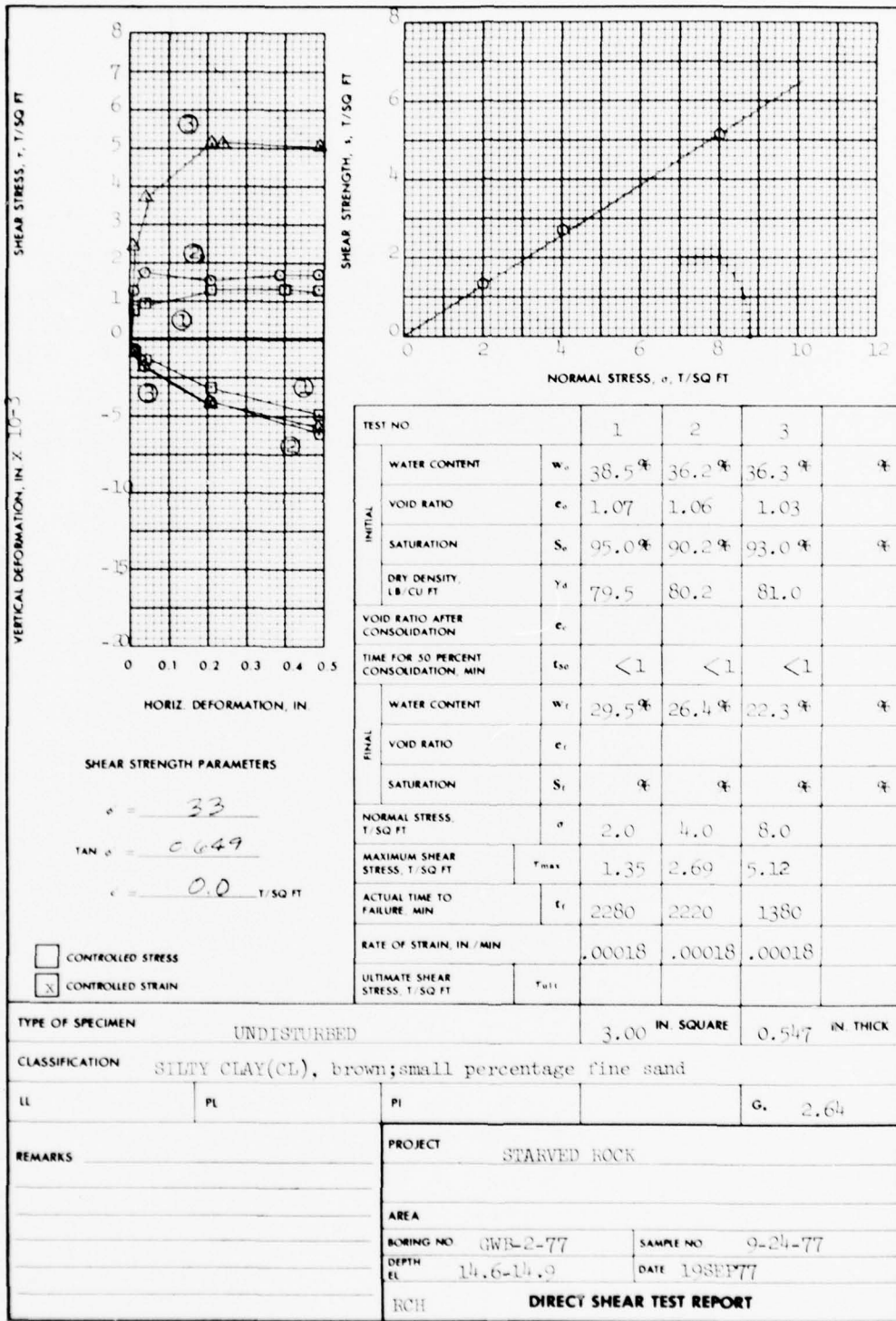


PLATE 21



6



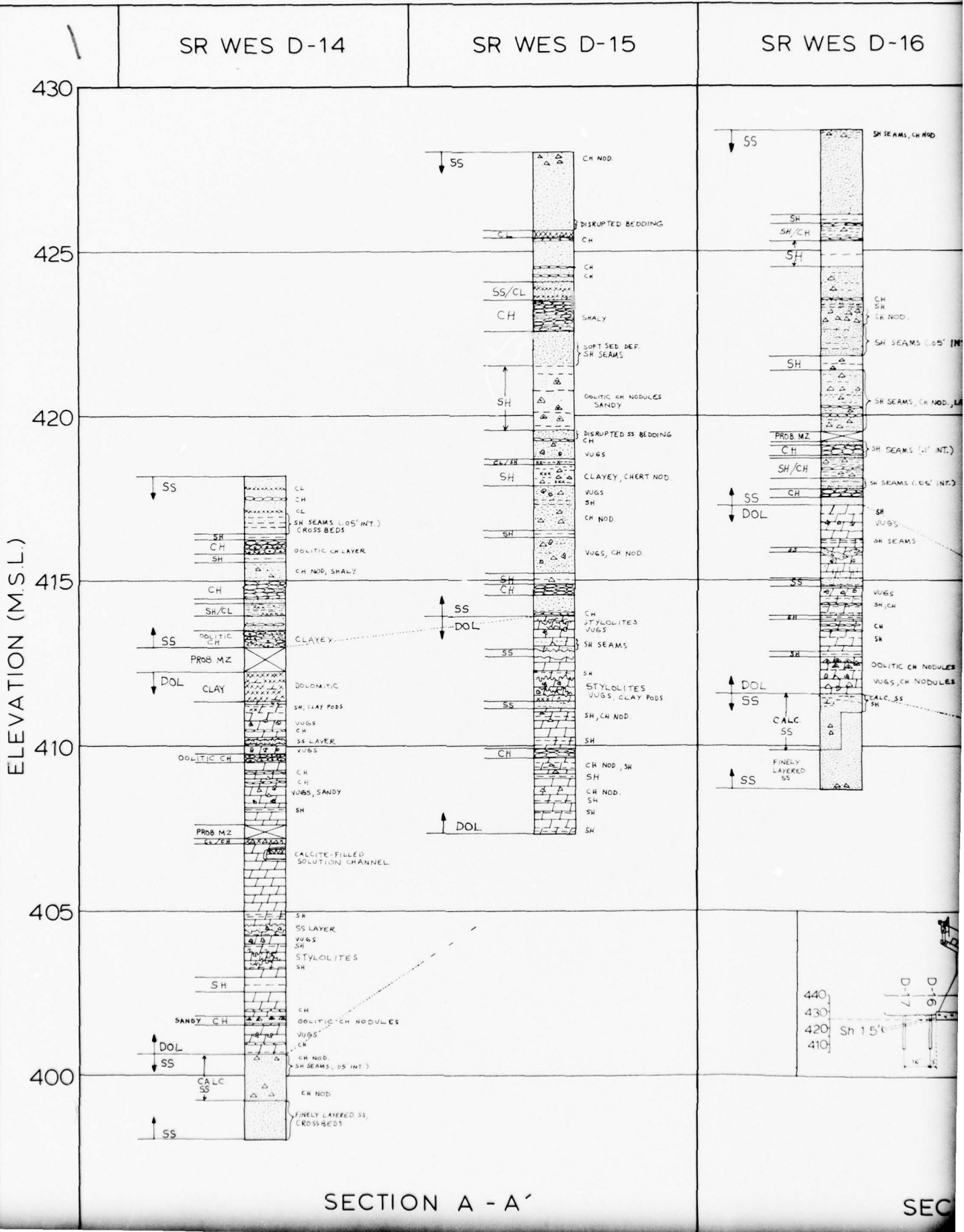
APPENDIX A

DETAIL GEOLOGIC AND
STRUCTURAL CROSS SECTIONS

STARVED ROCK LOCK AND DAM
ILLINOIS WATERWAY

DETAIL GEOLOGIC AND
STRUCTURAL CROSS SECTIONS

Because of the complex nature of the foundation, it was necessary to draw detail geologic and structural cross sections. The sections were used to assist in the selection of representative rock for laboratory testing and to correlate strata over the lock and dam site. The geologic sections were made first and were used to compile the general log of borings and the geologic cross sections presented in the text. Boring and section lines are shown on key location maps on each of the four cross section plates.

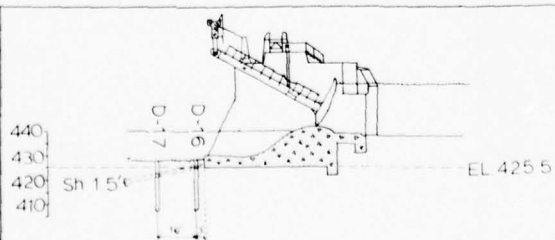
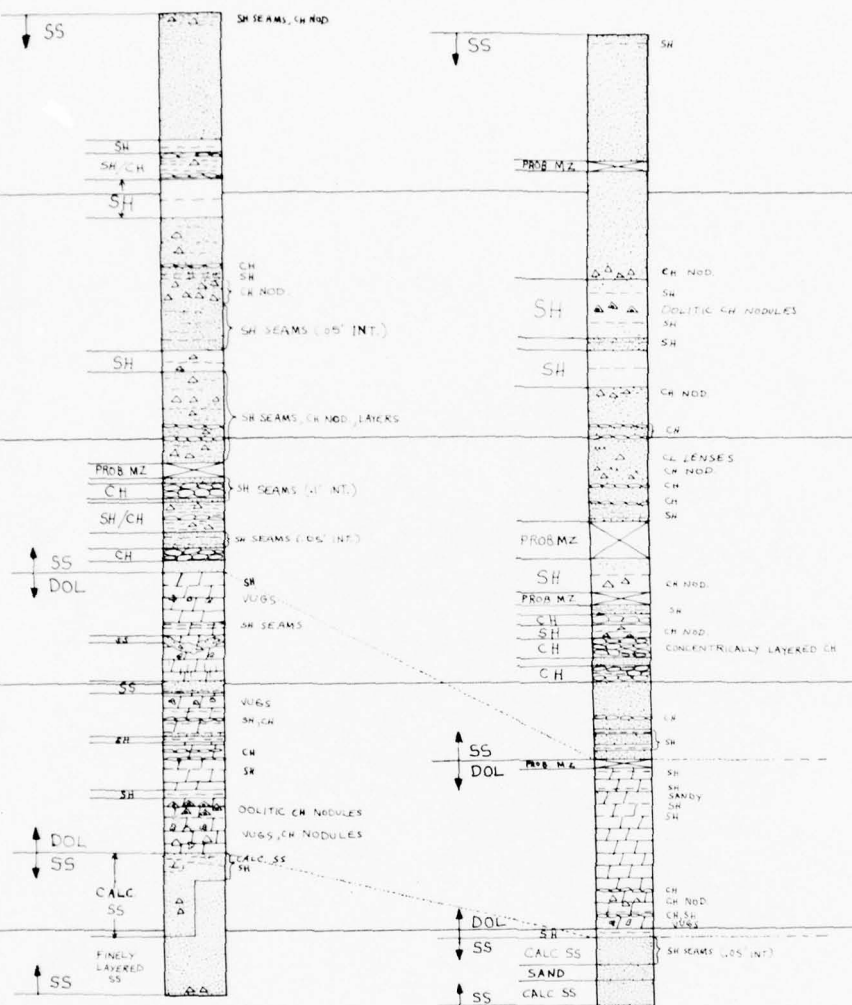


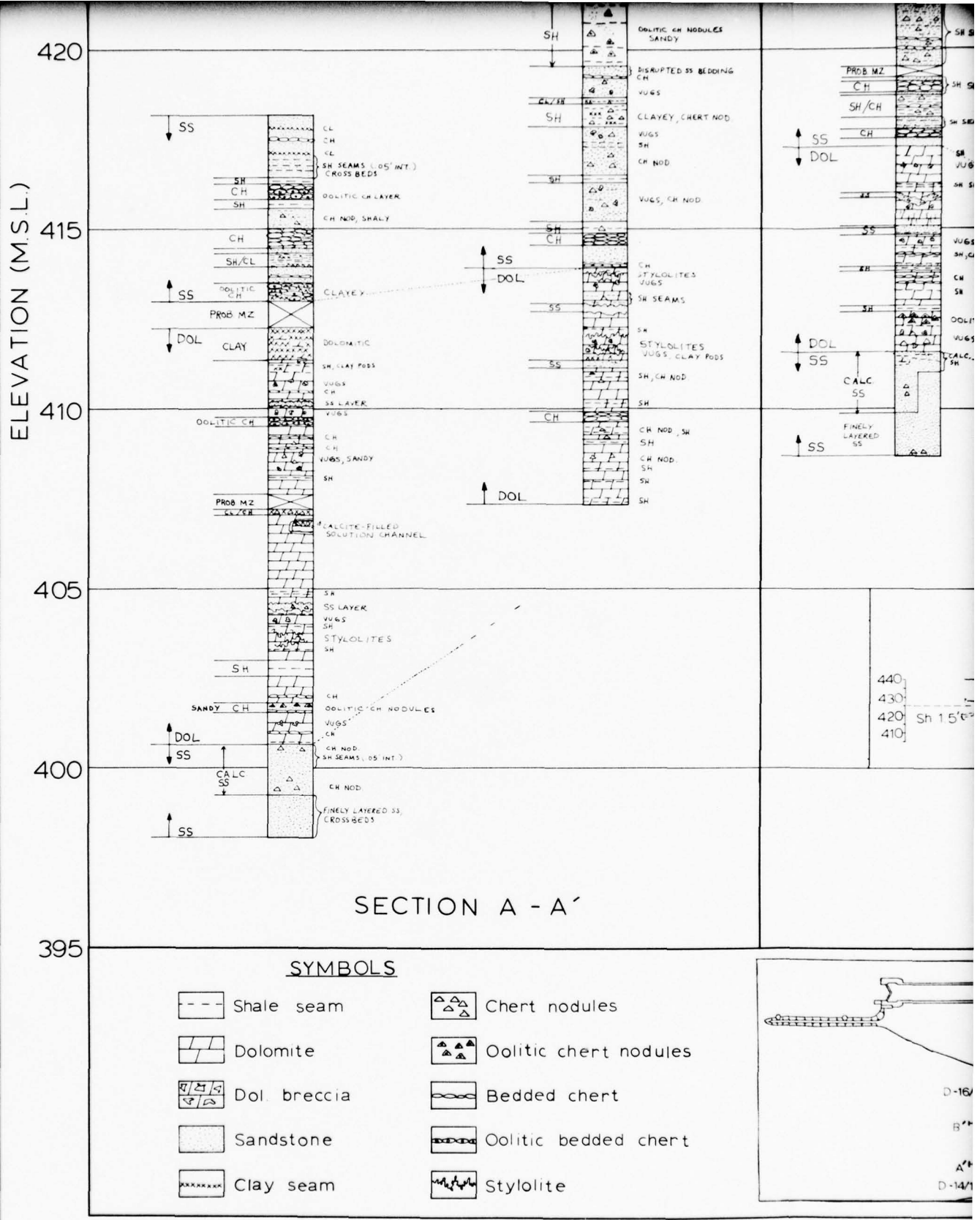
D-15

SR WES D-16

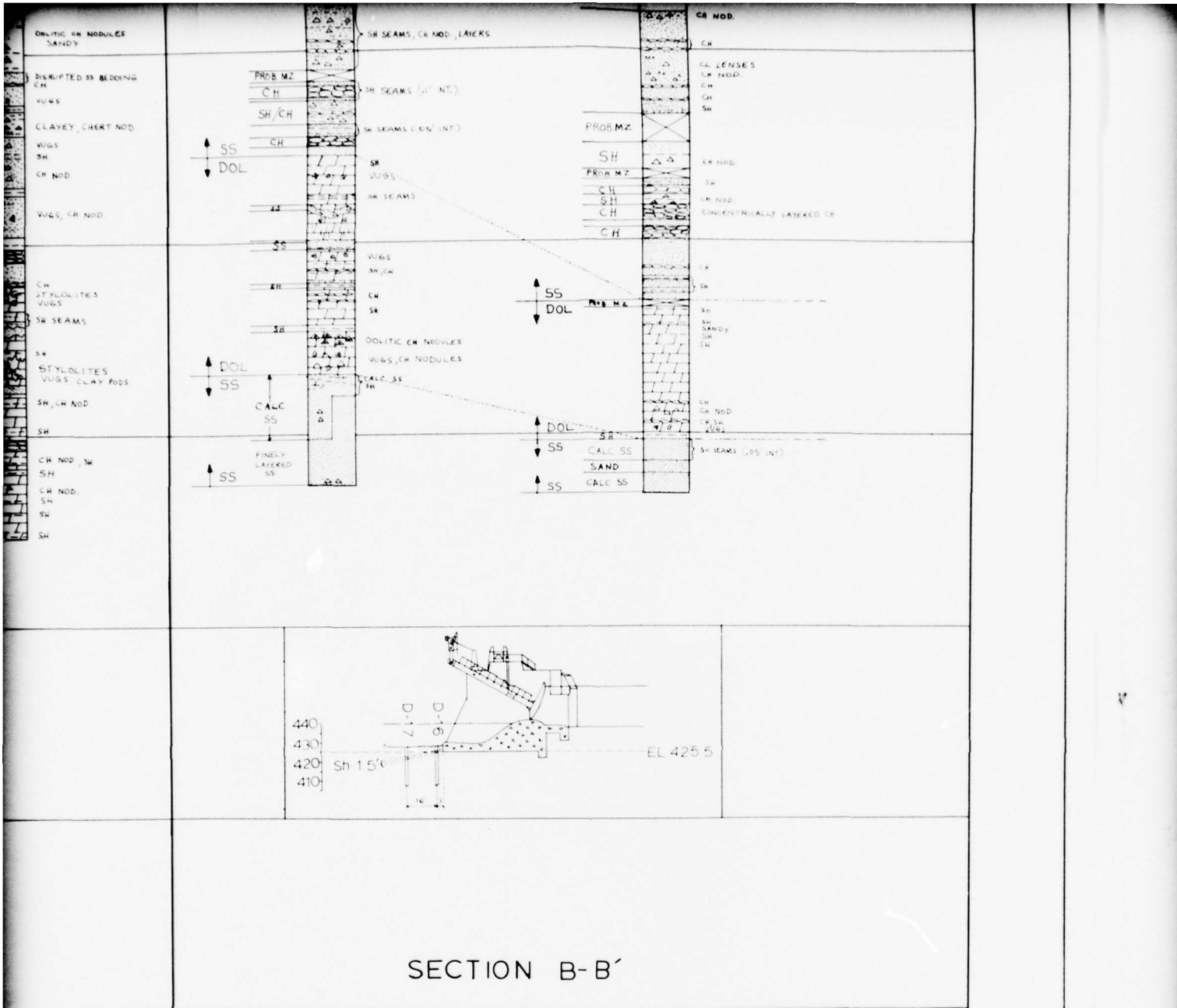
SR WES D-17

2



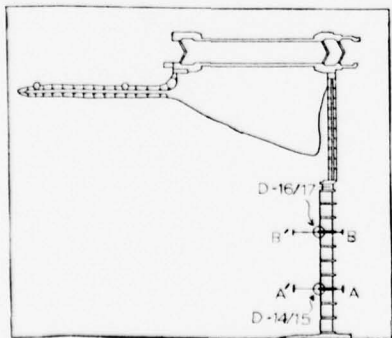


SECTIONS A-A' & B-B'



SECTION B-B'

s
nODULES
rt
ed chert

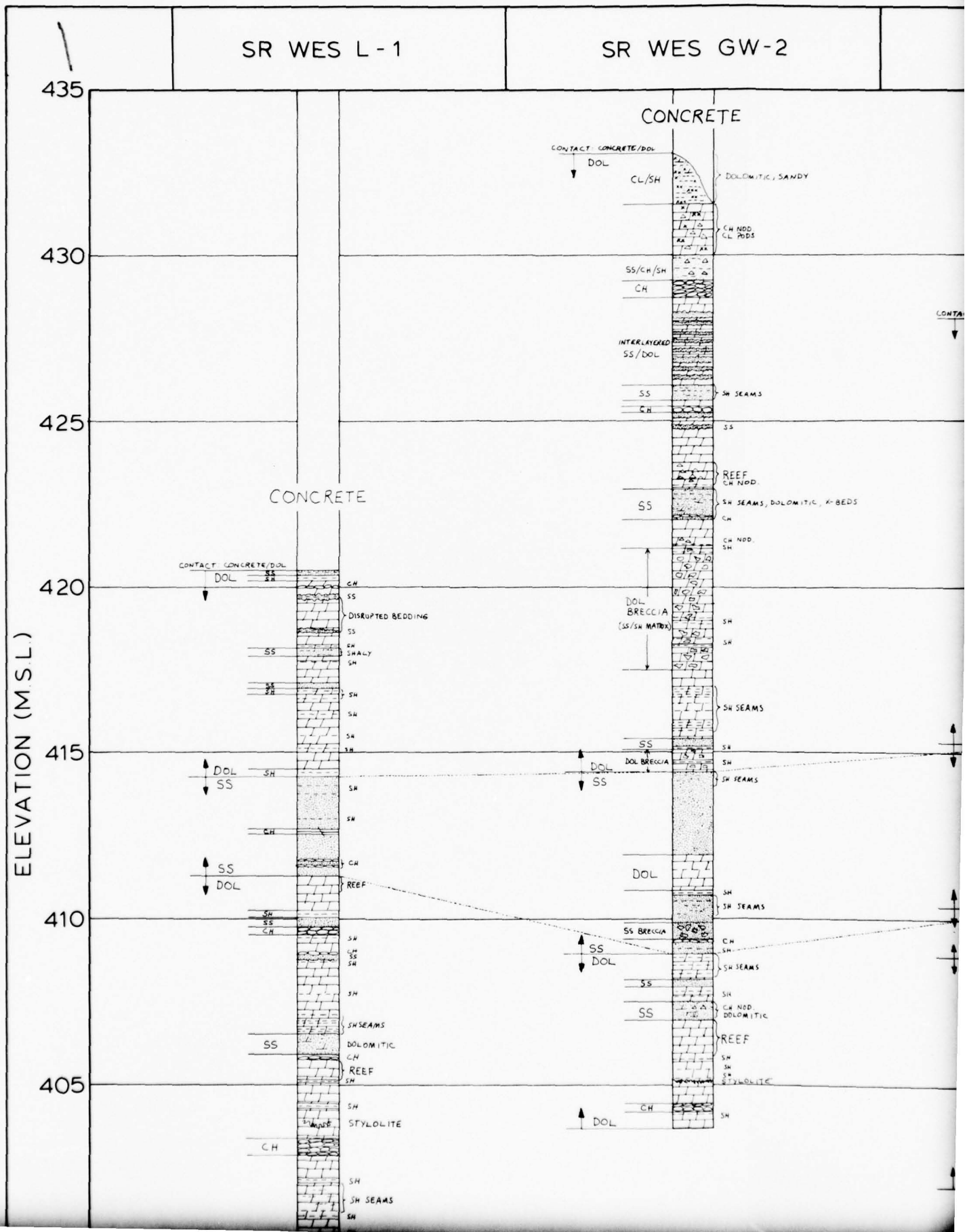


PREPARED FOR
U. S. ARMY ENGINEER DISTRICT
CORPS OF ENGINEERS
CHICAGO, ILLINOIS
STARVED ROCK LOCK & DAM
ILLINOIS WATERWAY, ILL.
GEOLOGIC CROSS-SECTION

PREPARED BY _____
DRAWN BY _____
DATE _____
SHEET ____ OF _____

PREPARED BY
U. S. ARMY ENGINEER
WATERWAYS EXPERIMENT STATION
CORPS OF ENGINEERS
VICKSBURG, MISSISSIPPI

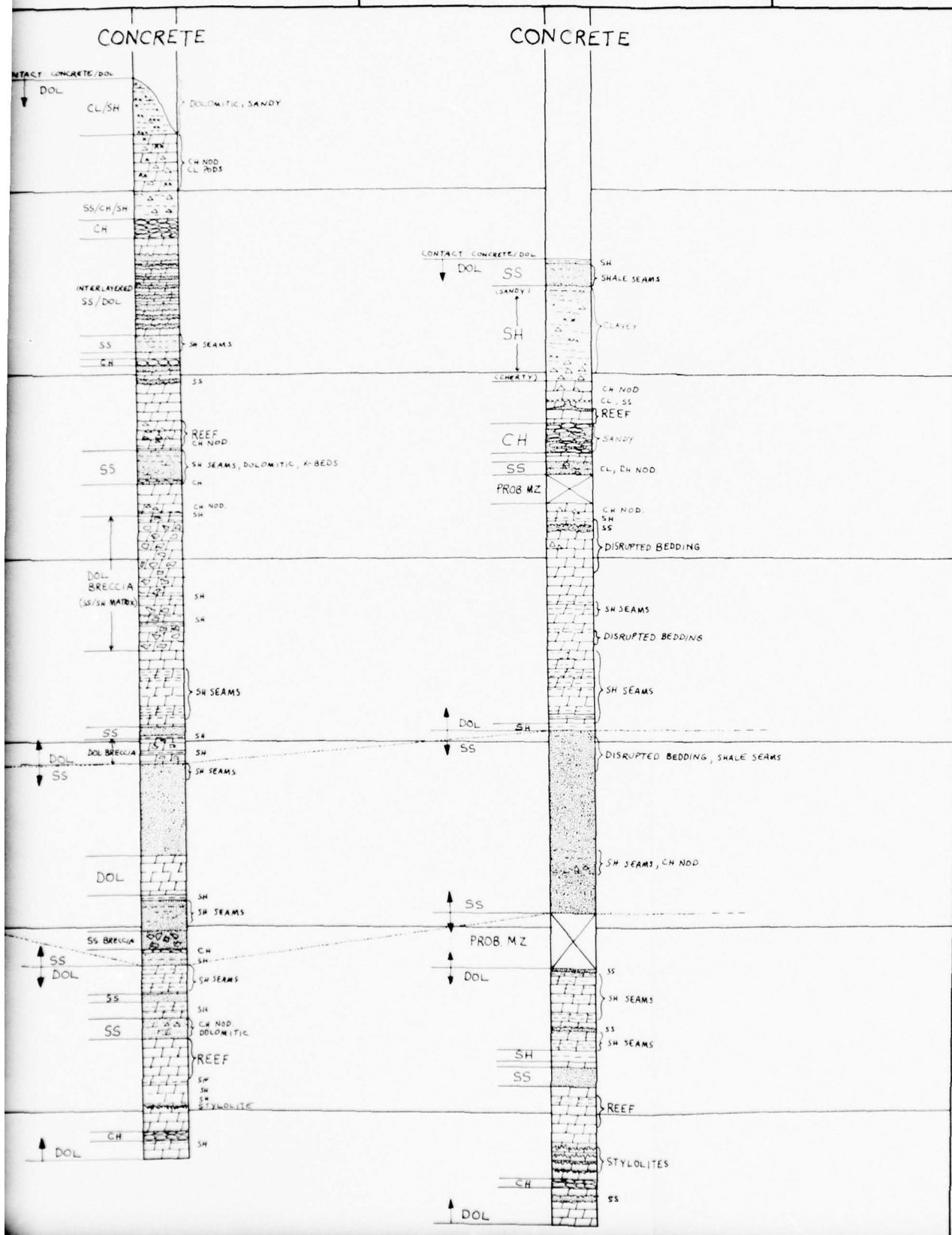
4

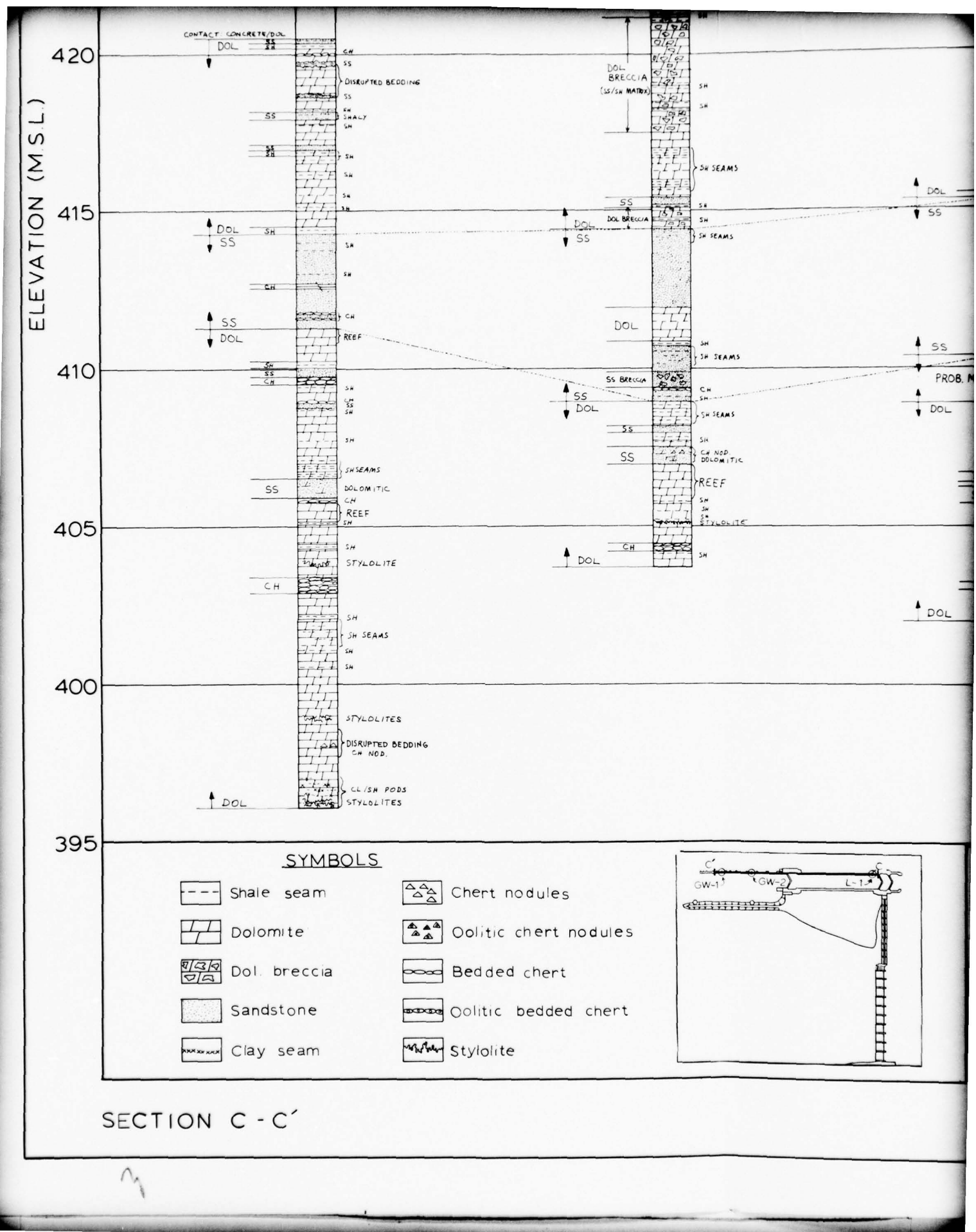


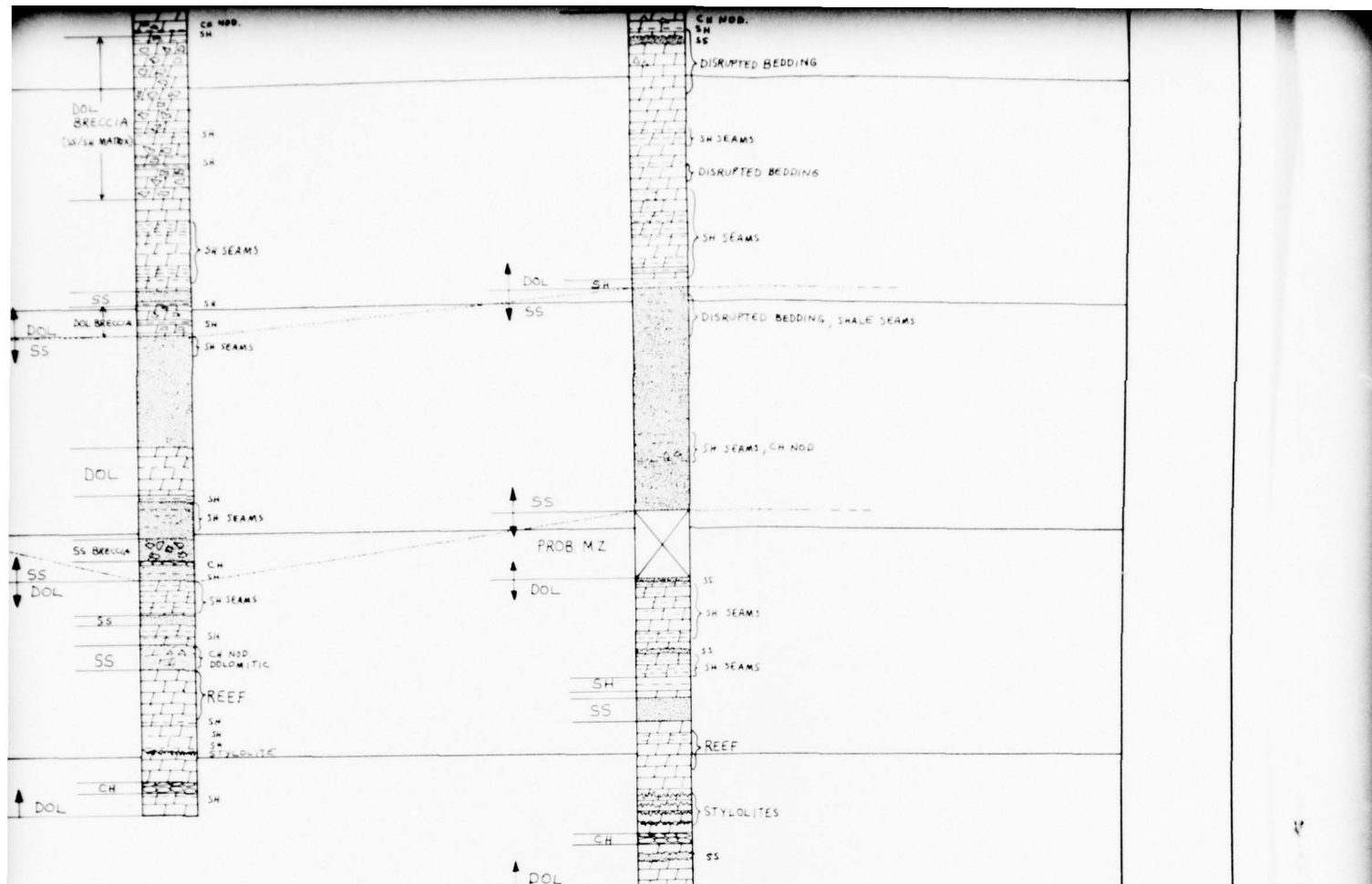
SR WES GW-2

SR WES GW-1

2

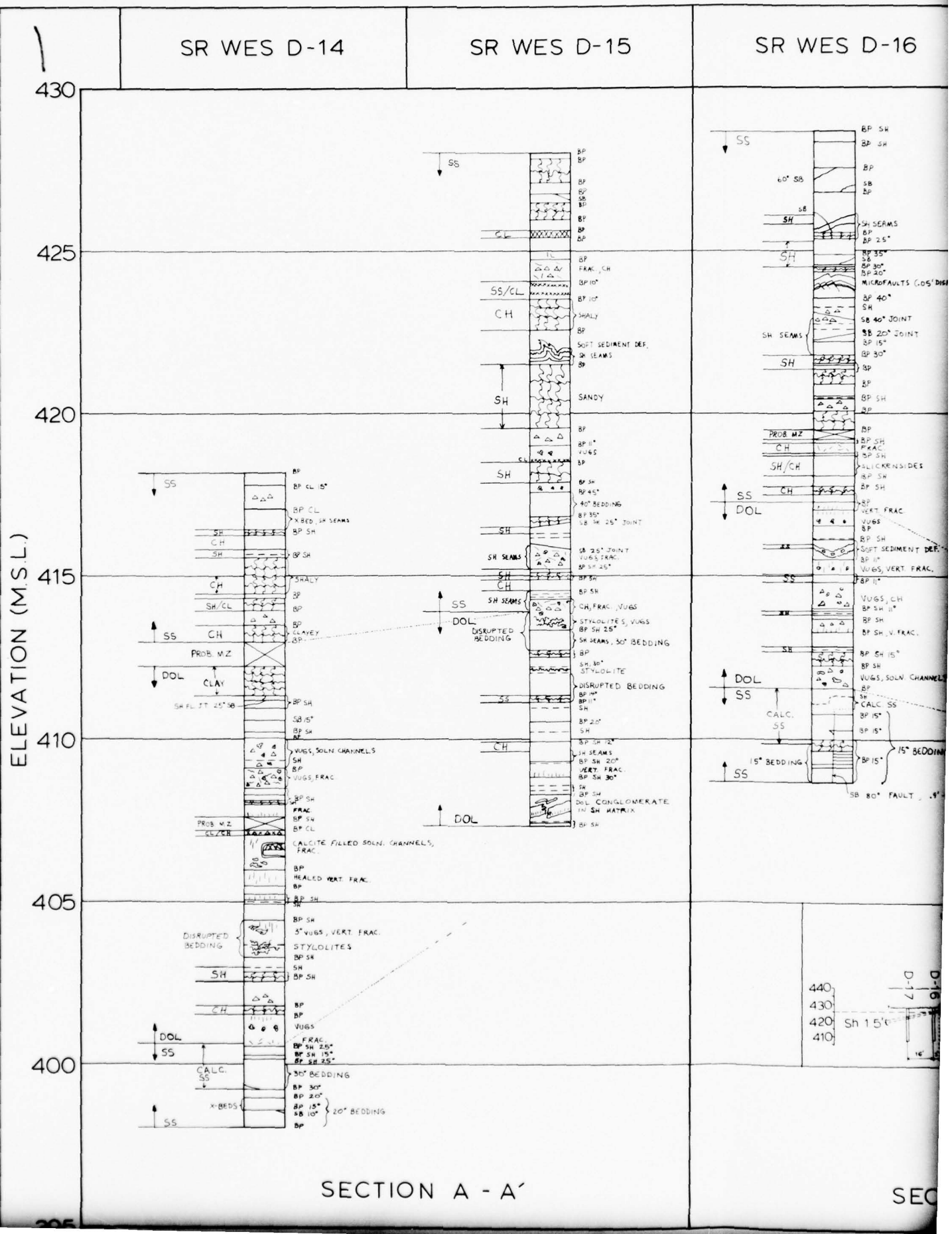






	<p>PREPARED FOR U. S. ARMY ENGINEER DISTRICT CORPS OF ENGINEERS CHICAGO, ILLINOIS STARVED ROCK LOCK & DAM ILLINOIS WATERWAY, ILL. GEOLOGIC CROSS-SECTION</p> <table border="1" style="width: 100%; border-collapse: collapse;"> <tr> <td style="width: 50%;">PREPARED BY _____</td> <td style="width: 50%;">PREPARED BY _____</td> </tr> <tr> <td>DRAWN BY _____</td> <td>U. S. ARMY ENGINEER</td> </tr> <tr> <td>DATE _____</td> <td>WATERWAYS EXPERIMENT STATION</td> </tr> <tr> <td>SHEET _____ OF _____</td> <td>CORPS OF ENGINEERS VICKSBURG, MISSISSIPPI</td> </tr> </table>	PREPARED BY _____	PREPARED BY _____	DRAWN BY _____	U. S. ARMY ENGINEER	DATE _____	WATERWAYS EXPERIMENT STATION	SHEET _____ OF _____	CORPS OF ENGINEERS VICKSBURG, MISSISSIPPI
PREPARED BY _____	PREPARED BY _____								
DRAWN BY _____	U. S. ARMY ENGINEER								
DATE _____	WATERWAYS EXPERIMENT STATION								
SHEET _____ OF _____	CORPS OF ENGINEERS VICKSBURG, MISSISSIPPI								

PLATE A2

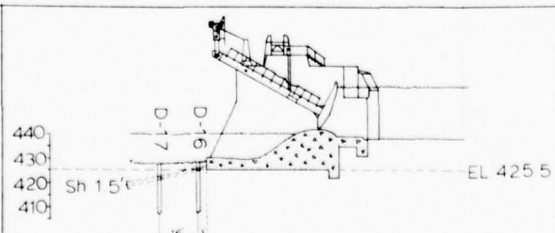
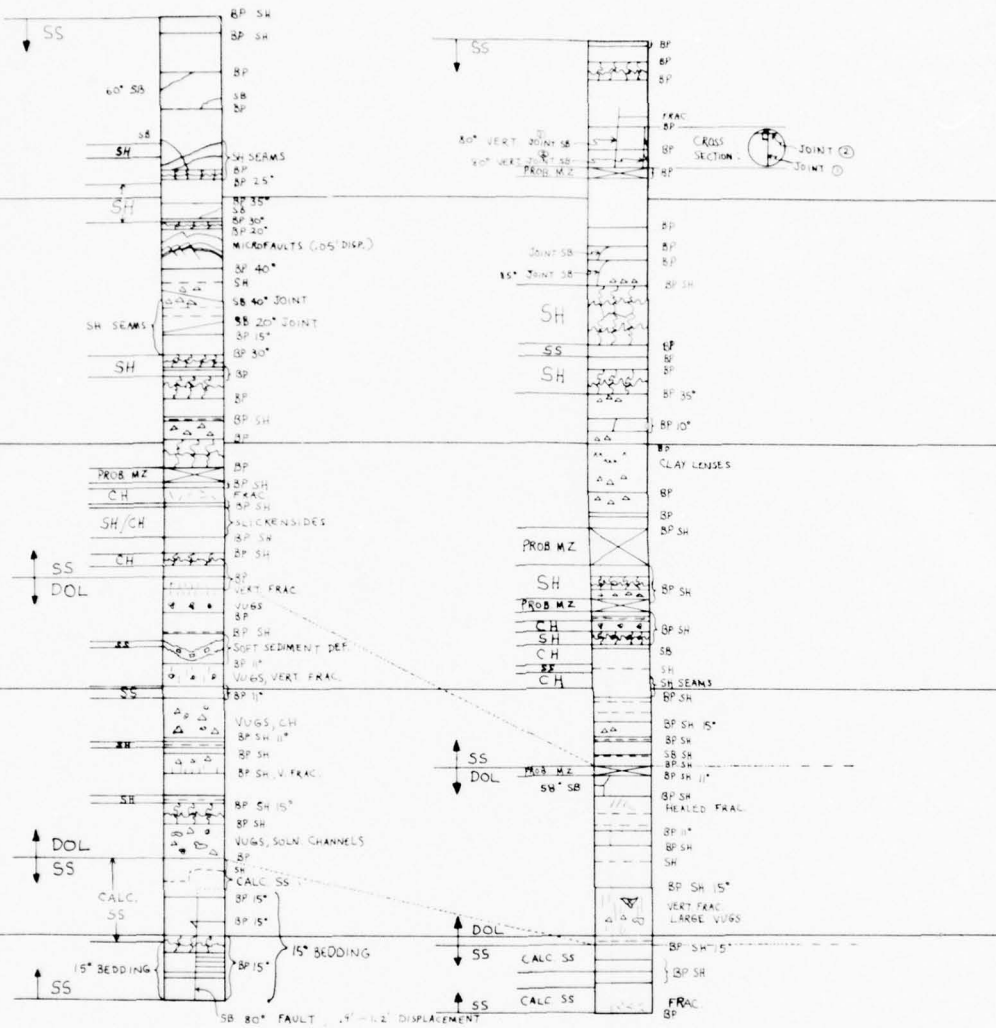


5 D-15

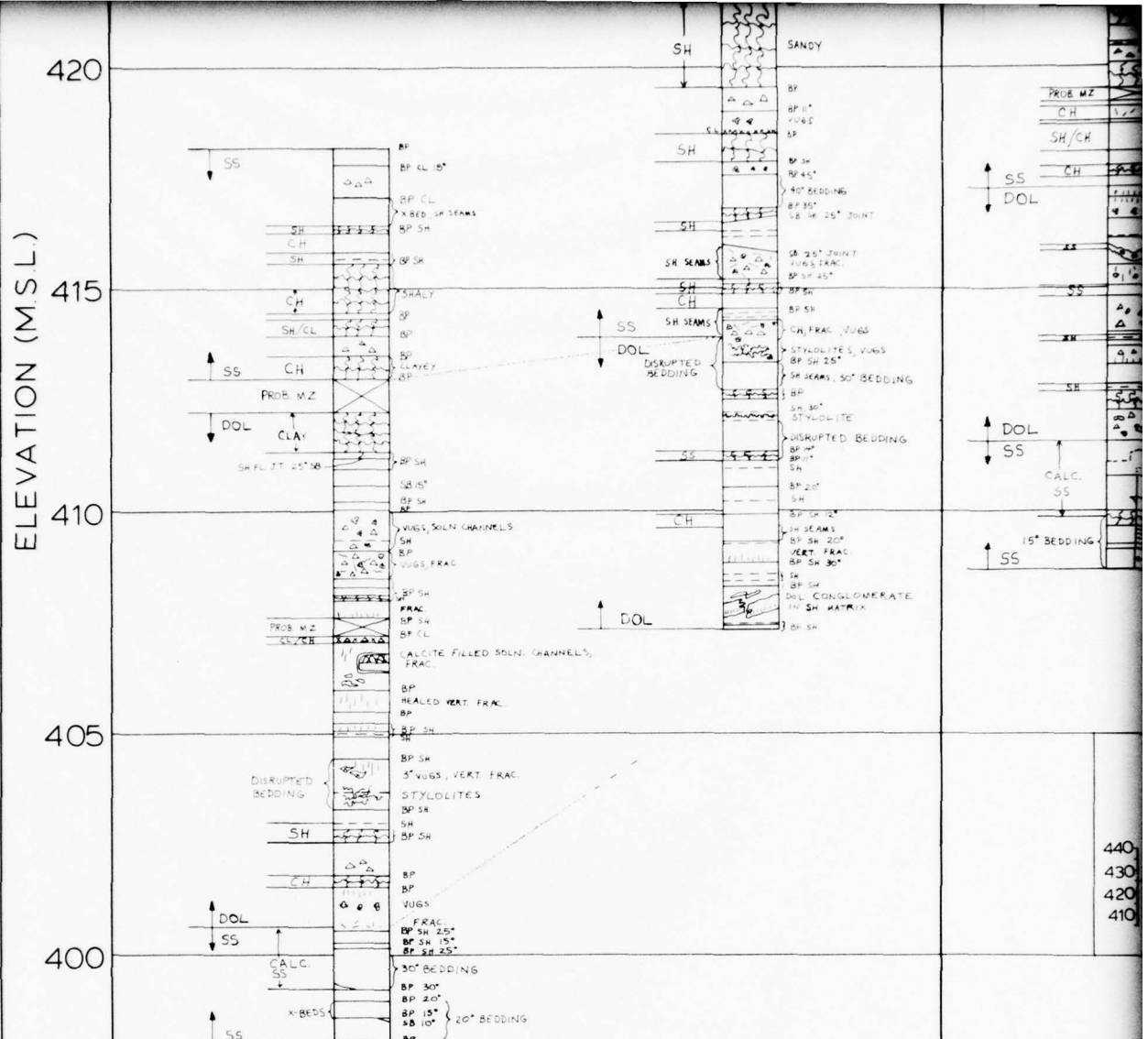
SR WES D-16

SR WES D-17

2



SECTION B-B'

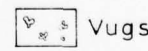


SECTION A - A'

SYMBOLS



Loss



Vugs



Stylolite



- Shale seam

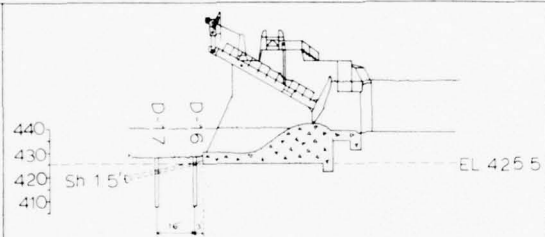
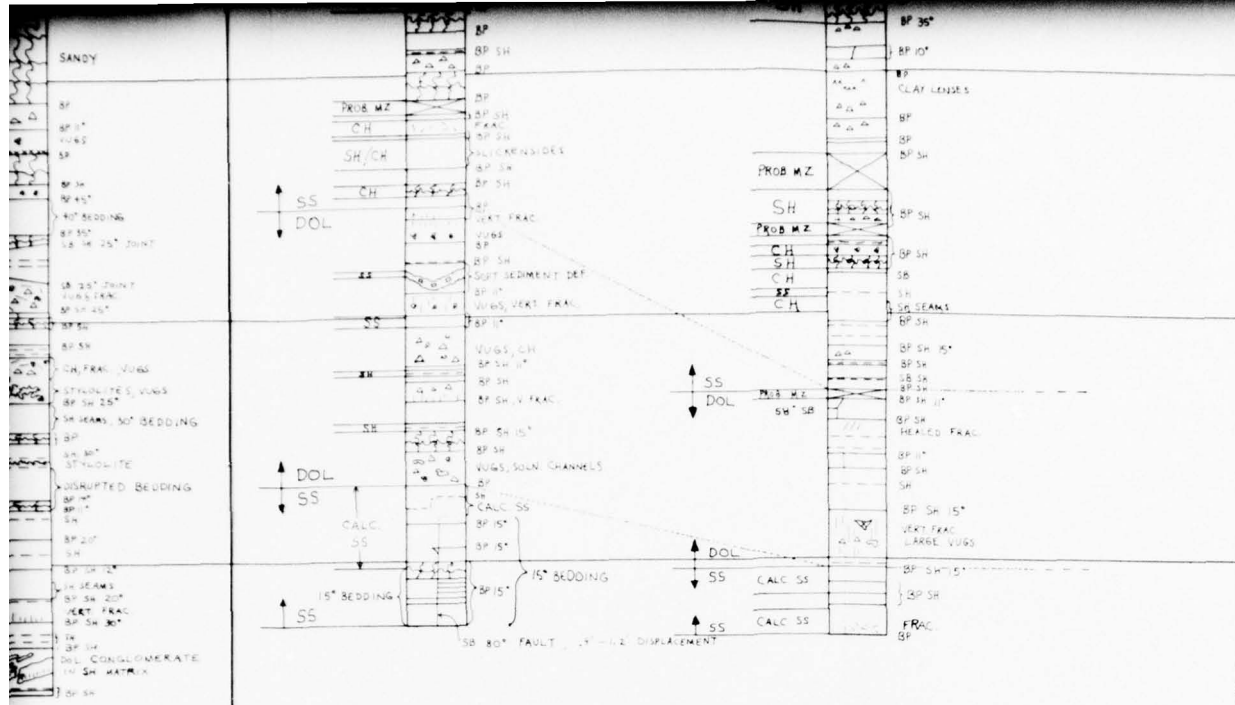


Reef

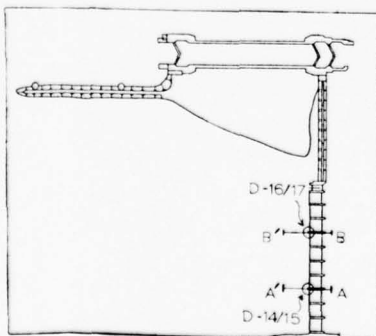


Fractured rock

SECTIONS A-A' & B-B'



SECTION B-B'



PREPARED FOR
U. S. ARMY ENGINEER DISTRICT
CORPS OF ENGINEERS

CHICAGO, ILLINOIS

BEDROCK STRUCTURAL CHARACTERISTICS RELEVANT TO FOUNDATIONS

PREPARED BY _____

PREPARED BY

DRAWN BY _____

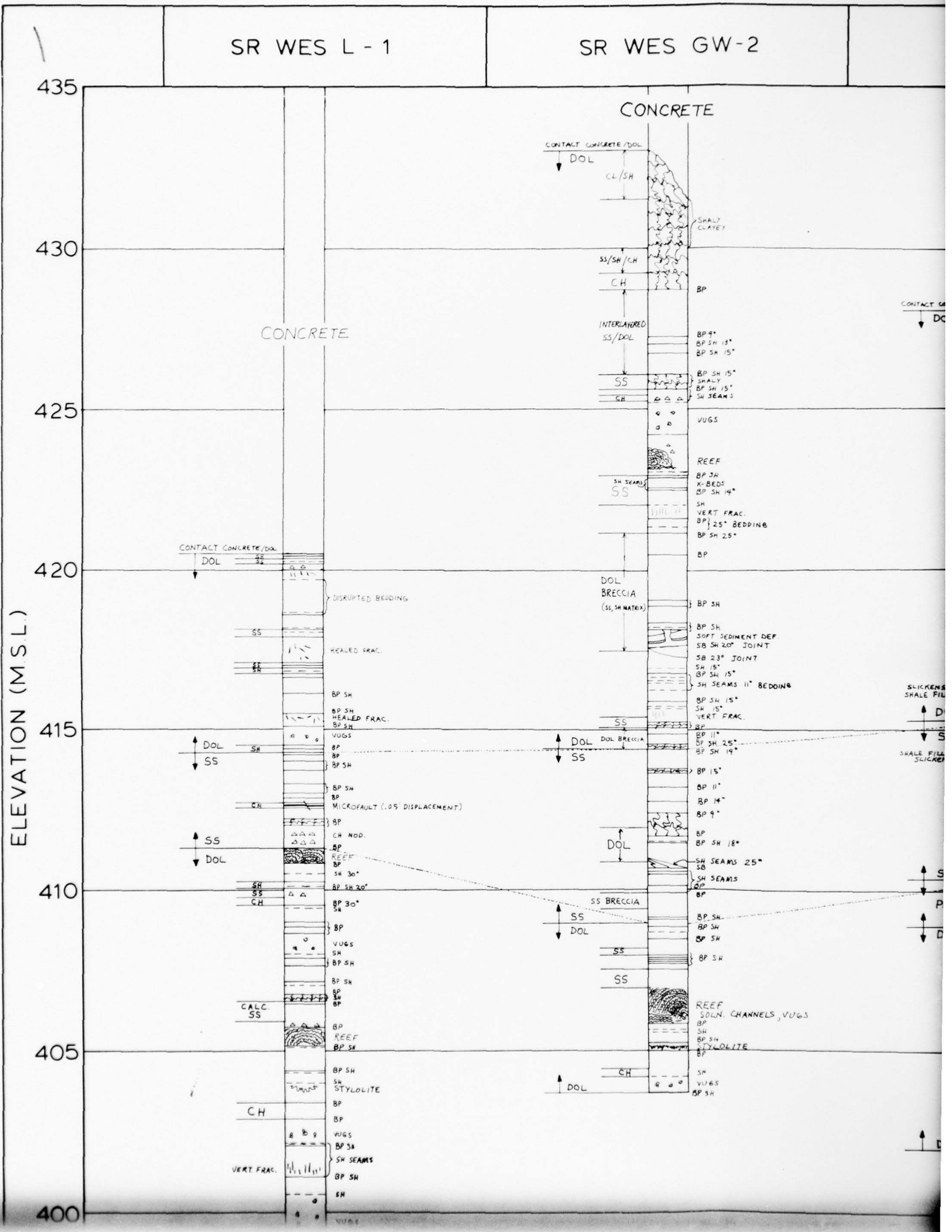
U. S. ARMY ENGINEER
WATERWAYS EXPERIMENT STATION
CORPS OF ENGINEERS

SHEET OF

VICKSBURG, MISSISSIPPI

— 1 —

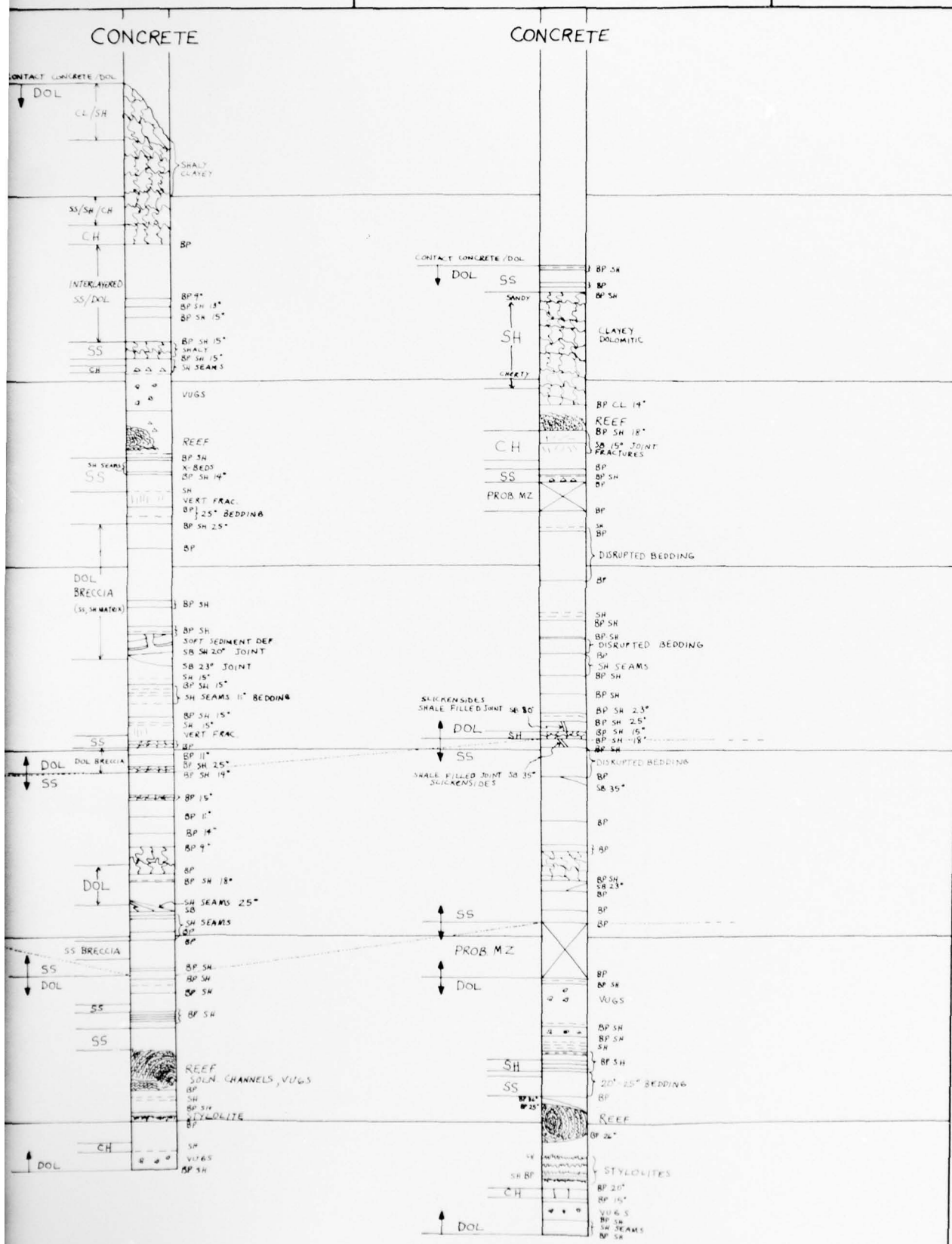
PLATE A3

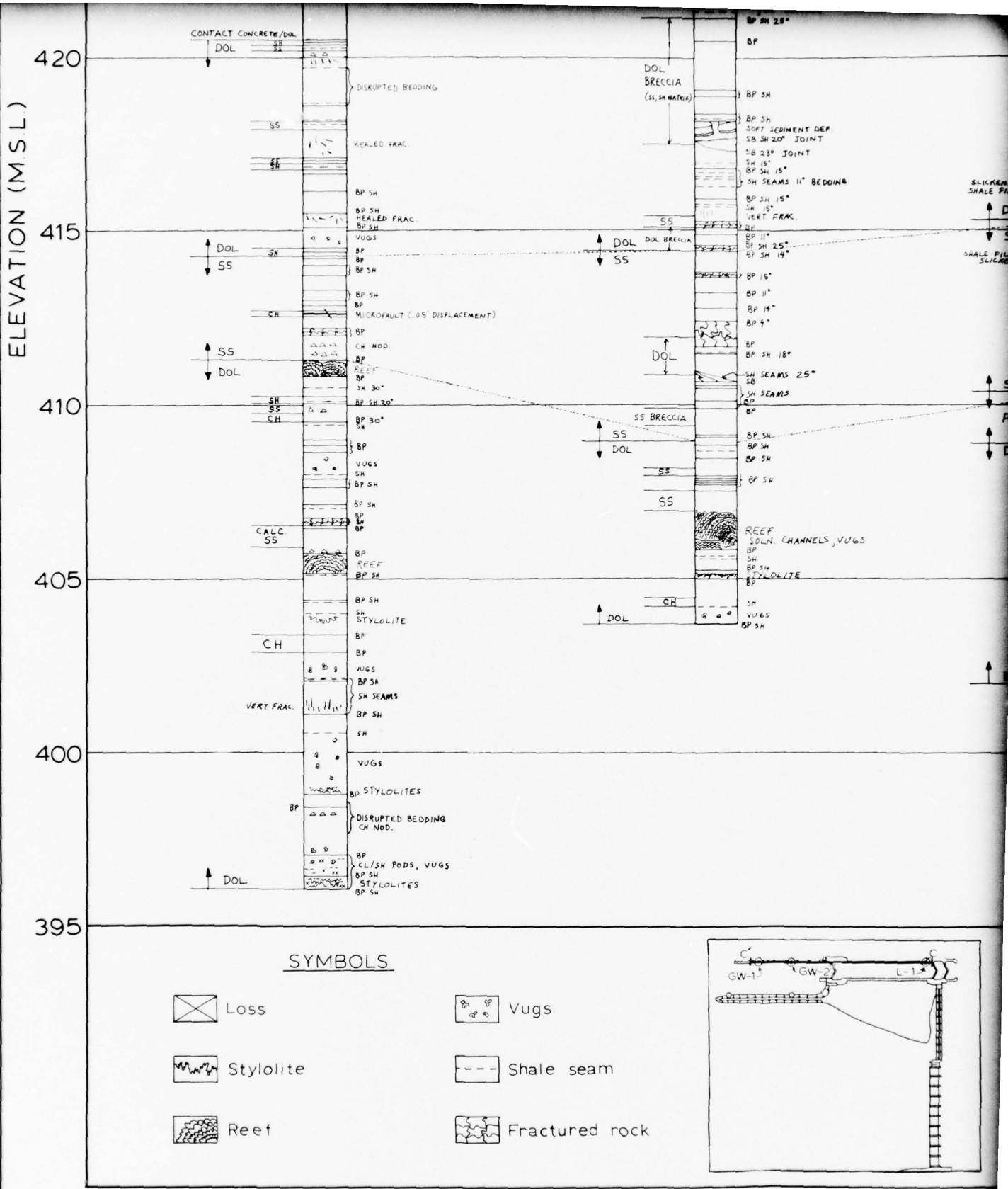


SR WES GW-2

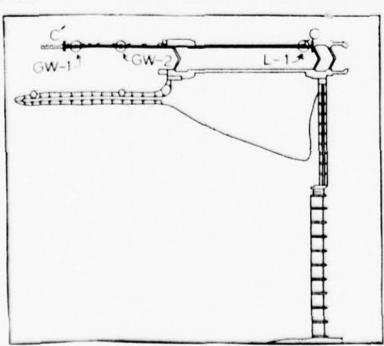
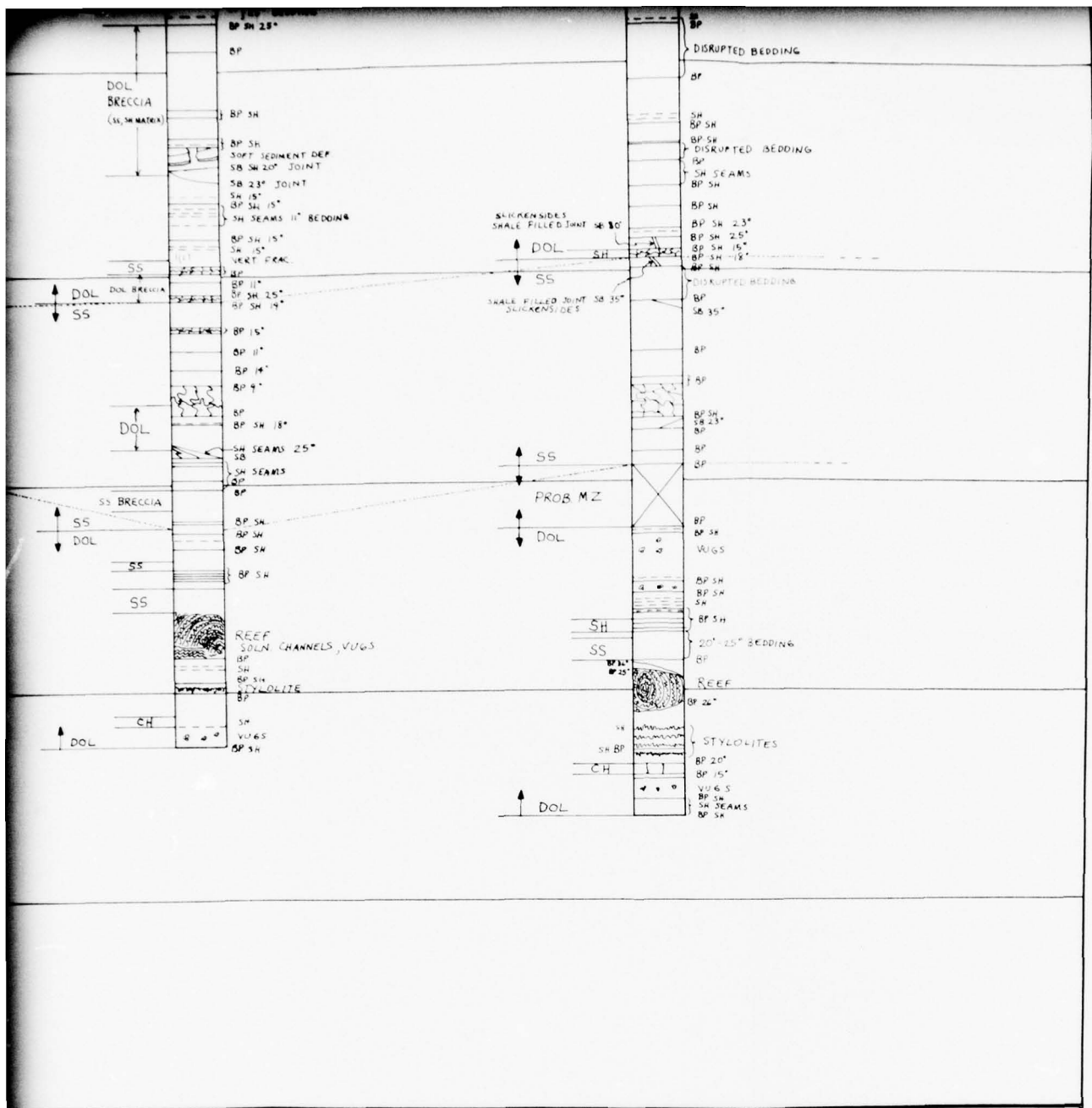
SR WES GW-1

2





SECTION C - C'



seam

ured rock

PREPARED FOR
U. S. ARMY ENGINEER DISTRICT
CORPS OF ENGINEERS
CHICAGO, ILLINOIS

STARVED ROCK LOCK & DAM
ILLINOIS WATERWAY, ILL.

BEDROCK STRUCTURAL CHARACTERISTICS
RELEVANT TO FOUNDATIONS

PREPARED BY _____
DRAWN BY _____
DATE _____
SHEET ____ OF _____

PREPARED BY
U. S. ARMY ENGINEER
WATERWAYS EXPERIMENT STATION
CORPS OF ENGINEERS
VICKSBURG, MISSISSIPPI

APPENDIX B
RESULTS OF
PETROGRAPHIC REPORT
STARVED ROCK LOCK AND DAM
MAJOR REHABILITATION

RESULTS OF
PETROGRAPHIC REPORT

1. The Concrete Laboratory serial numbers, depth of core, and field identification for all core taken during the resurfacing phase of the work is presented in Table B1.

2. A general description of the concrete from 41 borings are presented in Plates B1-B10. Concrete from cores GW-1, -3, -4, -9, and -13; D-1, -6, -9, -20, -21, -22, and -26 was selected for detailed petrographic examination. These specimens were chosen because they represented the general condition of the concrete from a specific part of the lock or dam. The detailed logs are presented in Plates B11-B22.

3. Cores GW-1 and GW-2 were in similar physical condition. The new surface concrete to depths of 0.8 ft and 0.7 ft, respectively, contained many fractures going through the paste and aggregate subparallel and parallel to the surface. The cracking is believed to be caused by frost action. The structure was built before air entrainment was introduced; and except for some resurfacing and filled areas, none of the concrete contained any entrained air. The concrete in these two holes was in good condition except for the region near the surface.

4. The composition of the near surface cement paste in core GW-1 was like that of the cement paste in the concrete deeper in the hole. The paste consisted of quartz, dolomite, ettringite, tetracalcium aluminate hydrate, calcite, and plagioclase feldspars. The last three were aggregate contamination of the samples.

5. The concrete from cores GW-1, -4, -6, and -11 is in good condition except for a longitudinal crack extending from exterior surface end of the core to depths of about 0.5 and 1.5 ft in cores GW-1, -4, and -11; see Plate B1. All of the cracks were old. The cracked surfaces were partially coated with calcite; there was also some alkali-silica gel around some aggregate particles visible on the broken surfaces. Alkali-silica reaction was probably responsible for producing these longitudinal cracks. The concrete in core GW-6 was not cracked and is in good condition (Plate B1).

6. Boring L-1 was a vertical core drilled into the land-side lock wall near the upper gates. The top 6 in. was new concrete with 1/2-in. maximum-size aggregate. The concrete below was older, and contained 3-in. maximum-size aggregate. All of the concrete from this hole was in good condition.

7. Cores GW-7, -8, and -9 showed the effects of freezing and thawing damage as cracking in the upper parts of the cores (Plate B2). The cores showed subparallel to parallel cracks near the surface to a depth of about 0.5 ft (Plate B2). Photograph B1 shows the near-surface concrete from core GW-9.

8. Cores GW-5, -12, and -13 drilled in the upper guide wall at about 533 ft, 754 ft, and 917 ft from the center line of the lock, respectively, and at the same elevation, were in good condition. All of the cores contained many reinforcing bars. A general description of the cores is given in Plate B3.

9. Six cores were taken from piers No. 6 and No. 18 in the headgate section. Cores D-21 and D-24, drilled from the sill adjacent to these piers, were in good condition and did not show any signs of deterioration. However, the other concrete cores from these locations were in poor condition caused by freezing and thawing and alkali-silica reaction as shown in Plate B4. Cores D-22 and D-25 contained incipient cracks below a depth of 1 ft. All of the cracks tended to be subparallel to the long axis of the core and passed through the aggregate and the cement paste. The crack surfaces in core D-26 were coated with algae, and D-23 has a parabolic crack at about 0.8 ft depth. The cause of the near surface cracking was probably frost action. The deeper longitudinal cracks probably were caused by alkali-silica reaction. Photograph B2 illustrates the cracking described above.

10. Core D-20 was drilled in the ice chute pier. The core was fractured to a depth of 1.7 ft with fractures that were parallel or subparallel to the surface and passed through aggregate and cement paste. These fractures were probably caused by frost action. The core below 1.7 ft was also fractured but these fractures passed around aggregate and were not parallel to the surface. The paste had been eroded from the core

surface during drilling, leaving a sandy textured cored surface. This could indicate a wet concrete mixture or damage of the mortar by freezing and thawing or both. X-ray diffraction examination of the cement paste revealed no unusual crystalline component.

11. Cores D-18 and D-19 were also drilled into the ice chute pier. The maximum depth of frost damage was found at 0.5 ft and 1.6 ft, respectively. Other information about these three cores is in Plate B5.

12. Eighteen cores were drilled in five piers in the tainter gate section of the dam. The depth of frost damage in each of the 18 is shown in Plates 6 through 10. The concrete was in good condition in piers No. 4 and No. 6 with only minor frost damage in core D-8 from pier No. 6. Cores from piers No. 2, No. 7, and No. 9 were in similar physical condition. Cores D-6, D-9, and D-30 from similar locations in the different piers showed freezing and thawing damage to 1.5 ft, 1 ft, and 0.7 ft, respectively. Cores D-1, D-5, and D-9 showed freezing and thawing damage to 2.0 ft, 1.5 ft, and 0.3 ft, respectively. The other cores in these piers had frost penetration less than 0.3 ft depth except for core D-10 in which frost damage penetrated to 0.9 ft depth.

13. Cores D-1, -2, -6, -7, and -9 contained some longitudinal cracks. The longitudinal cracks in cores D-6 and D-7 were horizontal and could be traced back to metal plates supporting the tainter gates. There was good correlation of old breaks in the concrete in cores D-27 and D-28 with the horizontal cracks in D-6 and D-7. Photograph B3 shows the deterioration of old concrete below new concrete in core D-1.

14. The other longitudinal cracks contained some alkali-silica gel in some air voids, but this was not believed extensive enough to cause the cracks.

15. Core D-28 was topped with 2 ft of new concrete which was air entrained and in good condition. The old concrete from 2.0 ft to 2.5 ft depth is cracked by freezing and thawing. The remainder of the concrete is in good condition (Plate B7).

Summary

16. This structure was built with non-air-entrained concrete and gravel aggregate, characteristic of the area, up to 3-in. maximum size. The aggregate contains dolomite, chert, siltstone, limestone, shale, and other varieties of rock. The maximum size of the aggregate varies from core to core and within cores. Examination of the core logs shows that while some of the concrete is in good condition from the finished surface to the greatest depth drilled, many of the cores show cracks subparallel to the free surface of the concrete and to depths ranging from 2 in. to 1-1/2 ft or more. Cores D-1, -18, -20, and -28 are damaged to greater depths. Inside the frost-damaged zone some of the cores contain cracks normal to the free surface of the concrete, frequently associated with white chert and alkali-silica gel. The longitudinal cracks normal to the free surface and characteristic of alkali-silica reaction in hydraulic structures and some bridges, and represent the expansion of the less restrained exterior part of the concrete in the structure. The expansive force and the restraint combined govern the extent and frequency of the cracks normal to the surface. Photograph B1 illustrates a crack subparallel to the finished surface, resulting from freezing and thawing, and several cracks within aggregate particles or extruding from an aggregate particle to the paste that suggest alkali-silica reaction. Photograph B2 illustrates a core showing closely spaced subparallel cracks produced by frost action, which curve farther back from the free face toward a major crack normal to the free face. At the left of the major crack is a broken particle white chert, apparently the most reactive aggregate in the structure. Photograph B3 shows the complete destruction of concrete back of an air-entrained repair. Some of the cracking in the largest fragment of rubble suggests that alkali-silica reaction and freezing and thawing contributed to this failure.

17. The most severe freezing and thawing damage appears to have taken place in the ice chute (Plate B5). The distribution of alkali-silica reaction is harder to summarize. It is usually found behind the depth of frost damage; it is apparently absent in the land-side guide wall; it is

present in some of the cores from headgate pier 18 and in several tainter gate piers. Nevertheless the substantial alkali-silica reaction has not penetrated the concrete that is more than about 4 ft back of a free surface, and concrete farther into the piers or sill is unaffected by either freezing and thawing or alkali-silica reaction.

18. Since the serious alkali-silica reaction seems to be expressed most often in and associated with cracks normal to free surfaces, it seems reasonable to assume that the alkali-silical reaction was encouraged when the exterior concrete began to crack up because of freezing and thawing, progressively letting water penetrate into the concrete. Possibly the alkali-silica reaction began in the cracked concrete. Some of the frost-damaged concrete is gone; much of it has been wasted repeatedly, so gel that perhaps was present in the concrete next to the free surfaces has been removed. In the zone of longitudinal cracks normal to free surfaces substantial but apparently not general alkali-silica reaction has taken place. Since the cracks are located normal to horizontal and vertical surfaces there is no basis that we can find for an assumption that there is a regular difference in alkali content of the cement with the high alkali cement confined to the zone of longitudinal cracking.

19. Inspection of the deepest cores and of cores from depths of 8.5 ft shows that they manifest little or no alkali-silica reaction. If the structure is repaired by the removal of fragile concrete and the addition of air-entrained concrete as repairs, the structure should be stable in terms of the anticipated behavior of the concrete.

Table B1
Boring Identification Numbers

CL Serial No.	Depth, ft/EL*	Field Identification
<u>Backfill</u>		
CL-1	0-26 458.5	SR WES GWB-1: backfill, 802 ft downstream of center line lock, behind lower guide wall
CL-2	0-18 458.5	SR WES GWB-2: backfill, 797 ft downstream of center line lock, behind lower guide wall
CL-3	0-19 455.5	SR WES GWB-2: backfill 791 ft downstream of center line of lock, behind lower guide wall
<u>Guidewall</u>		
CON-5	0-3.1 452.9	SR WES GW-3: 6-in.-diameter concrete core from about 795 ft downstream on land guidewall. Horizontal hole
CON-6	0-30.9 459.0	SR WES GW-1: 6-in.-diameter concrete core concrete core from about 795 ft downstream on land guide wall. Vertical hole
DC-5	30.9-57.0 459.0	6-in.-diameter rock core from SR WES GW-1
CON-7	0.3.3 445.3	SR WES GW-4: 6-in.-diameter concrete core from about 795 ft downstream on land guide wall. Horizontal hole
CON-8	0-3.0 454.2	SR WES GW-11: 6-in.-diameter concrete core from about 580 ft downstream on land guide wall. Horizontal hole
CON-9	0-27.5 459.0	SR WES GW-2: 6-in.-diameter concrete core from about 580 ft downstream on land guide wall. Vertical hole
DC-6	27.5-54.8 459.0	6-in.-diameter rock core from SR WES GW-2
CON-10	0-3.5 444.3	SR WES GW-6: 6-in.-diameter concrete core from about 580 ft downstream on land guide wall. Horizontal hole
(Continued)		

* MSL, elevation is for top of hole for vertical drilled holes and entry point for horizontal drilled holes

Table B1 (Continued)

CL Serial No.	Depth, ft/EL	Field Identification
CON-11	0-3.0 455.7	SR WES GW-10: 6-in.-diameter concrete core from lower gate recess land side wall. Horizontal hole
CON-12	0-3.2 461.3	SR WES GW-7: 6-in.-diameter concrete core from upper gate recess land side wall. Horizontal hole
CON-13	0-3.0 460.7	SR WES GW-8: 6-in.-diameter concrete core from upper gate recess river wall. Horizontal hole
CON-14	0-3.2 460.5	SR WES GW-9: 6-in.-diameter concrete core from emergency gate recess river wall. Horizontal hole
CON-15	0-3.0 460.8	SR WES GW-5: 6-in.-diameter concrete core from about 533 ft upstream river side guide wall. Horizontal hole
CON-16	0-3.1 460.8	SR WES GW-12: 6-in.-diameter concrete core from about 754.5 ft upstream river side guide wall. Horizontal hole
CON-17	0-3.1 461.0	SR WES GW-13: 6-in.-diameter concrete core from about station 947 ft upstream river side guide wall. Horizontal hole
CON-18	0-2.9 448.9	SR WES D-23: 6-in.-diameter concrete core from south side pier No. 18. Horizontal hole
CON-19	0-3.0 442.8	SR WES D-24: 6-in.-diameter concrete core from sill floor near pier No. 17. Vertical hole
CON-20	0-3.0 457.7	SR WES D-26: 6-in.-diameter concrete core from downstream face of pier No. 18. Horizontal hole
CON-21	0-3.1 448.8	SR WES D-22: 6-in.-diameter concrete core from north side of pier No. 6. Horizontal hole
CON-22	0-3.1 442.8	SR WES D-21: 6-in.-diameter concrete core from sill floor near pier No. 7. Vertical hole
CON-23	0-3.3 456.7	SR WES D-25: 6-in.-diameter concrete core from downstream face of pier No. 6. Horizontal hole

(Continued)

(Sheet 2 of 4)

Table B1 (Continued)

CL Serial No.	Depth, ft/EL	Field Identification	
		<u>Ice Chute</u>	
CON-24	0-3.5	SR WES D-19:	6-in.-diameter concrete core
	454.2	from the north pier ice chute.	Horizontal hole
CON-25	0-3.0	SR WES D-18:	6-in.-diameter concrete core
	448.3	from north pier of ice chute.	Horizontal hole
CON-26	0-3.1	SR WES D-20:	6-in.-diameter concrete core
	469.0	from ice chute.	Vertical hole
<u>Tainter Gate</u>			
CON-27	0-3.3	SR WES D-4:	6-in.-diameter concrete core
	445.5	from pier No. 9 downstream hole.	Horizontal hole
CON-28	0-3.4	SR WES D-5:	6-in.-diameter concrete core
	461.0	from pier No. 9 middle hole.	Horizontal hole
CON-29	0-3.1	SR WES D-6:	6-in.-diameter concrete core
	461.4	from pier No. 9 upstream hole.	Horizontal hole
CON-30	0-13.0	SR WES D-28:	6-in.-diameter concrete core
	468.0	from pier No. 9 upstream hole.	Vertical hole
DC-7	0-19.8	SR WES D-17:	6-in.-diameter vertical rock
	428.2	core from 19 ft downstream of pier No. 8	
DC-8	0-19.9	SR WES D-16:	6-in.-diameter vertical rock
	428.6	core from 2.5 ft downstream from down-	
		stream edge of concrete apron pier No. 8	
CON-31	0-3.1	SR WES D-31:	6-in.-diameter concrete core
	444.2	from south side of pier No. 7 downstream	
		hole.	Horizontal hole
CON-32	0-3.3	SR WES D-29:	6-in.-diameter concrete core
	461.6	from south side of pier No. 7, middle hole.	
		Horizontal hole	
CON-33	0-3.0	SR WES D-30:	6-in.-diameter concrete core
	462.3	from south side of pier No. 7, upstream	
		hole.	Horizontal hole
CON-34	0-3.2	SR WES D-9:	6-in.-diameter concrete core
	445.3	from south side of pier No. 6, downstream	
		hole.	Horizontal hole

(Continued)

(Sheet 3 of 4)

Table B1 (Concluded)

CL Serial No.	Depth, ft/EL	Field Identification
CON-35	0-3.5 461.3	SR WES D-8: 6-in.-diameter concrete core from south side of pier No. 6, middle hole. Horizontal hole
CON-36	0-2.9 460.8	SR WES D-7: 6-in.-diameter concrete core from south side of pier No. 6, upstream hole. Horizontal hole
CON-37	0-11.1 468.0	SR WES D-27: 6-in.-diameter concrete core from upstream end of pier No. 6. Vertical hole
DC-9	0-20.7 428.0	SR WES D-15: 6-in.-diameter rock core from 19 ft downstream from pier No. 4. Vertical hole
DC-10	0-20.1 418.2	SR WES D-14: 6-in.-diameter rock core from 4.0 ft downstream of downstream edge of concrete apron near pier No. 4
CON-38	0-3.0 444.7	SR WES D-34: 6-in.-diameter concrete core from south side of pier No. 4, downstream hole. Horizontal hole
CON-39	0-2.9 460.9	SR WES D-32: 6-in.-diameter concrete core from south side of pier No. 4, middle hole. Horizontal hole
CON-40	0-3.4 462.9	SR WES D-33: 6-in.-diameter concrete core from south side of pier No. 4. Upstream hole. Horizontal hole
CON-41	0-5.1 452.5	SR WES D-10: 6-in.-diameter concrete core from south side of pier No. 2, downstream hole. Horizontal hole
CON-42	0-3.3 446.3	SR WES D-3: 6-in.-diameter concrete core from south side of pier No. 2 downstream hole. Horizontal hole
CON-43	0-3.3 465.7	SR WES D-1: 6-in.-diameter concrete core from south side of pier No. 2, middle hole. Horizontal hole
CON-44	0-2.9 461.0	SR WES D-2: 6-in.-diameter concrete core from south side of pier No. 2, upstream hole. Horizontal hole

400

CH	BP
	BP
	VUGS
	BP SH
VERT. FRACT.	SH SEAMS
	BP SH
	SH
	VUGS



Core SR WES GW-9-77 contained traverse cracks near the top of the core and incipient cracks deeper in the core.

Photograph B1



Core SR WES D-22-77 is typical of several cores showing subparallel to parallel fractures going through both aggregate and paste indicating frost damage near the surface and a transition to horizontal cracking related to alkali-silica reaction deeper in the hole.

Photograph B2



Core SR WES D-1-77 has been resurfaced with a layer of new air-entrained concrete. The zone directly beneath the resurfacing was damaged by frost action and disaggregated during drilling.

Photograph B3

SPECI
STARVED ROCK LICK AND DAM, ILLINOIS WATER
General Description of Concrete Cores, Lower Approach Wall

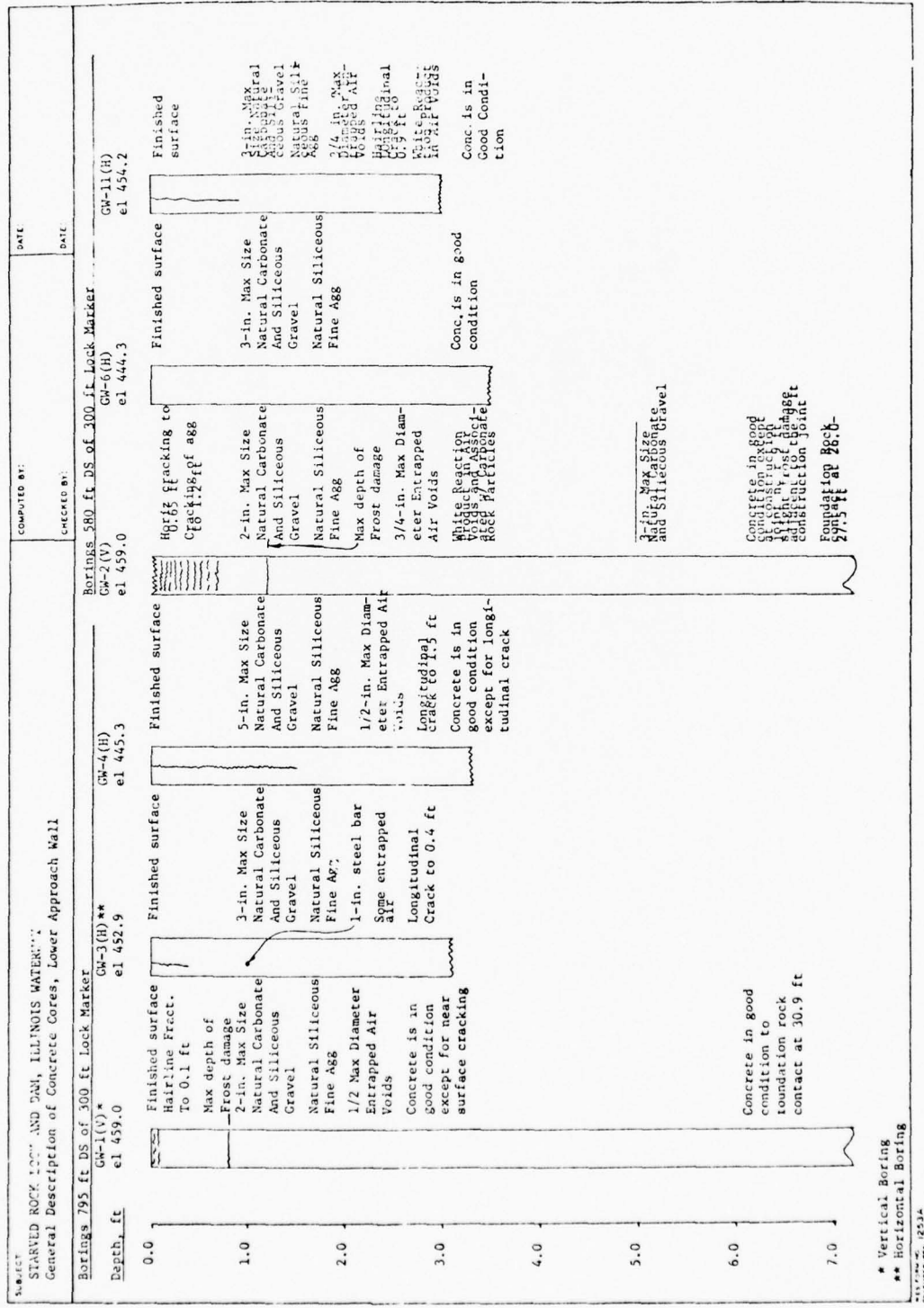


PLATE B1

Section	Starved Rock Lock and Dam, Illinois Waterway Geological Description of Concrete Cores, Lock & Gate Recesses	Completed by	Date
Depth, ft	L-1(V) Concrete Trough	Upper Gate L-1(H)	Lower Gate L-1(G)
0.0	el 464.0 Finished surface 1 1/2-in. Max Size Agg New Conc	el 461.3 Finished surface para- llel to gate structures 0.1 ft Tax Depth of frost damage 1/2-in. Max Size Agg Sand Silica Gravel Natural Siliceous Fine Agg	el 460.7 Finished surface para- llel to gate structures 0.1 ft Tax depth of frost damage 1/2-in. Max Size Agg Sand Silica Gravel Natural Siliceous Fine Agg
1.0	Concrete Production Sand Silica Gravel Natural Siliceous Fine Agg	el 460.5 Frost damage 1/2-in. Max Size Agg Sand Silica Gravel Natural Siliceous Fine Agg	el 460.5 Frost damage 1/2-in. Max Size Agg Sand Silica Gravel Natural Siliceous Fine Agg
2.0	Some Entrapped Air Concrete is brittle Good G.4 Condition	el 460.5 1/2-in. Max Size Agg Sand Silica Gravel Voids	el 460.5 1/2-in. Max Size Agg Sand Silica Gravel Voids
3.0	Old Concrete Steel Bar	el 460.5 White in Air Pockets Quality of concrete is good	el 460.5 White in Air Pockets Quality of concrete is good
4.0			
5.0		Concrete is in good condition	
6.0		Old Break	
7.0			

PLATE B2

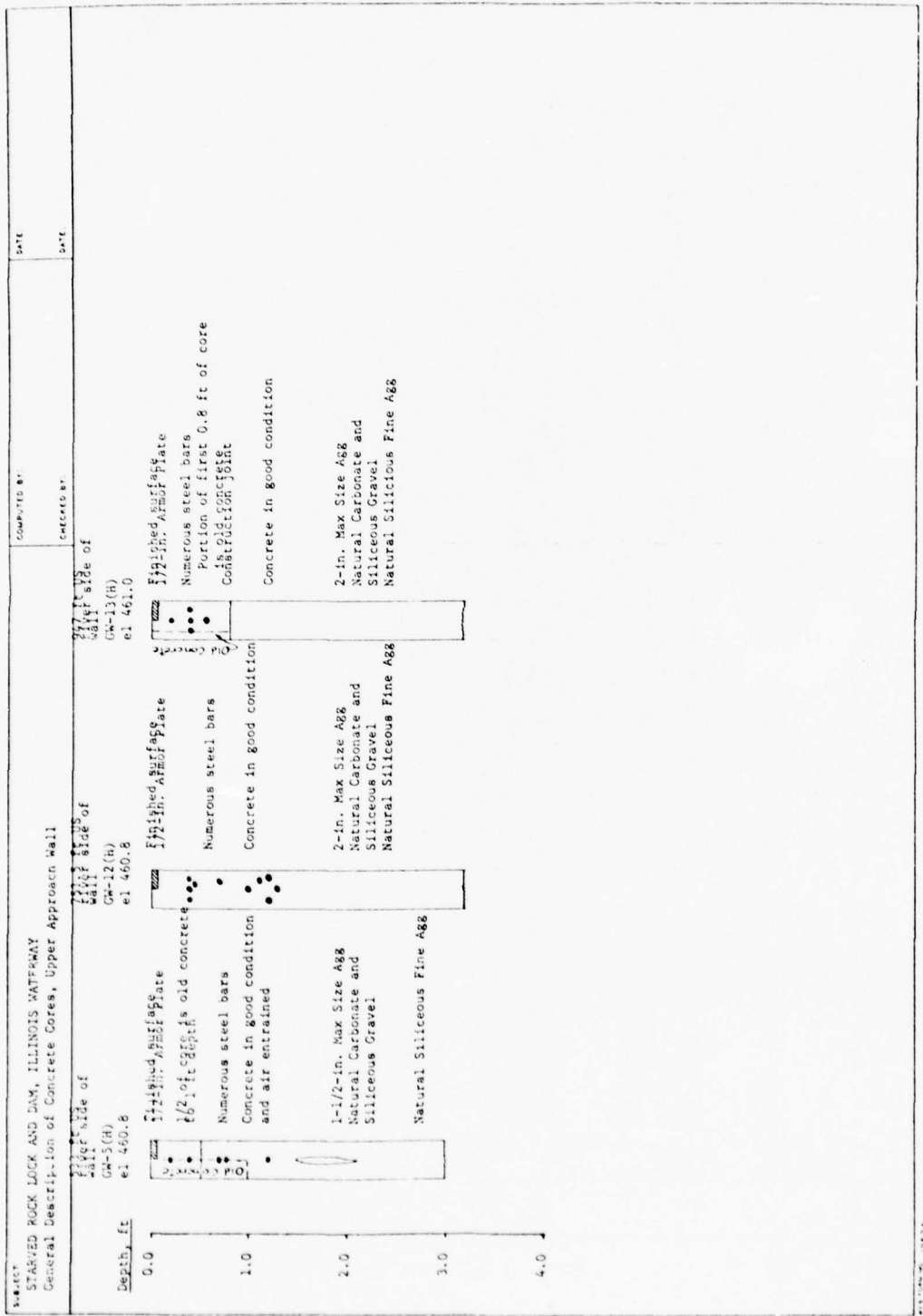
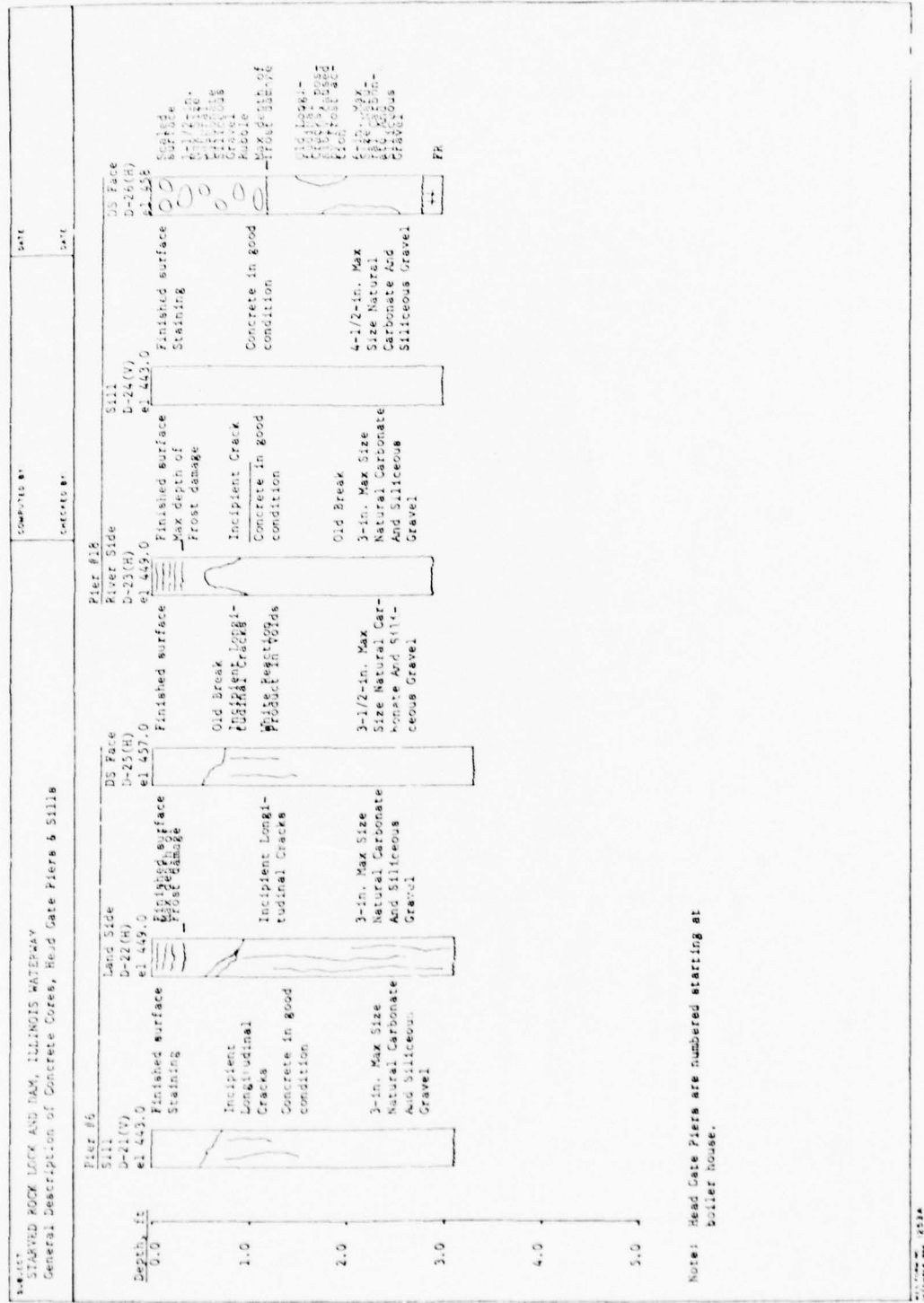


PLATE B3

STANDARD ROCK LOCK AND DAM, ILLINOIS WATERWAY
General Description of Concrete Cores, Head Gate Piers & Silos



Note: Head Gate Piers are numbered starting at
Boiler house.

PLATE B4

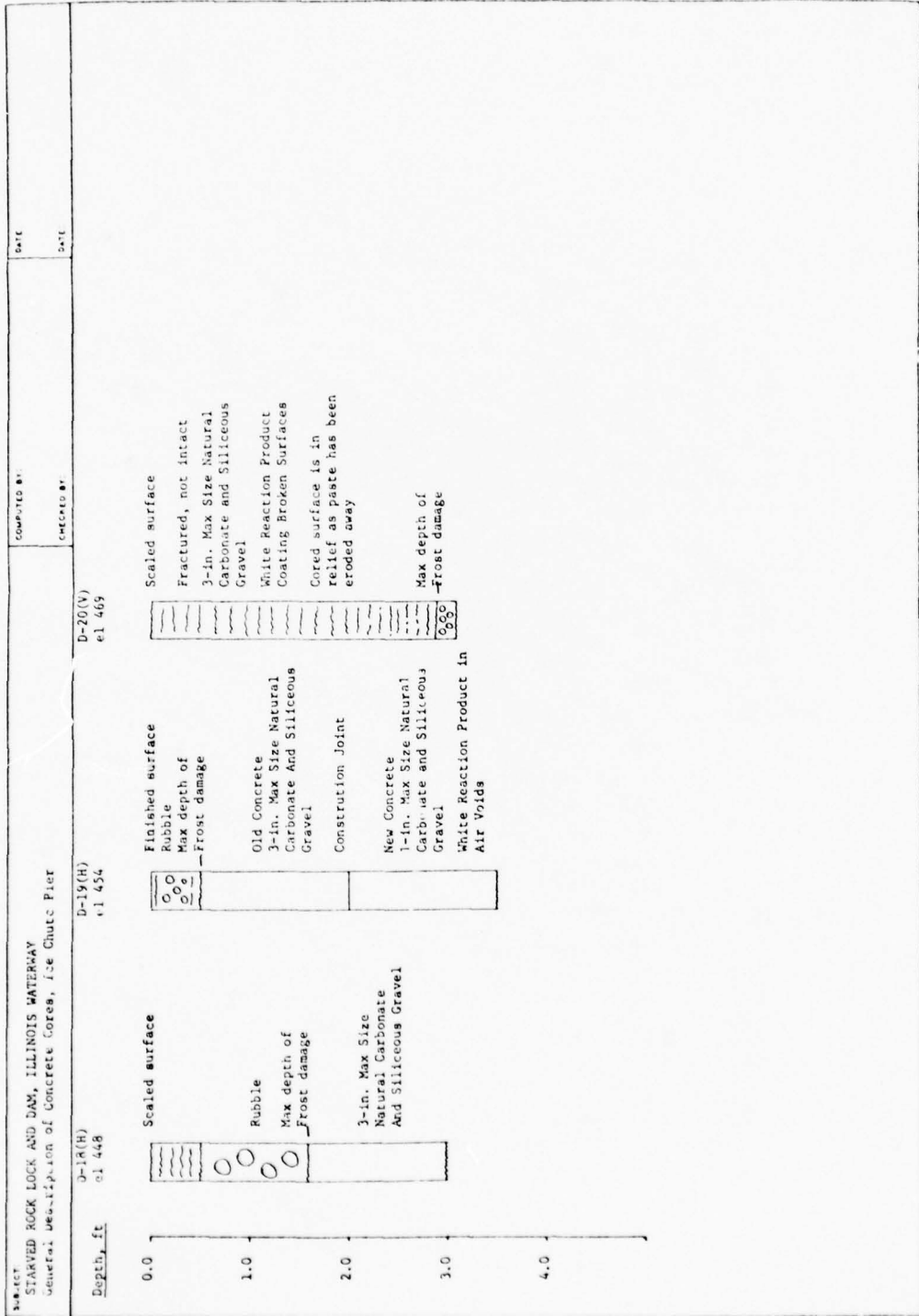


PLATE B5

STAKED ROCK DOCK AND DAM, ILLINOIS WATERWAY
General Description of Concrete Cores, Lainter Gate Pier

PLATE B6		COMPLETED BY	DATE
		CONCRETE BY	
Pier #2			
Depth, ft			
0.0	D-2 (H) el 466.0	D-3 (I) el 446.0	D-10 (G) el 452.0
	- Faded Surface. - Rubble 0.0 Fragmented 0.0 Siliceous Gravel 0.0 Rubble	- Bubble 0.0 Max depth of Frost damage Concrete in Good Condition	- Finished surface
1.0	- Tight fractures 0.0 Natural Carbonate And Siliceous Gravel	- Max depth of Frost damage Concrete in Good Condition	- Max depth of Frost damage
2.0	- Max depth of Frost damage	- 3-in. Max Size Natural Carbonate And Siliceous Gravel White RF product on broken surfaces	- 4-in. Max Size Natural Carbonate And Siliceous Gravel
3.0	-	-	-
4.0	-	-	-
5.0	-	-	-
6.0	-	-	-

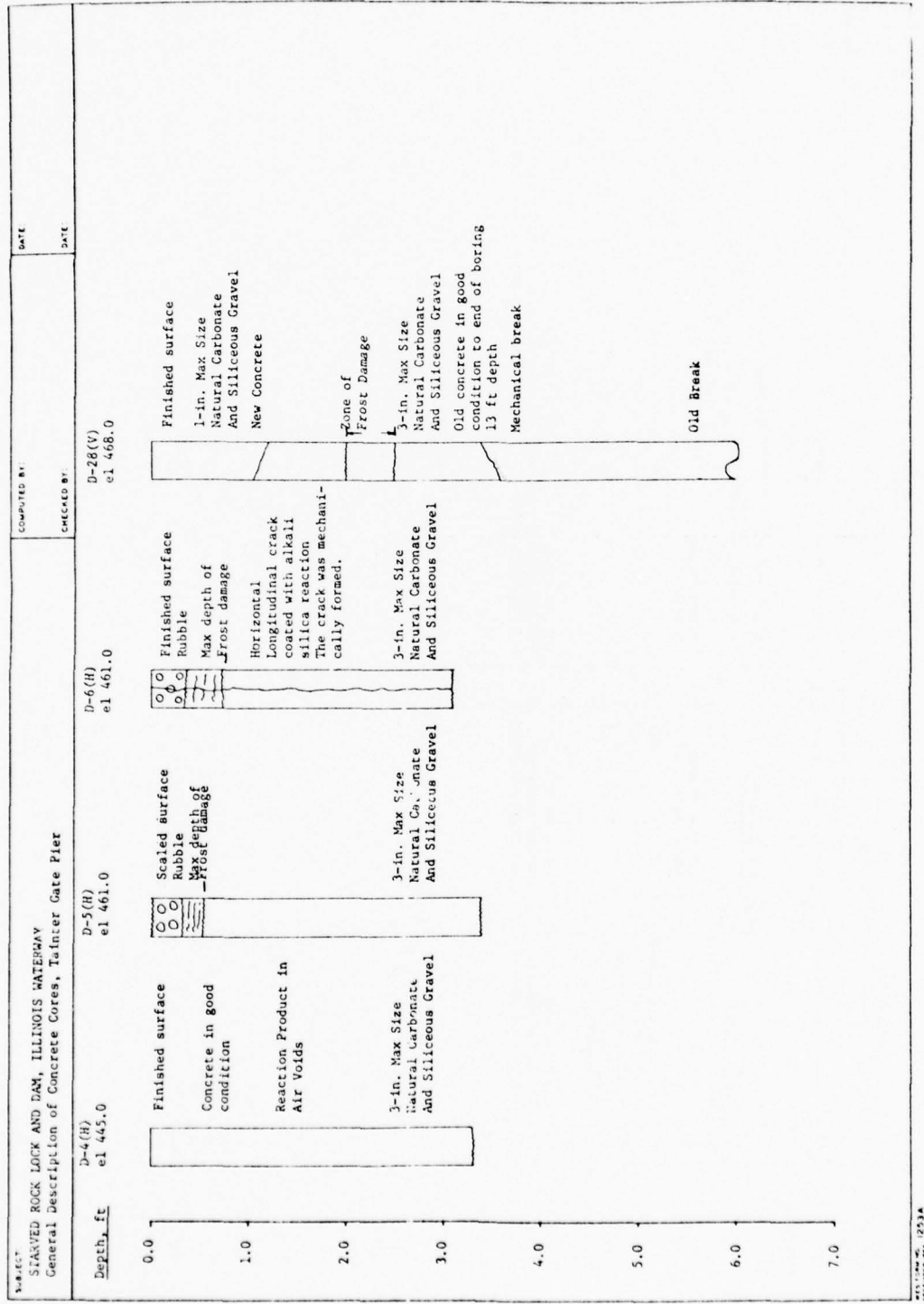


PLATE B7

STAKED ROCK LOCK AND DAM, ILLINOIS WATERWAY
General Description of PIER NO. 6, Tailwater Caisse Pier

Description of Caisse Pier		Components of Caisse Pier		Date
Depth, ft	Pier No.	Component No.	Condition	Comments
0.0	Pier #6 el 461.0	D-7(H) el 461.0	Finished surface Local Frost damage FR	U-7(V) el 445.0
1.0		D-8(H) el 461.0	Finishe[d] surface of Frost damage Old Longitudinal Crack Concrete in good condition	U-9(H) el 468.0
2.0			Concrete in good condition	
3.0			White reaction product on horizontal and longitudinal cracks. Cracks caused by chemical reaction.	
4.0				
5.0				
6.0				
7.0			Natural Break	

PLATE B8

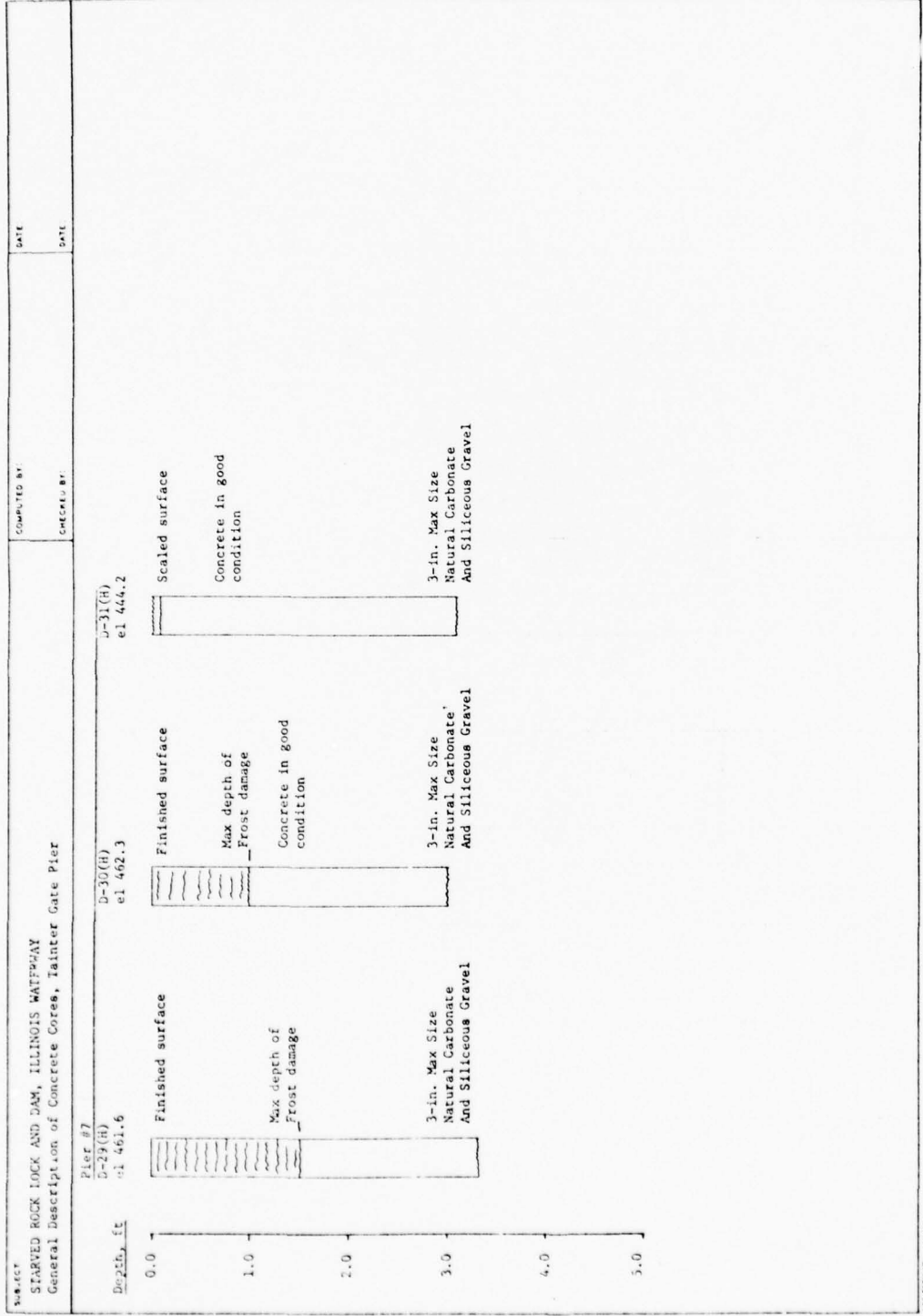


PLATE B9

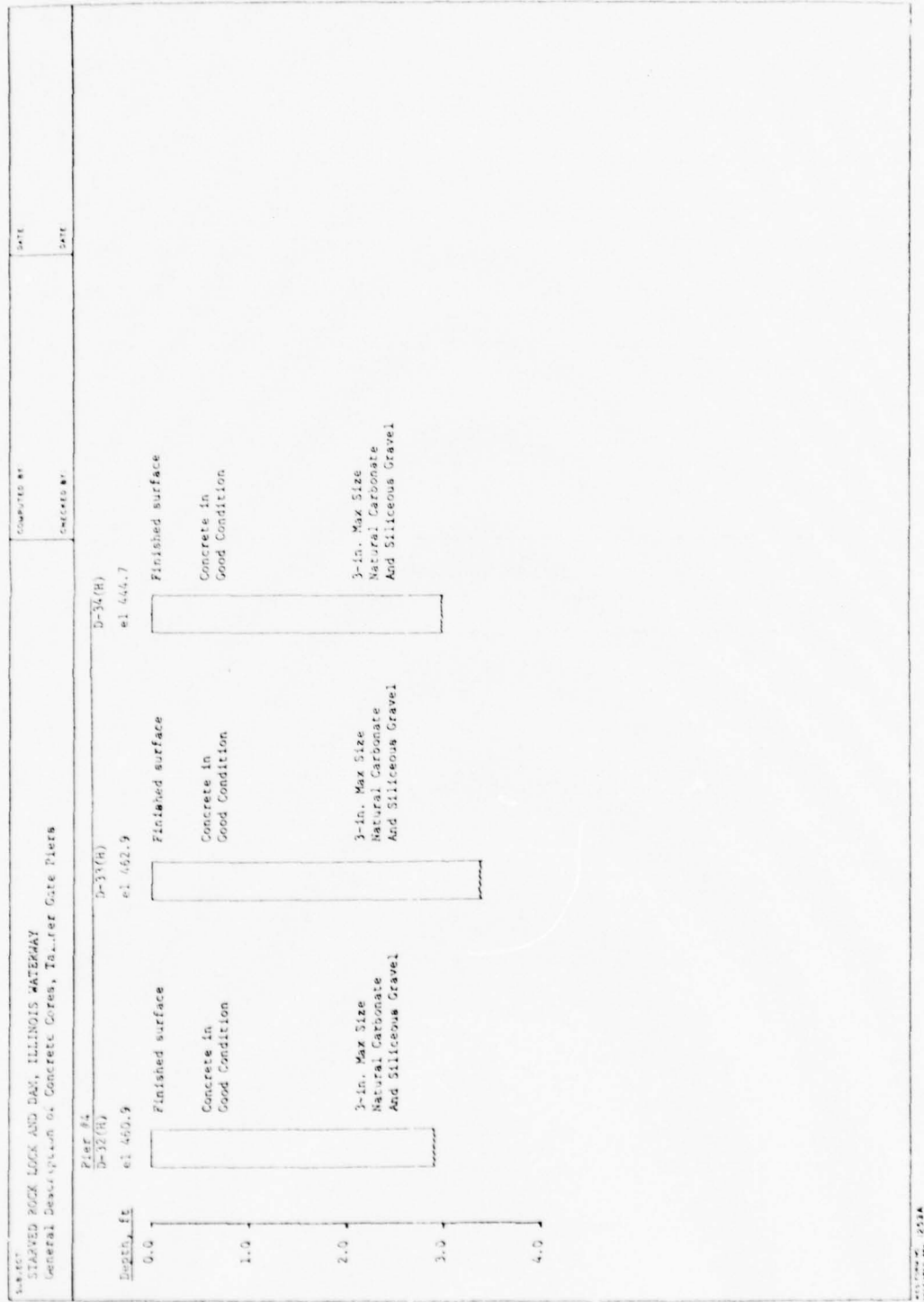


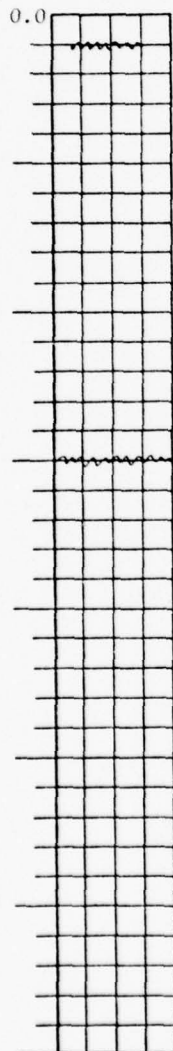
PLATE B10

STARVED ROCK LOCK AND DAM
ILLINOIS WATERWAY, CHICAGO DISTRICT
6-in.-Diameter Vertical Concrete Core

SR WES GW-1-77

Depth

ft.



Finished Surface
FR

1-1/2-in. maximum size aggregate
natural carbonate coarse aggregate
with some igneous rock particles
Natural siliceous fine aggregate

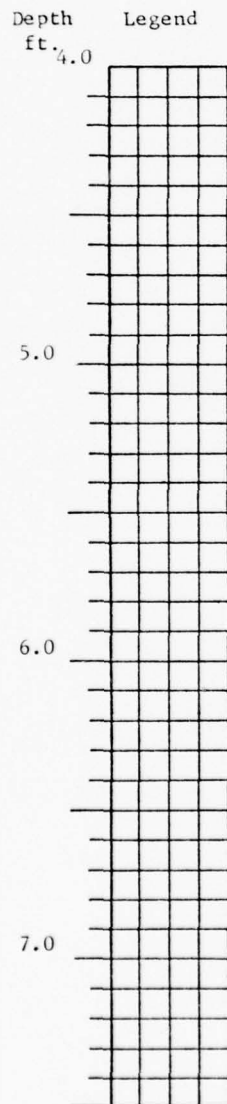
Maximum depth
of frost
damage

Air-Entrained
Some entrapped air

No detailed petrography

Concrete is in good condition
from 1.5 to 8.0 ft

STARVED ROCK LOCK AND DAM
ILLINOIS WATERWAY, CHICAGO DISTRICT
6-in.-Diameter Concrete Core

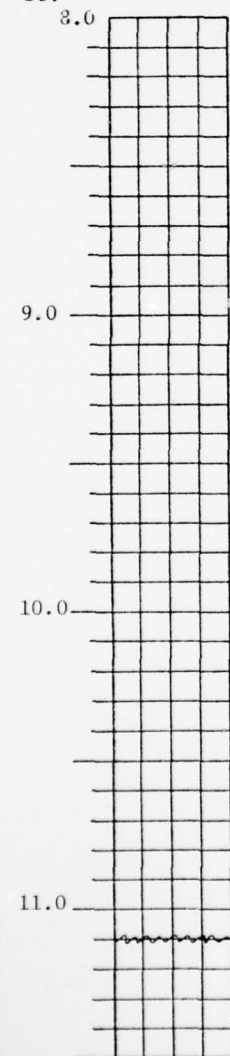


STARVED ROCK LOCK AND DAM
ILLINOIS WATERWAY, CHICAGO DISTRICT

6-in.-Diameter

Concrete Core

Depth Legend
ft.



8.0

2-in. maximum size aggregate
Natural carbonate coarse aggregate
with some igneous rock particles

Natural siliceous fine aggregate
Air-entrained
Some entrapped air
Concrete in good condition

9.0

Lift Joint

1-1/2-in. maximum size aggregate
Natural carbonate coarse aggregate
with some igneous rock particles
Natural siliceous fine aggregate
Not air-entrained
Some entrapped
Concrete is in good condition

10.0

No detailed petrography

Concrete examined at greater depths
is like the concrete described below
9.1 ft depth with 3-in. maximum size
aggregate

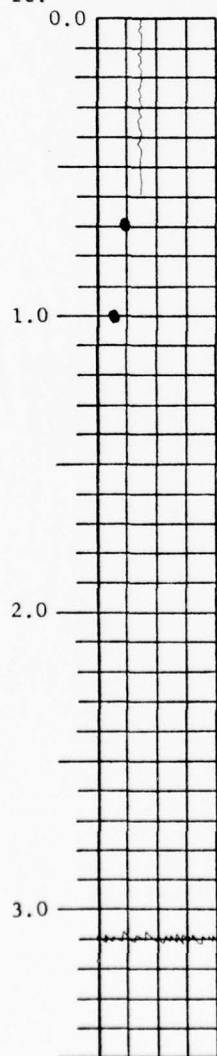
11.0

STARVED ROCK LOCK AND DAM
ILLINOIS WATERWAY, CHICAGO DISTRICT
6-in.-Diameter Horizontal Concrete Core

Horizontal Concrete Core

SR WES GW-3-77

Depth Legend
ft.



Finished Surface

3-in. maximum size aggregate
Natural carbonate coarse aggregate
with some igneous rock particles
Natural siliceous fine aggregate

Not air-entrained

Some entrapped air

Longitudinal crack is old with some alkali-silica gel but not very extensive

PLATE B12

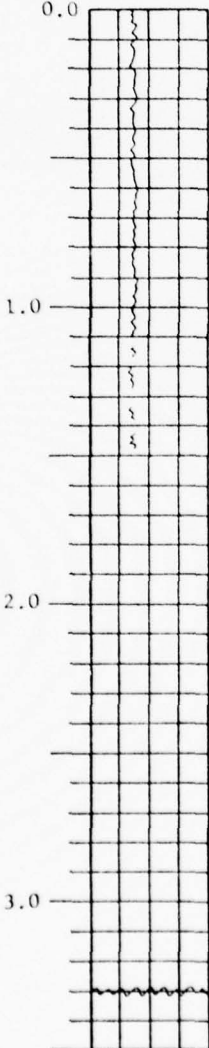
STARVED ROCK LOCK AND DAM
ILLINOIS WATERWAY, CHICAGO DISTRICT
6-in.-Diameter Horiz

Horizontal Concrete Core

SR WES GW-4-77

Depth Legend
ft.

Finished Surface



3-in. maximum size aggregate
Natural carbonate coarse aggregate
with some igneous rock particles
Natural siliceous fine aggregate
Not air-entrained

Some entrapped air

Longitudinal crack is old with some secondary calcite deposit in voids along crack

Concrete is in good condition except for longitudinal crack

PLATE B13

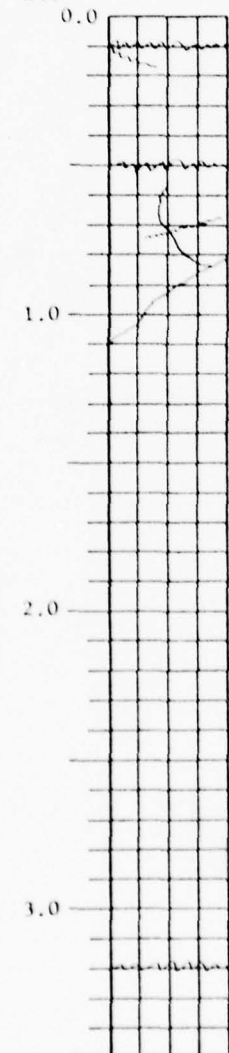
STARVED ROCK LOCK AND DAM

ILLINOIS WATERWAY, CHICAGO DISTRICT

6-in.-Diameter

Horizontal Concrete Core

SR WES GW-9-77

Depth Legend
ft.

Finished Surface

3-in. maximum size aggregate

Natural carbonate coarse aggregate
with some igneous rock particles
Natural siliceous fine aggregate
Not air-entrained

Some alkali-silica gel in some
voids but is not very extensive

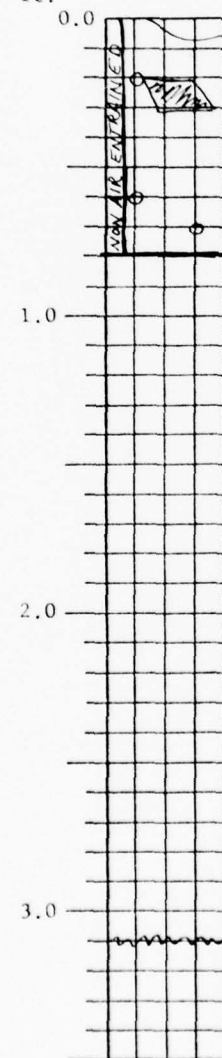
STARVED ROCK LOCK AND DAM
ILLINOIS WATERWAY, CHICAGO DISTRICT

6-in.-Diameter

Horizontal Concrete Core

SR WES GW-13-77

Depth Legend
ft.



0.0	Finished Surface	1-in. maximum size aggregate
	Steel armor plate	Natural carbonate coarse aggregate
	FR	
	1/2-in. steel flat iron	
	1-1/2-in. steel bar, 1/2-in. steel bar	Some poor consolidation around steel
	1/2-in. steel bar	Concrete is air-entrained except
	3/4-in. steel bar	where indicated
	Construction Joint	

Some alkali-silica gel in voids

3-in. maximum size aggregate
Natural carbonate coarse aggregate

Natural siliceous fine aggregate
Air-entrained

Concrete is in good condition

3.0 End of boring

v

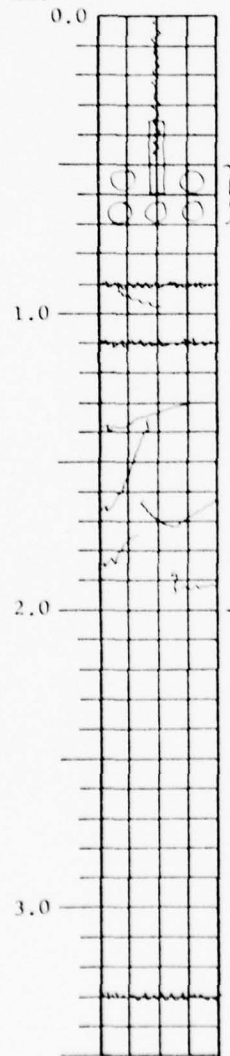
STARVED ROCK LOCK AND DAM

ILLINOIS WATERWAY, CHICAGO DISTRICT

6-in.-Diameter

Horizontal Concrete Core

SR WES D-1-77

Depth Legend
ft.

3/4-in. maximum size aggregate
 Natural carbonate coarse aggregate
 Natural siliceous fine aggregate
 Longitudinal crack is old
Air-entrained

3-in. maximum size aggregate
 Natural carbonate coarse aggregate with some igneous rock particles
 Natural siliceous fine aggregate

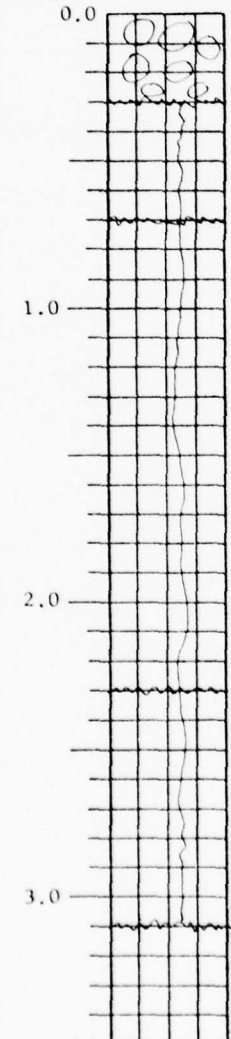
Not air-entrained
 Some entrapped air

Concrete is in good condition below
 below 2.0 ft.

STARVED ROCK LOCK AND DAM
ILLINOIS WATERWAY, CHICAGO DISTRICT
6-in.-Diameter Horizontal Concrete Core

SR WES D-6-77

Depth Legend
ft.



Formed Surface
Rubble
3-in. maximum size aggregate
Natural carbonate coarse aggregate
with some igneous rock particles
Natural siliceous fine aggregate

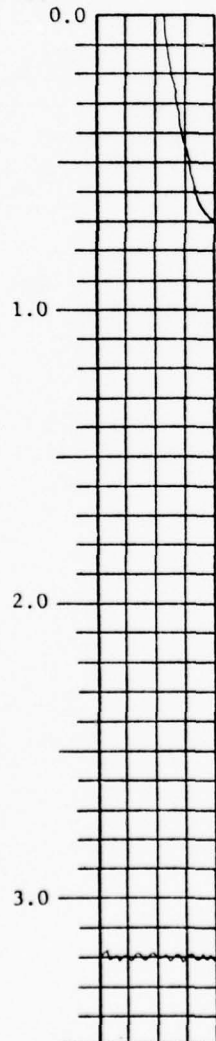
Maximum depth
of frost damage
Longitudinal crack coated with
alkali-silica gel. Appears not
to be cause of crack
Not air-entrained
Some entrapped air

Mortar has a sandy texture on cored
surface and may have been too wet
when placed

STARVED ROCK LOCK AND DAM
ILLINOIS WATERWAY, CHICAGO DISTRICT
6-in.-Diameter Horizontal Concrete Core

SR WES D-9-77

Depth Legend
ft.

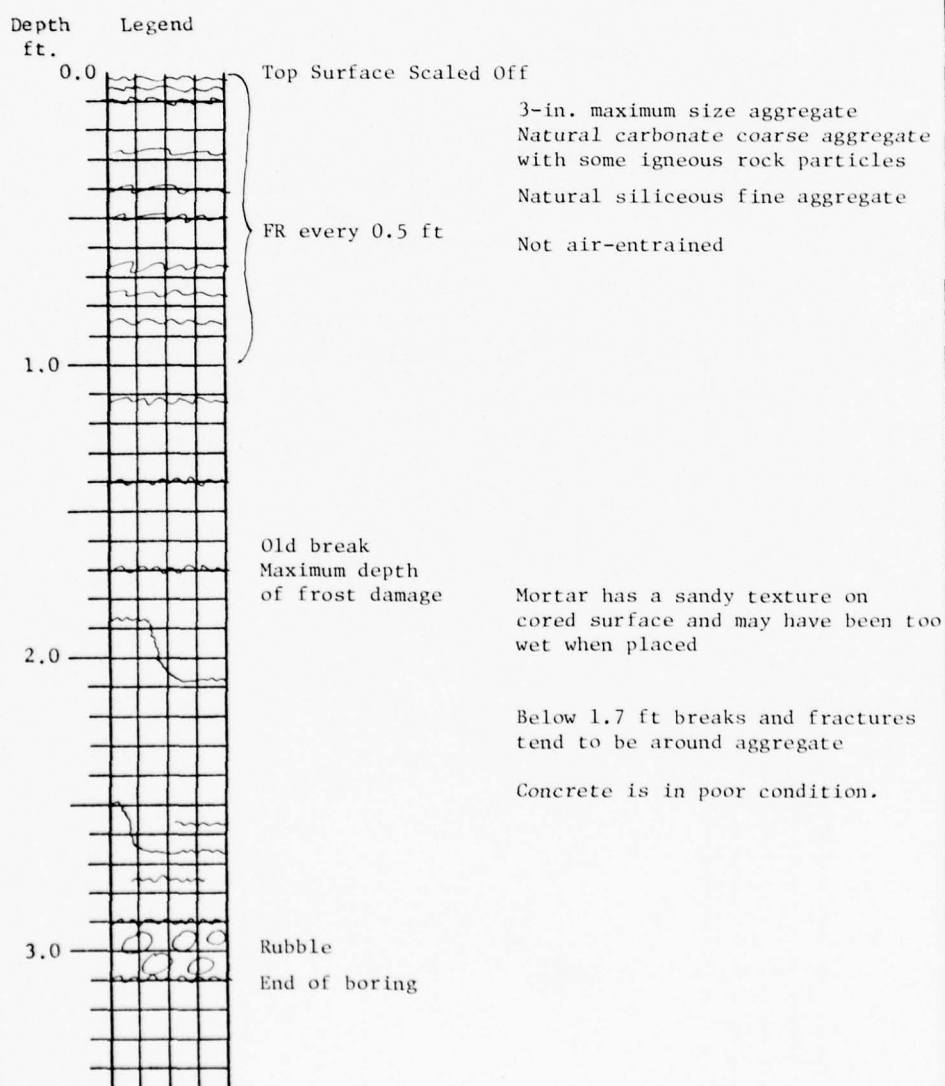


3-in. maximum size aggregate
Natural carbonate coarse aggregate
with some igneous rock particles
Natural siliceous fine aggregate
Longitudinal crack is old

Not air-entrained
Concrete is in good condition.

STARVED ROCK LOCK AND DAM
ILLINOIS WATERWAY, CHICAGO DISTRICT
6-in.-Diameter Vertical Concrete Core

SR WES D-20-77



STARVED ROCK LOCK AND DAM
ILLINOIS WATERWAY, CHICAGO DISTRICT
6-in.-Diameter Vertical Concrete Core

SR WES D-21-77

Depth ft. Legend

0.0 Finished Surface

3-in. maximum size aggregate
Natural carbonate aggregate
with some igneous rock particles
Natural siliceous aggregate

1.0 Not air-entrained
Some entrapped air

2.0

Concrete is in good condition

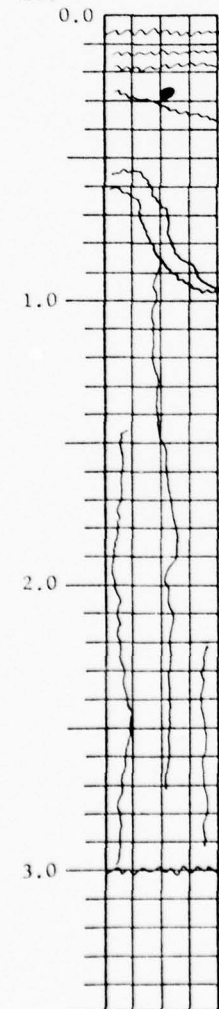
2.0

3.0 End of boring

This figure is a borehole log or soil profile diagram. It features a vertical axis on the left labeled 'Depth ft.' with major tick marks at 0.0, 1.0, 2.0, and 3.0. To the right of the axis, there is a legend titled 'Legend' and descriptive text for each depth interval. At the top, 'Finished Surface' is indicated. Below it, three aggregate types are listed: '3-in. maximum size aggregate', 'Natural carbonate aggregate with some igneous rock particles', and 'Natural siliceous aggregate'. The next section, from 1.0 to 2.0 feet, describes the presence of 'Not air-entrained' concrete with 'Some entrapped air'. The final section, from 2.0 to 3.0 feet, states that 'Concrete is in good condition'. The bottom of the log is marked as the 'End of boring'.

STARVED ROCK LOCK AND DAM
ILLINOIS WATERWAY, CHICAGO DISTRICT
6-in.-Diameter Horizontal Concrete Core

SR WES D-22-77

Depth Legend
ft.

Finished Surface

Broken surfaces are
carbonated
3/4-in. steel bar
Maximum depth
of frost damage

2-in. maximum size aggregate
Natural carbonate coarse aggregate with some igneous rock particles
Natural siliceous fine aggregate

Not air-entrained

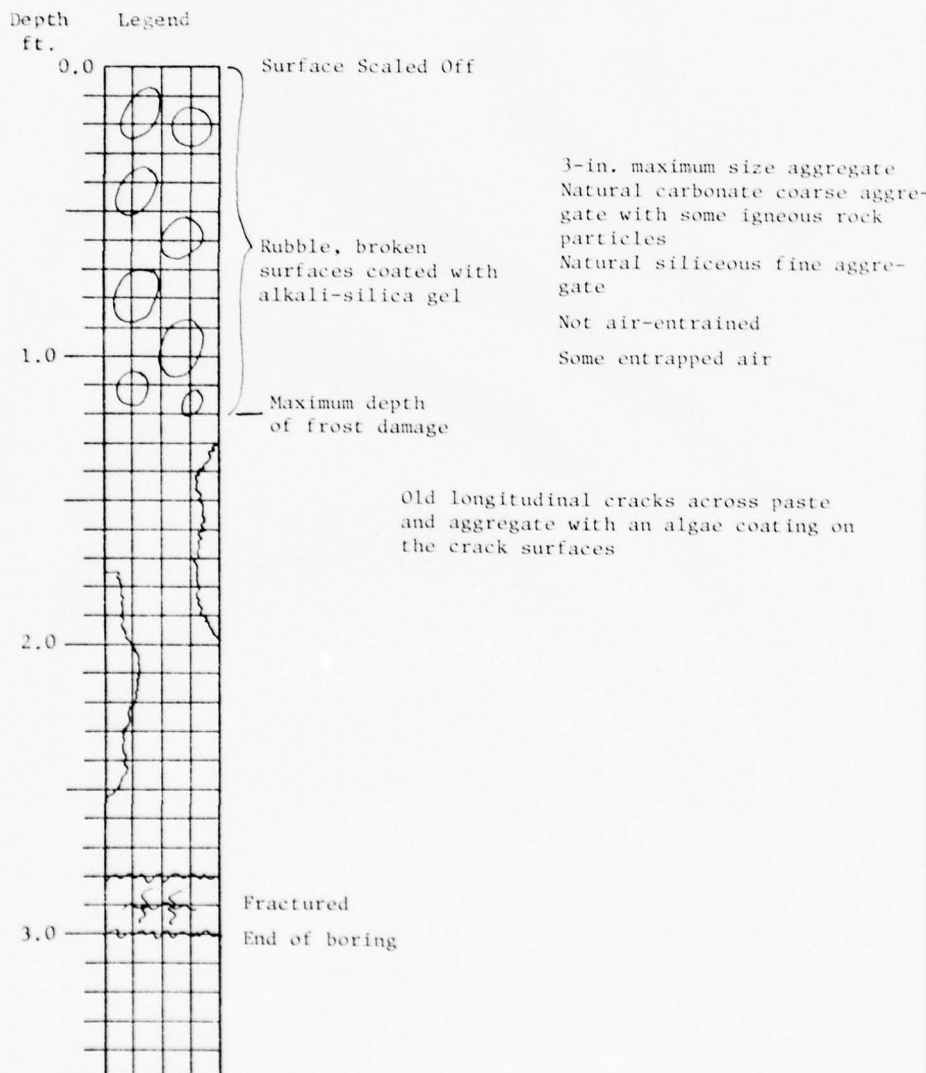
Several incipient longitudinal cracks opened when struck with a sledge hammer. No reaction product was observed

2.0

End of boring

STARVED ROCK LOCK AND DAM
ILLINOIS WATERWAY, CHICAGO DISTRICT
6-in.-Diameter Horizontal Concrete Core

SR WES D-26-77



V
APPENDIX C

SEISMIC COEFFICIENT

STARVED ROCK LOCK AND DAM
ILLINOIS WATERWAY



DEPARTMENT OF THE ARMY
WATERWAYS EXPERIMENT STATION, CORPS OF ENGINEERS
P. O. BOX 631
VICKSBURG, MISSISSIPPI 39180

IN REPLY REFER TO WESCC

25 May 1978

SUBJECT: Use of Seismic Coefficient for Starved Rock Installation

District Engineer
U.S. Army Engineer District, Chicago
ATTN: Chief, Foundations, Materials, and Surveying Branch
219 S. Dearborn St.
Chicago, IL 60604

1. In regards to your comments on the Starved Rock Rehabilitation Project submitted by W.E.S., especially comment 4, I found it necessary to answer in detail.

2. The comment was stated:

"Page 15, para. 28; The sandwich Fault is a major structure although not too active to date. Does W.E.S. have any reservations about using the standard zone value for seismic coefficient for the Illinois Waterway System as found in Figure 6 of EM1110-2-1902?"

3. I spoke with several earthquake engineers at W.E.S. in the Structures Branch and was told that considerable care should be taken when using the seismic coefficient method. In the Corps this method is gradually being replaced by more accurate analyses. They recommended using Response Spectrum or Time History Methods for determining Earthquake Analysis figures for a particular structure. In any case, calculating a design-basis earthquake for Starved Rock is beyond the scope of our study and would require an additional study if it were deemed sufficiently important.

4. However, the study done for the Atomic Energy Commission by Sargent and Lundy in 1973 on a proposed nuclear power plant to be built in LaSalle County has some information which may be applicable to Starved Rock Installation. The detailed Earthquake Analysis indicates that "of all earthquake events which can be postulated for the design-basis earthquake, the maximum level of horizontal ground motion of 20% (.2 g) of gravity would result from the occurrence at or

WESCC

SUBJECT: Use of Seismic Coefficient for Starved Rock Installation

near the plant site of an earthquake similar to the 1900 northern Illinois Intensity VII shock." This is probably a better estimate than the 5% (.05 g) given in the seismic coefficient map in EM1110-2-1902. It has not been calculated whether the Lock and Dam could withstand an earthquake of this magnitude. For additional information on the Atomic Energy Commission report, see the 1973 Appendix A-Soils and Geology Report for Starved Rock.

5. If more information is needed about the newer earthquake analysis methods or the calculations of the design-basis earthquake for Starved Rock, contact Dean Norman, Structures Division, Weapons Effects Laboratory, W.E.S.

FOR THE COMMANDER AND DIRECTOR:

BARBARA PAVLOV
Concrete and Rock Properties Branch
Structures Laboratory

CF:
Structures Lab, Dean Norman

APPENDIX D
HYPOTHETICAL SLIDE WEDGES
STARVED ROCK LOCK & DAM
ILLINOIS WATERWAY

This appendix contains paper exercises intended as examples to show the possibility of rock wedges forming in the foundation rock at Starved Rock. The discussion of possible rock wedges, as presented in para 103, is in response to comment No. 26 of NCCED-F letter, subject, "Concrete and Rock Tests, Major Rehabilitation, Starved Rock Lock and Dam, Illinois Waterway, Chicago District," the letter containing comments to subject report.

v

Dam Scour azimuth = $115^{\circ}/295^{\circ}$

Prominent joints in order of frequency from Reference 5.

	<u>Strike</u>	<u>Dip</u>	<u>Dip Dir.</u>
1	$0^{\circ}/180^{\circ}$	16°	90°
2	$144^{\circ}/324^{\circ}$	17°	234°
3	$90^{\circ}/270^{\circ}$	10°	0°
4	$52^{\circ}/232^{\circ}$	20°	322°
5	$61^{\circ}/241^{\circ}$	8°	151°

Bedding			
B	$45^{\circ}/255^{\circ}$	10°	135°

Visual checking of failure possibility:

S-1-2 - to N, No. Maybe to S	S-2-4 No	S-3-5 N
S-1-3 - Maybe to N	S-3-4 No	S-4-5 S
S-2-3 - Neither way	S-1-5 No	
S-1-4 - Yes to N	S-2-5 S	

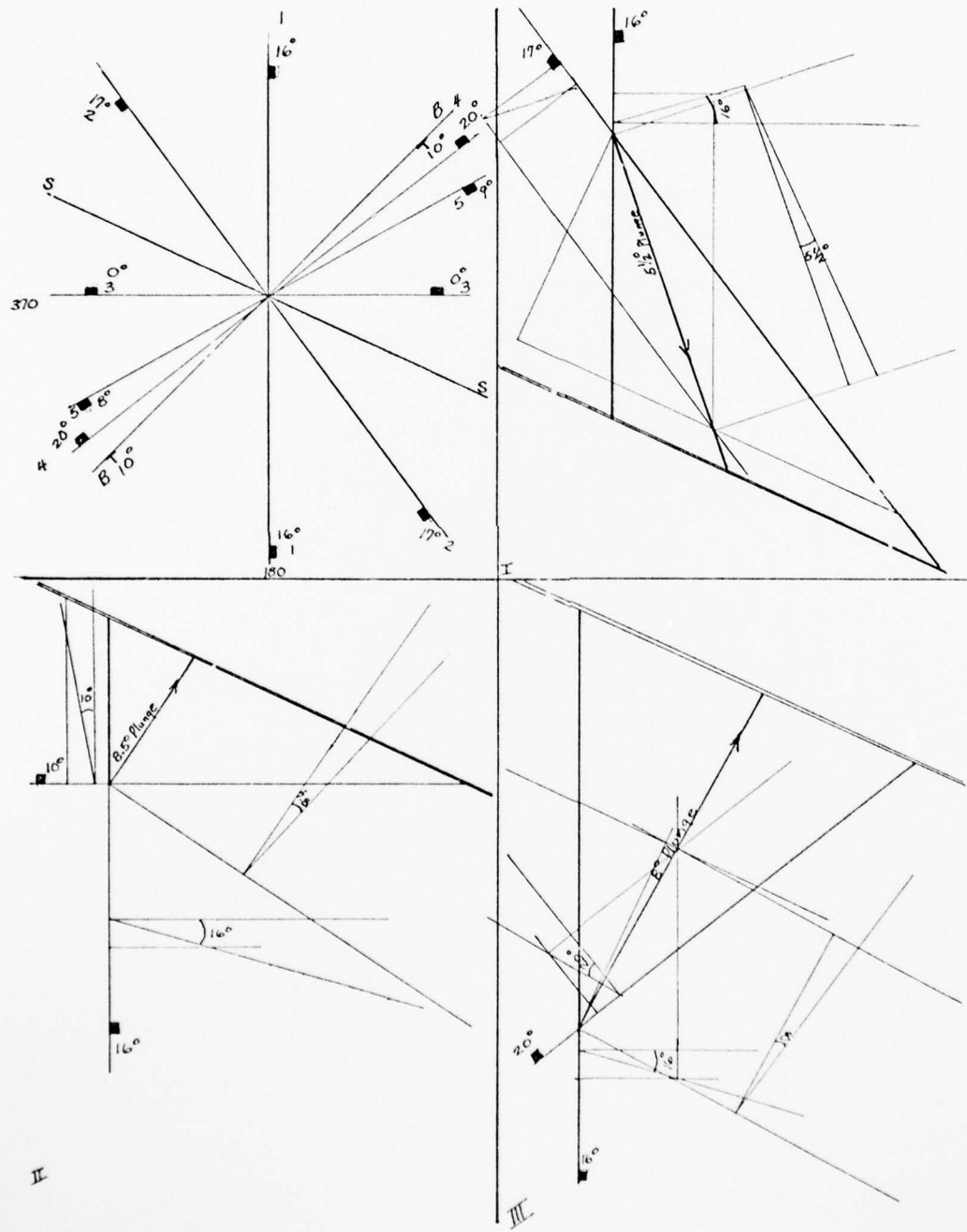
S-B-1 No.	2 plane possibilities
S-B-2 S	
S-B-3 N	I S-1-2 to South
S-B-4 N	II S-1-3 to North
S-B-5 No.	III S-1-4 to North
	IV S-2-5 to South
	V S-3-5 to North
	VI S-4-5 to South
	VII S-B-2 to South
	VIII S-B-3 to North
	IX S-B-4 to North

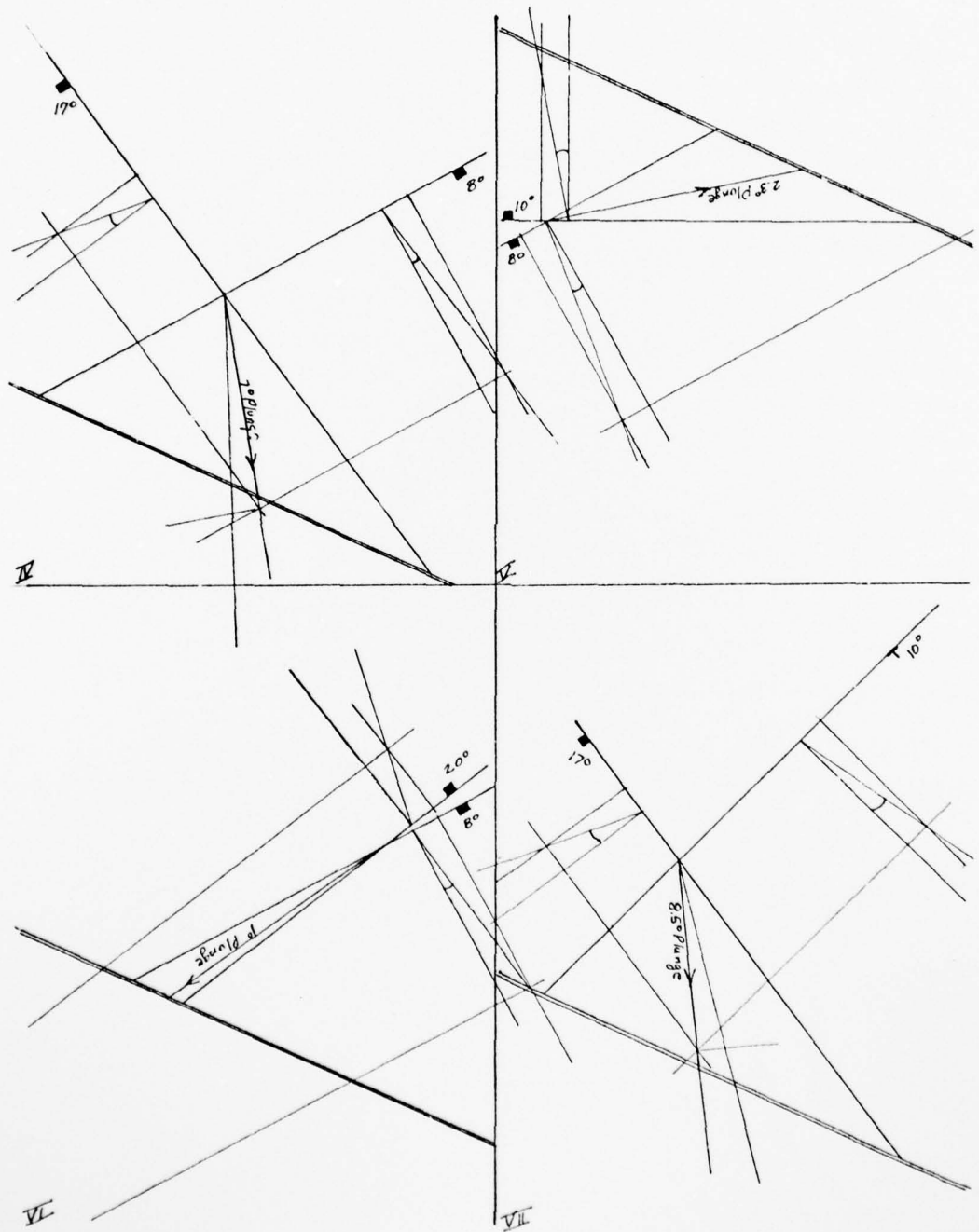
Wet weight 150pcf

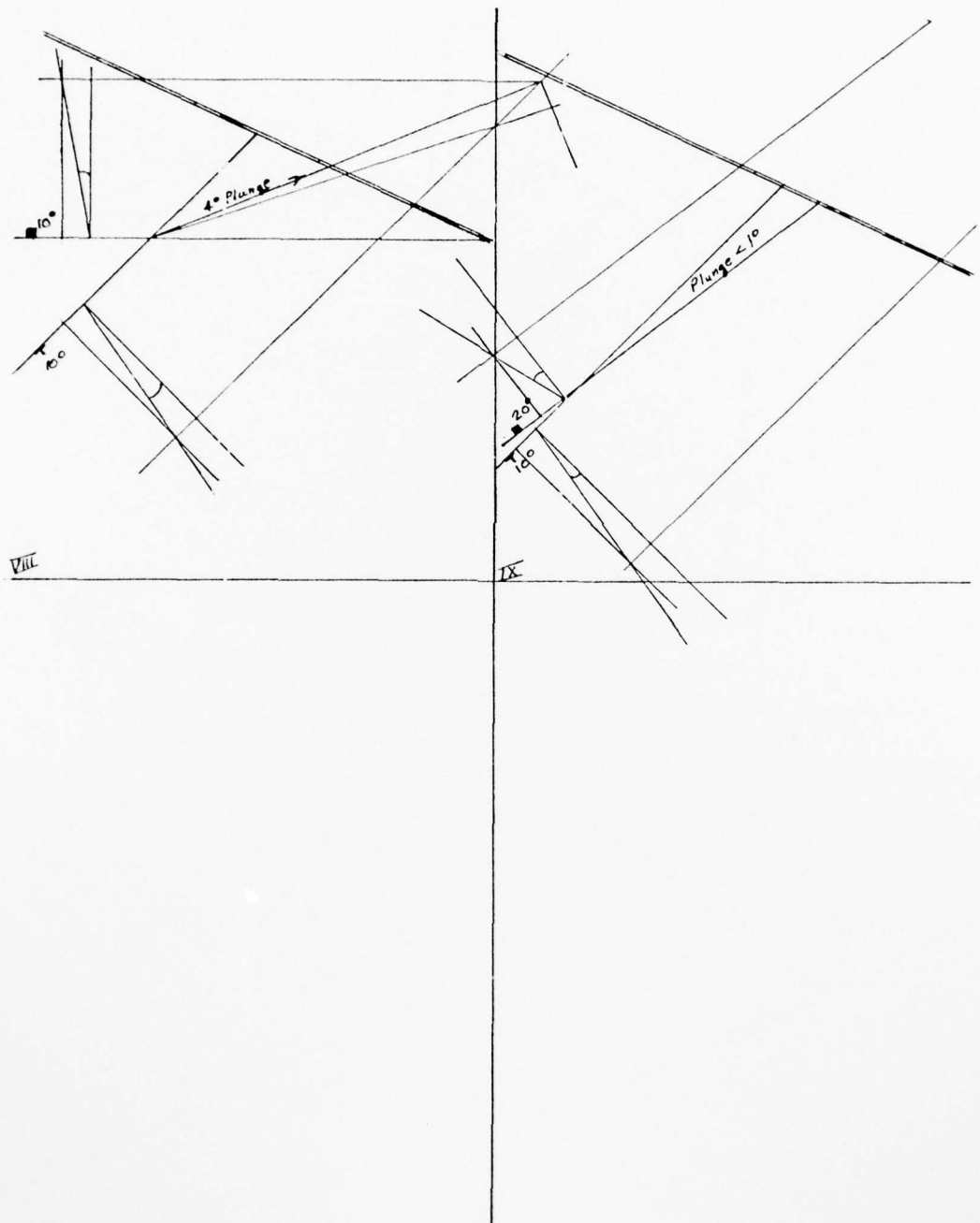
$\phi = 13.7^{\circ}$

$\alpha = 90^{\circ}$

$\delta = 0^{\circ}$







Hendron, A. J., E. J. Carding, and A. K. Aiger, Analytical and Graphical Methods for the Analysis of Slopes in Rock Masses. NCG Technical Report No. 36, 1971. WES contract report.

$$2.13 \quad \vec{u} = (\cos \beta, \sin \beta, 0)$$

$$2.14 \quad \vec{v} = (\cos \gamma, \sin \beta, -\cos \gamma \cos \beta, -\sin \gamma)$$

$$2.15 \quad \vec{w} = \vec{w} \times \vec{v} = \begin{vmatrix} \vec{i} & \vec{j} & \vec{k} \\ u_x & u_y & u_z \\ v_x & v_y & v_z \end{vmatrix}$$

$$= \{(u_y v_z - u_z v_y), (u_z v_x - u_x v_z), (u_x v_y - u_y v_x)\}$$

$$= \{u_y v_z, -u_x v_z, (u_x v_y - u_y v_x)\}$$

$$3.4 \quad F.S. = \frac{(\vec{w} \cdot \vec{w}) \tan \phi}{(\vec{w} \cdot \vec{v})} \quad (\text{single plane})$$

$$2.16 \quad \vec{x}_{12} = \vec{w}_2 \times \vec{w}_1$$

$$= \{(W_{2y} W_{1z} - W_{2z} W_{1y}), (W_{2z} W_{1x} - W_{2x} W_{1z}), (W_{2x} W_{1y} - W_{2y} W_{1x})\}$$

$$3.15 \quad \vec{s}_{12} = \vec{x}_{12} \times \vec{w} \\ = \{(x_{12y} W_z - x_{12z} W_y), (x_{12z} W_x - x_{12x} W_z), (x_{12x} W_y - x_{12y} W_x)\}$$

Vector Analyses of nine possible wedges.

I. S-1-2

Plane 1	Plane 2
$\beta_1 = 115^\circ$	$\beta_2 = 152^\circ$
$\gamma_1 = 16^\circ$	$\gamma_2 = 17^\circ$

$$\begin{aligned} u_1 &= (-0.423, 0.906, 0) \\ v_1 &= (0.871, 0.406, -0.276) \\ w_1 &= (-0.250, -0.117, -0.961) \end{aligned}$$

$$\begin{aligned} u_2 &= (-0.883, 0.469, 0) \\ v_2 &= (0.449, 0.844, -0.292) \\ w_2 &= (-0.137, -0.258, -0.956) \end{aligned}$$

$$\begin{aligned} \bar{R} &= (0.0, -W) \\ \bar{R} \cdot \bar{W} &= 0 + 0 + (-0.961)(-W) = 0.961W > 0 \\ \bar{R} \cdot \bar{W} &= 0.956W > 0 \quad \text{Sliding } \underline{\text{cannot}} \text{ occur on 2} \end{aligned}$$

$$\begin{aligned} \bar{x}_{12} &= (0.136, 0.107, -0.048) \\ x_{12} &= 0.032 \\ \bar{s}_{12} &= (-0.108, 0.143, 0.011) \\ \bar{s}_{12} &= (-0.115, 0.137, -0.020) \\ \epsilon_x &= -24.16^\circ \end{aligned}$$

$$\begin{aligned} I. \quad \bar{R} \cdot \bar{s}_{12} &= 0.011W < 0 \\ \bar{R} \cdot \bar{s}_{12} &= 0.020W < 0 \\ \bar{x}_{12} &\text{ sliding impossible} \\ \bar{R} \cdot \bar{w}_1 &= 0.961W > 0 \\ \text{plane 1 sliding possible.} \end{aligned}$$

Single plane sliding on plane 1 by dead weight,

$$\begin{aligned} F.S. &= \frac{0.961W \tan 13.7}{0.276W} = \underline{\underline{0.849}} \\ \text{requires } \phi &\geq 16.0^\circ \text{ to make static F.S. } \geq 1. \end{aligned}$$

II. S-3-1

Plane 3	Plane 1
$\beta_1 = 24.5^\circ$	$\beta_2 = 115^\circ$
$\gamma_1 = 10^\circ$	$\gamma_2 = 16^\circ$

$$\begin{aligned} u_1 &= (0.910, 0.415, 0) \\ v_1 &= (0.408, -0.896, -0.174) \\ w_1 &= (-0.072, 0.158, -0.985) \end{aligned}$$

$$\begin{aligned} u_2 &= (-0.423, 0.906, 0) \\ v_2 &= (0.871, 0.406, -0.276) \\ w_2 &= (-0.250, -0.117, -0.961) \end{aligned}$$

$$\begin{aligned} \bar{R} &= (0, 0, -W) \\ \bar{R} \cdot W_1 &= 0.985W > 0 \quad \text{no tension} \\ \bar{R} \cdot W_2 &= 0.961W > 0 \quad \text{tensile breaks} \end{aligned}$$

Single plane sliding on plane 3 by dead weight.

$$F.S. = \frac{0.985W \tan 13.7}{0.174W} = \underline{\underline{1.38}}$$

Lateral loading or pore pressure could initiate movement but otherwise stable.

III. S-4-1

Plane 4	Plane 1
$\beta_1 = 63^\circ$	$\beta_2 = 115^\circ$
$\gamma_1 = 20^\circ$	$\gamma_2 = 16^\circ$

$$\begin{aligned} u_1 &= (0.454, 0.891, 0) \\ v_1 &= (0.837, -0.427, -0.343) \\ w_1 &= (-0.306, 0.156, -0.940) \end{aligned}$$

$$\begin{aligned} u_2 &= (-0.423, 0.906, 0) \\ v_2 &= (0.871, 0.406, -0.276) \\ w_2 &= (-0.250, -0.117, -0.961) \end{aligned}$$

$$\begin{aligned} \bar{R} &= (0, 0, -W) \\ \bar{R} \cdot W_1 &= 0.940W > 0 \quad \text{no tension} \\ \bar{R} \cdot W_2 &= 0.961W > 0 \quad \text{tensile} \end{aligned}$$

Single plane sliding on plane 4 by dead weight.

$$F.S. = \frac{0.940W \tan 13.7}{0.343W} = \underline{\underline{0.668}}$$

requires $\phi \geq 20.0^\circ$ to make static F.S. ≥ 1 .

IV. S-5-2

Plane 5

$$\beta_1 = 53^\circ$$

$$\gamma_1 = 8^\circ$$

Plane 2

$$\beta_2 = 152^\circ$$

$$\gamma_2 = 17^\circ$$

$$u_1 = (0.602, 0.799, 0)$$

$$v_1 = (0.791, -0.596, -0.139)$$

$$w_1 = (-0.111, 0.084, -0.991)$$

$$u_2 = (-0.883, 0.469, 0)$$

$$v_2 = (0.449, 0.844, -0.292)$$

$$w_2 = (-0.137, -0.258, -0.956)$$

$$\bar{R} = (0, 0, -W)$$

$$\bar{R} \cdot \bar{W}_1 = 0.991W > 0 \quad \text{no tension}$$

$$\bar{R} \cdot \bar{W}_2 = 0.956W > 0 \quad \text{tensile}$$

Single plane sliding on plane 5 by dead weight.

$$F.S. = \frac{0.991W \tan 13.7}{0.139W} = \underline{\underline{1.738}}$$

stable under dead weight alone.

V. S-3-5

Plane 3

$$\beta_1 = 24.5^\circ$$

$$\gamma_1 = 10^\circ$$

Plane 5

$$\beta_2 = 53^\circ$$

$$\gamma_2 = 8^\circ$$

$$u_1 = (0.910, 0.415, 0)$$

$$v_1 = (0.480, -0.896, -0.174)$$

$$w_1 = (-0.072, 0.158, -0.985)$$

$$u_2 = (0.602, 0.799, 0)$$

$$v_2 = (0.791, -0.596, -0.139)$$

$$w_2 = (-0.111, 0.084, -0.991)$$

$$\begin{aligned}\bar{R} &= (0, 0, -W) \\ \bar{R} \cdot \bar{w}_1 &= +0.985W > 0 \quad \text{no tension} \\ \bar{R} \cdot \bar{w}_2 &= 0.991W > 0 \quad \text{tensile}\end{aligned}$$

Single plane sliding on plane 3 by dead weight.

$$F.S. = \frac{0.985W \tan 13.7}{0.174W} = \underline{\underline{1.380}}$$

stable under dead weight alone.

VI. S-5-4

Plane 5	Plane 4
$\beta_1 = 53^\circ$	$\beta_2 = 63^\circ$
$\gamma_1 = 8^\circ$	$\gamma_2 = 20^\circ$

$$\begin{aligned}u_1 &= (0.602, 0.799, 0) \\ v_1 &= (0.791, -0.596, -0.139) \\ w_1 &= (-0.111, 0.085, -0.991)\end{aligned}$$

$$\begin{aligned}u_2 &= (0.454, 0.891, 0) \\ v_2 &= (0.837, -0.427, -0.343) \\ w_2 &= (-0.306, 0.156, -0.940)\end{aligned}$$

$$\begin{aligned}\bar{R} &= (0, 0, -W) \\ \bar{R} \cdot \bar{w}_1 &= 0.991W > 0 \quad \text{no tension} \\ \bar{R} \cdot \bar{w}_2 &= 0.940W > 0 \quad \text{tensile}\end{aligned}$$

Single plane sliding on plane 5 by dead weight.

$$F.S. = \frac{0.991W \tan 13.7}{0.139W} = \underline{\underline{1.738}}$$

stable under dead weight alone.

VII. S-B-2

Plane B

$\beta_1 = 70^\circ$

$\gamma_1 = 10^\circ$

Plane 2

$\beta_2 = 152^\circ$

$\gamma_2 = 17^\circ$

$u_1 = (0.342, 0.940, 0)$

$v_1 = (0.925, -0.337, -0.174)$

$w_1 = (-0.164, 0.060, -0.985)$

$u_2 = (-0.883, 0.469, 0)$

$v_2 = (0.449, 0.844, -0.292)$

$w_2 = (-0.137, -0.258, -0.956)$

$\bar{R} = (0, 0, -W)$

$\bar{R} \cdot \bar{w}_1 = 0.985W > 0 \quad \text{no tension}$

$\bar{R} \cdot \bar{w}_2 = 0.956W > 0 \quad \text{tensile}$

Single plane sliding on bedding by dead weight.

$F.S. = \frac{0.985W \tan 13.7}{0.174W} = \underline{\underline{1.380}}$

stable under dead weight alone.

VIII. S-3-B

Plane 3

$\beta_1 = 24.5^\circ$

$\gamma_1 = 10^\circ$

Plane B

$\beta_2 = 70^\circ$

$\gamma_2 = 10^\circ$

$u_1 = (0.910, 0.415, 0)$

$v_1 = (0.480, -0.896, -0.174)$

$w_1 = (-0.072, 0.158, -0.985)$

$u_2 = (0.342, 0.940, 0)$

$v_2 = (0.925, -0.337, -0.174)$

$w_2 = (-0.164, 0.060, -0.985)$

$$\begin{aligned}\bar{R} &= (0, 0, -W) \\ \bar{R} \cdot \bar{w}_1 &= 0.985W > 0 \quad \text{no tension} \\ \bar{R} \cdot \bar{w}_2 &= 0.985W > 0 \quad \text{tensile}\end{aligned}$$

Single plane sliding on plane 3 by dead weight.

$$\text{F.S.} = \frac{0.985W \tan 13.7}{0.174W} = \underline{\underline{1.380}}$$

stable under dead weight alone.

IX.	S-4-B
Plane 4	Plane B
$\beta_1 = 63^\circ$	$\beta_2 = 70^\circ$
$\gamma_1 = 20^\circ$	$\gamma_2 = 10^\circ$

$$\begin{aligned}u_1 &= (0.454, 0.891, 0) \\ v_1 &= (0.837, -0.427, -0.343) \\ w_1 &= (-0.306, 0.156, -0.940)\end{aligned}$$

$$\begin{aligned}u_2 &= (0.342, 0.940, 0) \\ v_2 &= (0.925, -0.337, -0.174) \\ w_2 &= (-0.164, 0.060, -0.985)\end{aligned}$$

$$\begin{aligned}\bar{R} &= (0, 0, -W) \\ \bar{R} \cdot \bar{w}_1 &= 0.940W > 0 \quad \text{no tension} \\ \bar{R} \cdot \bar{w}_2 &= 0.985W > 0 \quad \text{tensile}\end{aligned}$$

Single plane sliding on plane 4 by dead weight.

$$\text{F.S.} = \frac{0.940W \tan 13.7}{0.343W} = \underline{\underline{0.668}}$$

requires $\phi \geq 20.0^\circ$ to make static F.S. ≥ 1 .

AD-A061 711 ARMY ENGINEER WATERWAYS EXPERIMENT STATION VICKSBURG MISS F/G 13/2
CONCRETE AND ROCK CORE TESTS, MAJOR REHABILITATION OF STARVED R--ETC(U)
SEP 78 R L STOWE, B A PAVLOV, G S WONG

UNCLASSIFIED

WES-MP-C-78-12

NL

3 of 3
AD
A061711



END
DATE
FILMED
2-79
DDC

Conclusions

Sliding on single plane only possible for cases I, III, and IX.

Case I: Sliding on plane 1, tensile crack on plane 2, and friction angle (ϕ) of 13.7° produces F.S. = 0.85. Requires ϕ of 16.0° to make static F.S. of 1.

Case III: Sliding on plane 4, tensile crack on plane 1, and friction angle (ϕ) of 13.7° produces F.S. = 0.67. Requires ϕ of 20.0° to make static F.S. of 1.

Case IX: Sliding on plane 4, tensile crack on bedding, and friction angle (ϕ) of 13.7° produces F.S. = 0.67. Requires ϕ of 20.0° to make static F.S. of 1.

Most critical discontinuities

Plane 4: strike = 52° ; dip = 20° NW

Plane 1: strike = 0° ; dip = 16° E

Plane 2: strike = 144° ; dip = 17° SW

Bedding: strike = 45° ; dip = 10° SE

Possible Volumes

Assume 10-ft height of vertical free face of slide wedges.

$$\begin{aligned} \text{Case I: Volume} &= \frac{1}{2} \times 79 \times 109 \times \frac{1}{3} \times 10 = 14,352 \text{ ft}^3 \\ &= 532 \text{ yd}^3 \end{aligned}$$

$$\begin{aligned} \text{Case III: Volume} &= \frac{1}{3} \times \frac{1}{2} \times 72 \times 69 \times 10 = 8,280 \text{ ft}^3 \\ &= 307 \text{ yd}^3 \end{aligned}$$

Case IX: Configuration appears very unlikely but would make a crack-like subsidence about 500 ft long normal to free face and 60 ft wide at free face

$$\begin{aligned} \text{Volume} &= \frac{1}{3} \times \frac{1}{2} \times 60 \times 500 \times 10 = 50,000 \text{ ft}^3 \\ &= 1,850 \text{ yd}^3 \end{aligned}$$

APPENDIX E

CAPPING EXPOSED SURFACES
OF CONCRETE

STARVED ROCK LOCK AND DAM
ILLINOIS WATERWAY



DEPARTMENT OF THE ARMY
WATERWAYS EXPERIMENT STATION, CORPS OF ENGINEERS
P. O. BOX 631
VICKSBURG, MISSISSIPPI 39180

IN REPLY REFER TO: WESCC

22 July 1977

MEMORANDUM FOR RECORD

SUBJECT: Capping exposed surfaces of Concrete, Tainter Gate Piers,
Starved Rock and Dresden Island Dams, Illinois Waterway

1. The undersigned visited Starved Rock and Dresden Island on 8-9 July 1977 for purposes of inspecting certain sections of the locks and dams containing deteriorated concrete. I met with Mr. Ignas Juzenas (Chief of the Structure Section), Chicago District), Mr. Jim Przwoznik (Chicago District), Mr. Vic Gernais (Joliet Area Office), and Mr. Don Byczynski (Lockmaster of Starved Rock Lock and Dam). Mr. Juzenas asked several questions concerning resurfacing the tainter gate piers which I could not answer. After returning to WES, I called a meeting of laboratory personnel to get their opinions on these questions. Those in attendance are listed in Incl 1.
2. The questions Mr. Juzenas asked me were presented:
 - a. If 9 in. of deteriorated concrete were removed from the exposed surfaces of a tainter gate pier. Would 9 in. of new concrete be an adequate cap over the pier?
 - b. What would be the best way to fasten on the concrete cap to the old cap considering that the cap could be subjected to large impact?
3. I explained that Mr. Juzenas and I were concerned about covering up the deteriorated concrete that was not removed. The piers are 8 ft. wide and in places there is 3.1 ft. of deteriorated concrete as observed in core taken in the horizontal direction on one side of the pier. Assuming that the opposite side of the pier contained an equal depth of bad concrete, then a large volume of deteriorated concrete would remain under a concrete cap. Mr. Hoff expressed concern that if the porous concrete under a 9 in. cap contained water, it would probably freeze and could crack the cap. He thought it worthwhile to consider injecting an epoxy resin or chemical grout into the porous concrete. An epoxy resin would both fill voids and increase the concrete strength. The least

WESCC

22 July 1977

MEMORANDUM FOR RECORD

SUBJECT: Capping exposed surfaces of Concrete, Tainter Gate Piers,
Starved Rock and Dresden Island Dams, Illinois Waterway

amount of space for water and hence freezable water would be a minimum.

4. Mr. Hoff suggested that fiber concrete be considered for capping the piers. Fiber concrete would be stronger than regular concrete. The technology exists for making a good quality fiber concrete, and the techniques of placing and handling are readily learned.

5. It was the consensus that a concrete cap should be included in the first layer of steel reinforcement in the pier. This would help the cap become an integral part of the pier. It was felt that a 9 in. concrete cap adequately anchored and bonded to the old concrete would be a sufficient cover over a pier.

6. Mr. Pace suggested that the concrete cap contain steel rock bolts on a similar device that was anchored into the old concrete. The bolts would hold the cap to the pier. Mr. Husbands recommended that the new concrete be bonded to the old concrete using an epoxy resin. A stronger bond would result using epoxy as opposed to placing the new concrete directly on old concrete. He stated that he would be available to assist field personnel in the proper application of the adhesive. With the cap properly tied and bonded to the old concrete, the cap would still be subject to breaking if shock loaded by large impact, but so would the original pier.

1 Incl

as

CF

Mr. L. Juzenas, NCC

R.L. Stowe

Concrete and Rock Properties Branch
Concrete Laboratory

Attendance at Meeting
Concrete Laboratory, 11 July 1977

Richard L Stowe; Con. & Rock Prop. Br.
Kenneth L Saucier; Con. & Rock Prop. Br.
Tony B. Husbands; Chief, Chemistry & Plastics Br.
George C. Hoff; Chief, Materials Properties Br.
Carl E. Pace; Structures Br.
Tony Liu; Structures Br.

APPENDIX F

Dol - Dolomite
Sh - Shale
Ch - Chert
Cl - Clay
Chy - Cherty
Sty - Stylolitic Bed
Interb - Interbedded
Sf - Soft
Inc - Inclusion
Lyr - Layer
Nod - Nodule
W/ - With
V - Very
Vert - Vertical
Slg - Slightly
Mod - Moderately
Fi - Fine
Bl - Blue
Br - Brown
Gry - Gray
Grn - Green
Drk - Dark
Fr - Fracture
Ptg - Parting
Jt - Joint
SB - Structural Break
BP - Bedding Plane
Prob MZ - Probably Missing Zone
FA - Fine Aggregate
CA - Coarse Aggregate
Nat - Natural
Conc - Concrete
Pc - Piece
Const - Construction
Lt - Light
Gr - Grain
U/S - Upstream
D/S - Downstream

In accordance with letter from DAEN-RDC, DAEN-ASI dated 22 July 1977, Subject: Facsimile Catalog Cards for Laboratory Technical Publications, a facsimile catalog card in Library of Congress MARC format is reproduced below.

Stowe, Richard L.

Concrete and rock core tests, major rehabilitation of Starved Rock Lock and Dam, Illinois Waterway, Chicago District, phase I, rehabilitation / by Richard L. Stowe, Barbara A. Pavlov, Ging S. Wong. Vicksburg, Miss. : U. S. Waterways Experiment Station ; Springfield, Va. : available from National Technical Information Service, 1978.

i, 55, [50] p., [51] leaves of plates : ill. ; 27 cm. (Miscellaneous paper - U. S. Army Engineer Waterways Experiment Station ; C-78-12)

Prepared for U. S. Army Engineer District, Chicago, Chicago, Ill.

References: p. 55.

1. Concrete cores.
 2. Concrete tests.
 3. Core drilling.
 4. Rock cores.
 5. Rock foundations.
 6. Rock tests (Laboratory).
 7. Starved Rock Lock and Dam.
- I. Pavlov, Barbara A., joint author.
- II. Wong, Ging S., joint author.
- III. United States. Army. Corps of Engineers. Chicago District.
- IV. Series: United States. Waterways Experiment Station, Vicksburg, Miss. Miscellaneous paper ; C-78-12.

TA7.W34m no.C-78-12